DZero Note 4338

Single EM Trigger Efficiency Using a Diem Tag and Probe Method

John Gardner

Abstract

The electron trigger efficiency using single EM triggers is studied with 177 pb^{-1} of data taken between September 2002 and September 2003. Efficiencies for the following triggers are studied: EM_HI_SH, EM_HI_2EM5_SH, EM_HI, EM_MX_SH, EM_MX, E1_SHT20, E2_SHT20, E3_SHT20, E1_SH30 and a combined efficiency using all these triggers. Additionally, the L1, L2 and L3 components of these triggers are examined separately.

Contents

1 Procedure

1.1 Trigger Selection

The following triggers from the global CMT 8 to 11 trigger lists:

- EM_HI_SH
- EM_HI_2EM5_SH
- EM_HI
- EM_MX_SH
- EM_MX

and the global CMT 12 trigger list:

- E1_SHT20
- E2_SHT20
- E3_SHT20
- E1_SH30

are selected for study in this note. These are commonly used EM triggers with trigger conditions that can be easily studied with a tag & probe method. In order to gain more statistics it is common to use several triggers. Sets of triggers are used in combination with the preferences shown below. This lists in order the combinations of triggers to use with the requirement that all triggers in the set be unprescaled. For an event to be used, a candidate electron must fire an unprescaled trigger from the lists below.

global CMT 8 to 11 trigger combinations (runs $\leq$ 178721)

- EM_HI_SH or EM_HI_2EM5_SH
- EM_HI_SH
- EM_HI
- EM_MX_SH
- EM_MX.

global CMT 12 trigger combinations (runs $\geq$ 178722)

- E1_SHT20, E2_SHT20, E3_SHT20 or E1_SH30
- E1_SHT20, E2_SHT20 or E1_SH30
- E1_SHT20 or E1_SH30
- E1_SHT20

For runs $\geq$ 174845, The level 1 trigger detector eta coverage was extended from $|\eta_{det}| < 2.4$ to $|\eta_{det}| < 3.2$. For pre global CMT 12 triggers, the level 2 and level 3 eta coverage is $|\eta_{det}| < 3.0$ and all CMT 12, L3 triggers cut on physics eta where $|\eta_{physics}| < 3.6$. These η coverages must be taken into account so that efficiency is only measured within the η range covered. Due to these eta coverages, a maximum $|\eta_{det}|$ of 2.3 is used for all EC efficiency plots unless otherwise stated. See Table 1 for a trigger summary.

1.2 Electron Selection

Electrons are selected using the version of EMcandidate dated 10 December 2003 and applying the quality cuts recommended by the EMID group. Electromagnetic objects have to satisfy the following requirements:

- Probe electrons:
  - ID = 10 OR $\pm$ 11
  - EMFraction > 0.9
  - Isolation < 0.15
  - HMatrix7 < 12
  - $E_T > 25$ GeV
    (extended down to 15 GeV for E_T plots only)
  - $|\eta_{det}| < 1.05$ (for CC) OR $1.5 < |\eta_{det}| < 2.3$ (for EC)
    (extended EC($2.3 < |\eta_{det}| < 3.2$) also plotted for η_{det} and E_T distributions)
  - 'is_in_fiducial' in EMCandidate
  - Not in a problematic calorimeter region
- Tag electrons:
  - meet probe electron requirements
  - Electron Likelihood > 0.9
  - Track match with $P(\chi^2) > 0.01$
  - Trigger requirements must be satisfied for at least one trigger in the set.

Electromagnetic clusters from EMReco are assigned an ID of 10 if they have $E_T > 1.5$ GeV and EMFraction > 0.9. If the cluster also has a track loosely matched to it, it is given an ID of $\pm$11 depending on the sign of the track (note: electrons are given an ID of +11 and positrons are given an ID of -11). The isolation variable is defined as

$$iso = \frac{E_{tot}(0.4) - E_{EM}(0.2)}{E_{EM}(0.2)} \tag{1}$$

trigger	L1	L2	L3
EM_HI_SH	CEM(1,10)	EM(1,12)	ELE_LOOSE_SH_T(1,20)
EM_HI_2EM5_SH	CEM(2,5)	EM(1,12)	ELE_LOOSE_SH_T(1,20)
EM_HI	CEM(1,10)	EM(1,12)	ELE_LOOSE(1,30)
EM_MX_SH	CEM(1,15)	none	ELE_LOOSE_SH_T(1,20)
EM_MX	CEM(1,15)	none	ELE_LOOSE(1,30)
E1_SHT20	CEM(1,11)	none	ELE_NLV_SHT(1,20)
E2_SHT20	CEM(2,6)	none	ELE_NLV_SHT(1,20)
E3_SHT20	CEM(1,9)CEM(2,3)	none	ELE_NLV_SHT(1,20)
E1_SH30	CEM(1,11)	none	ELE_NLV_SH(1,30)

L1 triggers

CEM(1,10)	one EM trigger tower with $E_T > 10GeV$
CEM(2,5)	two EM trigger towers with $E_T > 5GeV$
CEM(1,15)	one EM trigger tower with $E_T > 15GeV$
CEM(1,11)	one EM trigger tower with $E_T > 11GeV$
CEM(2,6)	two EM trigger towers with $E_T > 6GeV$
CEM(1,9)CEM(2,3)	one EM trigger tower with $E_T > 9GeV$, another EM trigger tower with $E_T > 3GeV$

L2 triggers

EM(1,12)	one EM candidate with $E_T > 12GeV$ (not present for runs below 169524)

L3 triggers

ELE_LOOSE_SH_T(1,20)	one electron with $\|\eta\| < 3.0$ and $E_T > 20GeV$ passing loose requirements including shower shape cuts
ELE_LOOSE(1,30)	one electron with $\|\eta\| < 3.0$ and $E_T > 30GeV$ passing loose requirements
ELE_NLV_SHT(1,20)	one electron with $\|\eta\| < 3.6$ and $E_T > 20GeV$ passing tight shower shape cuts
ELE_NLV_SH(1,30)	one electron with $\|\eta\| < 3.6$ and $E_T > 30GeV$ passing loose shower shape cuts

Table 1: Single EM triggers

where $E_{tot}(R)$ and $E_{EM}(R)$ denote the total energy and EM energy within a cone of radius R.

The fiducial requirement avoids cryostat edges and removes electron candidates near the ϕ gaps due to module boundaries. Calorimeter quality cuts refer to the calorimeter areas that have an identified hardware problem.

The electron likelihood was developed to maximize discrimination between signal and background. Histograms of seven variables are input for a signal and background sample obtained from data. These variables are:

- EM fraction
- H-Matrix(8)
- Calorimeter E_T / Track P_T
- Track DCA
- Track spatial χ^2 probability
- Number of tracks in an 0.05 cone around (and including) the candidate track
- Total P_T of tracks in an 0.4 cone around the candidate track, but excluding the candidate track

The track matching algorithm is found in the em_util package and includes a cut on the χ^2 of the track match.

$$\chi^2_{CC} = \left(\frac{\Delta z}{\sigma(z)}\right)^2 + \left(\frac{\Delta\phi}{\sigma(\phi)}\right)^2 + \left(\frac{E_T/p_T - 1}{\sigma(E_T/p_T)}\right)^2 \quad (2)$$

$$\chi^2_{EC} = \left(\frac{\Delta z}{\sigma(z)}\right)^2 + \left(\frac{\Delta\phi}{\sigma(\phi)}\right)^2 \quad (3)$$

In the above expression, Δz and $\Delta\phi$ are the differences between the track position and the EM cluster position at the third floor of the calorimeter; E_T/p_T is the transverse energy of the EM cluster as measured by the calorimeter divided by the transverse momentum of the track; and the σ variables are the root-mean-squares of the experimental measurements of each quantity. In the EC region of the calorimeter the E_T/p_T term in the χ^2 is not used. For a good track match, the track matching χ^2 probability cut is $P(\chi^2) > 10^{-2}$.

The requirement that the "tag" electron passes trigger requirements for at least one unprescaled trigger in the set is especially important. This ensures the probe is not biased by the event trigger requirement. For an electron to pass a trigger's requirements, the EM object must have a matching trigger object at each level which passes all cuts for the corresponding trigger. The electron EM to trigger object matching requirements are:

- L1: $\Delta\phi < 0.4$ (L1 η information not available)

- L2: $\Delta R < 0.4$
- L3: $\Delta R < 0.4$

where $\Delta R = \sqrt{\Delta\phi^2 + \Delta\eta^2}$

The triggers EM_HI_2EM5_SH, E2_SHT20 and E3_SHT20 have at L1 a requirement of 2 high E_T trigger towers with no requirement that these towers be near each other. This complicates matters because the exact handling for this depends on what else is happening in the event. For example in di-electron events each electron will only have to fire one L1 tower while in single electron events the electron must fire both. To simplify matters for these triggers, the EM object must always be associated with 2 nearby high E_T L1 towers in order to pass trigger requirements. Likewise, this same requirement must be placed when considering these triggers for event selection.

1.3 Trigger Efficiency Determination

Efficiencies are found with a tag-probe method using Z candidate events. This is done by selecting events with at least two EM objects satisfying the requirements of the probe electron. Additionally a 70 < invariant mass < 110 GeV cut is placed on the two highest E_T probe electrons. Both of these are considered as possible tags. If the electron satsifies the requirements of a tag then the other electron becomes a probe.

A total of 7899 CC and 3151 EC probes for runs $\leq$ 178721(CMT 8 to 11) and 2845 CC and 1246 EC probes for runs $\geq$ 178722(CMT 12) are found. Trigger efficiency is then the fraction of probes passing the trigger requirements. A total of 7808 CC and 3000 EC probes pass trigger requirements for CMT 8 to 11 triggers and 2807 CC and 1158 EC probes for CMT 12, yielding average trigger efficiencies of 98.8% CC and 95.2% EC for CMT 8 to 11 and 98.7% CC and 92.9% EC for CMT 12.

All plots are in section 2. First, trigger efficiency plots using a combination of all triggers for all runs are shown, then CMT 8 to 11 only and CMT only. The following subsections cover each trigger individually. Each trigger subsection has subsubsections for efficiency separated into L1, L2(if present) and L3 components. L2 efficiency is defined as the efficiency for an electron passing L1 to also pass L2 while L3 efficiency is the efficiency for an electron passing L1 and L2 to also pass L3.

The following distributions are plotted:

- E_T for CC, EC and extended EC,
- detector η
- physics η for CC and EC
- instantaneous luminosity for combined CC and EC
- detector ϕ for CC and EC

1.4 CMT 12 Trigger Peculiarities

The most noticeable CMT 12 peculiarity is a large asymmetry visible in the E1_SHT20 plot vs. η_{det} shown in figure 181. This effect is produced at L3 as can be seen in figure 193. ELE_NLV_SHT, the L3 trigger of E1_SHT20, makes use of rescaled shower widths for shower shape cuts. One parameter in this rescaling is primary vertex z. A comparison of ELE_NLV_SHT efficiency, shown in figure 1, using only events with primary vertex z > 0 to events with z < 0 shows a very pronounced difference. The top plots, comparing η_{det}, show an even larger asymmetry for z > 0 while the z < 0 plot is symmetric. This suggests perhaps a missing absolute value sign for z somewhere within the rescaling equation. This same L3 trigger is also used in E2_SHT20 and E3_SHT20 where the asymmetry is also apparent. It is possible this effects E1_SH30 which uses loose shower shape cuts, but if so the asymmetry is much less apparent.

Another odd effect is seen in the CMT trigger combination plot vs E_T for CC shown in figure 53. There appears to be an odd bump at around 25 GeV. This is produced by the combination of E1_SHT20 and E1_SH30, which are set to turn on at L3 at 20 and 30 GeV respectively. A comparison of figures 179 and 233 shows E1_SHT20 turns on at 25 GeV and plateaus at around 95% while E1_SH30 turns on at 35 GeV and quickly reaches 100%. The plateau in figure 179 for E1_SHT20 is rather uneven which makes it questionable as to whether there is a peak at 25 GeV. This is caused by ELE_NLV_SHT as seen in the middle plots of figure 1. The bump is only apparent for z > 0 which suggests a relationship with the η_{det} peculiarity.

1.5 Background Check and Cut Dependence

Background in the sample will tend to fail the trigger requirements more often than real electrons therefore biasing efficiency low. Therefore invariant mass plots of probes failing trigger requirements should be especially sensitive to the presence of background. If background is a potential concern, these plots should show a large low mass tail. Figure 2 demonstrates that this is not a problem. There is a strong Z peak with very few statistics in the tail for both CC and EC.

For a precise measurement in a particular analysis, care should be taken to place identical cuts on the electron probe as used in the analysis. Trigger efficiency can be dependent on other cuts placed on the electron, especially if there is a definite correlation between these cuts and those of the trigger. For example, there is evidence that efficiency increases with the addition of a track requirement. This is especially apparent at low E_T for EC, as shown in figure 3. To verify this is not caused by background, the invariant mass of failed probes with the track requirement is compared to without. Figure 4 shows the amount of of background is quite similiar. This suggests background is not the problem but rather trigger efficiency is dependent either directly or indirectly on the presence of a track.

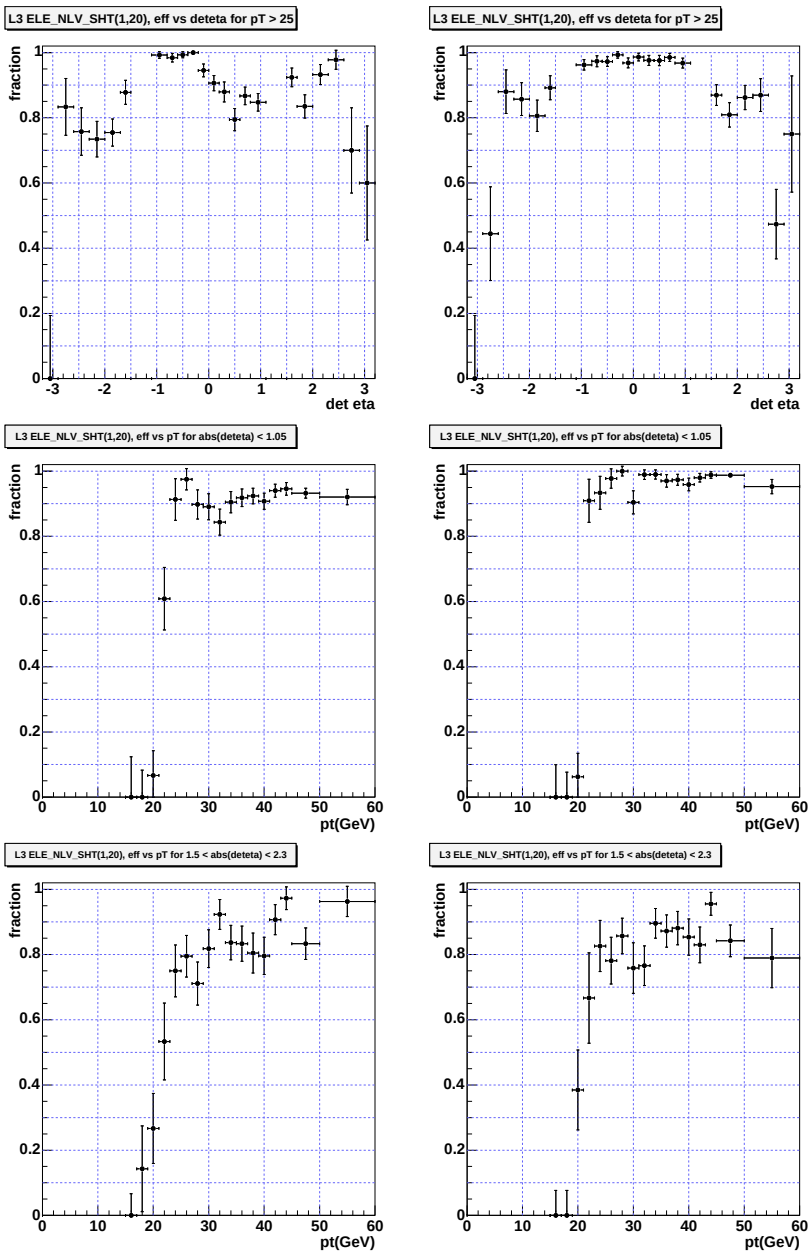

Figure 1: Comparison of events with primary vertex z > 0(left plots) to events with z < 0(right plots). The top row is for η_{det}, middle row is CC E_T and bottom row EC E_T. For a description refer to 1.4.

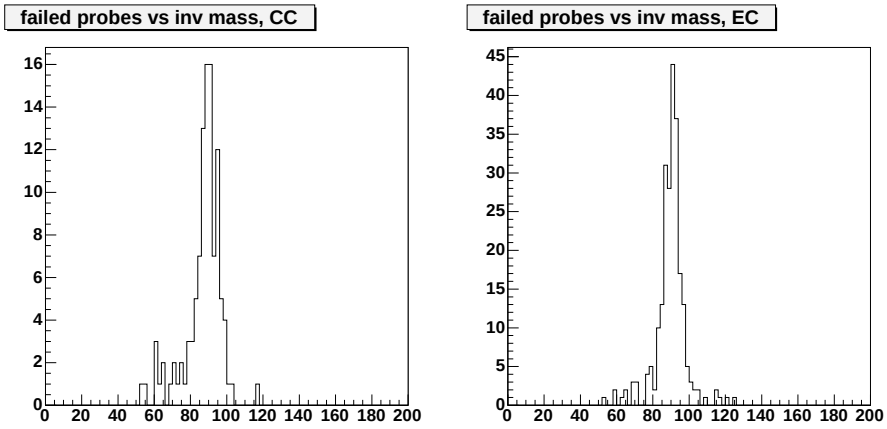

Figure 2: Invariant mass distributions(in GeV) of failed probes for CC(left) and EC(right)

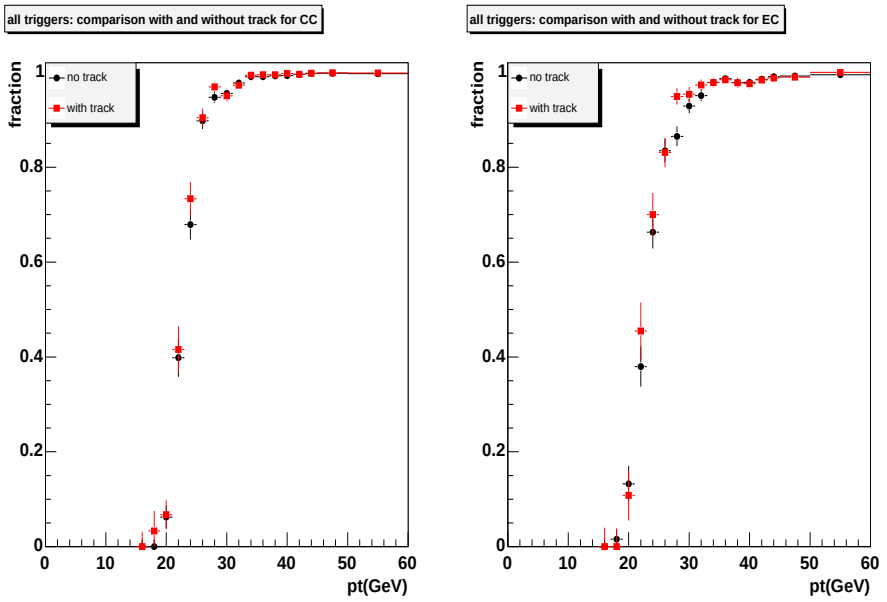

Figure 3: Comparison using all triggers of trigger efficiency with and without a track requirement on the probe for CC(left) and EC(right)

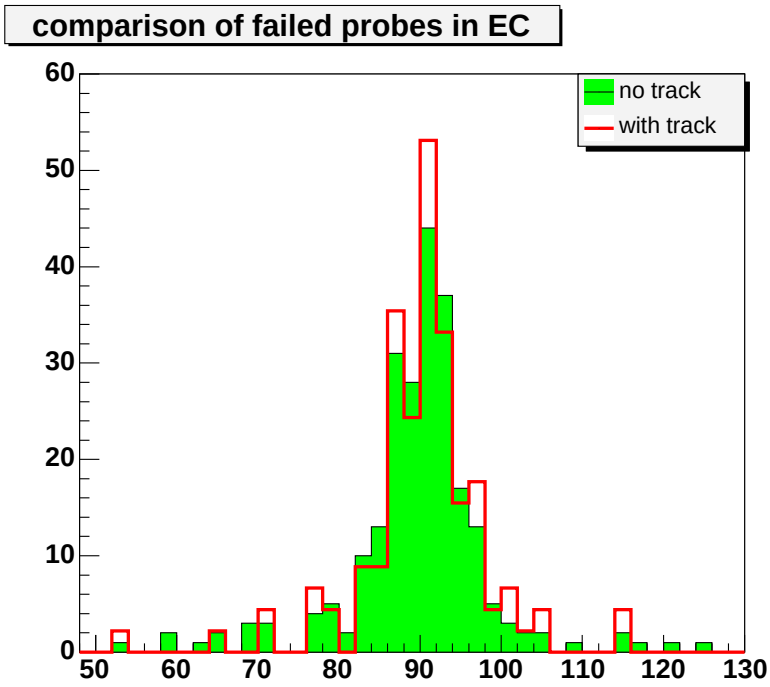

Figure 4: Invariant mass distributions(in GeV) in the EC comparing failed probes with and without a track requirement. Actual number of probes failing with a track requirement is roughly half that of without and is normalized to match.

2 Efficiency Plots

2.1 All Triggers Combined

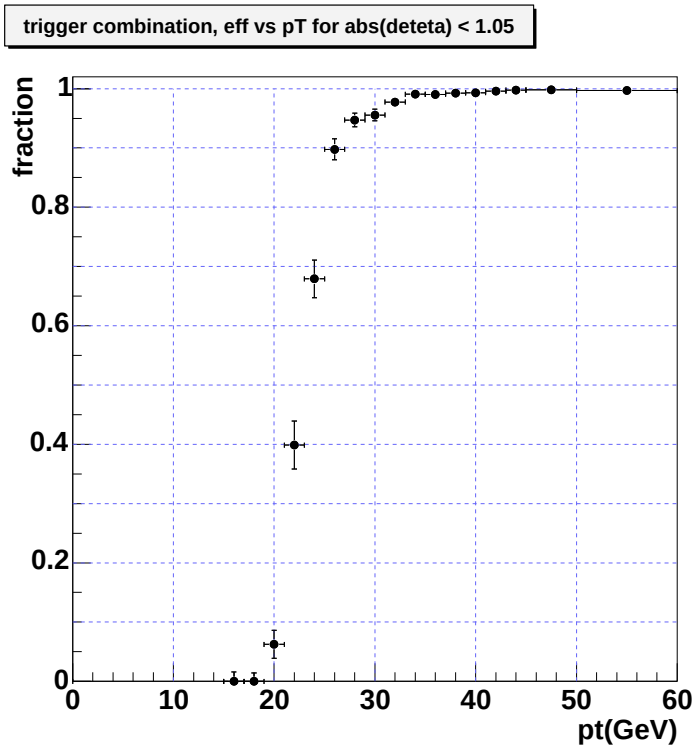

Figure 5: Electron trigger efficiency for all triggers as a function of E_T for CC.

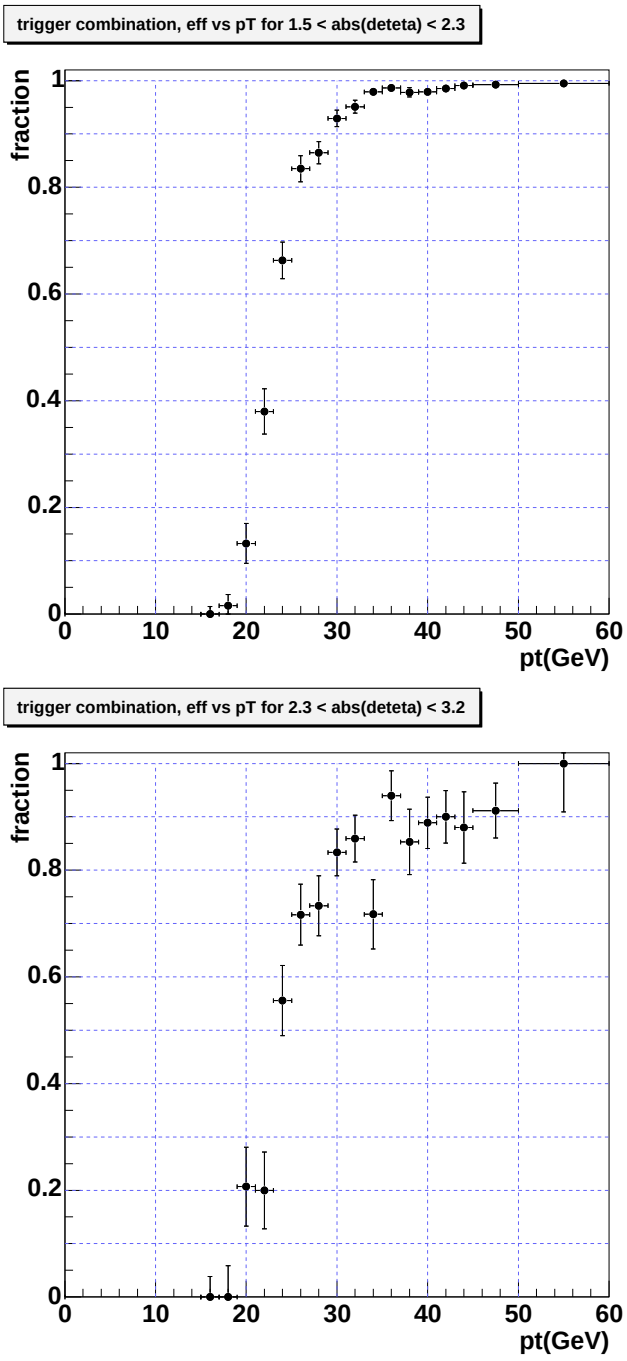

Figure 6: Electron trigger efficiency for all triggers as a function of E_T for EC(top) and extended EC($2.3 < |\eta_{detector}| < 3.2$) (bottom).

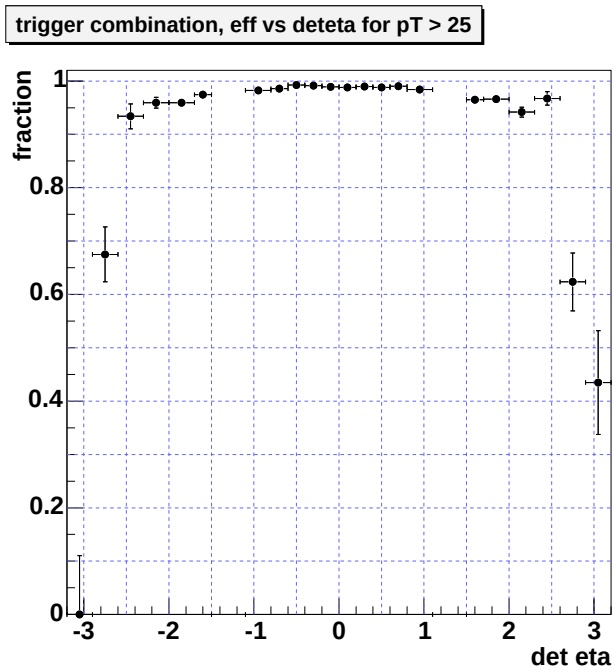

Figure 7: Electron trigger efficiency for all triggers as a function of detector η.

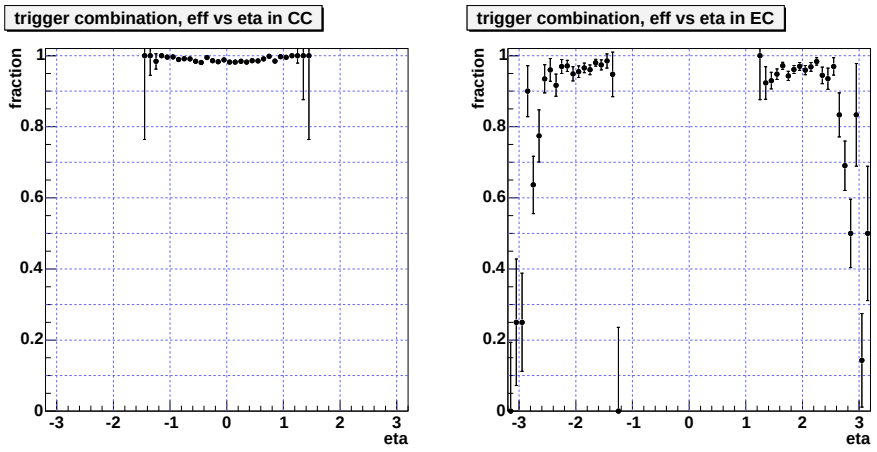

Figure 8: Electron trigger efficiency for all triggers as a function of physics η for CC(left) and EC(right).

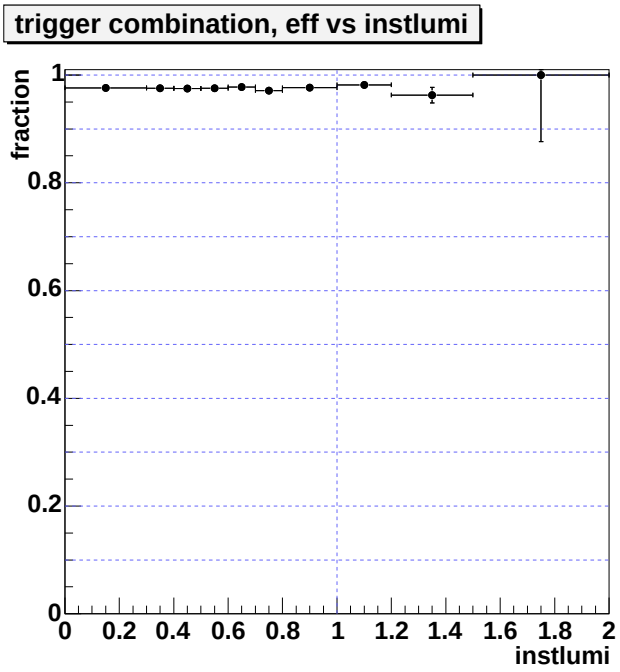

Figure 9: Electron trigger efficiency for all triggers as a function of instantaneous luminosity($10^{30} cm^{-2} s^{-1}$) for all probes.

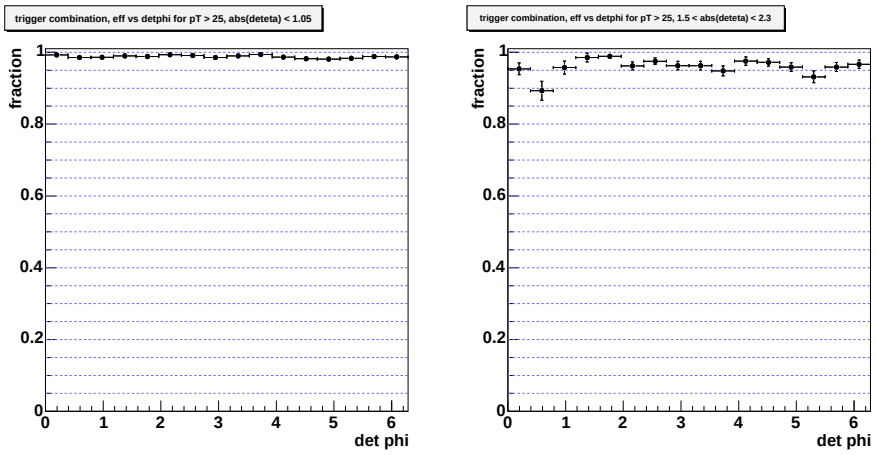

Figure 10: Electron trigger efficiency for all triggers as a function of detector ϕ for CC(left) and EC(right).

2.1.1 All Triggers Combined: L1

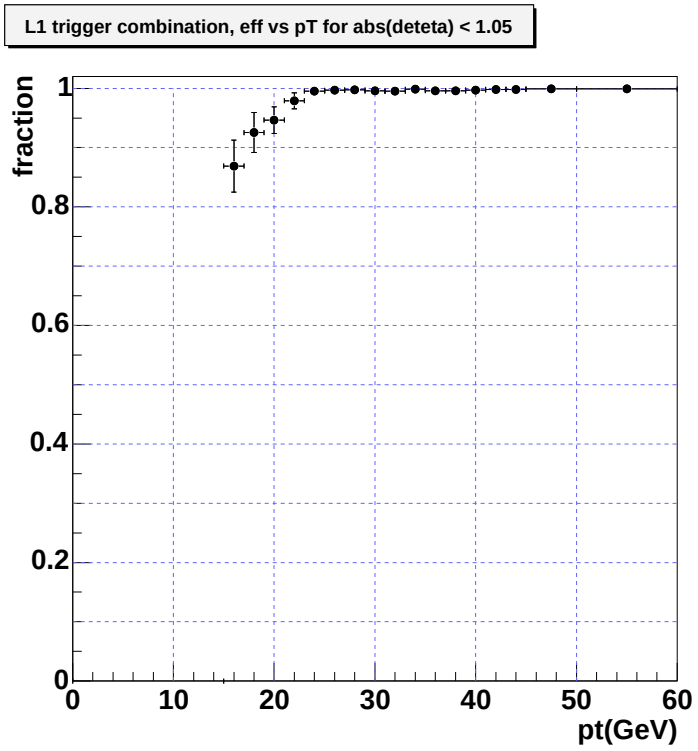

Figure 11: Electron trigger efficiency at L1 for all triggers as a function of E_T for CC.

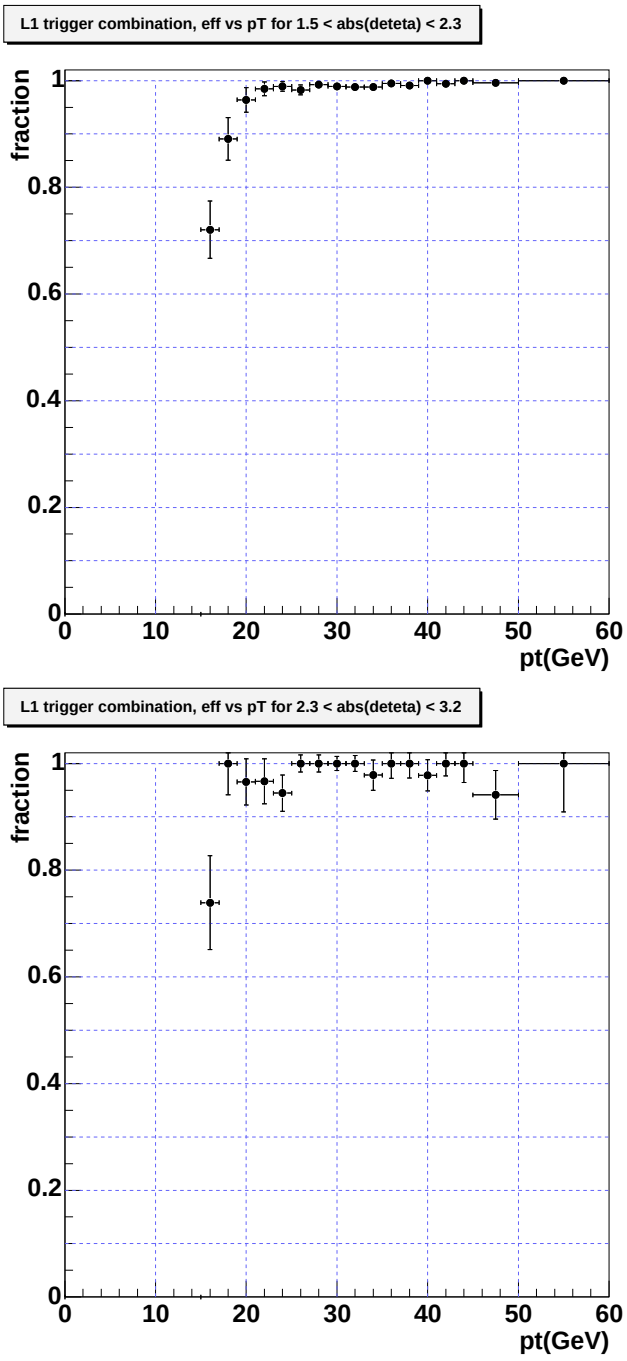

Figure 12: Electron trigger efficiency at L1 for all triggers as a function of E_T for EC(top) and extended EC($2.3 < |\eta_{detector}| < 3.2$) (bottom).

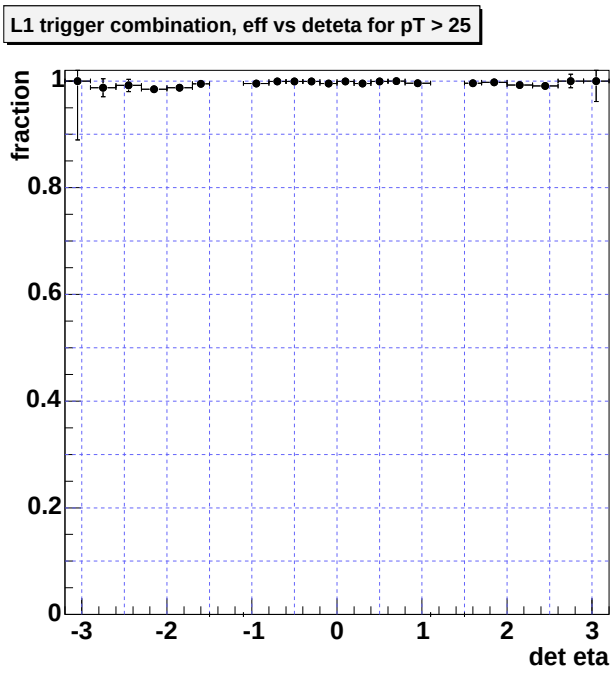

Figure 13: Electron trigger efficiency at L1 for all triggers as a function of detector η.

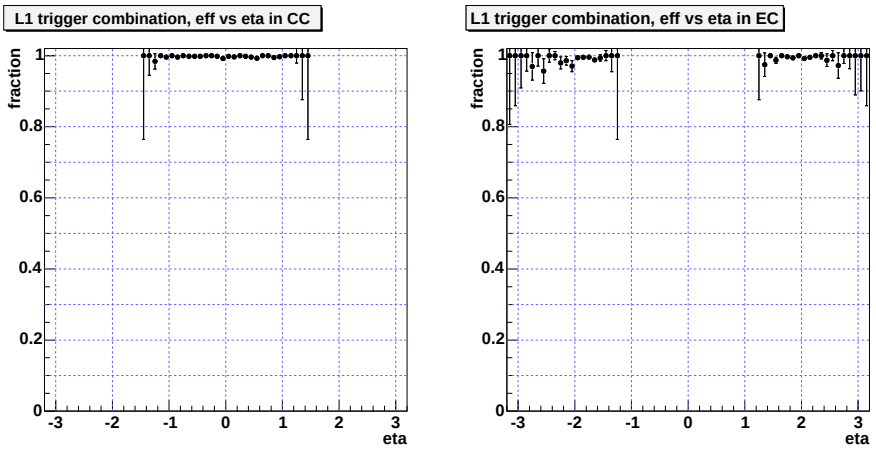

Figure 14: Electron trigger efficiency at L1 for all triggers as a function of physics η for CC(left) and EC(right).

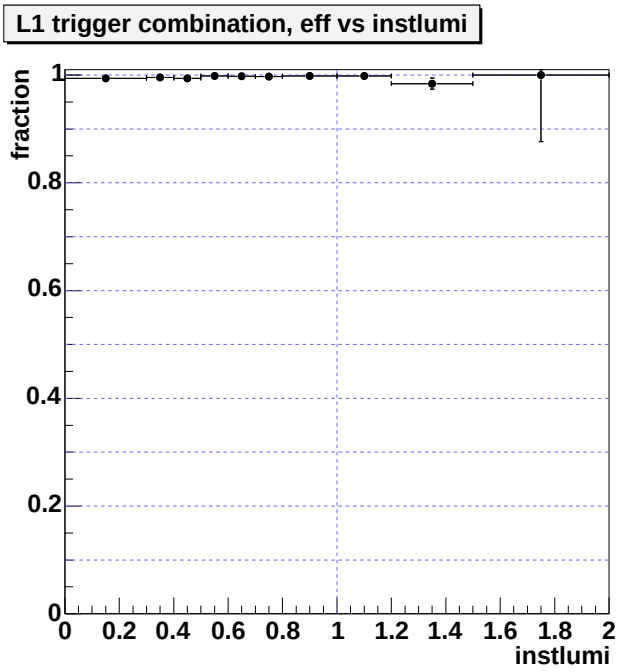

Figure 15: Electron trigger efficiency at L1 for all triggers as a function of instantaneous luminosity($10^{30} cm^{-2} s^{-1}$) for all probes.

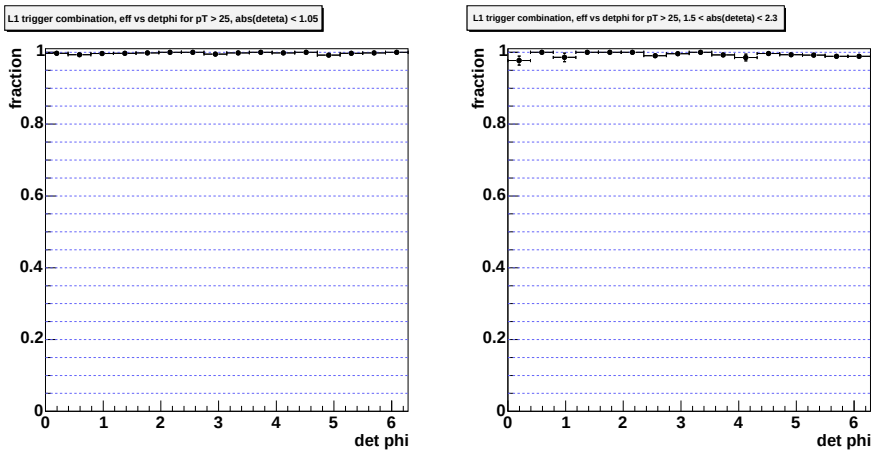

Figure 16: Electron trigger efficiency at L1 for all triggers as a function of detector ϕ for CC(left) and EC(right).

2.1.2 All Triggers Combined: L2

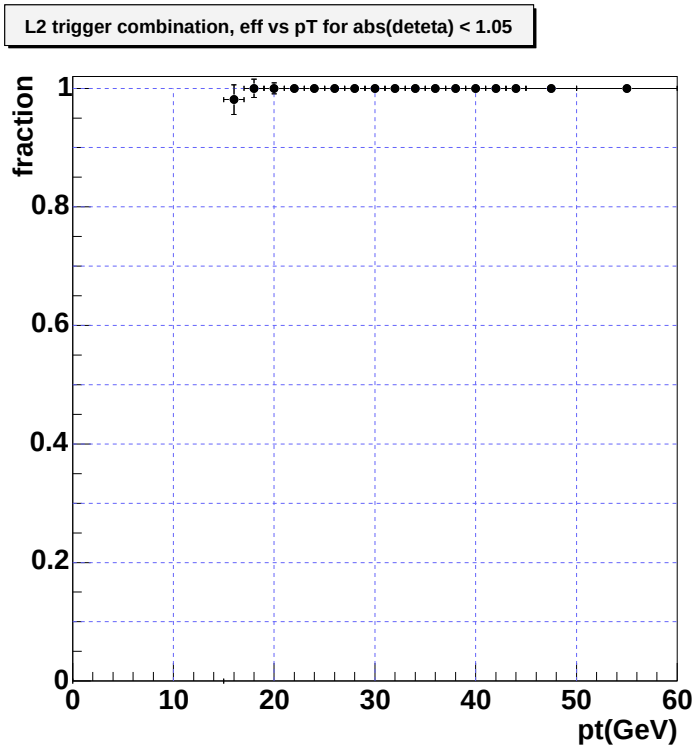

Figure 17: Electron trigger efficiency at L2 for all triggers as a function of E_T for CC.

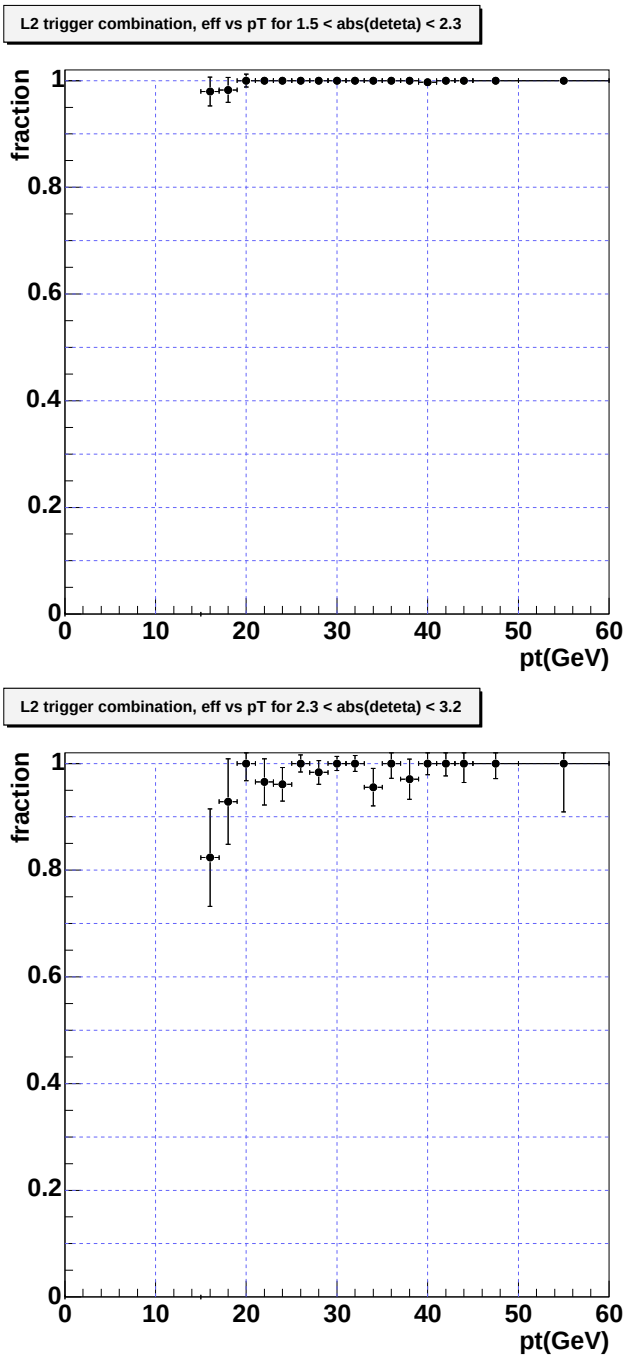

Figure 18: Electron trigger efficiency at L2 for all triggers as a function of E_T for EC(top) and extended EC($2.3 < |\eta_{detector}| < 3.2$) (bottom).

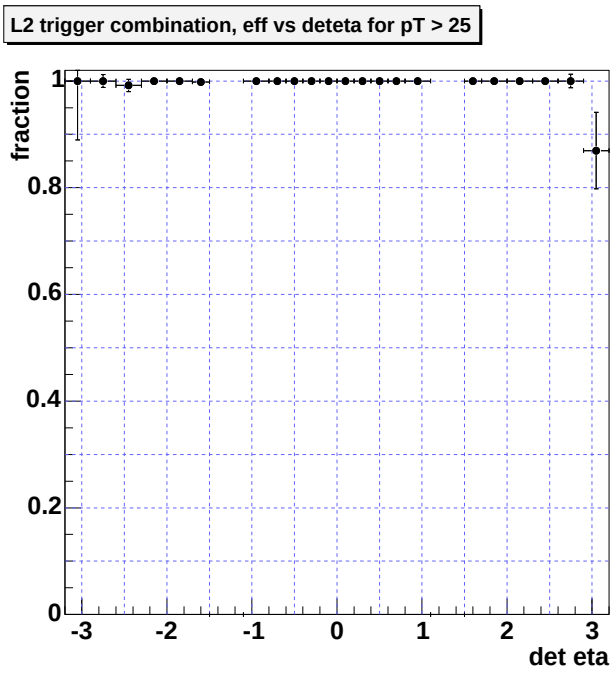

Figure 19: Electron trigger efficiency at L2 for all triggers as a function of detector η.

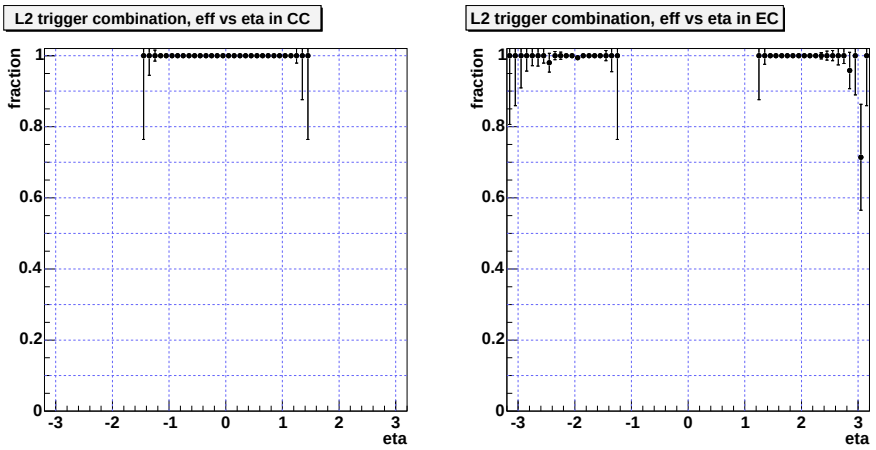

Figure 20: Electron trigger efficiency at L2 for all triggers as a function of physics η for CC(left) and EC(right).

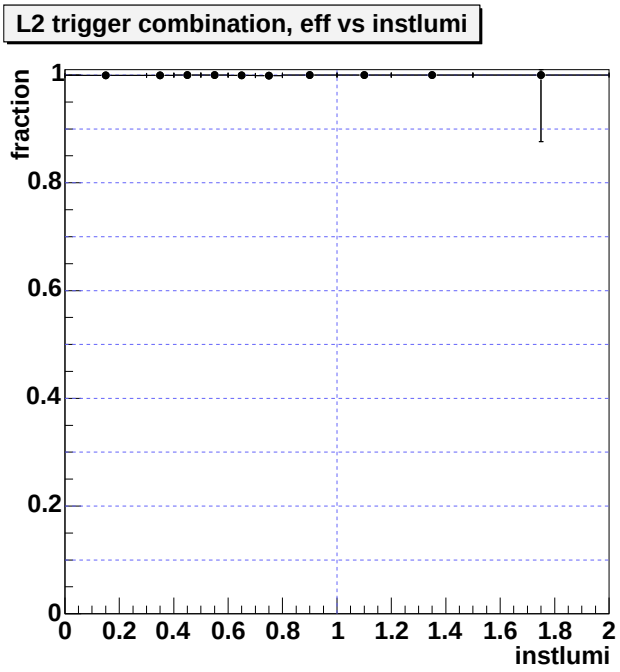

Figure 21: Electron trigger efficiency at L2 for all triggers as a function of instantaneous luminosity($10^{30} cm^{-2} s^{-1}$) for all probes.

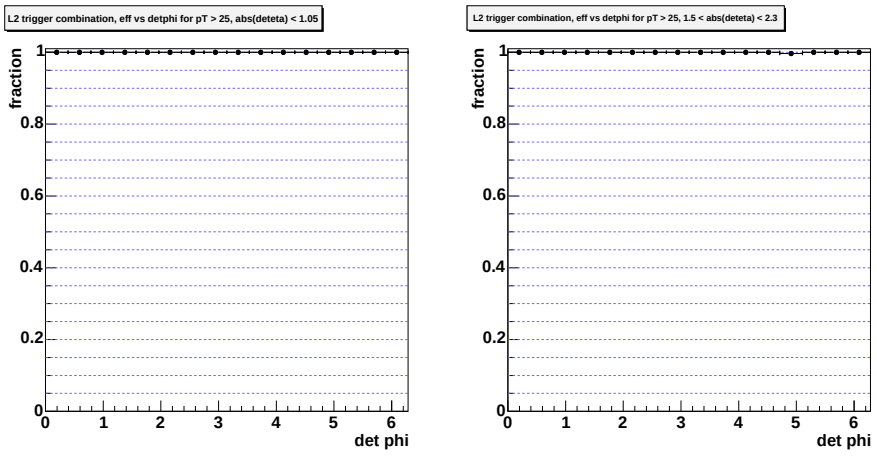

Figure 22: Electron trigger efficiency at L2 for all triggers as a function of detector ϕ for CC(left) and EC(right).

2.1.3 All Triggers Combined: L3

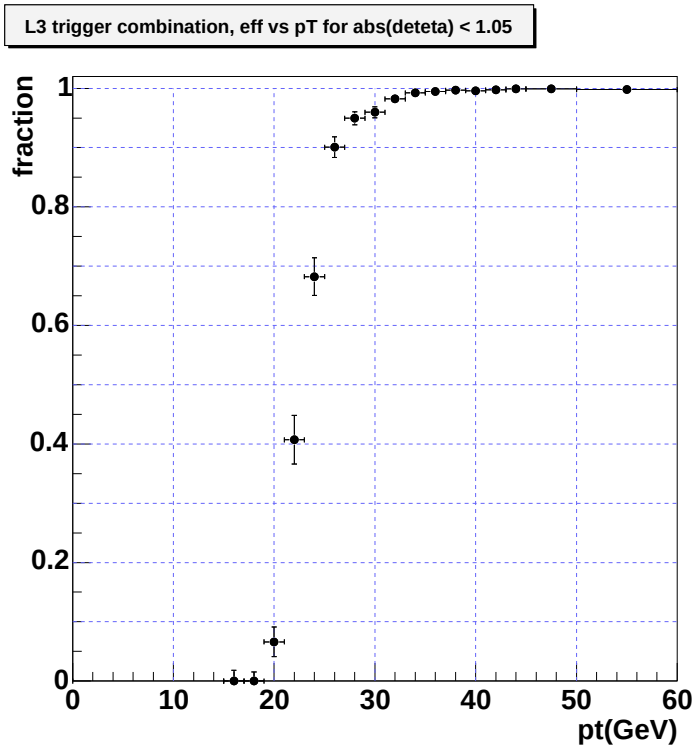

Figure 23: Electron trigger efficiency at L3 for all triggers as a function of E_T for CC.

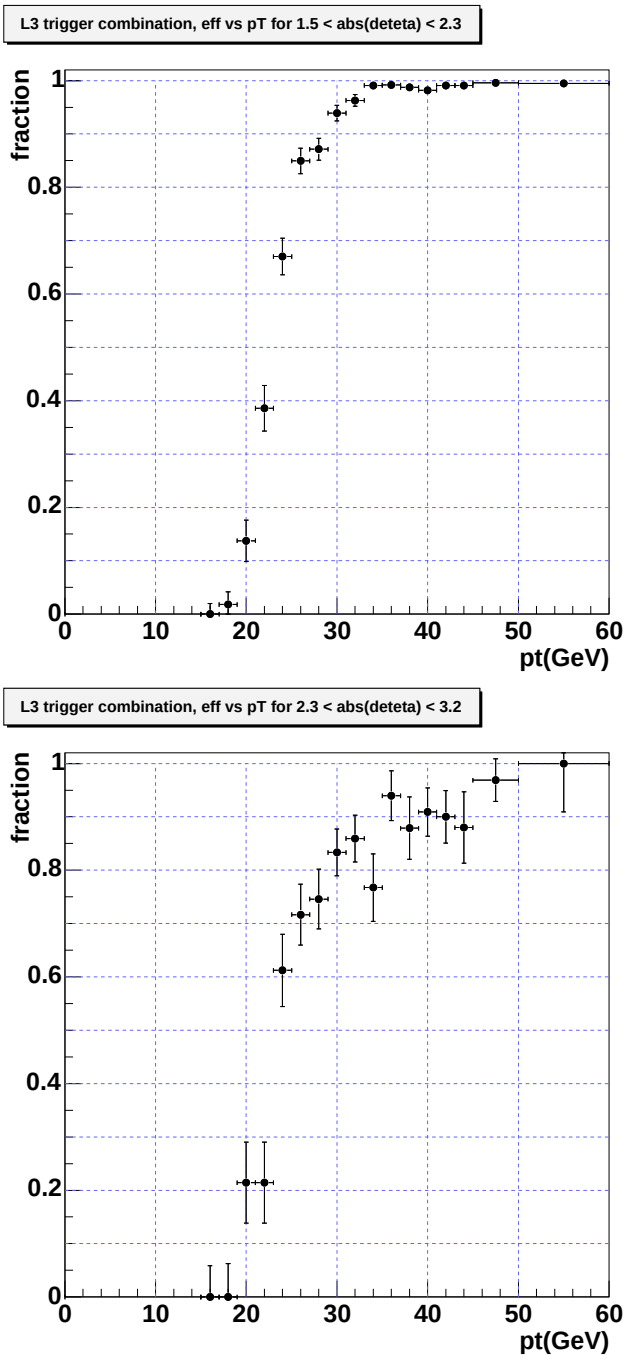

Figure 24: Electron trigger efficiency at L3 for all triggers as a function of E_T for EC(top) and extended EC($2.3 < |\eta_{detector}| < 3.2$) (bottom).

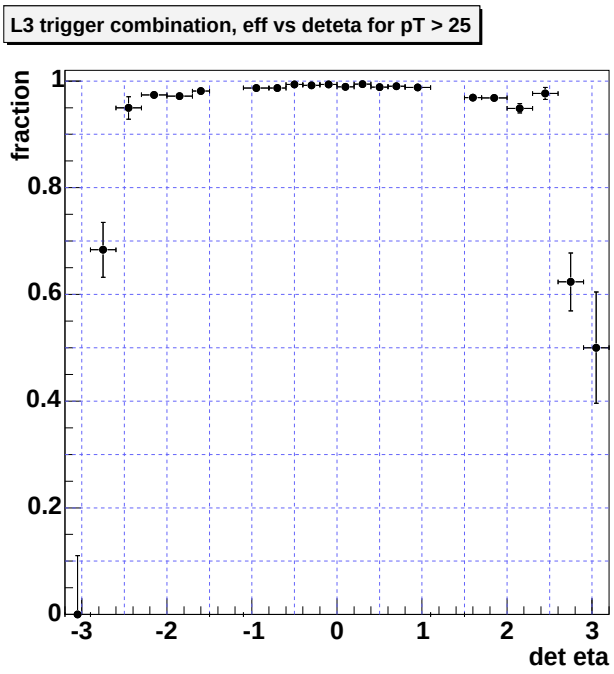

Figure 25: Electron trigger efficiency at L3 for all triggers as a function of detector η.

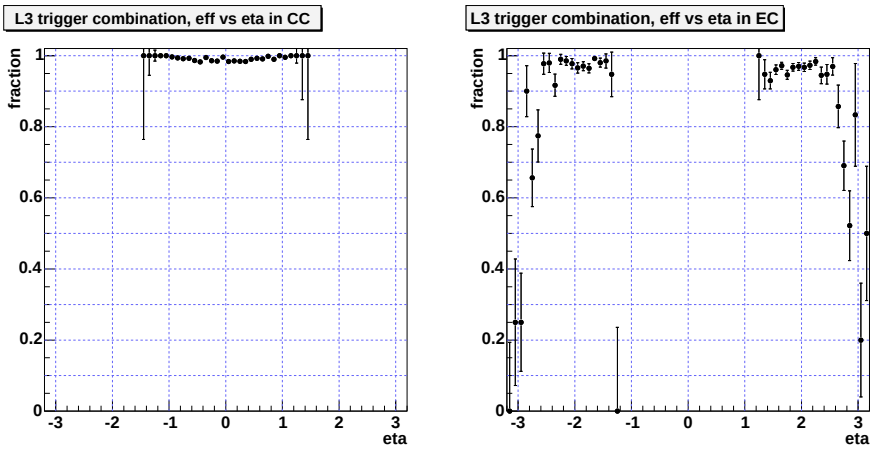

Figure 26: Electron trigger efficiency at L3 for all triggers as a function of physics η for CC(left) and EC(right).

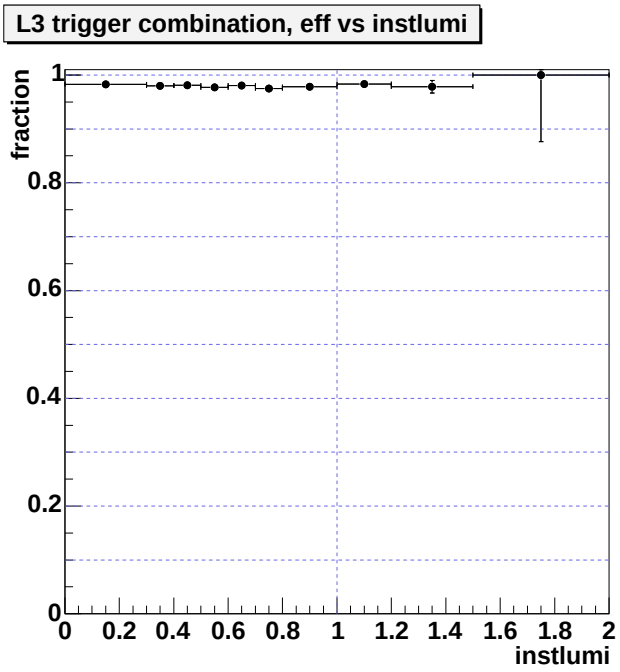

Figure 27: Electron trigger efficiency at L3 for all triggers as a function of instantaneous luminosity($10^{30} cm^{-2} s^{-1}$) for all probes.

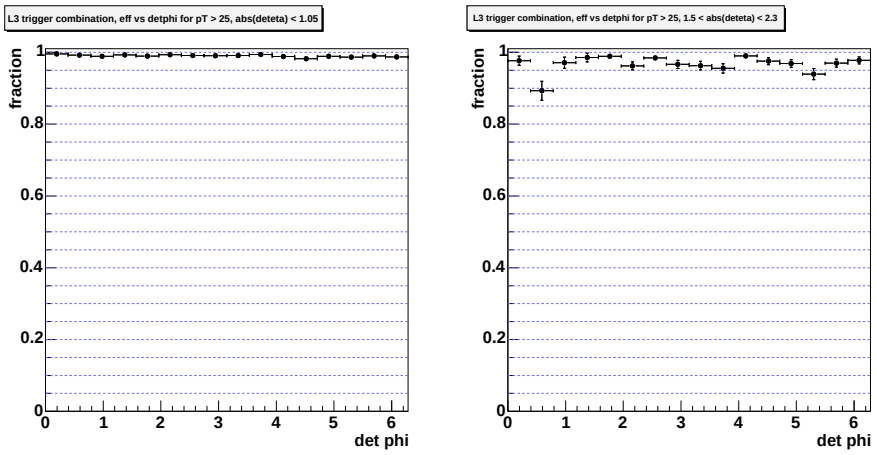

Figure 28: Electron trigger efficiency at L3 for all triggers as a function of detector ϕ for CC(left) and EC(right).

2.2 All Triggers Combined for CMT 8 to 11

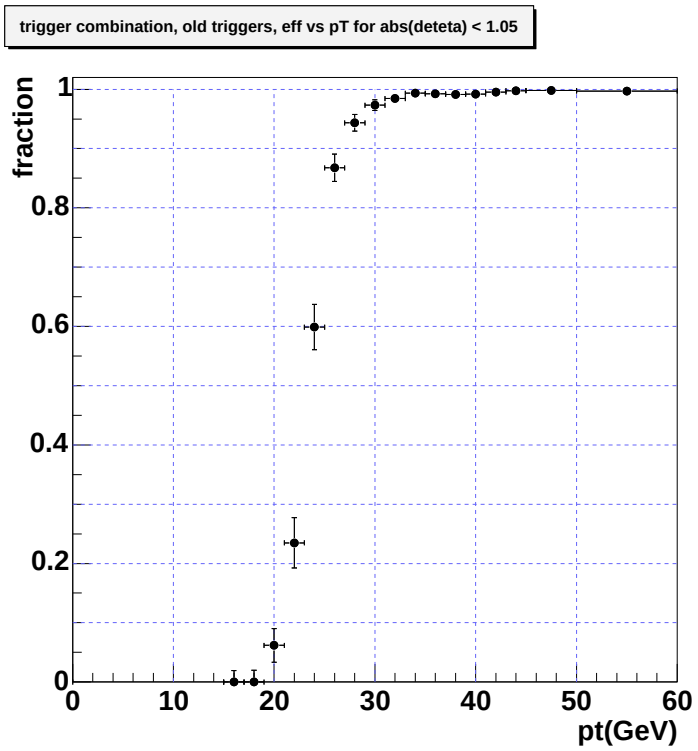

Figure 29: Electron trigger efficiency for all CMT 8 to 11 triggers as a function of E_T for CC.

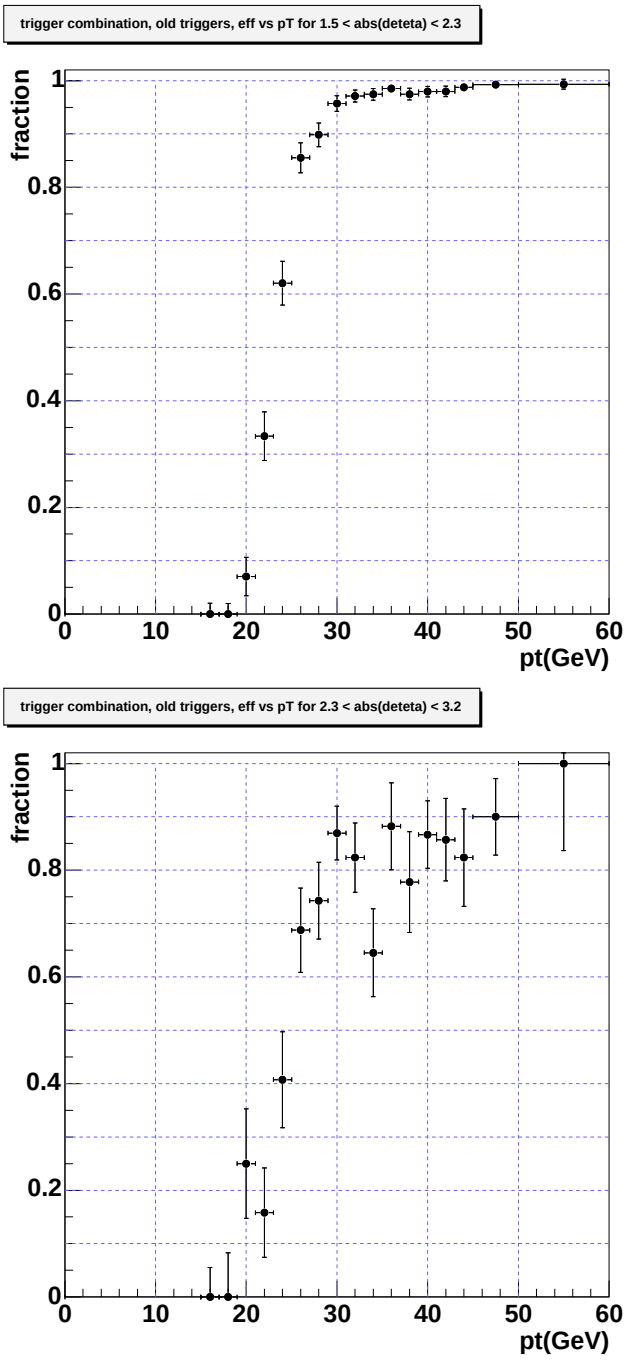

Figure 30: Electron trigger efficiency for all CMT 8 to 11 triggers as a function of E_T for EC(top) and extended EC($2.3 < |\eta_{detector}| < 3.2$) (bottom).

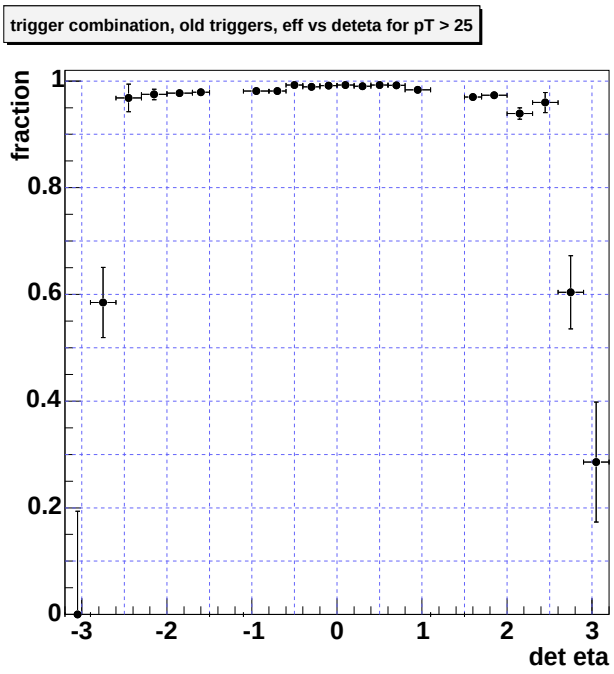

Figure 31: Electron trigger efficiency for all CMT 8 to 11 triggers as a function of detector η.

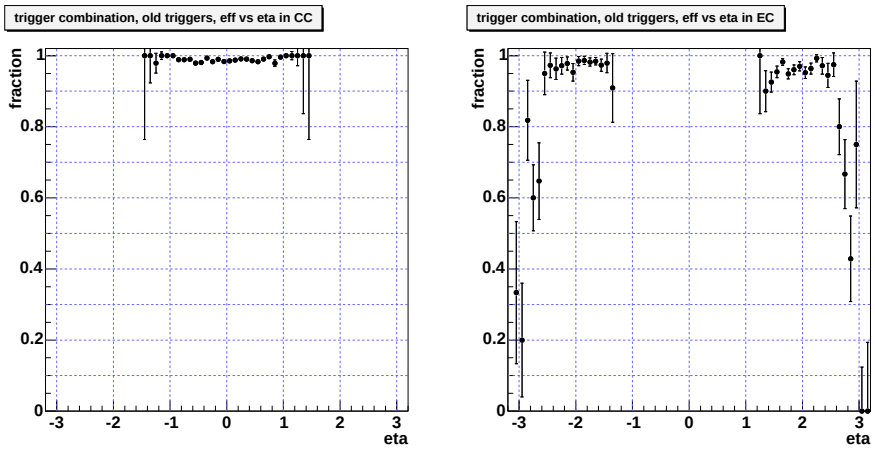

Figure 32: Electron trigger efficiency for all CMT 8 to 11 triggers as a function of physics η for CC(left) and EC(right).

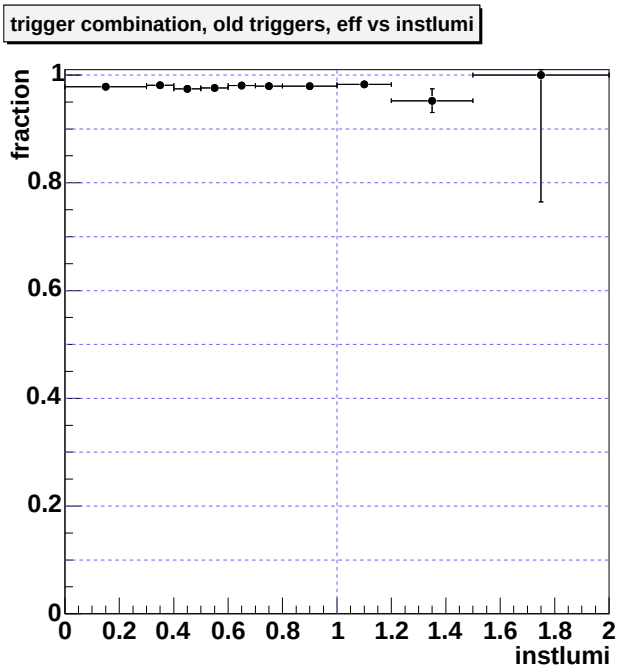

Figure 33: Electron trigger efficiency for all CMT 8 to 11 triggers as a function of instantaneous luminosity($10^{30} cm^{-2} s^{-1}$) for all probes.

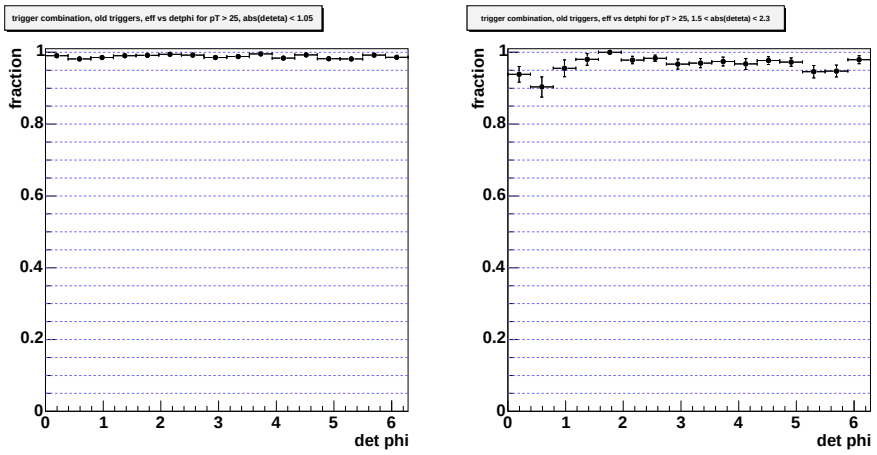

Figure 34: Electron trigger efficiency for all CMT 8 to 11 triggers as a function of detector ϕ for CC(left) and EC(right).

2.2.1 All Triggers Combined for CMT 8 to 11: L1

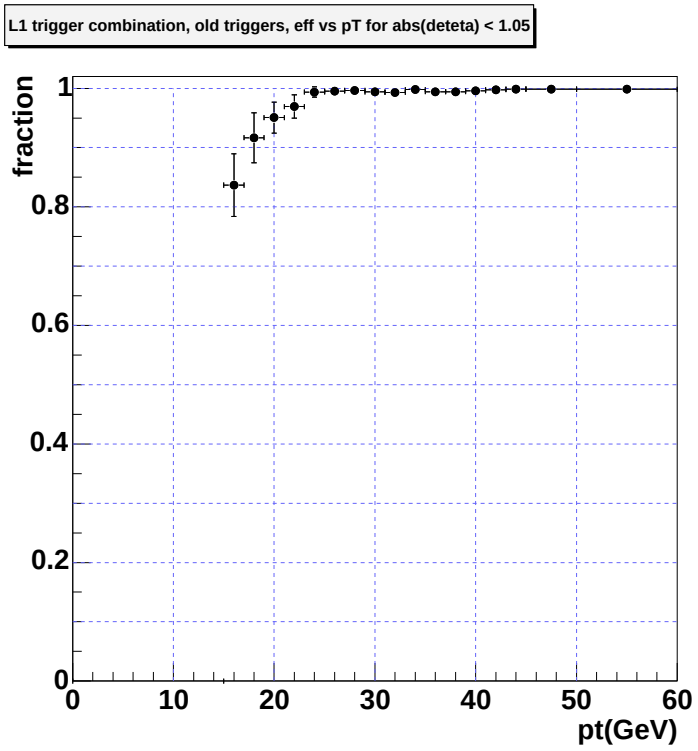

Figure 35: Electron trigger efficiency at L1 for all CMT 8 to 11 triggers as a function of E_T for CC.

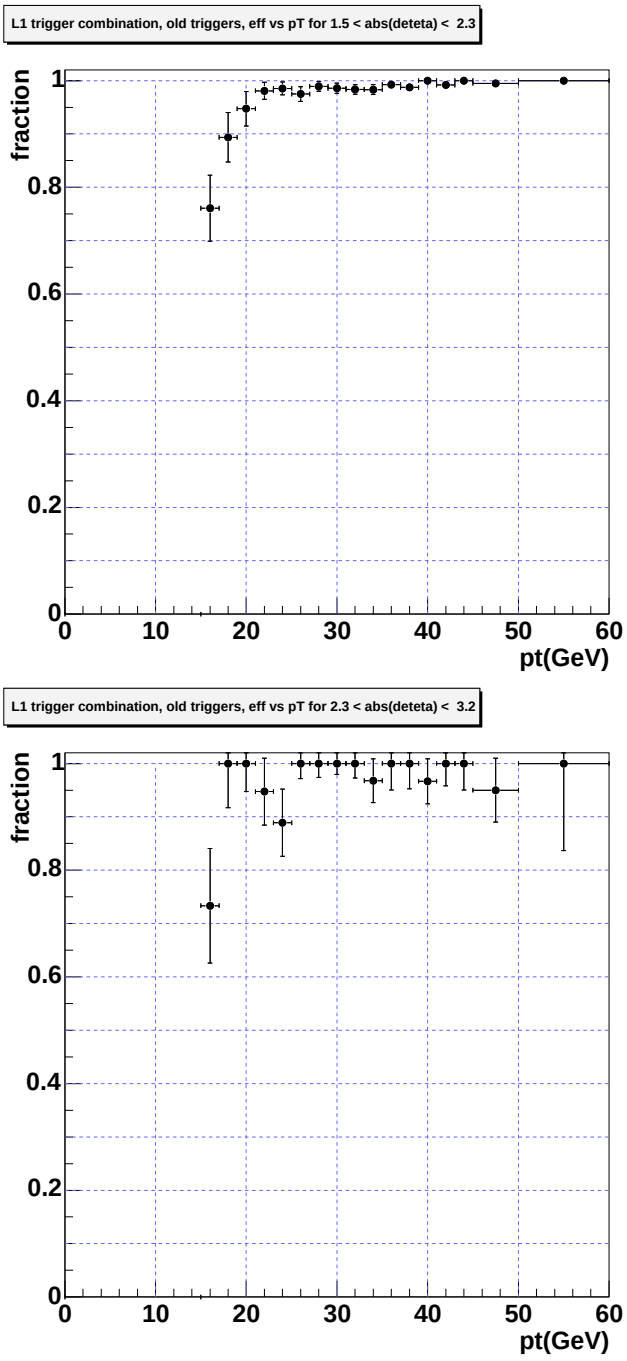

Figure 36: Electron trigger efficiency at L1 for all CMT 8 to 11 triggers as a function of E_T for EC(top) and extended EC($2.3 < |\eta_{detector}| < 3.2$) (bottom).

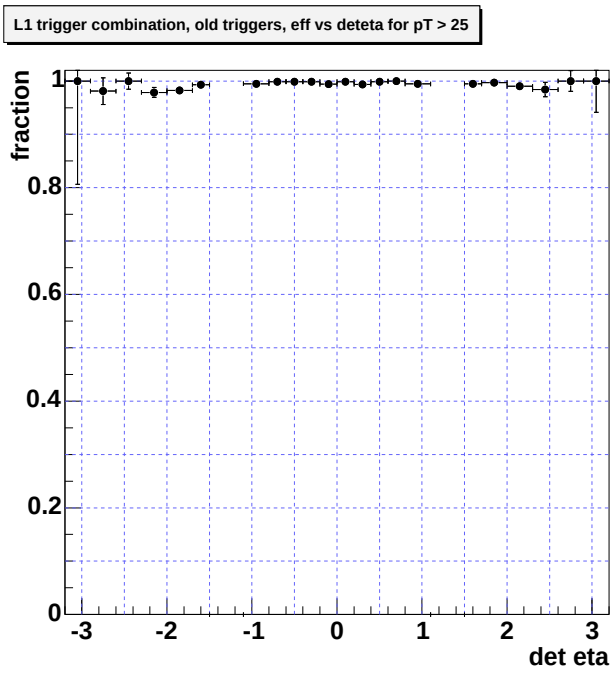

Figure 37: Electron trigger efficiency at L1 for all CMT 8 to 11 triggers as a function of detector η.

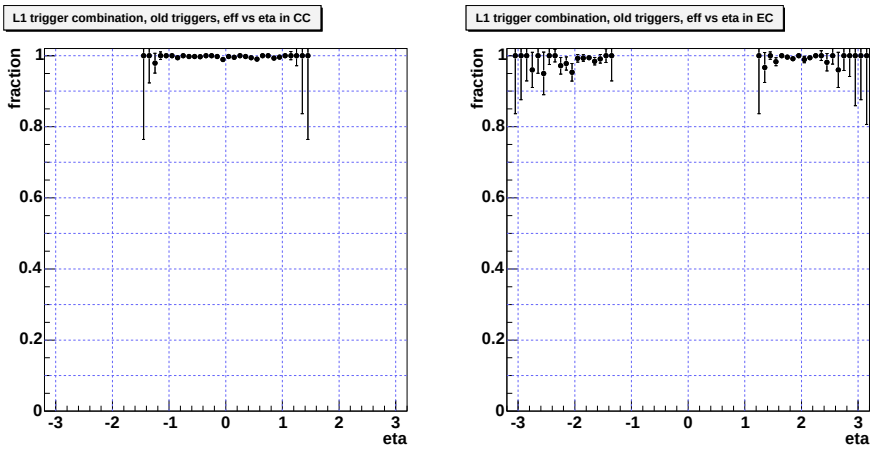

Figure 38: Electron trigger efficiency at L1 for all CMT 8 to 11 triggers as a function of physics η for CC(left) and EC(right).

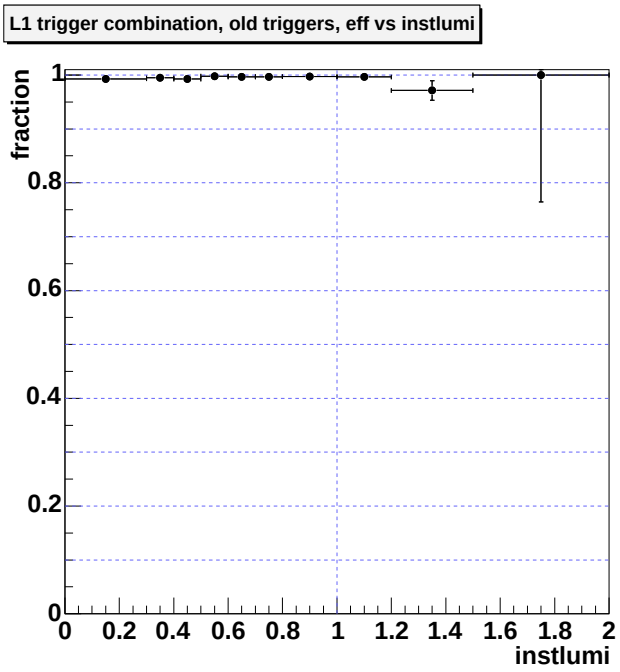

Figure 39: Electron trigger efficiency at L1 for all CMT 8 to 11 triggers as a function of instantaneous luminosity($10^{30} cm^{-2} s^{-1}$) for all probes.

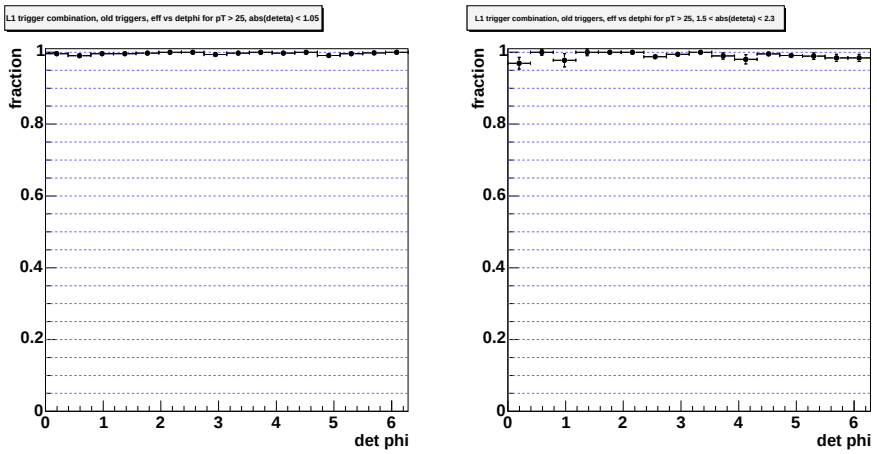

Figure 40: Electron trigger efficiency at L1 for all CMT 8 to 11 triggers as a function of detector ϕ for CC(left) and EC(right).

2.2.2 All Triggers Combined for CMT 8 to 11: L2

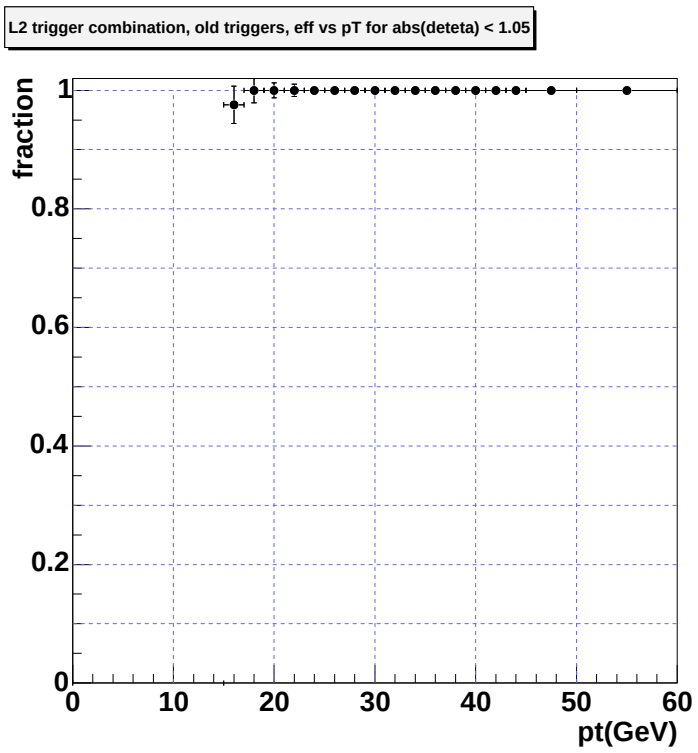

Figure 41: Electron trigger efficiency at L2 for all CMT 8 to 11 triggers as a function of E_T for CC.

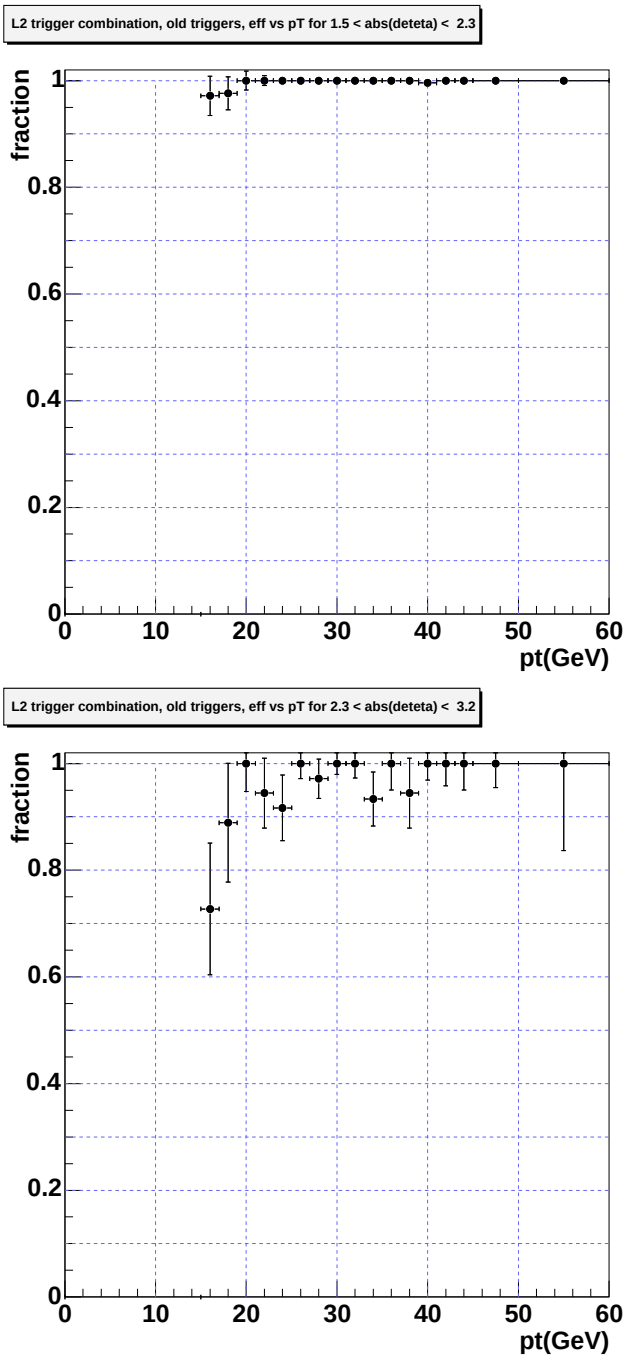

Figure 42: Electron trigger efficiency at L2 for all CMT 8 to 11 triggers as a function of E_T for EC(top) and extended EC($2.3 < |\eta_{detector}| < 3.2$) (bottom).

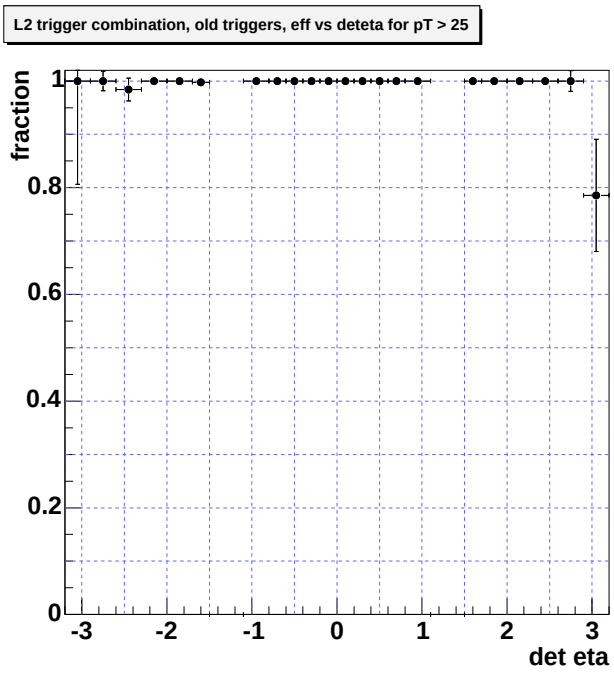

Figure 43: Electron trigger efficiency at L2 for all CMT 8 to 11 triggers as a function of detector η.

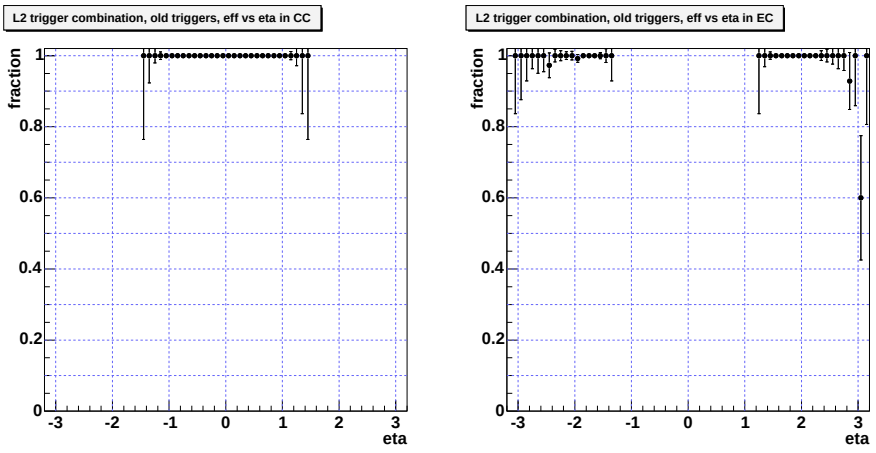

Figure 44: Electron trigger efficiency at L2 for all CMT 8 to 11 triggers as a function of physics η for CC(left) and EC(right).

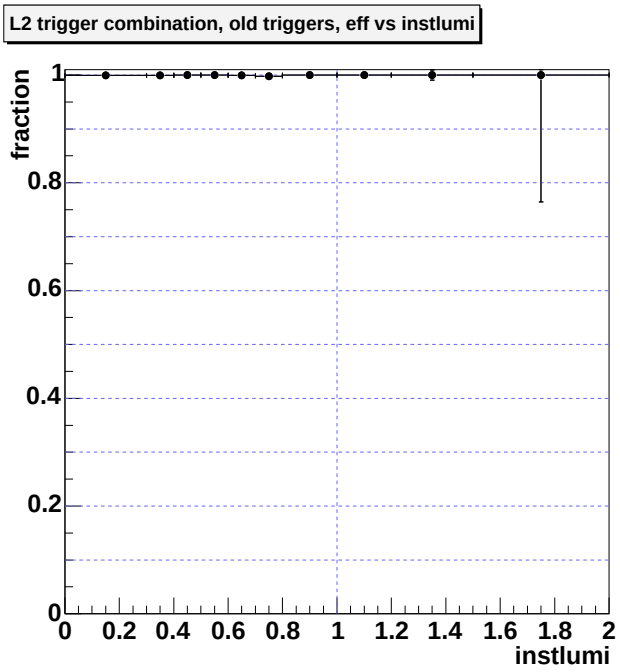

Figure 45: Electron trigger efficiency at L2 for all CMT 8 to 11 triggers as a function of instantaneous luminosity($10^{30} cm^{-2} s^{-1}$) for all probes.

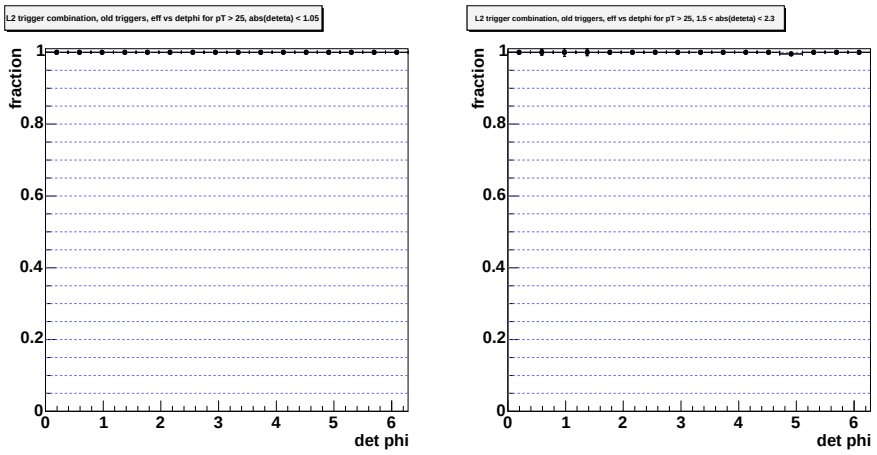

Figure 46: Electron trigger efficiency at L2 for all CMT 8 to 11 triggers as a function of detector ϕ for CC(left) and EC(right).

2.2.3 All Triggers Combined for CMT 8 to 11: L3

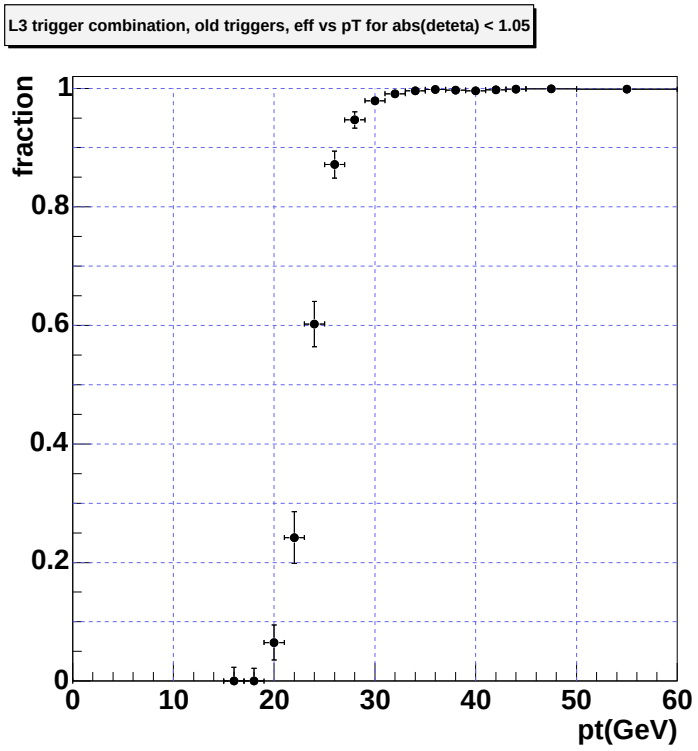

Figure 47: Electron trigger efficiency at L3 for all CMT 8 to 11 triggers as a function of E_T for CC.

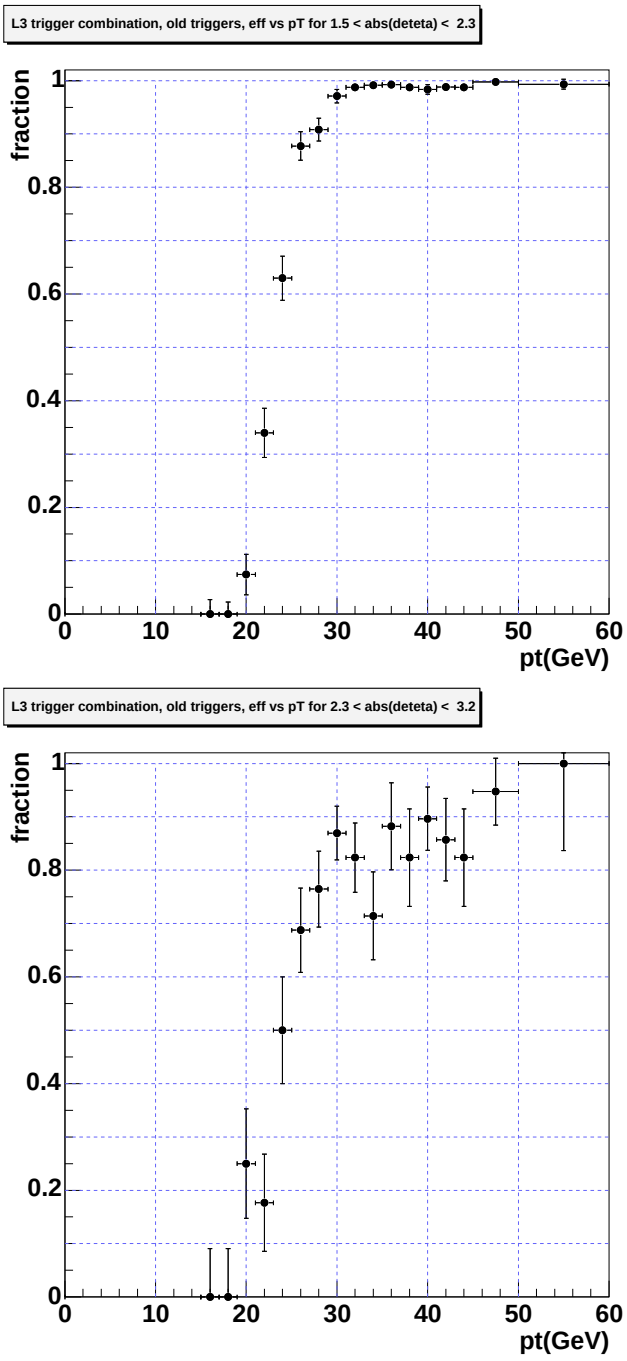

Figure 48: Electron trigger efficiency at L3 for all CMT 8 to 11 triggers as a function of E_T for EC(top) and extended EC($2.3 < |\eta_{detector}| < 3.2$) (bottom).

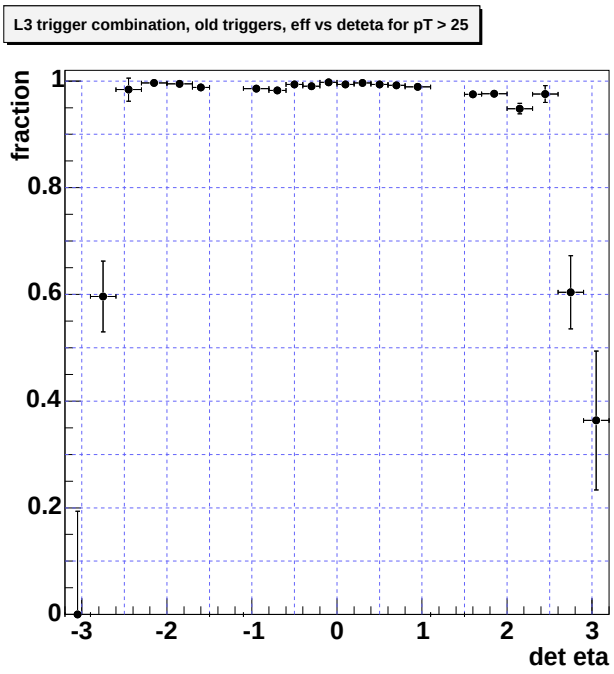

Figure 49: Electron trigger efficiency at L3 for all CMT 8 to 11 triggers as a function of detector η.

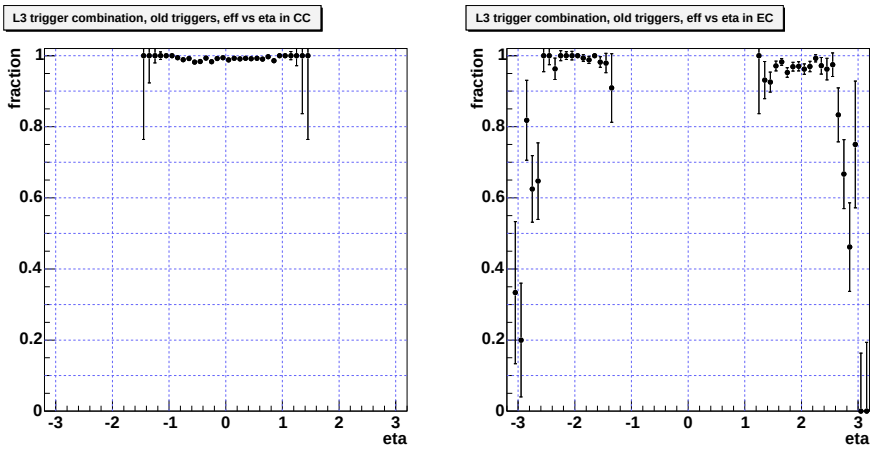

Figure 50: Electron trigger efficiency at L3 for all CMT 8 to 11 triggers as a function of physics η for CC(left) and EC(right).

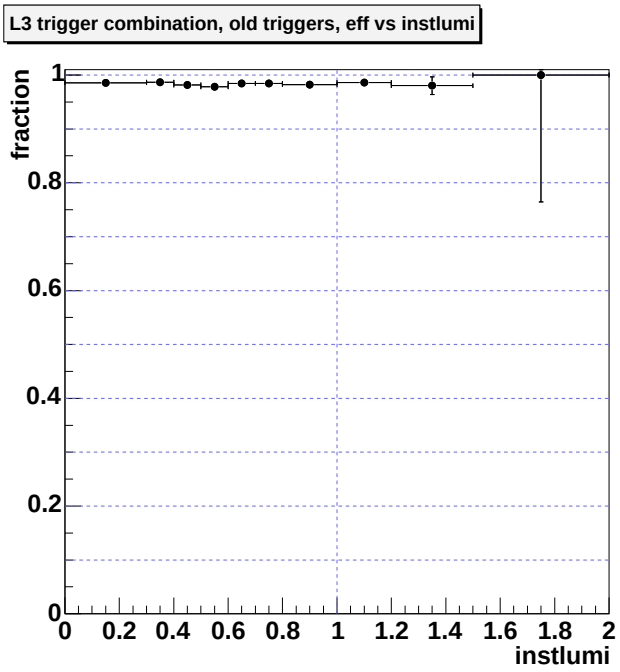

Figure 51: Electron trigger efficiency at L3 for all CMT 8 to 11 triggers as a function of instantaneous luminosity($10^{30} cm^{-2} s^{-1}$) for all probes.

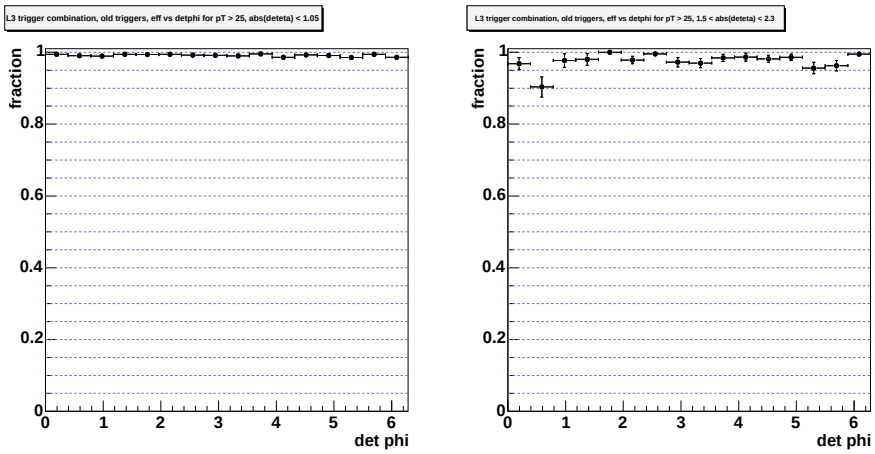

Figure 52: Electron trigger efficiency at L3 for all CMT 8 to 11 triggers as a function of detector ϕ for CC(left) and EC(right).

2.3 All Triggers Combined for CMT 12

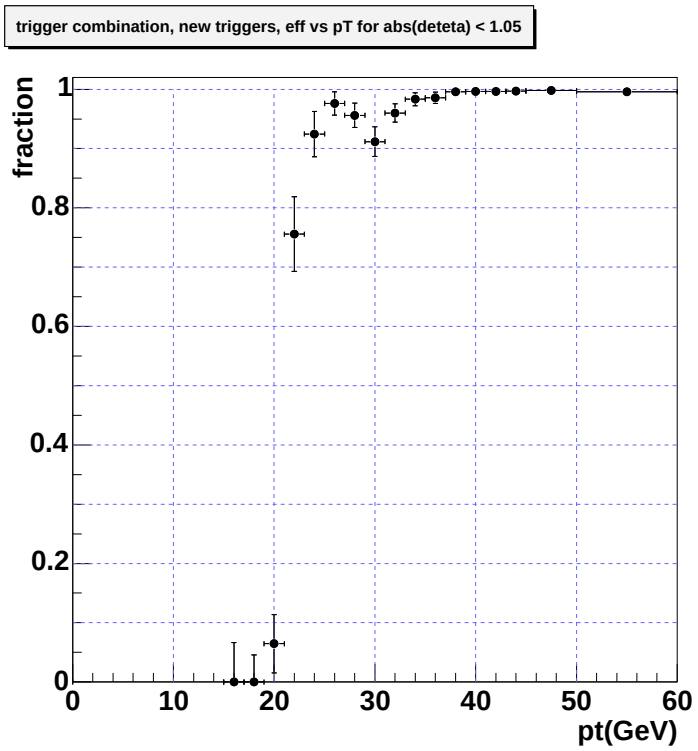

Figure 53: Electron trigger efficiency for all CMT 12 triggers as a function of E_T for CC.

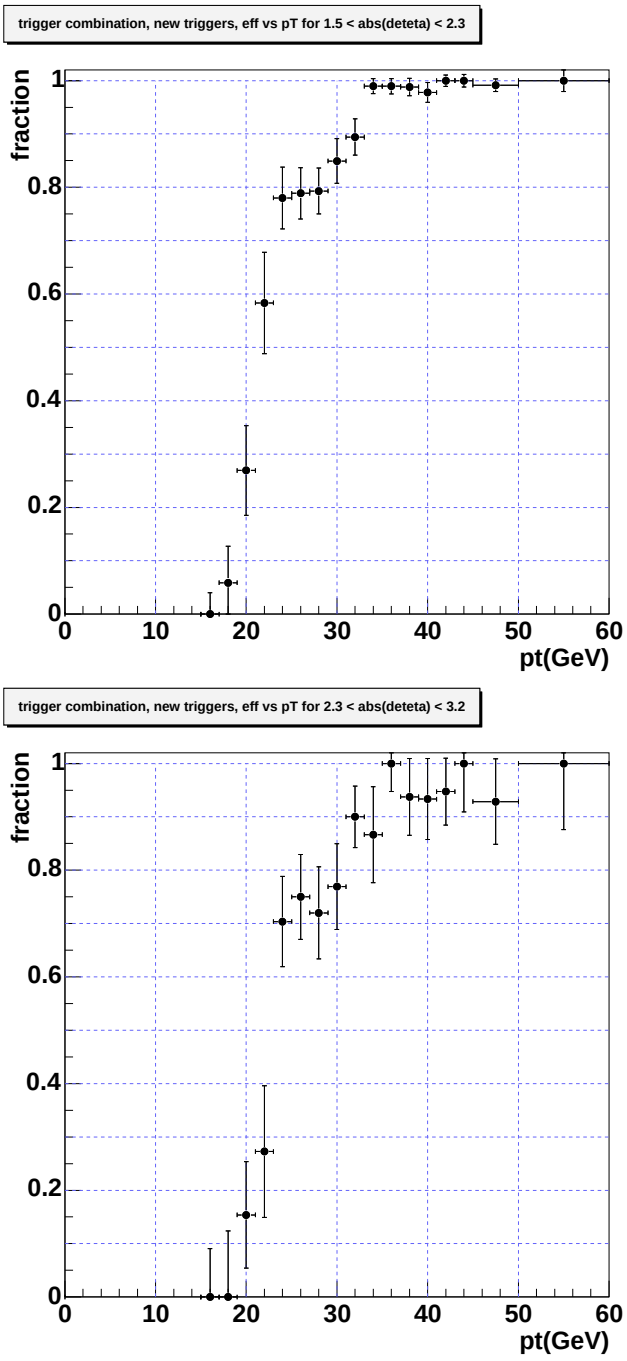

Figure 54: Electron trigger efficiency for all CMT 12 triggers as a function of E_T for EC(top) and extended EC($2.3 < |\eta_{detector}| < 3.2$) (bottom).

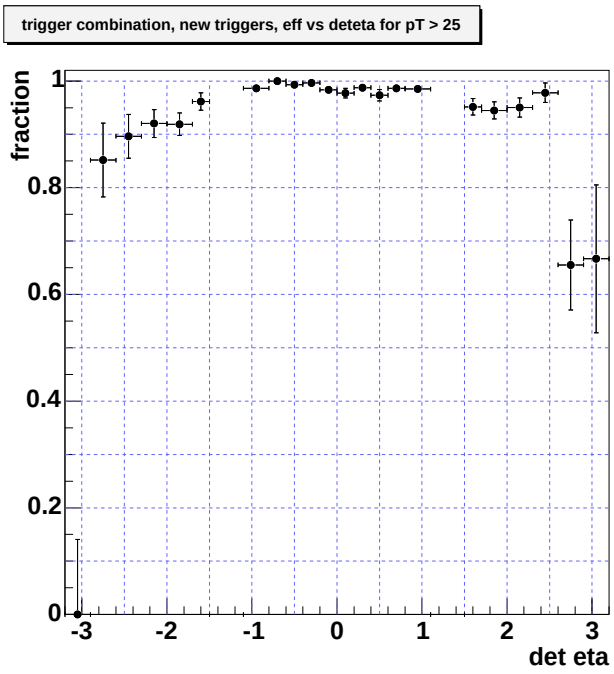

Figure 55: Electron trigger efficiency for all CMT 12 triggers as a function of detector η.

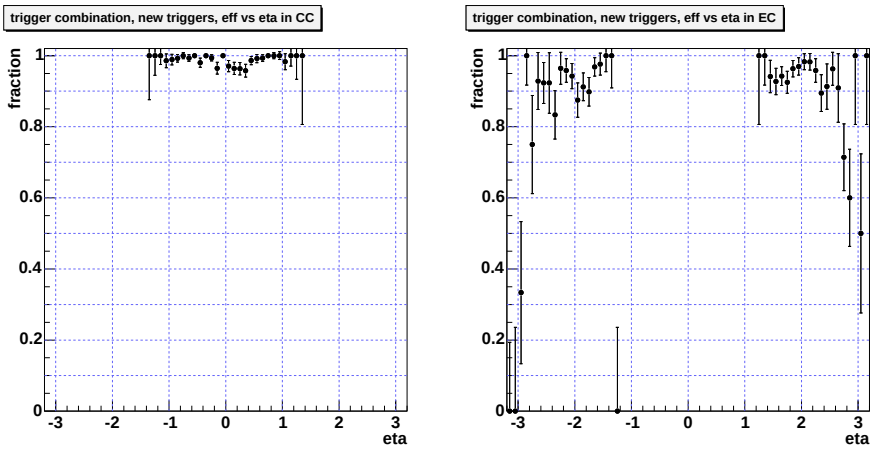

Figure 56: Electron trigger efficiency for all CMT 12 triggers as a function of physics η for CC(left) and EC(right).

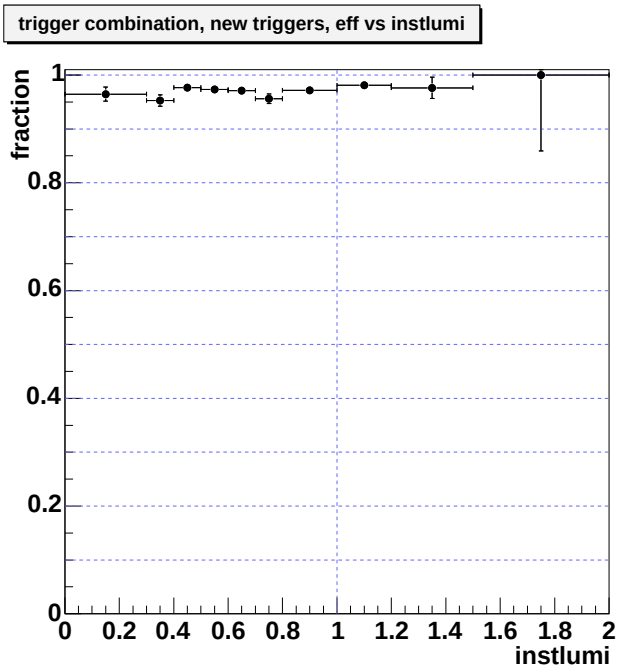

Figure 57: Electron trigger efficiency for all CMT 12 triggers as a function of instantaneous luminosity($10^{30} cm^{-2} s^{-1}$) for all probes.

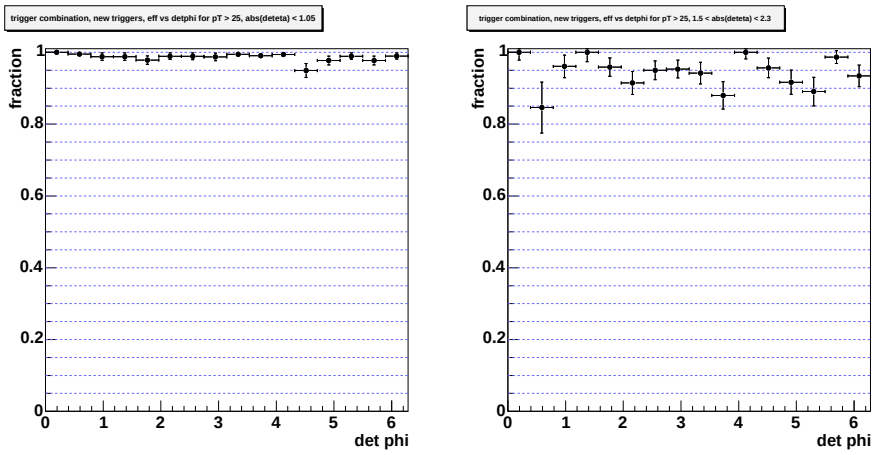

Figure 58: Electron trigger efficiency for all CMT 12 triggers as a function of detector ϕ for CC(left) and EC(right).

2.3.1 All Triggers Combined for CMT 12: L1

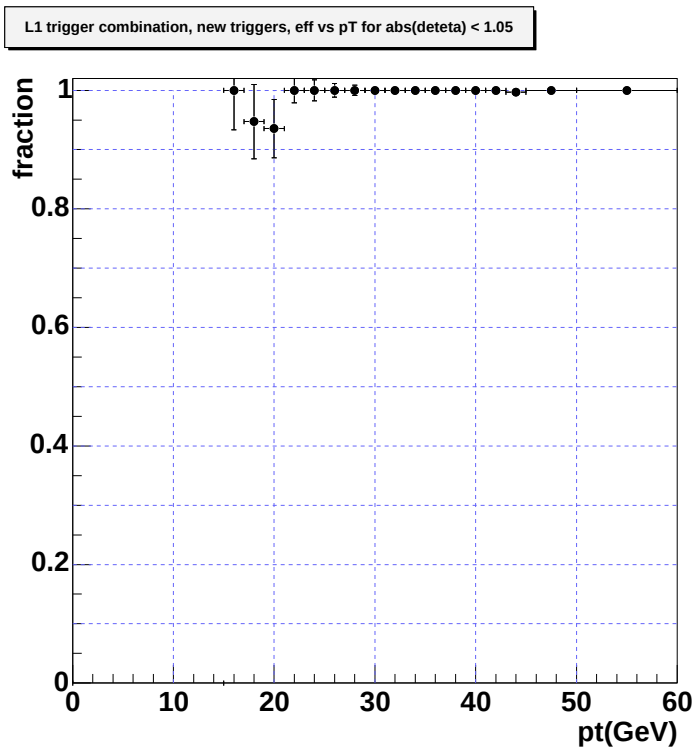

Figure 59: Electron trigger efficiency at L1 for all CMT 12 triggers as a function of E_T for CC.

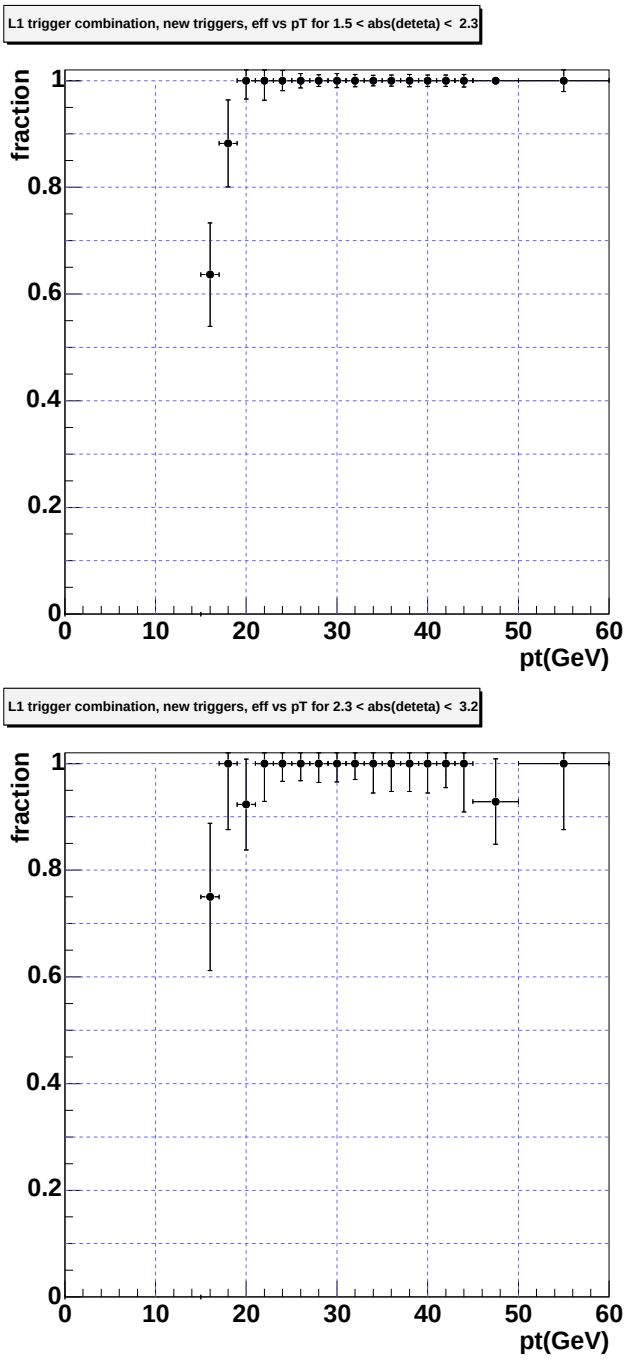

Figure 60: Electron trigger efficiency at L1 for all CMT 12 triggers as a function of E_T for EC(top) and extended EC($2.3 < |\eta_{detector}| < 3.2$) (bottom).

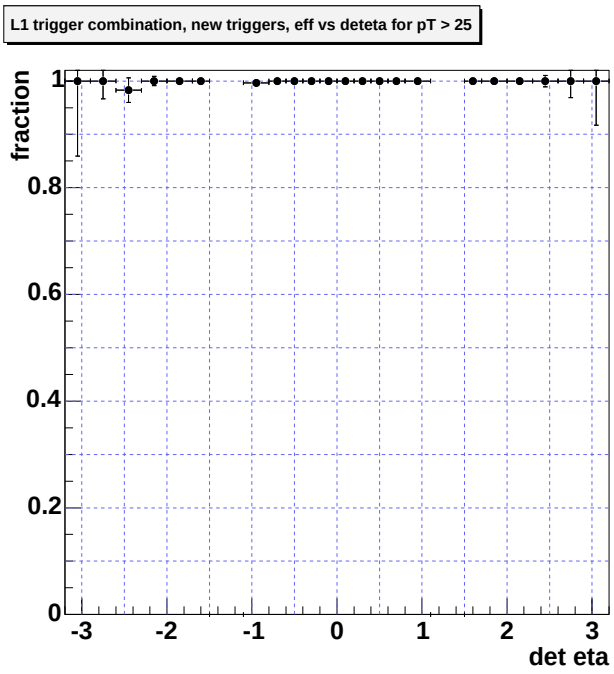

Figure 61: Electron trigger efficiency at L1 for all CMT 12 triggers as a function of detector η.

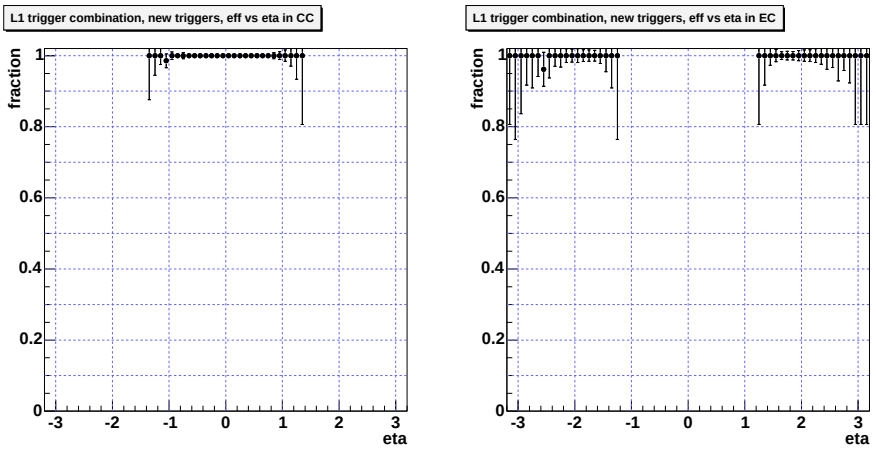

Figure 62: Electron trigger efficiency at L1 for all CMT 12 triggers as a function of physics η for CC(left) and EC(right).

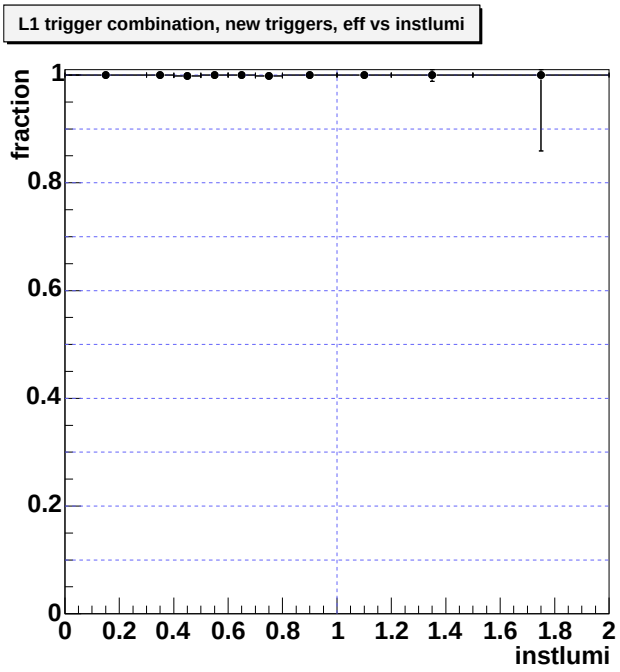

Figure 63: Electron trigger efficiency at L1 for all CMT 12 triggers as a function of instantaneous luminosity($10^{30} cm^{-2} s^{-1}$) for all probes.

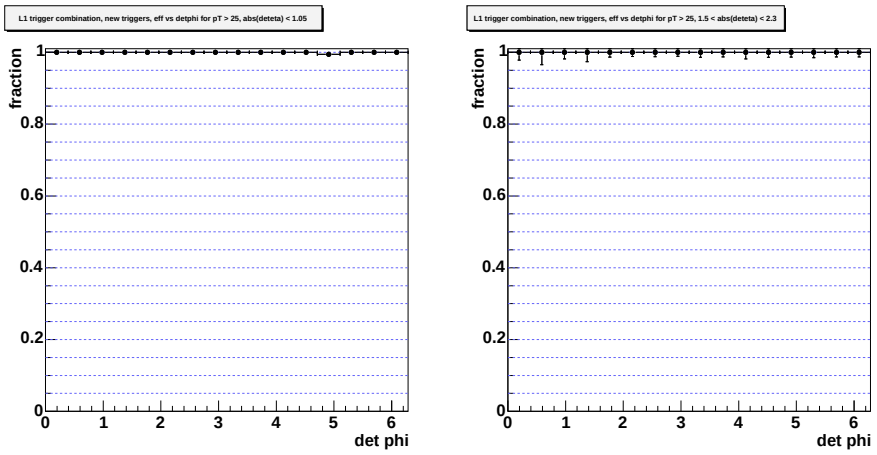

Figure 64: Electron trigger efficiency at L1 for all CMT 12 triggers as a function of detector ϕ for CC(left) and EC(right).

2.3.2 All Triggers Combined for CMT 12: L3

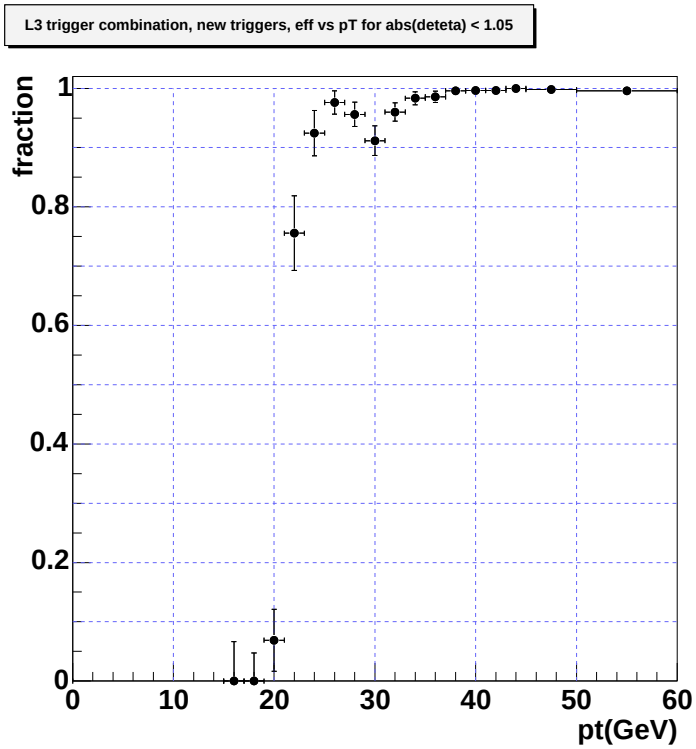

Figure 65: Electron trigger efficiency at L3 for all CMT 12 triggers as a function of E_T for CC.

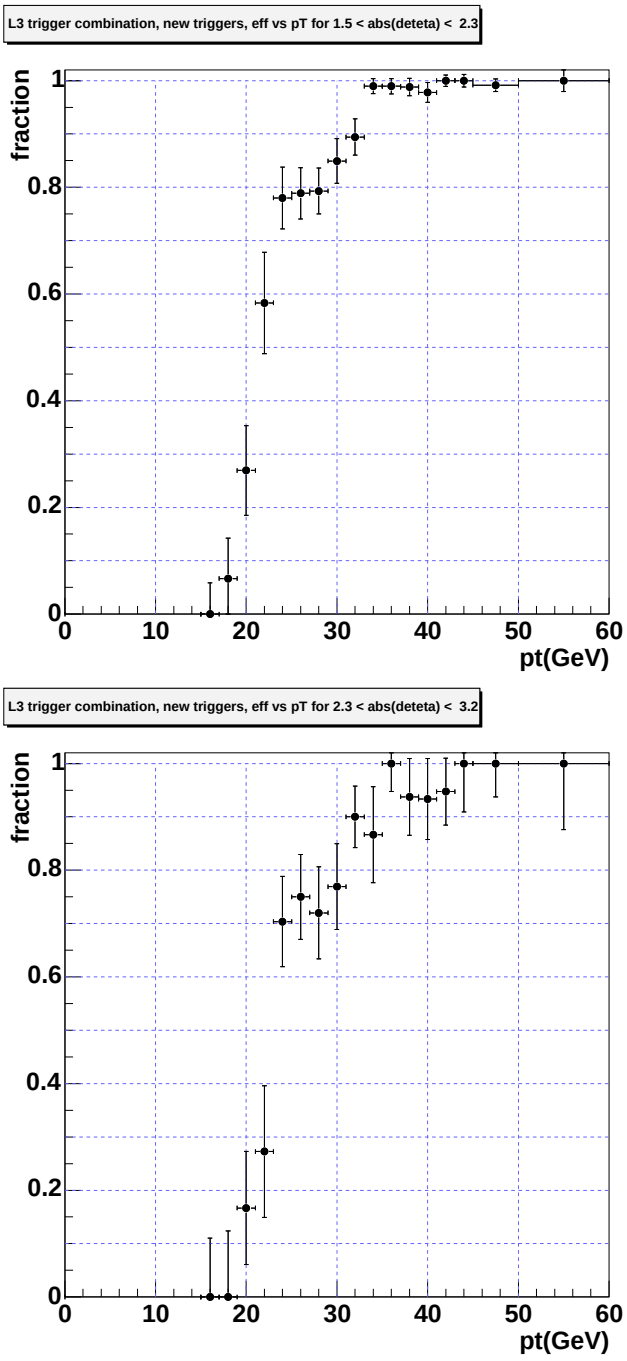

Figure 66: Electron trigger efficiency at L3 for all CMT 12 triggers as a function of E_T for EC(top) and extended EC($2.3 < |\eta_{detector}| < 3.2$) (bottom).

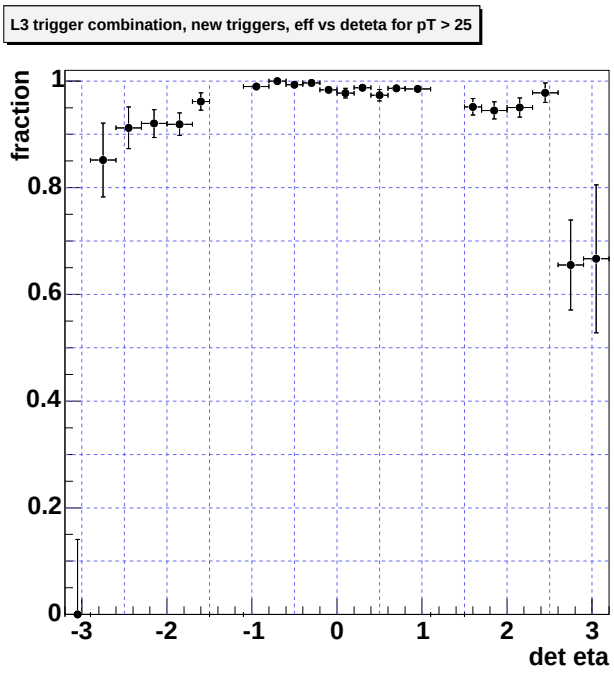

Figure 67: Electron trigger efficiency at L3 for all CMT 12 triggers as a function of detector η.

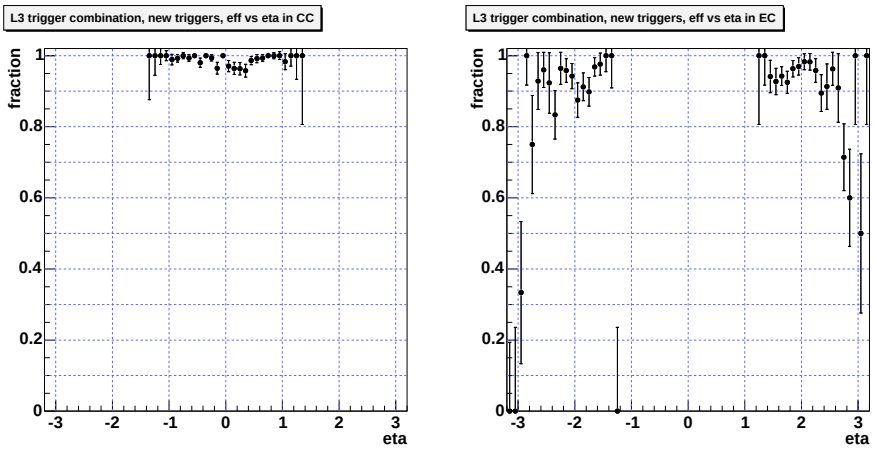

Figure 68: Electron trigger efficiency at L3 for all CMT 12 triggers as a function of physics η for CC(left) and EC(right).

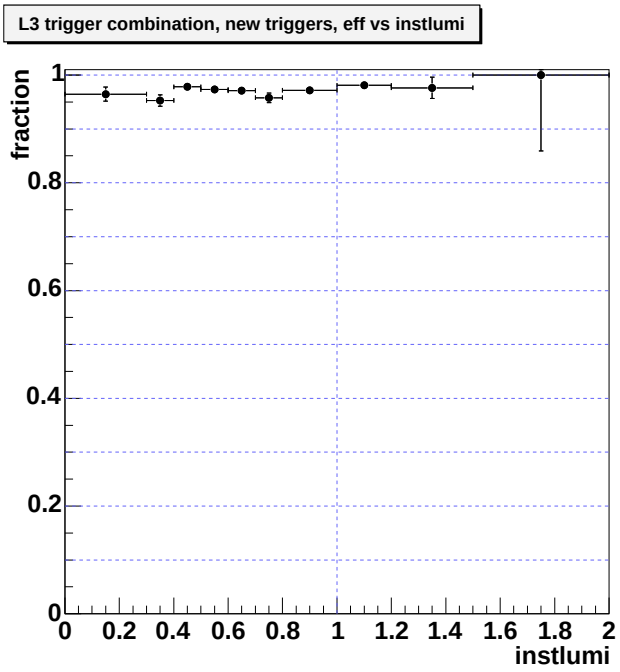

Figure 69: Electron trigger efficiency at L3 for all CMT 12 triggers as a function of instantaneous luminosity($10^{30} cm^{-2} s^{-1}$) for all probes.

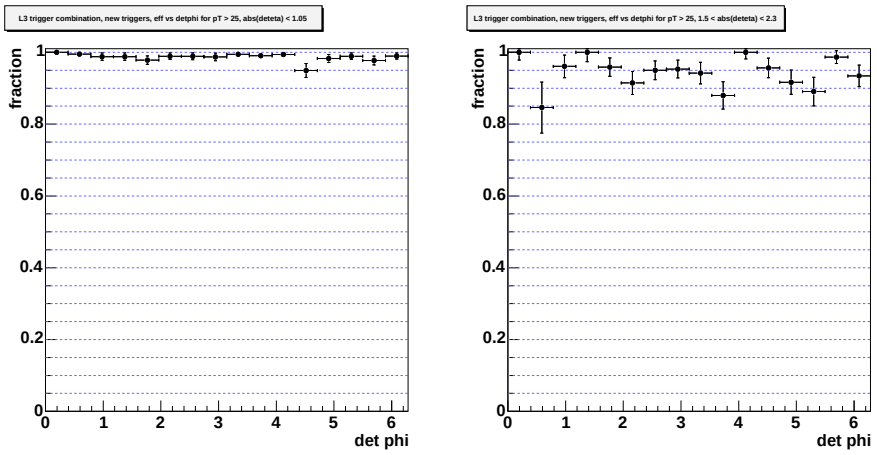

Figure 70: Electron trigger efficiency at L3 for all CMT 12 triggers as a function of detector ϕ for CC(left) and EC(right).

2.4 EM_HI_SH

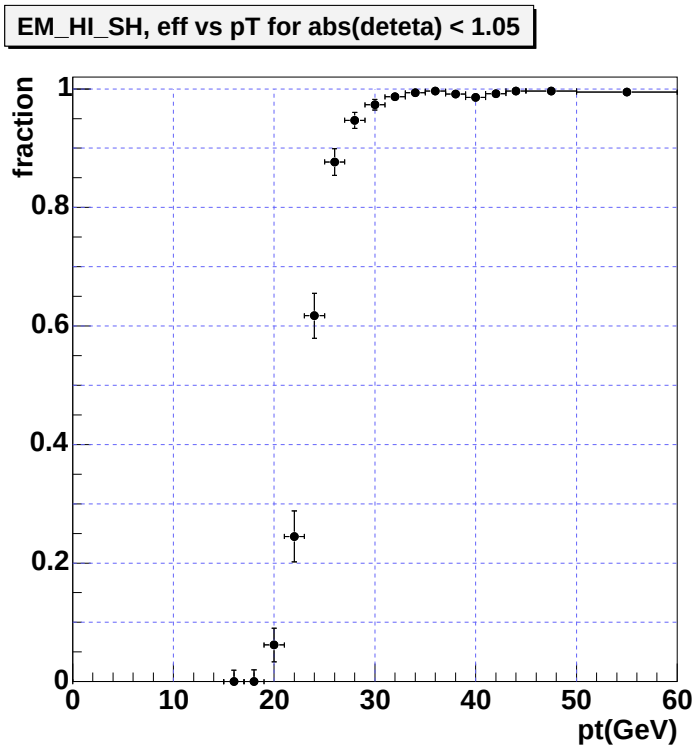

Figure 71: Electron trigger efficiency for EM_HI_SH as a function of E_T for CC.

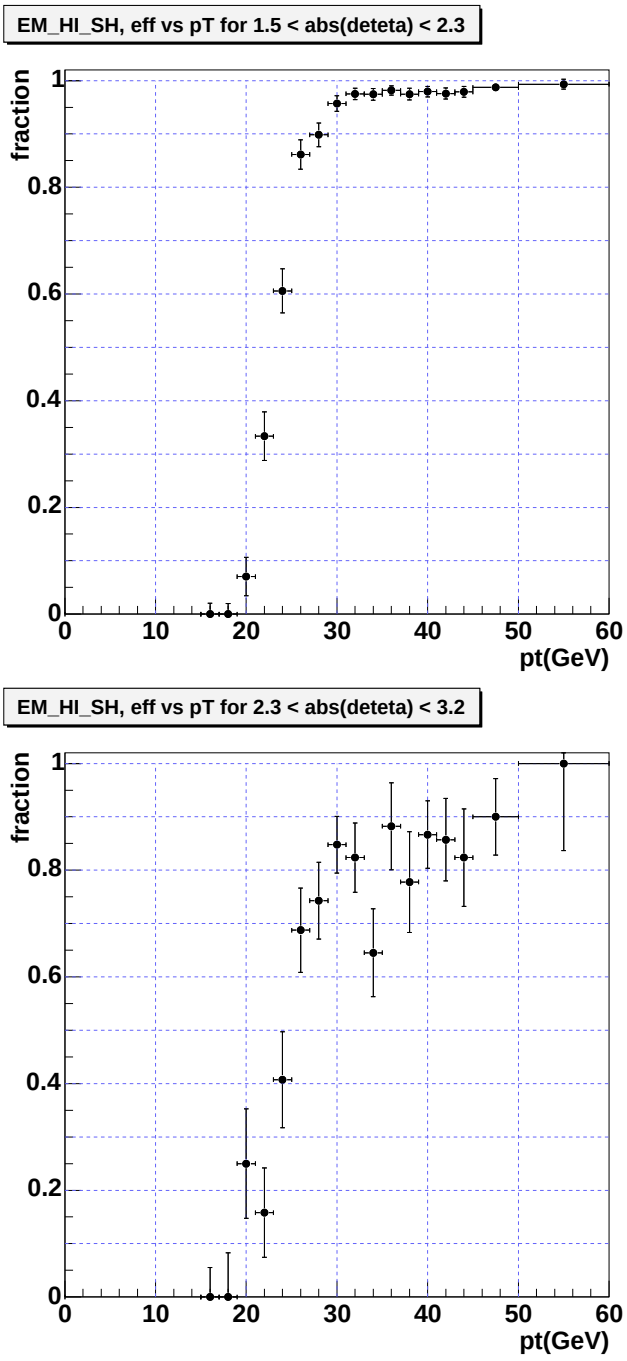

Figure 72: Electron trigger efficiency for EM_HI_SH as a function of E_T for EC(top) and extended EC($2.3 < |\eta_{detector}| < 3.2$) (bottom).

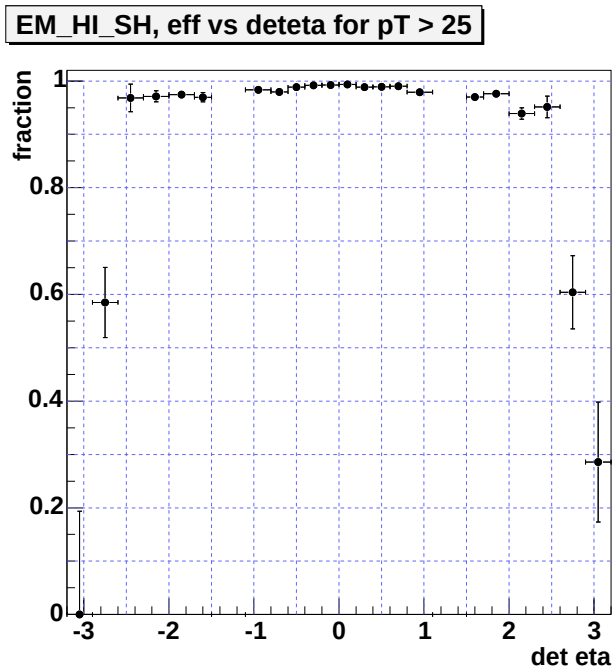

Figure 73: Electron trigger efficiency for EM_HI_SH as a function of detector η.

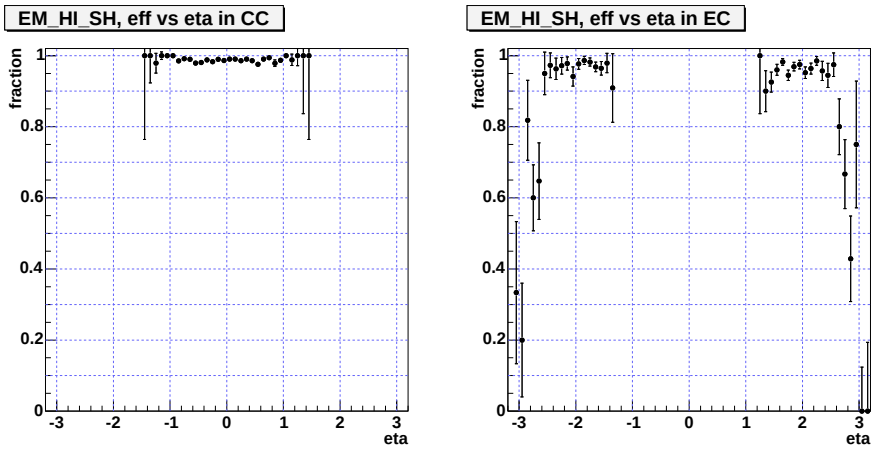

Figure 74: Electron trigger efficiency for EM_HI_SH as a function of physics η for CC(left) and EC(right).

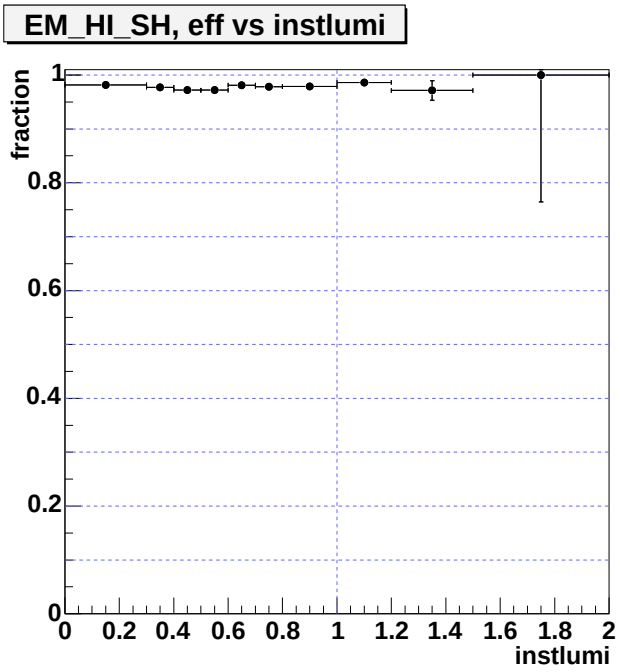

Figure 75: Electron trigger efficiency for EM_HI_SH as a function of instantaneous luminosity($10^{30} cm^{-2} s^{-1}$) for all probes.

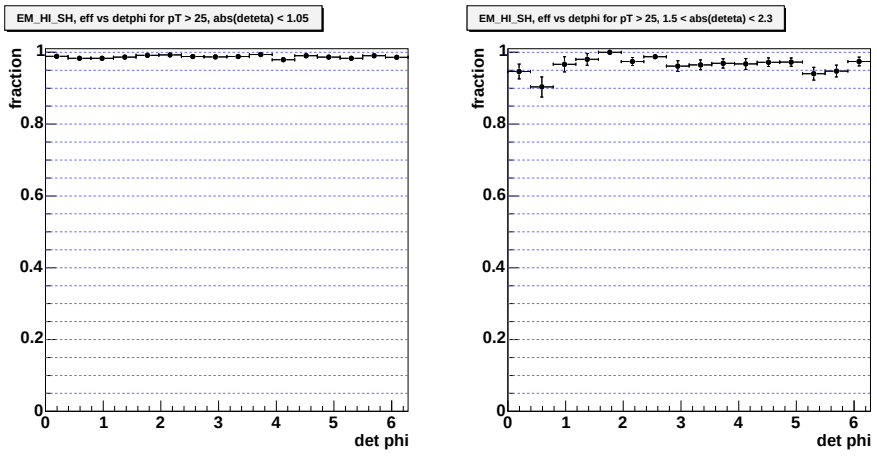

Figure 76: Electron trigger efficiency for EM_HI_SH as a function of detector ϕ for CC(left) and EC(right).

2.4.1 EM_HI_SH: L1

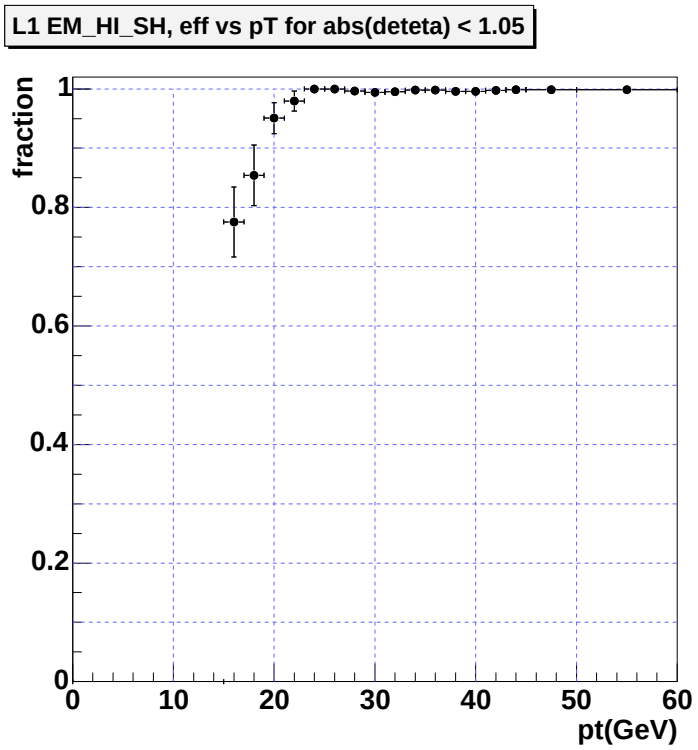

Figure 77: Electron trigger efficiency at L1 for EM_HI_SH as a function of E_T for CC.

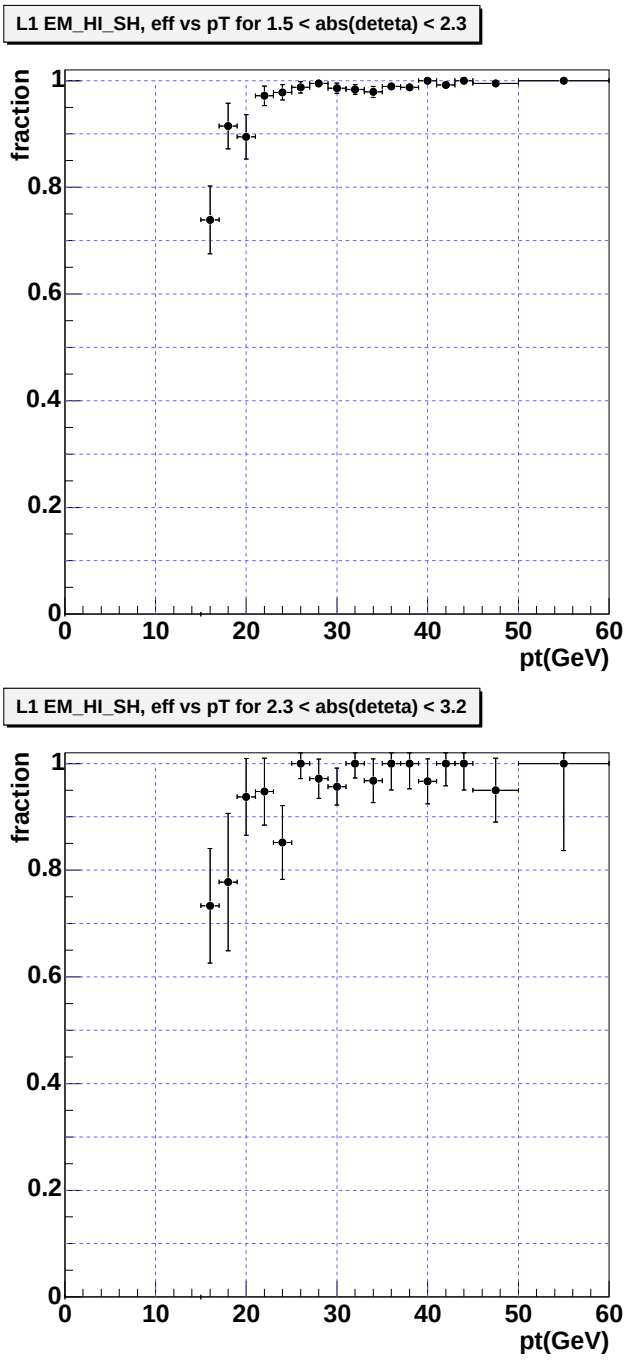

Figure 78: Electron trigger efficiency at L1 for EM_HI_SH as a function of E_T for EC(top) and extended EC($2.3 < |\eta_{detector}| < 3.2$) (bottom).

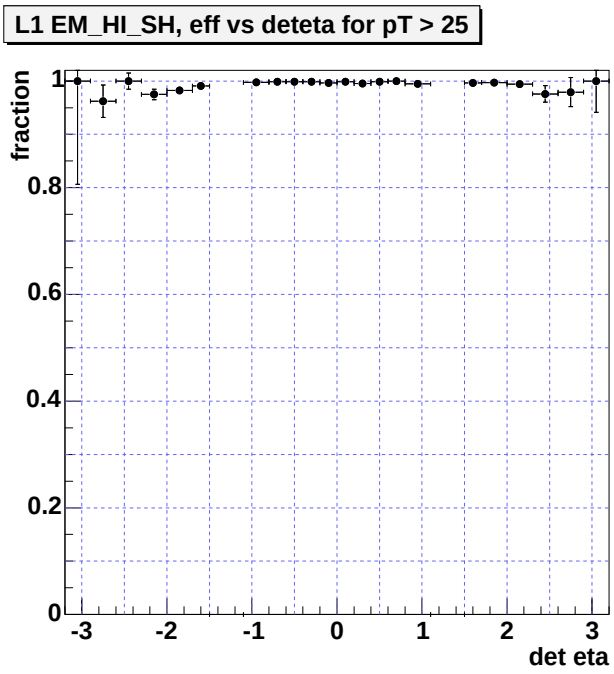

Figure 79: Electron trigger efficiency at L1 for EM_HI_SH as a function of detector η.

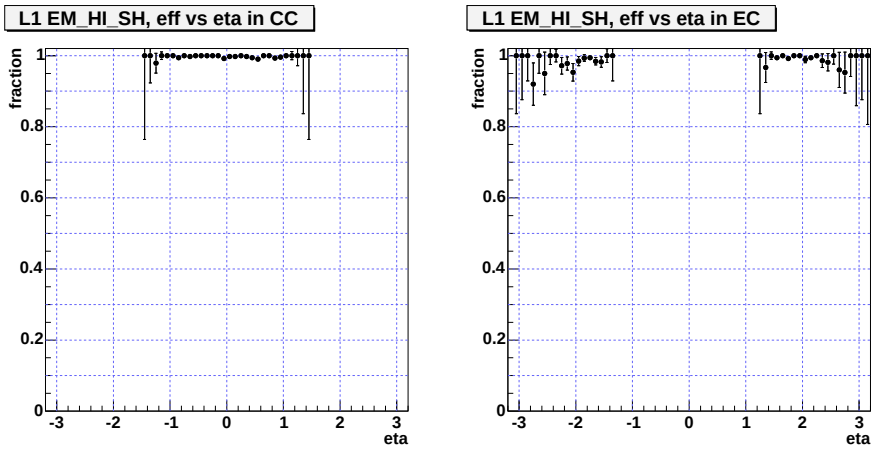

Figure 80: Electron trigger efficiency at L1 for EM_HI_SH as a function of physics η for CC(left) and EC(right).

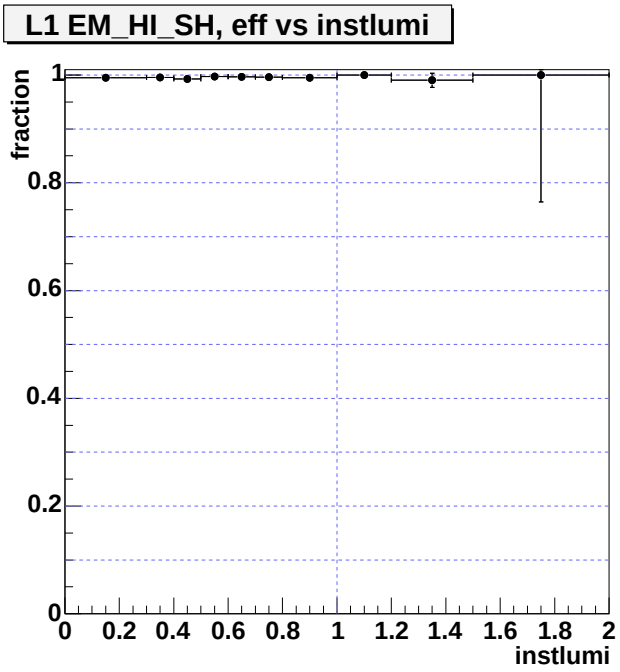

Figure 81: Electron trigger efficiency at L1 for EM_HI_SH as a function of instantaneous luminosity($10^{30} cm^{-2} s^{-1}$) for all probes.

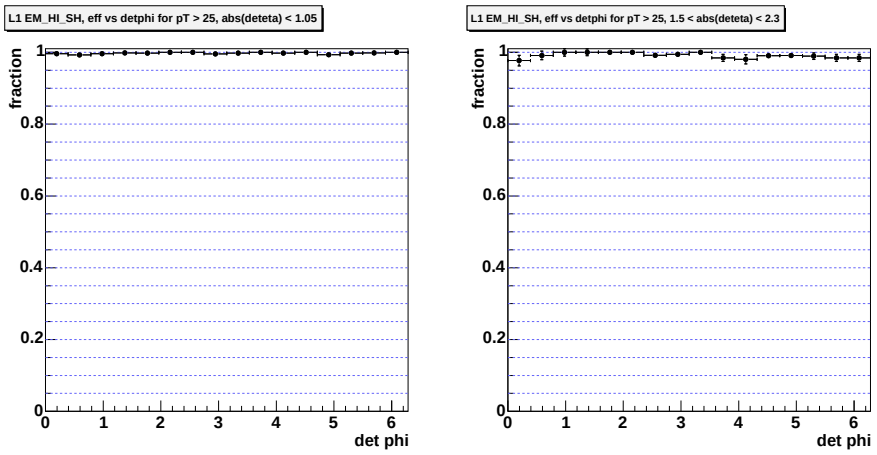

Figure 82: Electron trigger efficiency at L1 for EM_HI_SH as a function of detector ϕ for CC(left) and EC(right).

2.4.2 EM_HI_SH: L2

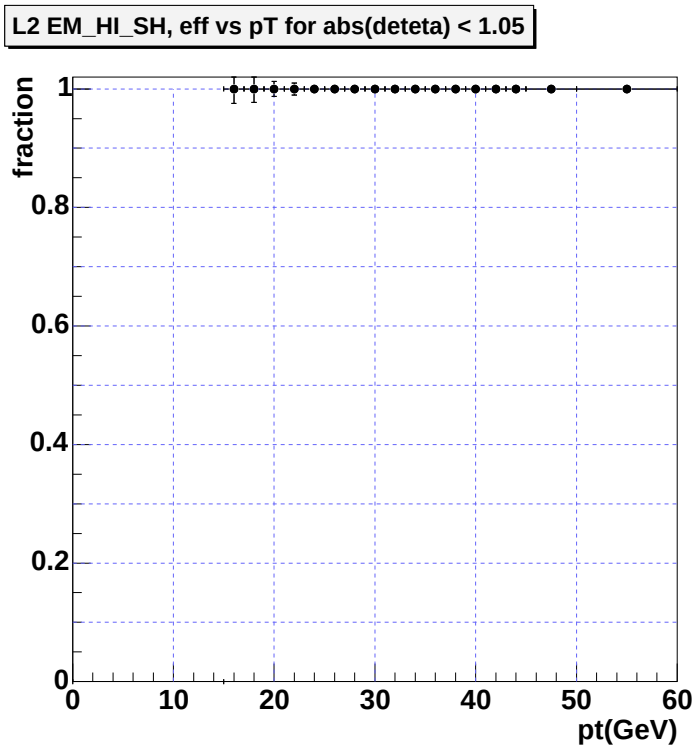

Figure 83: Electron trigger efficiency at L2 for EM_HI_SH as a function of E_T for CC.

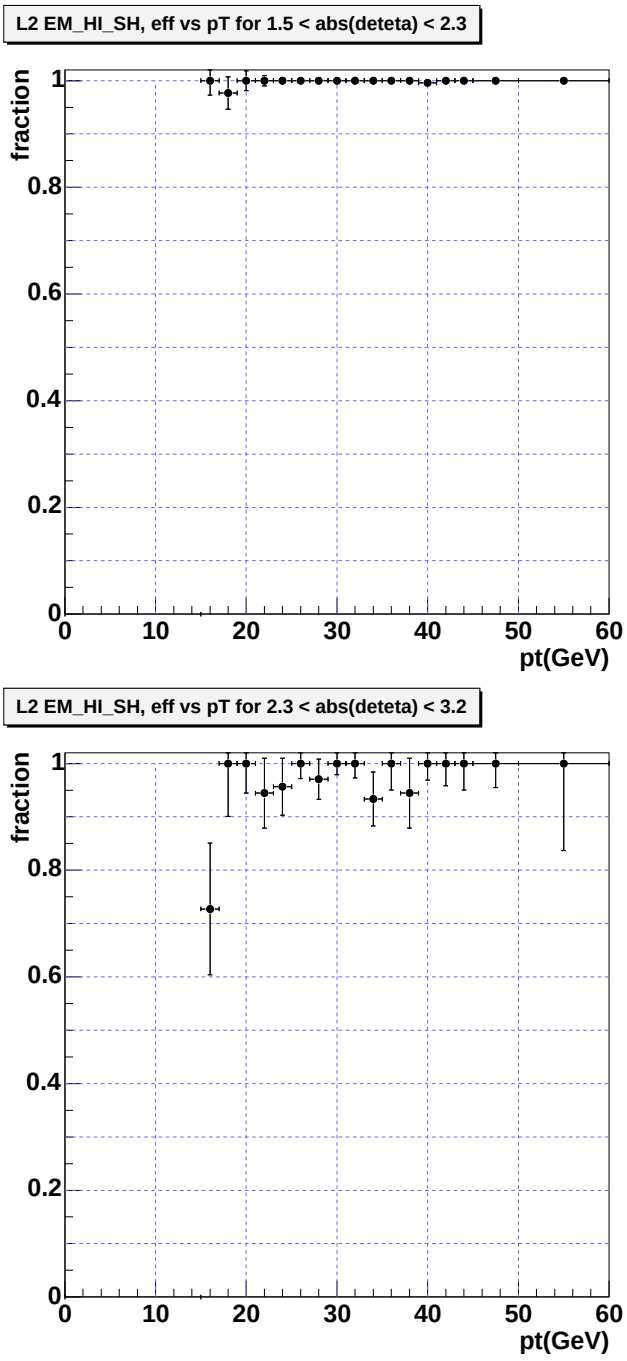

Figure 84: Electron trigger efficiency at L2 for EM_HI_SH as a function of E_T for EC(top) and extended EC($2.3 < |\eta_{detector}| < 3.2$) (bottom).

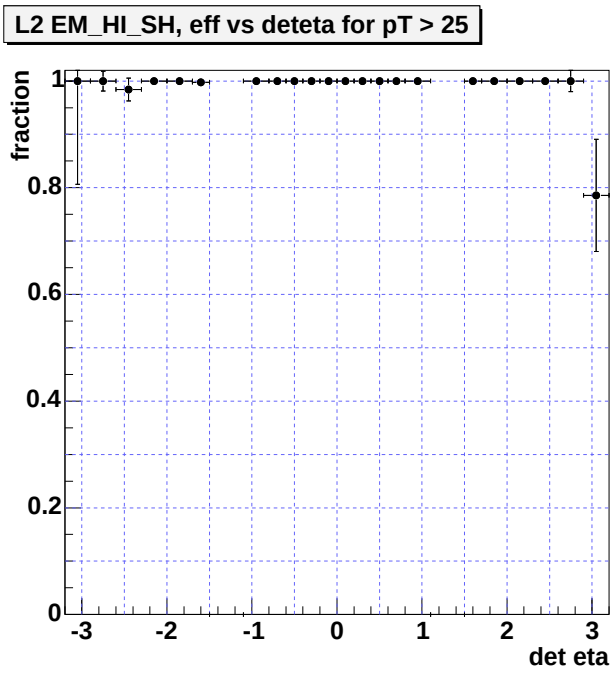

Figure 85: Electron trigger efficiency at L2 for EM_HI_SH as a function of detector η.

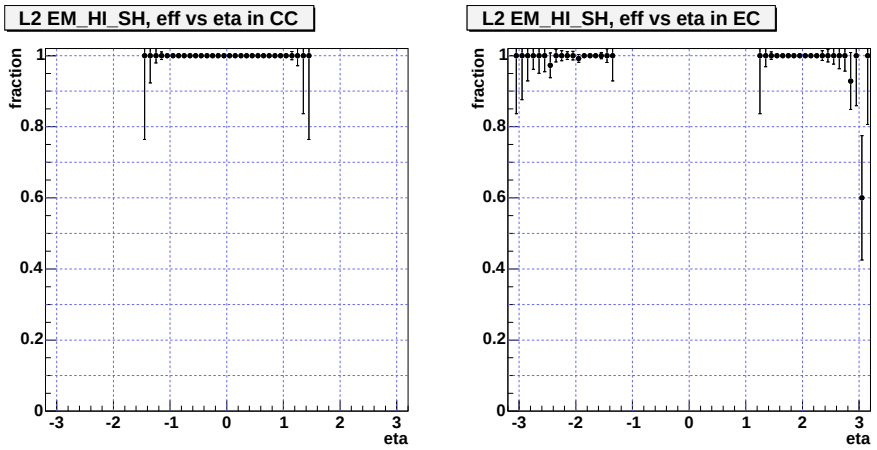

Figure 86: Electron trigger efficiency at L2 for EM_HI_SH as a function of physics η for CC(left) and EC(right).

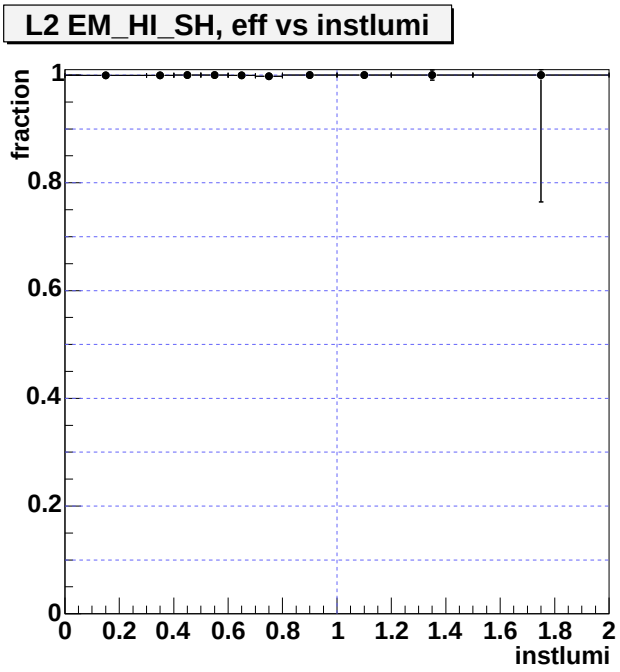

Figure 87: Electron trigger efficiency at L2 for EM_HI_SH as a function of instantaneous luminosity($10^{30} cm^{-2} s^{-1}$) for all probes.

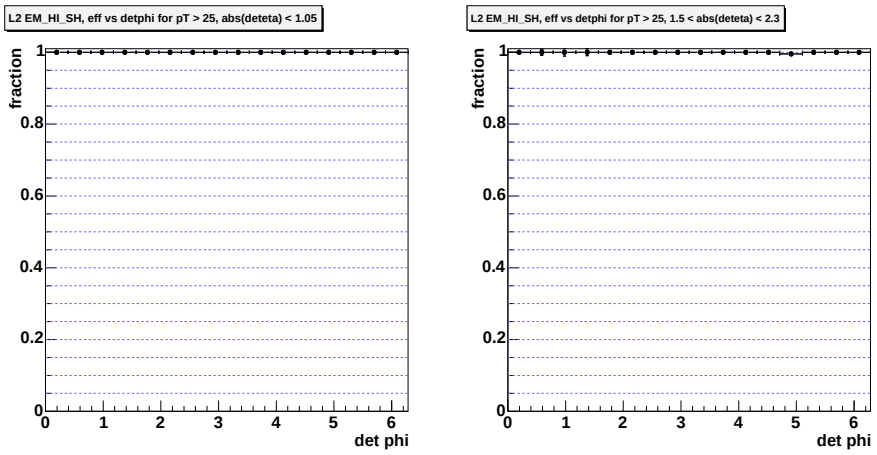

Figure 88: Electron trigger efficiency at L2 for EM_HI_SH as a function of detector ϕ for CC(left) and EC(right).

2.4.3 EM_HI_SH: L3

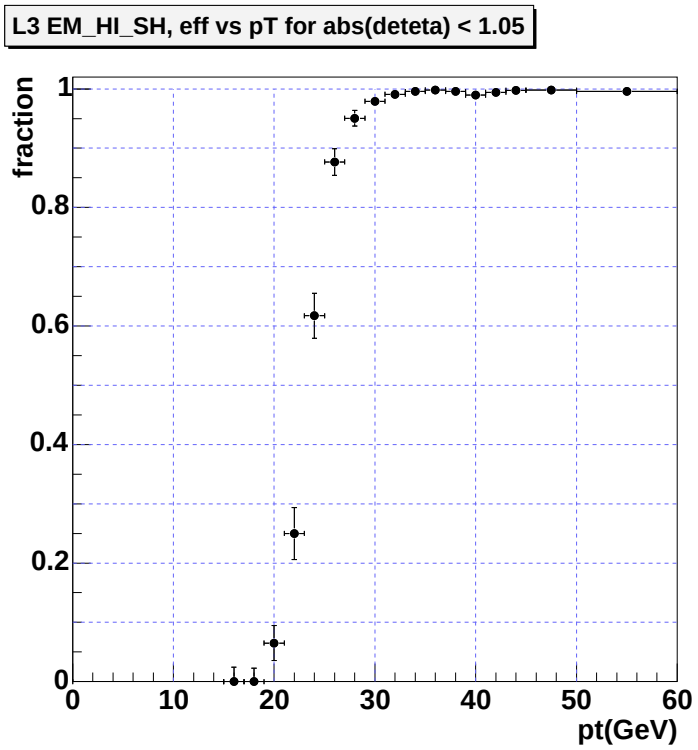

Figure 89: Electron trigger efficiency at L3 for EM_HI_SH as a function of E_T for CC.

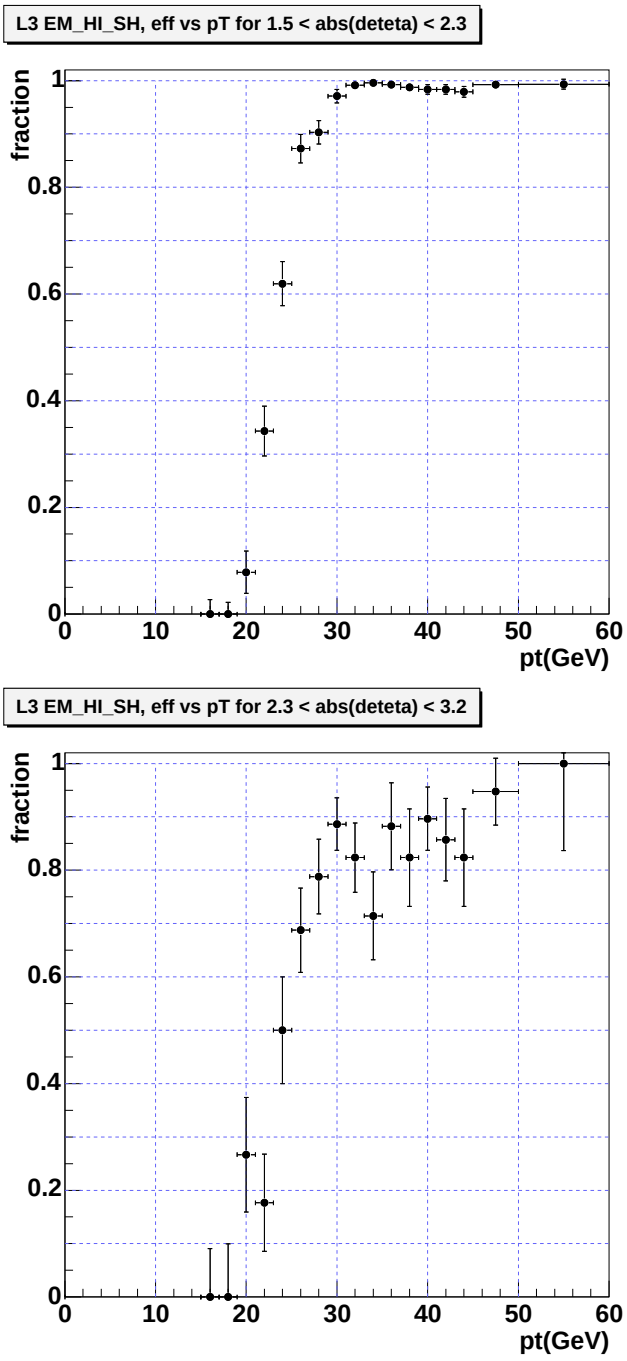

Figure 90: Electron trigger efficiency at L3 for EM_HI_SH as a function of E_T for EC(top) and extended EC($2.3 < |\eta_{detector}| < 3.2$) (bottom).

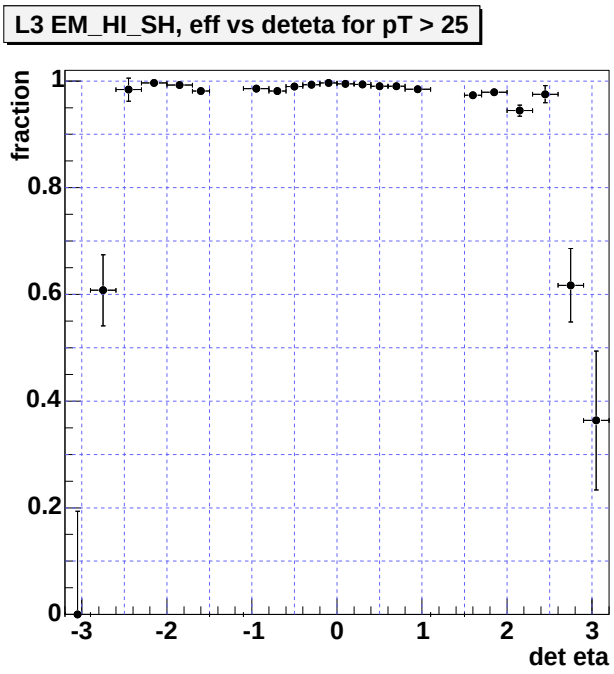

Figure 91: Electron trigger efficiency at L3 for EM_HI_SH as a function of detector η.

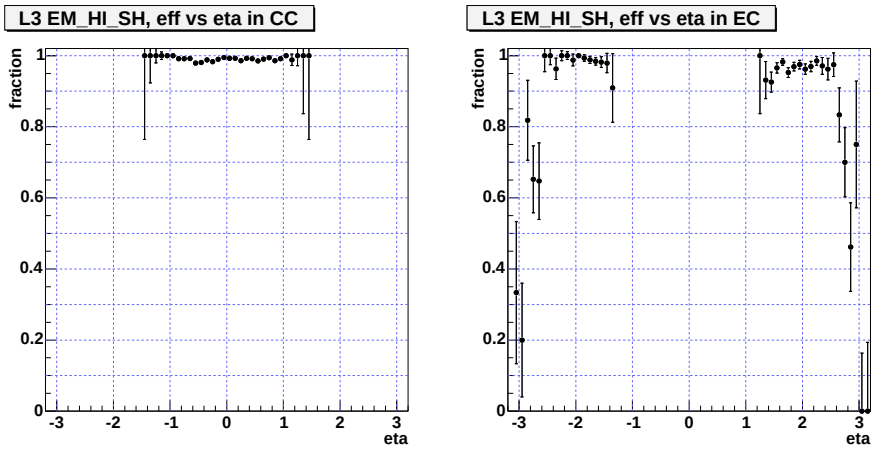

Figure 92: Electron trigger efficiency at L3 for EM_HI_SH as a function of physics η for CC(left) and EC(right).

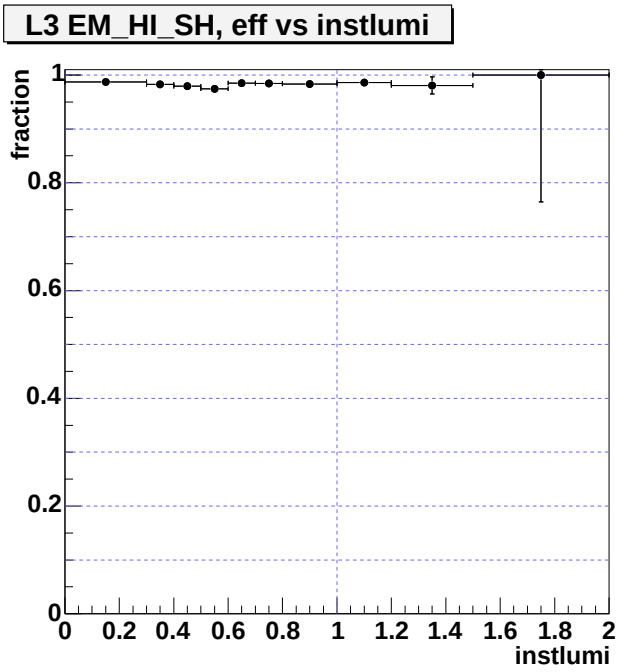

Figure 93: Electron trigger efficiency at L3 for EM_HI_SH as a function of instantaneous luminosity($10^{30} cm^{-2} s^{-1}$) for all probes.

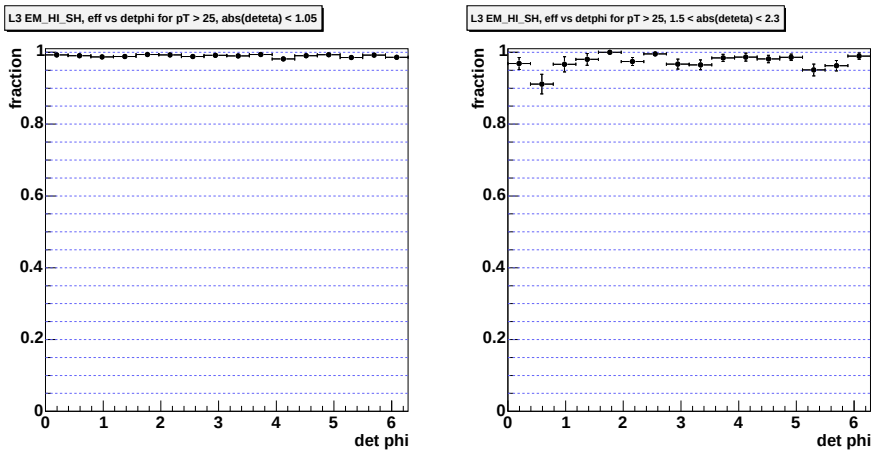

Figure 94: Electron trigger efficiency at L3 for EM_HI_SH as a function of detector ϕ for CC(left) and EC(right).

2.5 EM_HI_2EM5_SH

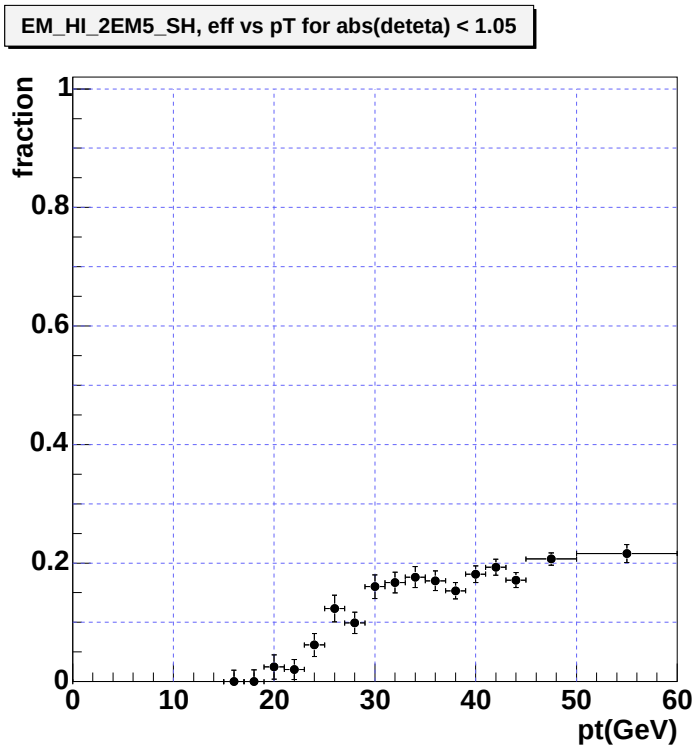

Figure 95: Electron trigger efficiency for EM_HI_2EM5_SH as a function of E_T for CC.

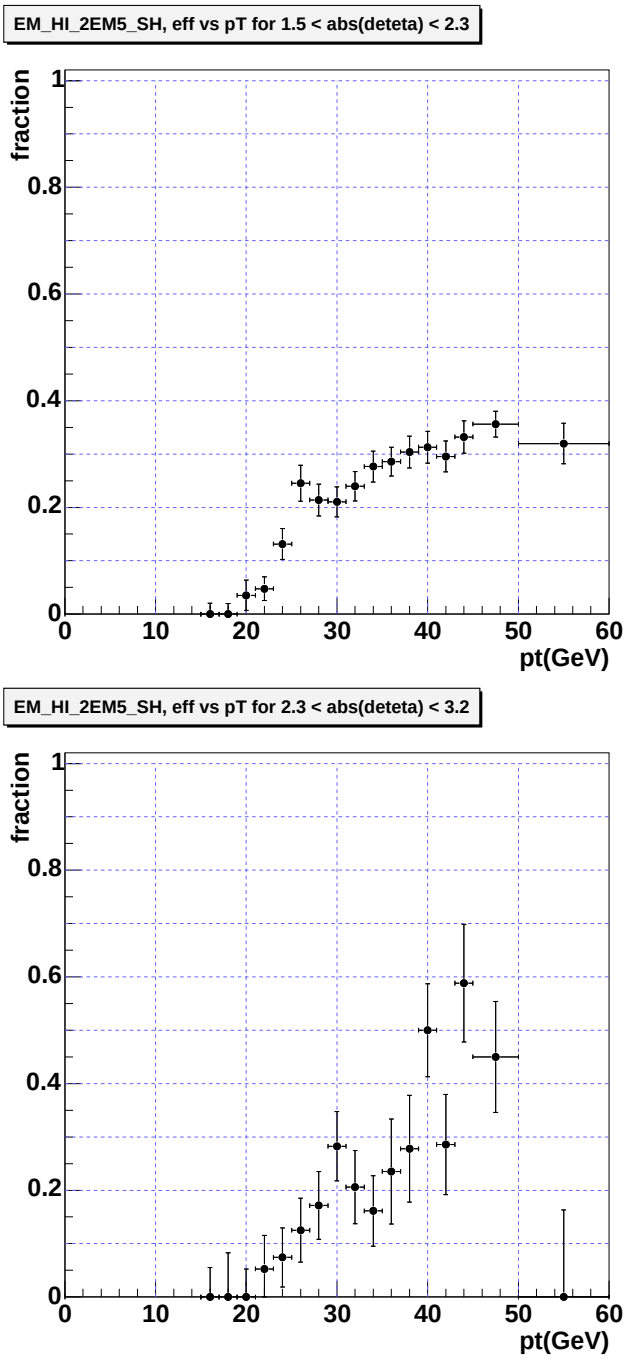

Figure 96: Electron trigger efficiency for EM_HI_2EM5_SH as a function of E_T for EC(top) and extended EC($2.3 < |\eta_{detector}| < 3.2$) (bottom).

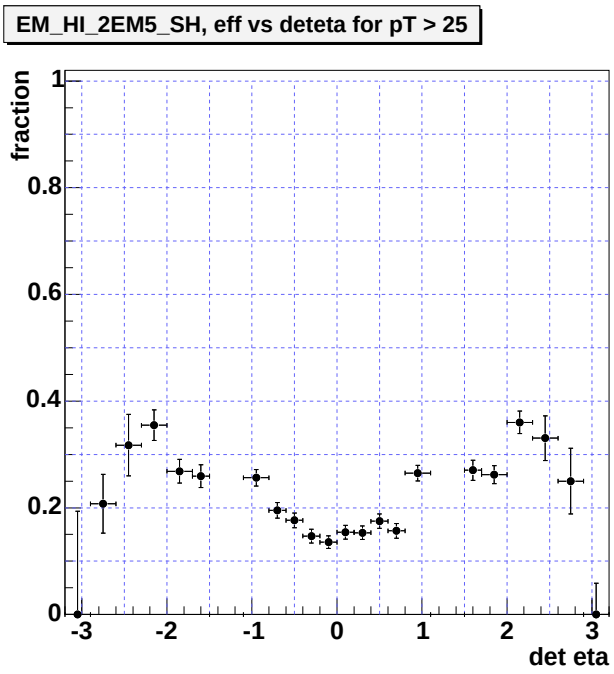

Figure 97: Electron trigger efficiency for EM_HI_2EM5_SH as a function of detector η.

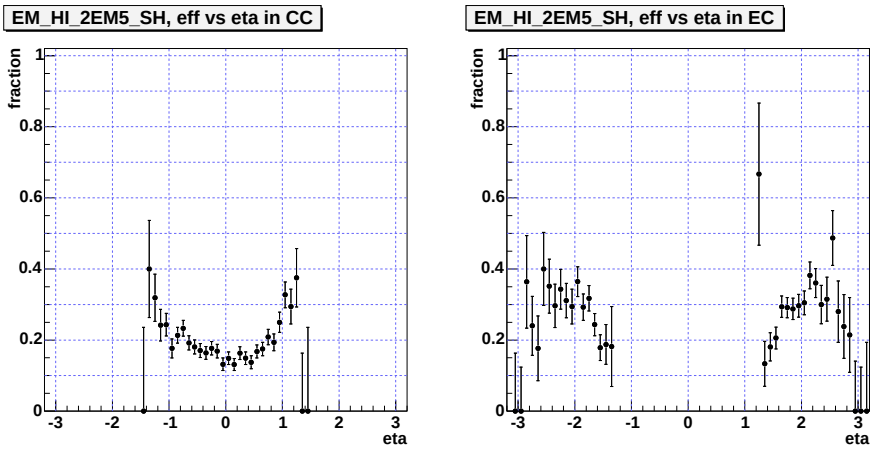

Figure 98: Electron trigger efficiency for EM_HI_2EM5_SH as a function of physics η for CC(left) and EC(right).

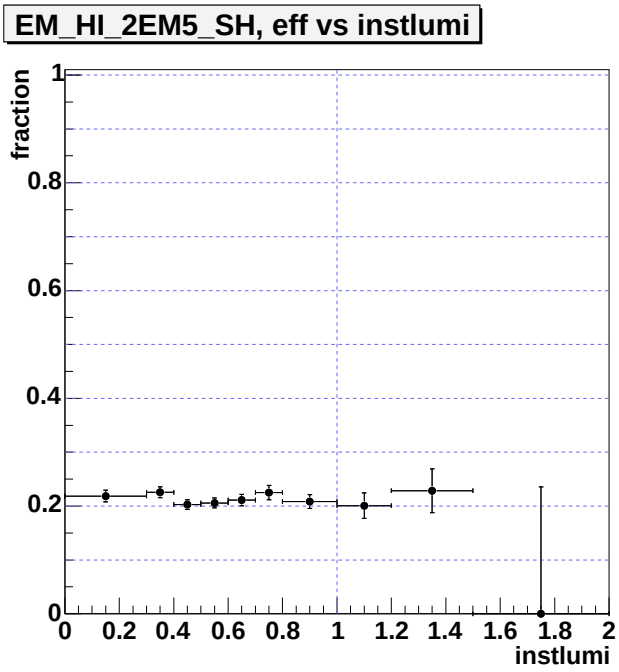

Figure 99: Electron trigger efficiency for EM_HI_2EM5_SH as a function of instantaneous luminosity($10^{30} cm^{-2} s^{-1}$) for all probes.

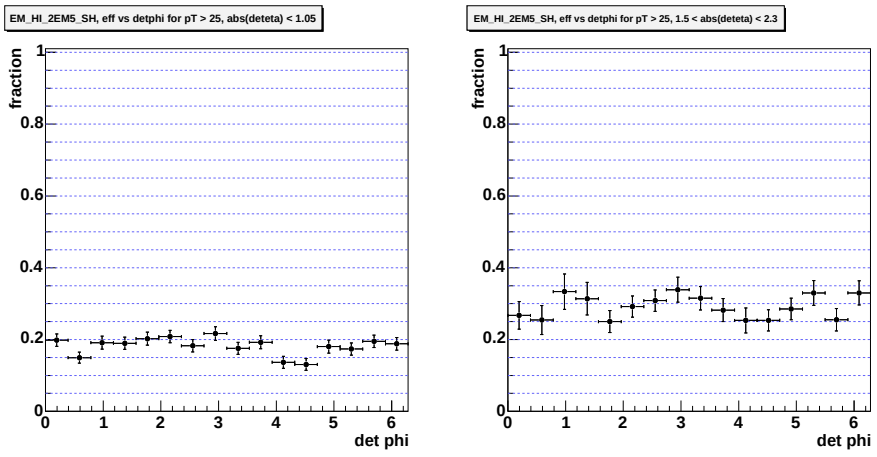

Figure 100: Electron trigger efficiency for EM_HI_2EM5_SH as a function of detector ϕ for CC(left) and EC(right).

2.5.1 EM_HI_2EM5_SH: L1

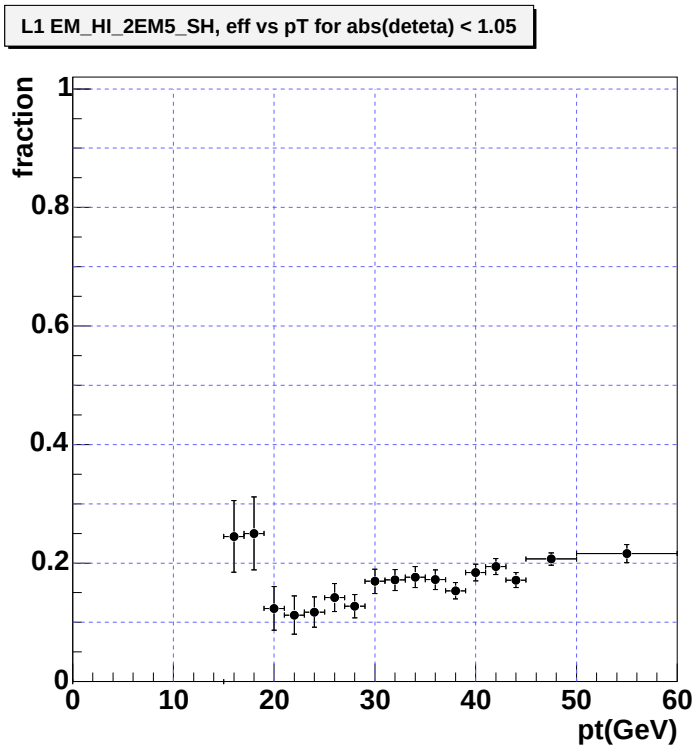

Figure 101: Electron trigger efficiency at L1 for EM_HI_2EM5_SH as a function of E_T for CC.

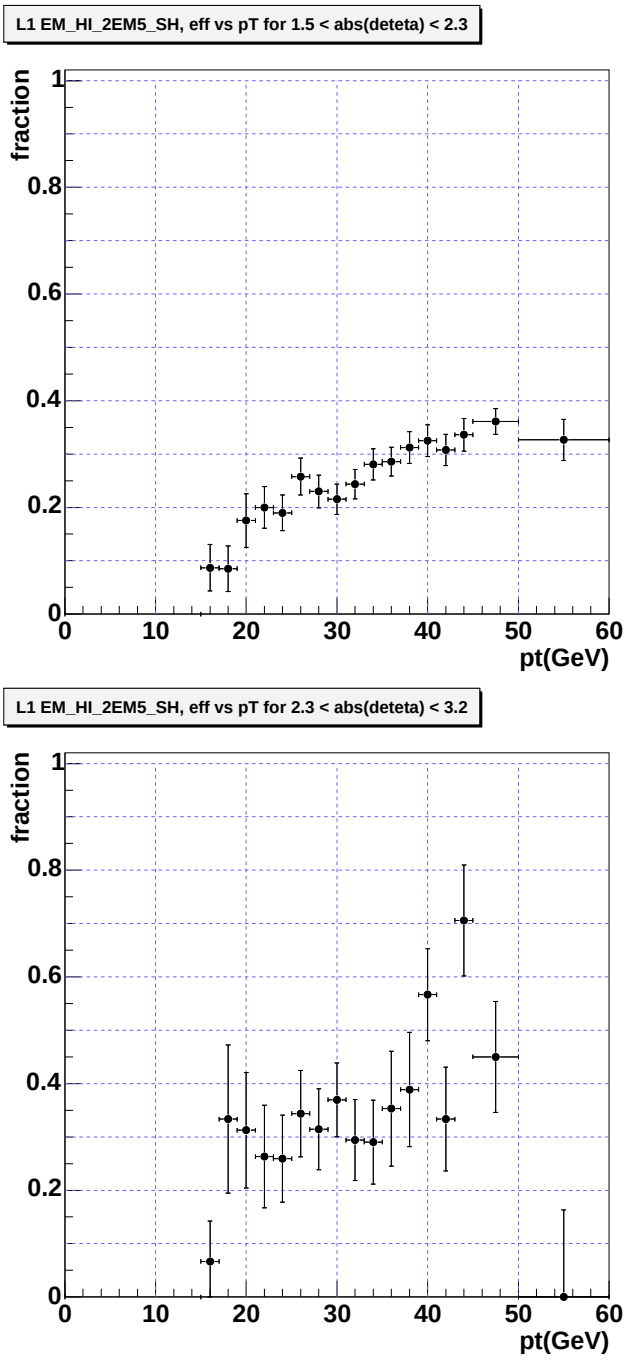

Figure 102: Electron trigger efficiency at L1 for EM_HI_2EM5_SH as a function of E_T for EC(top) and extended EC($2.3 < |\eta_{detector}| < 3.2$) (bottom).

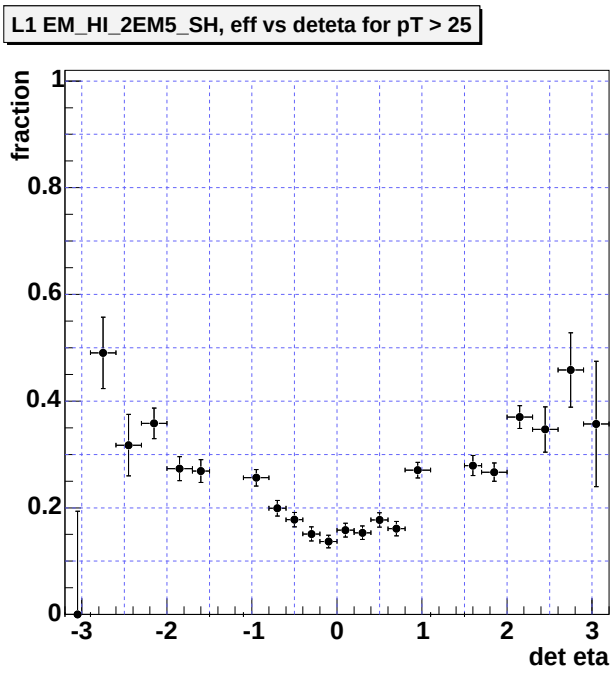

Figure 103: Electron trigger efficiency at L1 for EM_HI_2EM5_SH as a function of detector η.

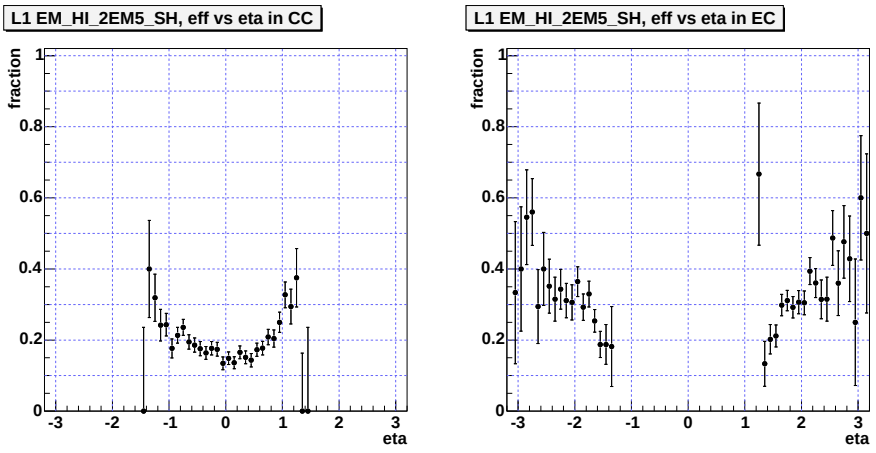

Figure 104: Electron trigger efficiency at L1 for EM_HI_2EM5_SH as a function of physics η for CC(left) and EC(right).

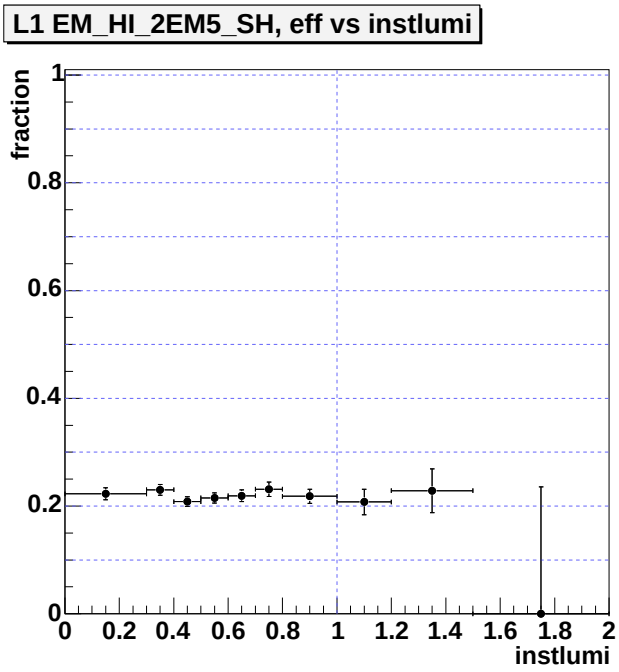

Figure 105: Electron trigger efficiency at L1 for EM_HI_2EM5_SH as a function of instantaneous luminosity($10^{30} cm^{-2} s^{-1}$) for all probes.

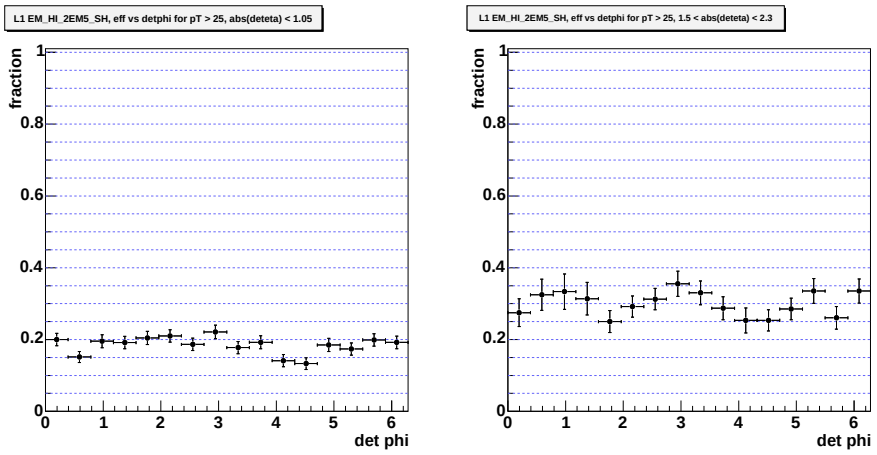

Figure 106: Electron trigger efficiency at L1 for EM_HI_2EM5_SH as a function of detector ϕ for CC(left) and EC(right).

2.5.2 EM_HI_2EM5_SH: L2

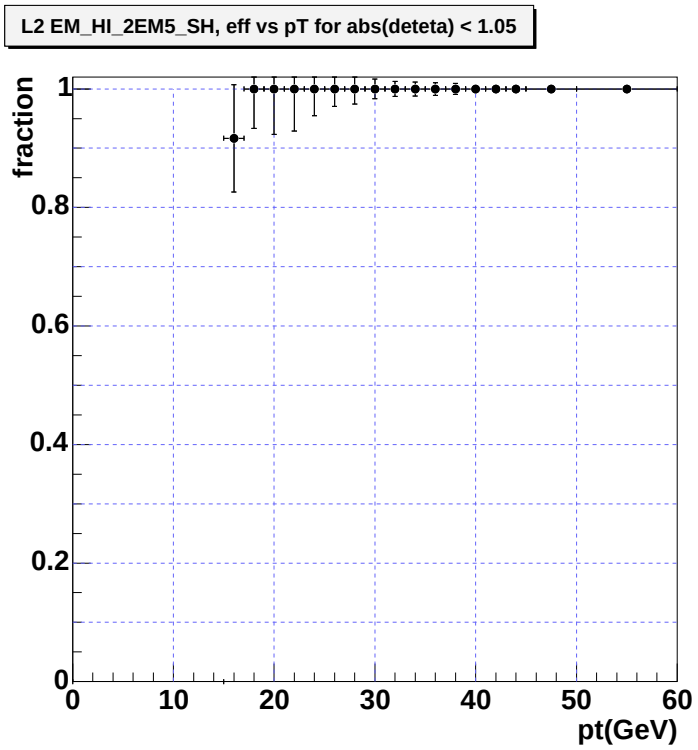

Figure 107: Electron trigger efficiency at L2 for EM_HI_2EM5_SH as a function of E_T for CC.

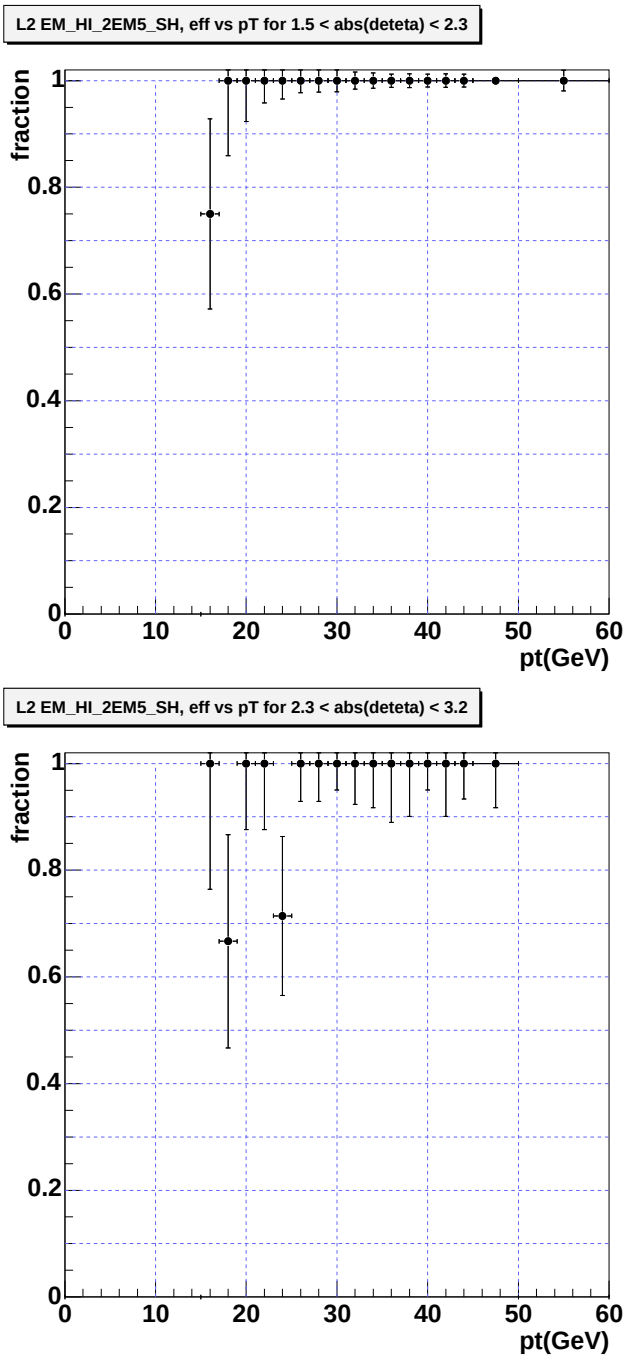

Figure 108: Electron trigger efficiency at L2 for EM_HI_2EM5_SH as a function of E_T for EC(top) and extended EC($2.3 < |\eta_{detector}| < 3.2$) (bottom).

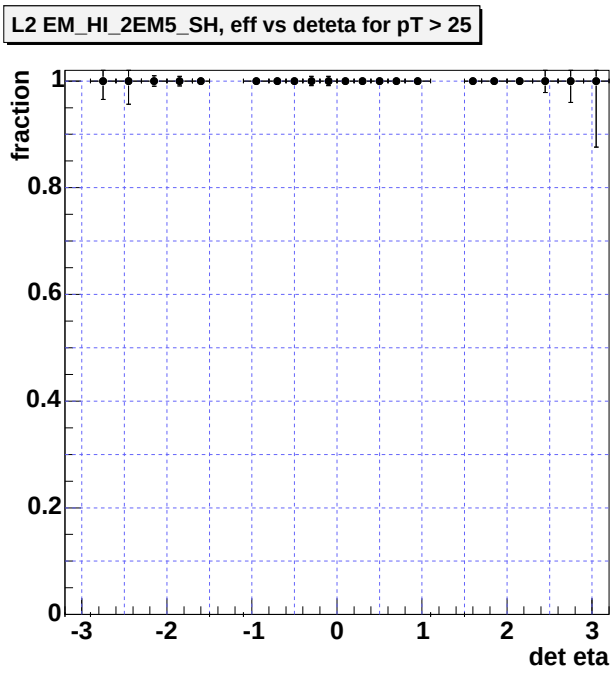

Figure 109: Electron trigger efficiency at L2 for EM_HI_2EM5_SH as a function of detector η.

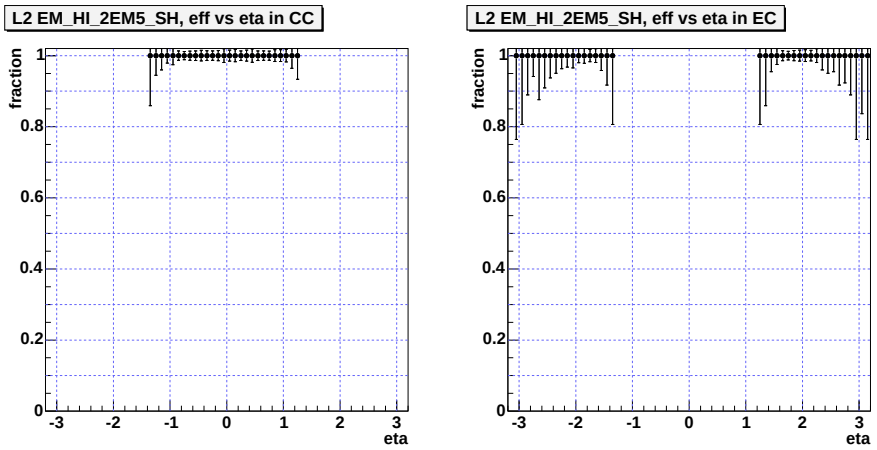

Figure 110: Electron trigger efficiency at L2 for EM_HI_2EM5_SH as a function of physics η for CC(left) and EC(right).

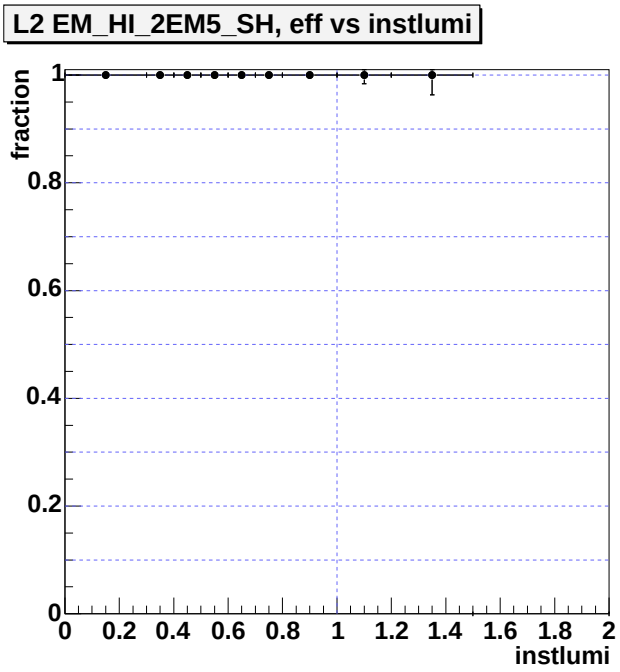

Figure 111: Electron trigger efficiency at L2 for EM_HI_2EM5_SH as a function of instantaneous luminosity($10^{30} cm^{-2} s^{-1}$) for all probes.

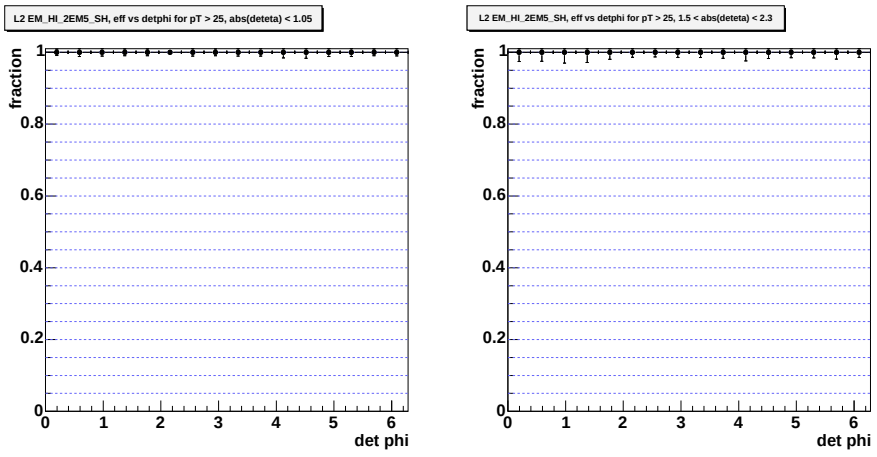

Figure 112: Electron trigger efficiency at L2 for EM_HI_2EM5_SH as a function of detector ϕ for CC(left) and EC(right).

2.5.3 EM_HI_2EM5_SH: L3

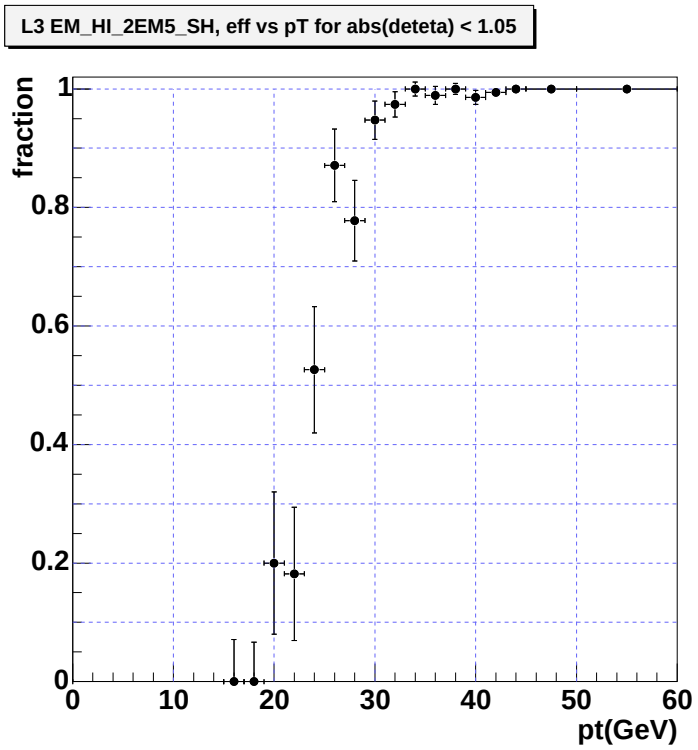

Figure 113: Electron trigger efficiency at L3 for EM_HI_2EM5_SH as a function of E_T for CC.

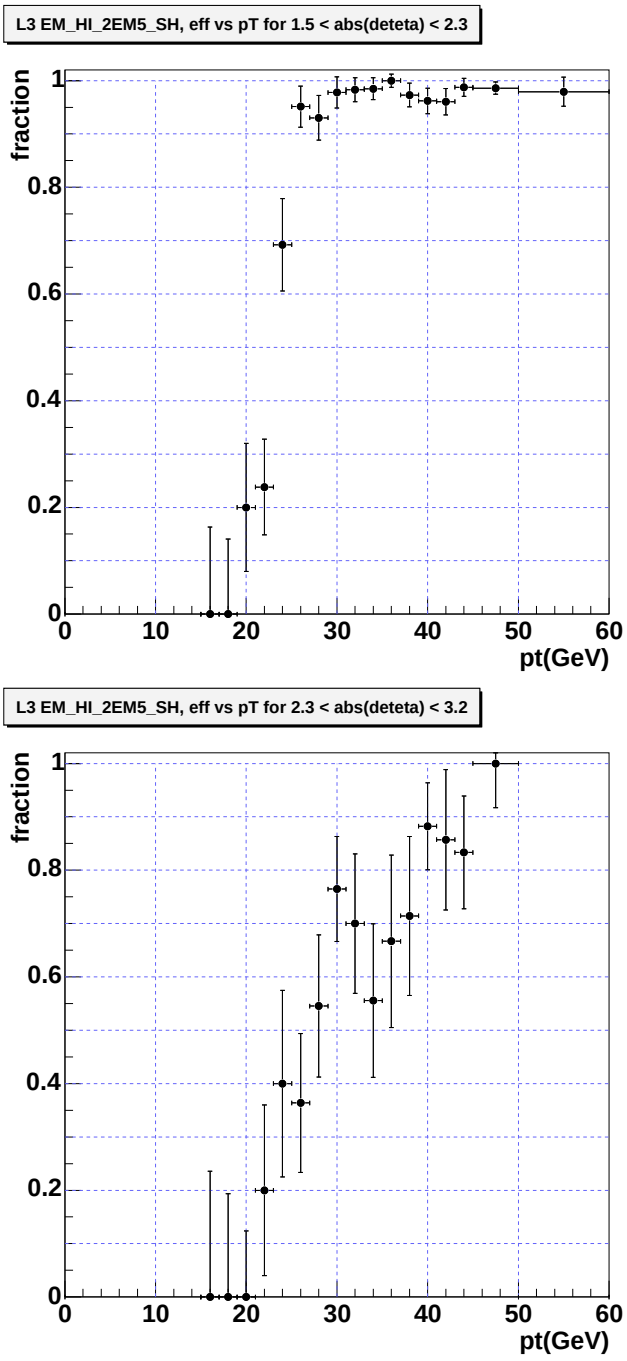

Figure 114: Electron trigger efficiency at L3 for EM_HI_2EM5_SH as a function of E_T for EC(top) and extended EC($2.3 < |\eta_{detector}| < 3.2$) (bottom).

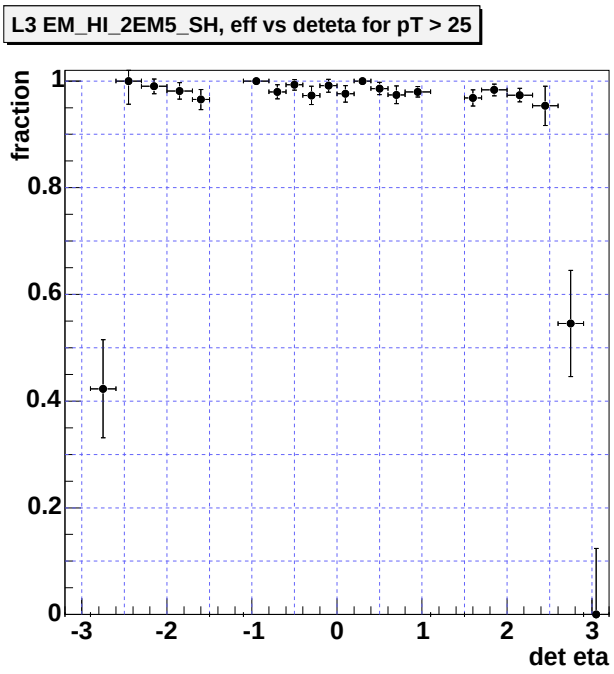

Figure 115: Electron trigger efficiency at L3 for EM_HI_2EM5_SH as a function of detector η.

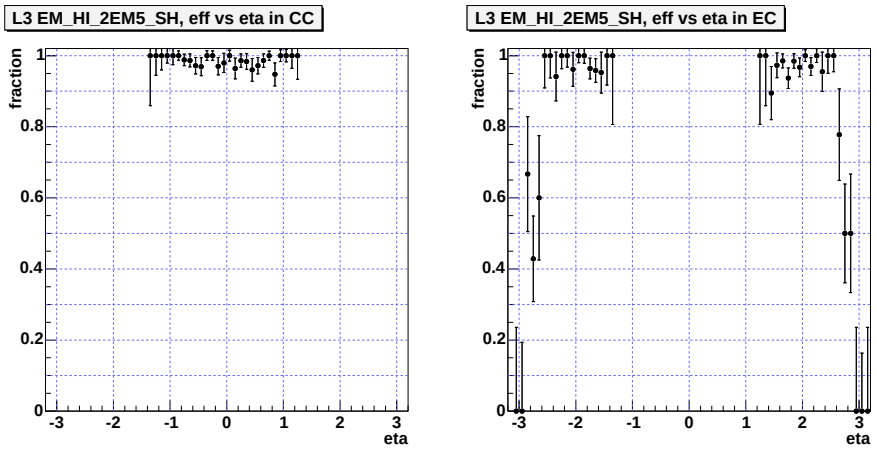

Figure 116: Electron trigger efficiency at L3 for EM_HI_2EM5_SH as a function of physics η for CC(left) and EC(right).

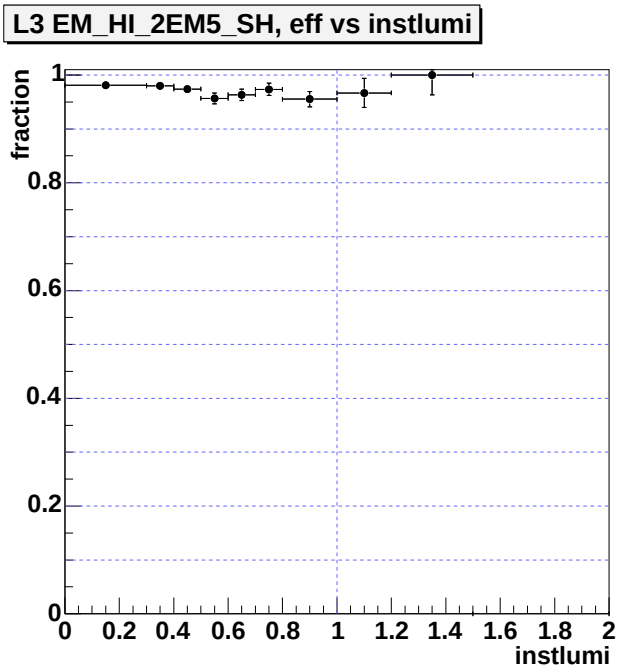

Figure 117: Electron trigger efficiency at L3 for EM_HI_2EM5_SH as a function of instantaneous luminosity($10^{30} cm^{-2} s^{-1}$) for all probes.

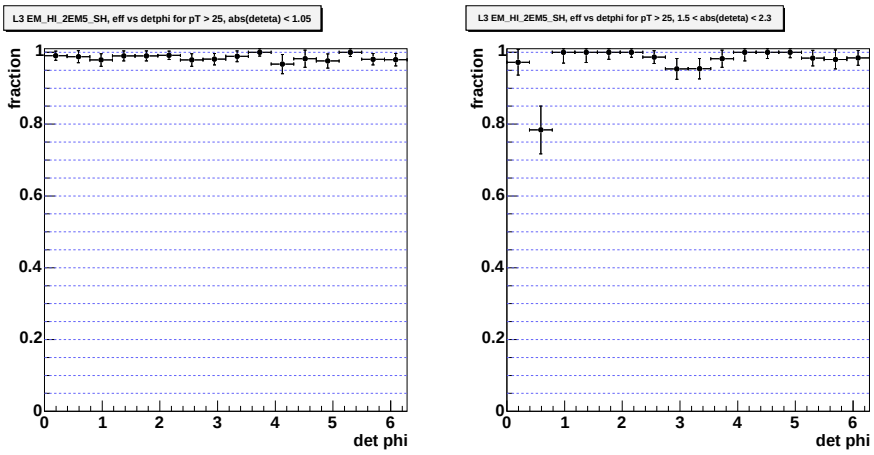

Figure 118: Electron trigger efficiency at L3 for EM_HI_2EM5_SH as a function of detector ϕ for CC(left) and EC(right).

2.6 EM_HI

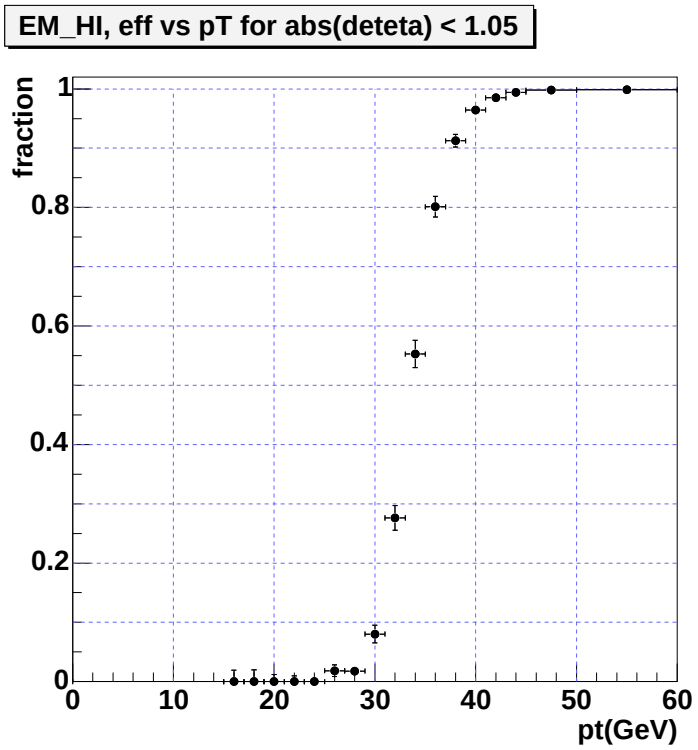

Figure 119: Electron trigger efficiency for EM_HI as a function of E_T for CC.

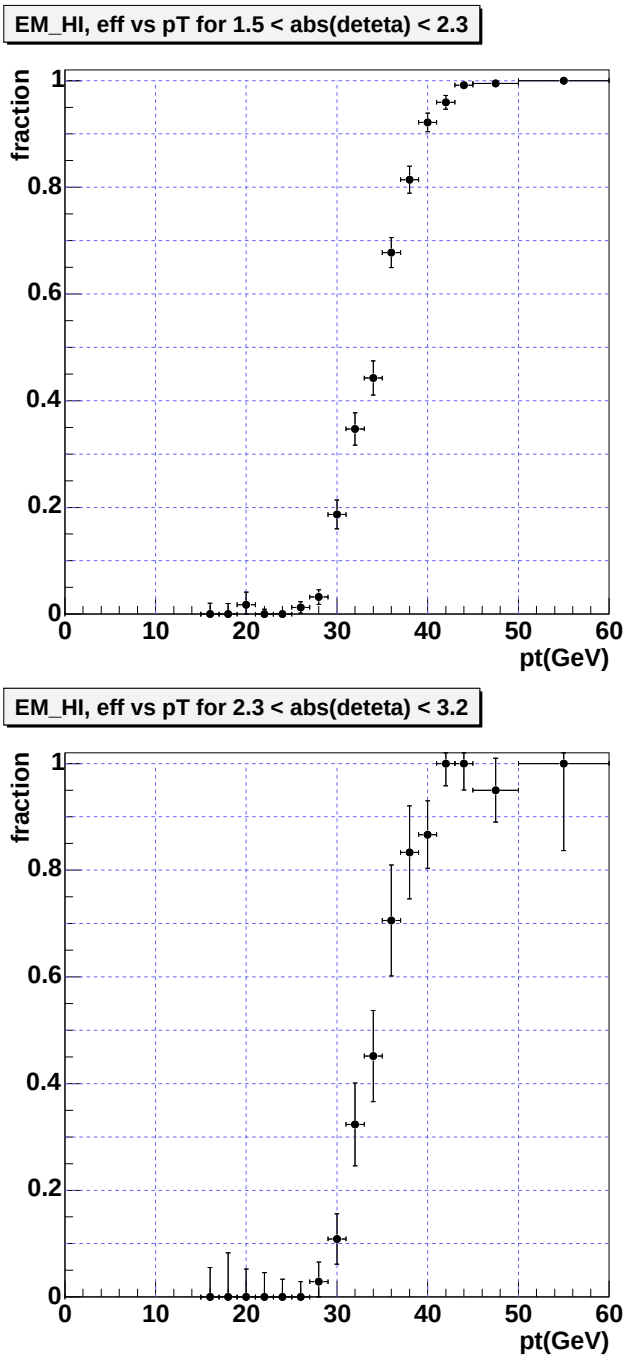

Figure 120: Electron trigger efficiency for EM_HI as a function of E_T for EC(top) and extended EC($2.3 < |\eta_{detector}| < 3.2$) (bottom).

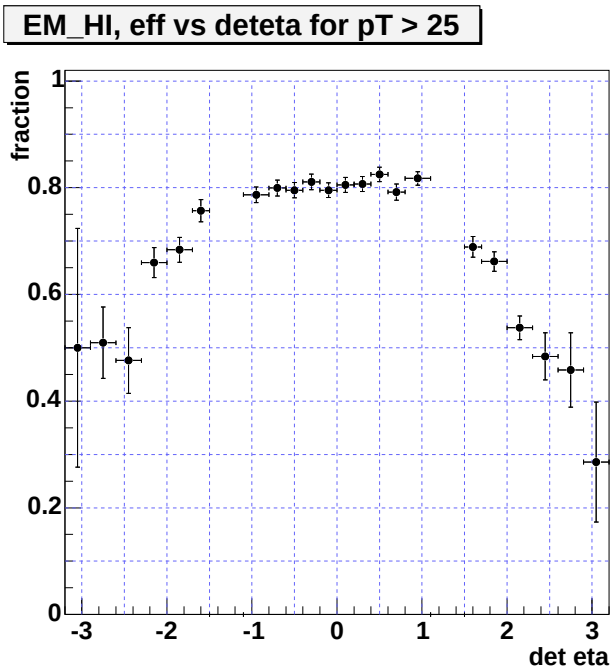

Figure 121: Electron trigger efficiency for EM_HI as a function of detector η.

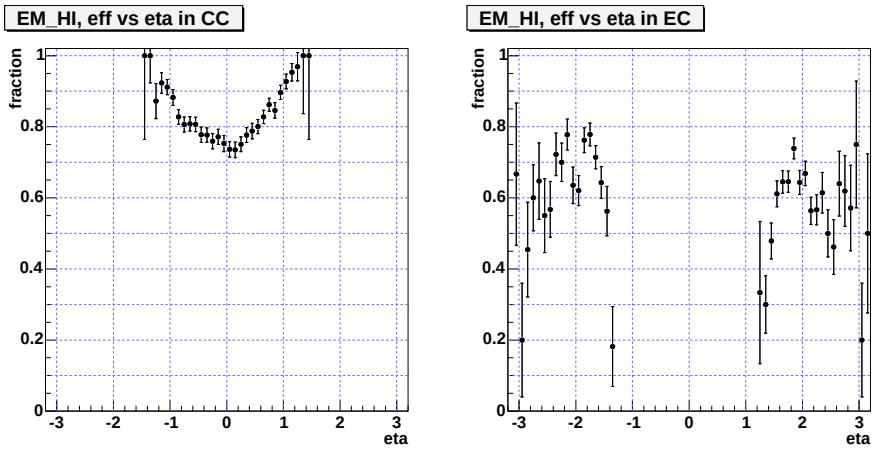

Figure 122: Electron trigger efficiency for EM_HI as a function of physics η for CC(left) and EC(right).

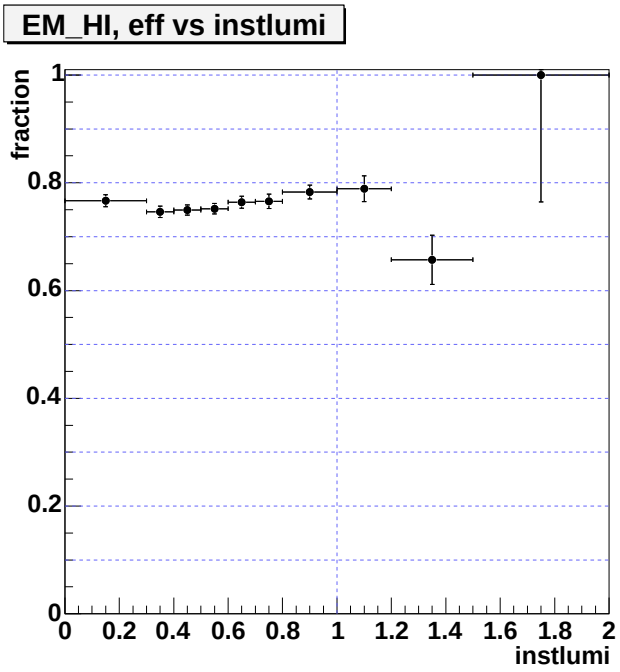

Figure 123: Electron trigger efficiency for EM_HI as a function of instantaneous luminosity($10^{30} cm^{-2} s^{-1}$) for all probes.

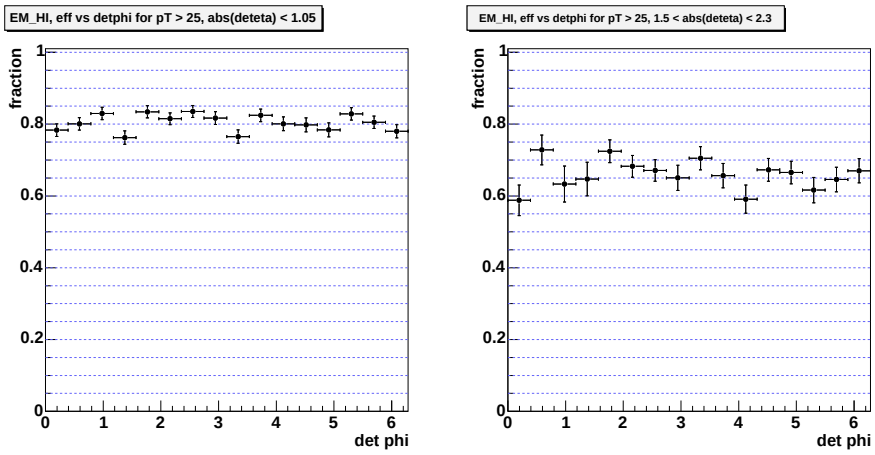

Figure 124: Electron trigger efficiency for EM_HI as a function of detector ϕ for CC(left) and EC(right).

2.6.1 EM_HI: L1

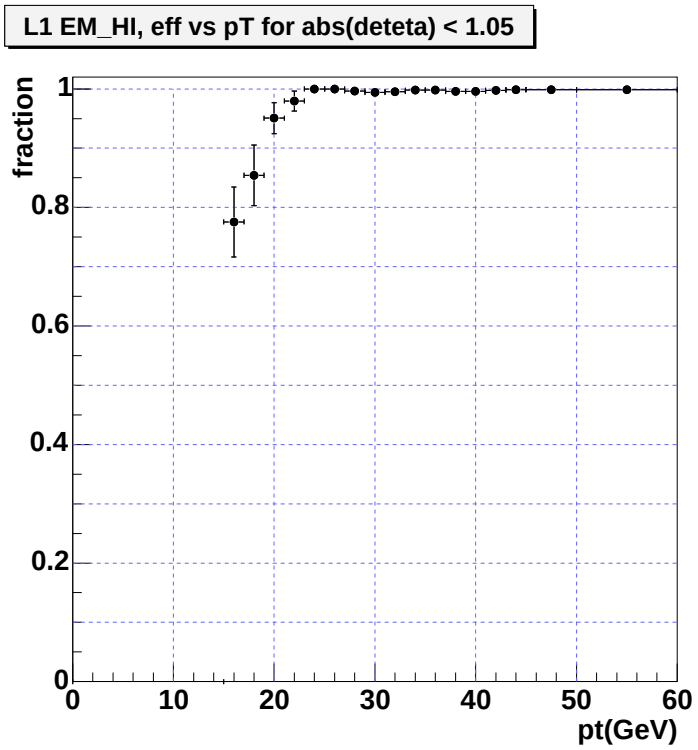

Figure 125: Electron trigger efficiency at L1 for EM_HI as a function of E_T for CC.

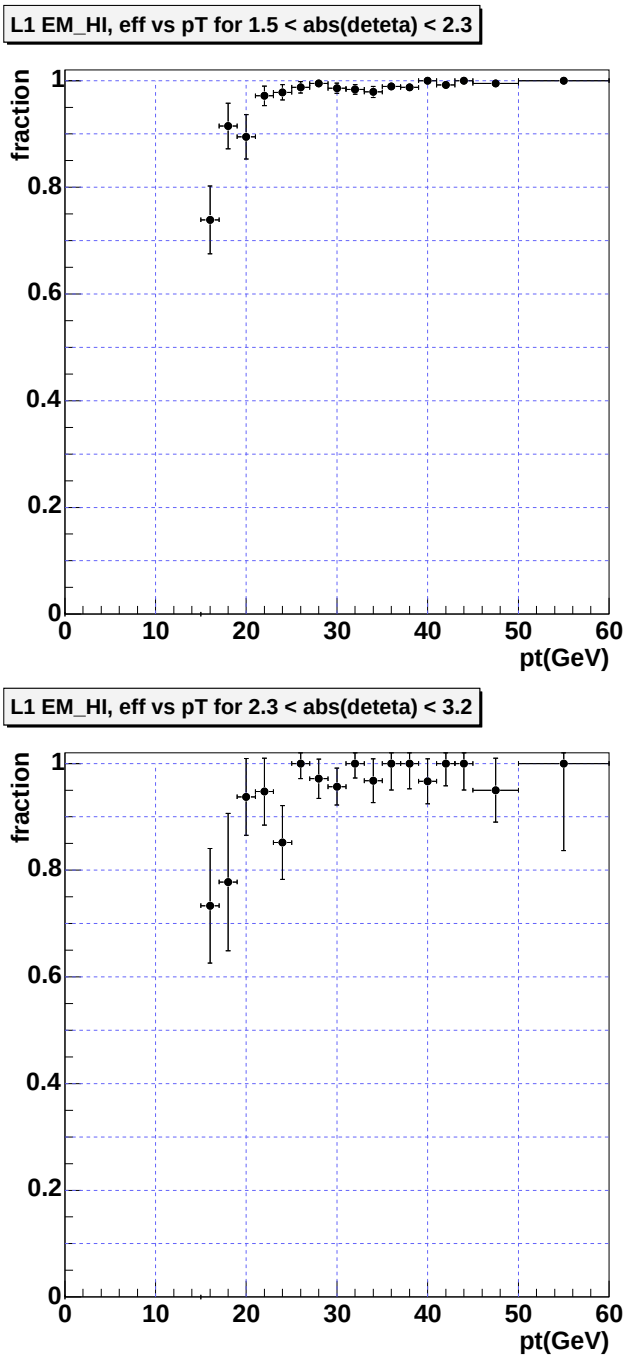

Figure 126: Electron trigger efficiency at L1 for EM_HI as a function of E_T for EC(top) and extended EC($2.3 < |\eta_{detector}| < 3.2$) (bottom).

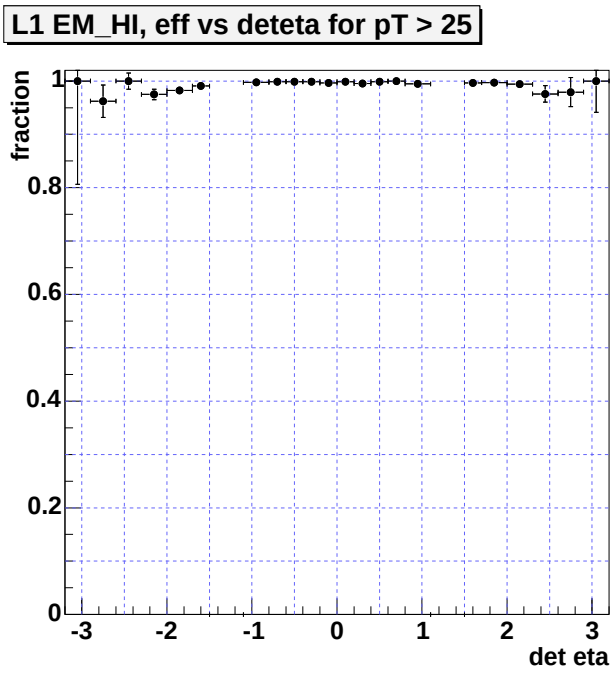

Figure 127: Electron trigger efficiency at L1 for EM_HI as a function of detector η.

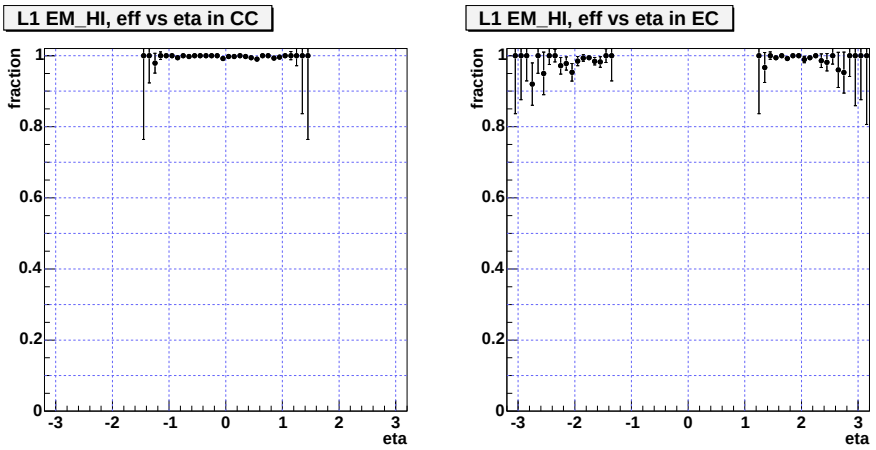

Figure 128: Electron trigger efficiency at L1 for EM_HI as a function of physics η for CC(left) and EC(right).

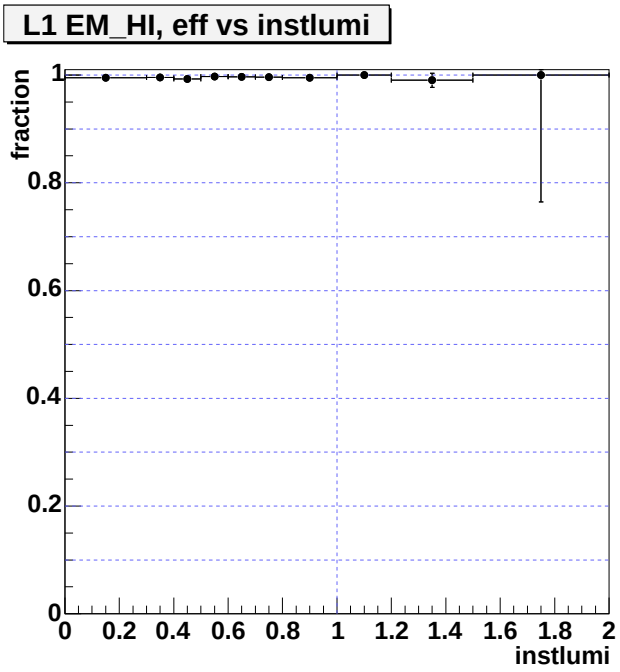

Figure 129: Electron trigger efficiency at L1 for EM_HI as a function of instantaneous luminosity($10^{30} cm^{-2} s^{-1}$) for all probes.

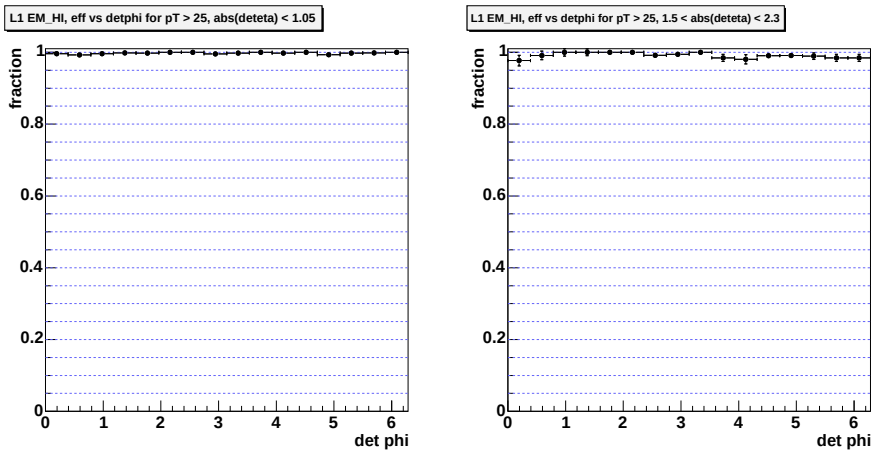

Figure 130: Electron trigger efficiency at L1 for EM_HI as a function of detector ϕ for CC(left) and EC(right).

2.6.2 EM_HI: L2

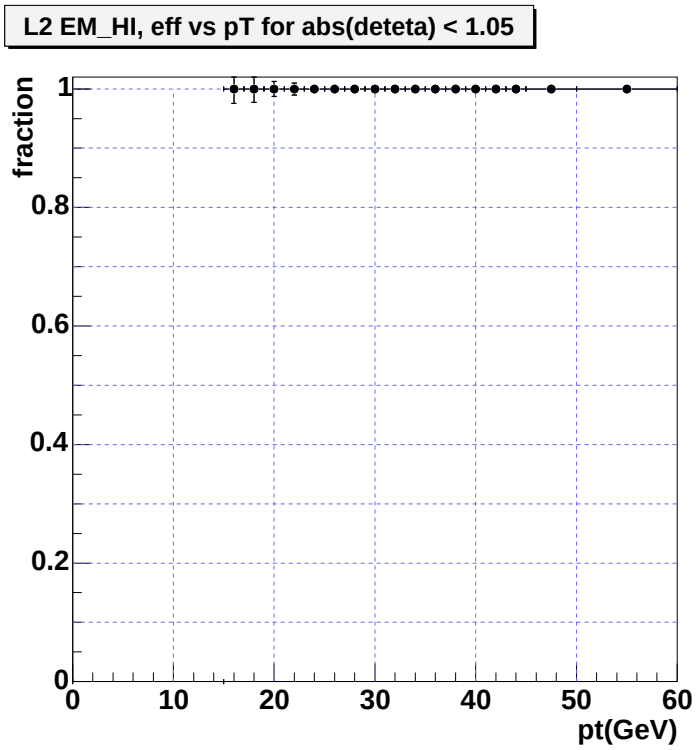

Figure 131: Electron trigger efficiency at L2 for EM_HI as a function of E_T for CC.

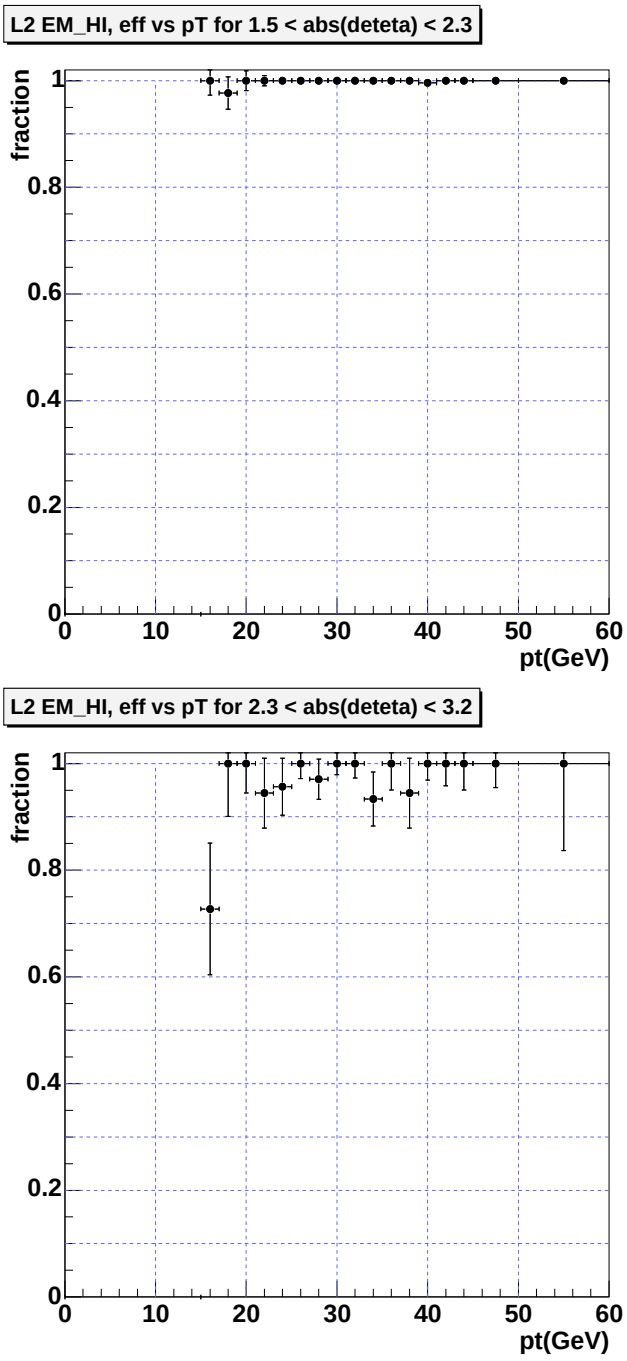

Figure 132: Electron trigger efficiency at L2 for EM_HI as a function of E_T for EC(top) and extended EC($2.3 < |\eta_{detector}| < 3.2$) (bottom).

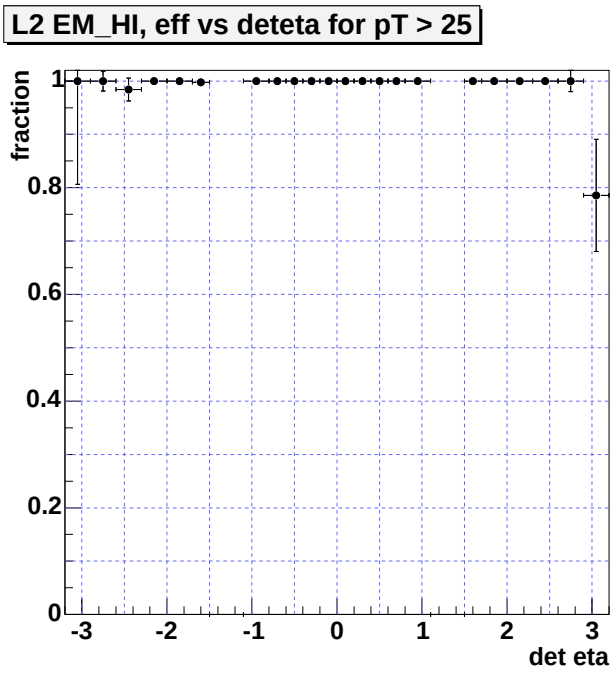

Figure 133: Electron trigger efficiency at L2 for EM_HI as a function of detector η.

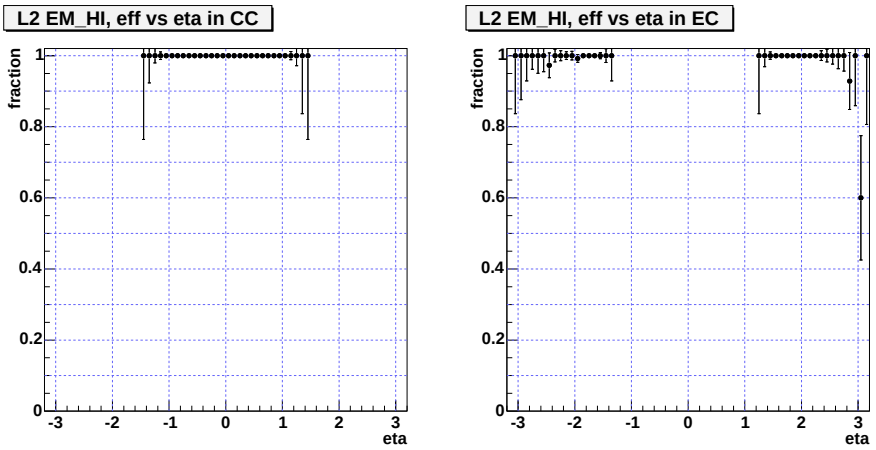

Figure 134: Electron trigger efficiency at L2 for EM_HI as a function of physics η for CC(left) and EC(right).

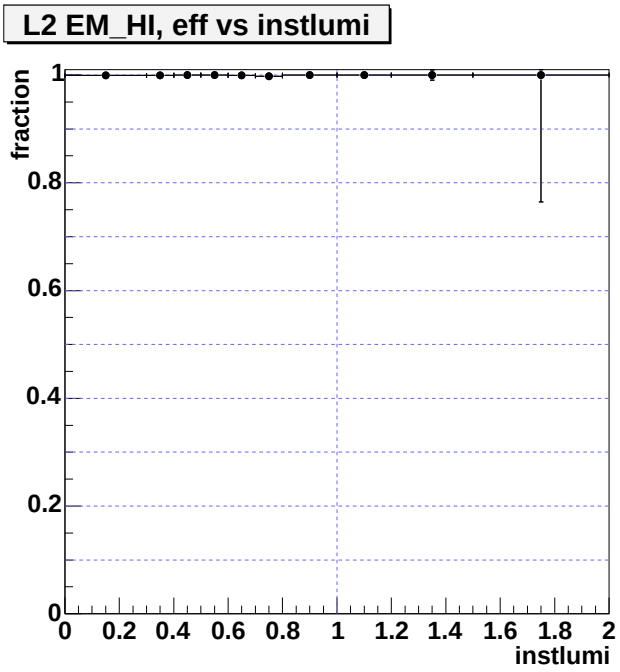

Figure 135: Electron trigger efficiency at L2 for EM_HI as a function of instantaneous luminosity($10^{30} cm^{-2} s^{-1}$) for all probes.

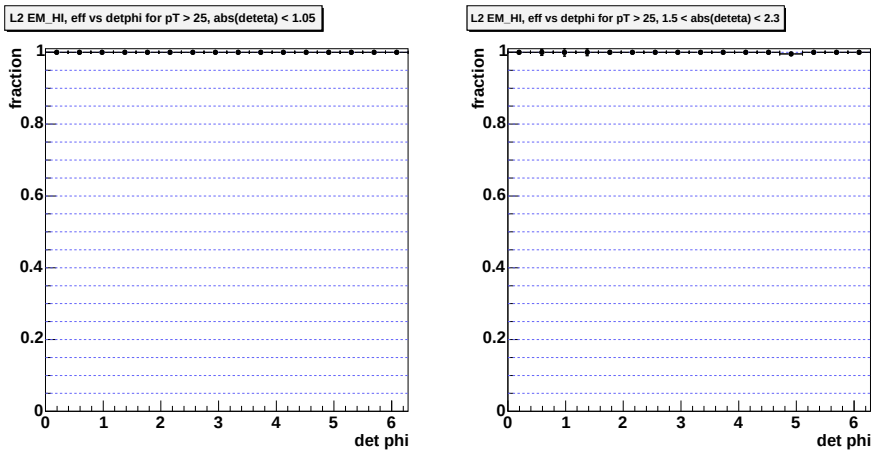

Figure 136: Electron trigger efficiency at L2 for EM_HI as a function of detector ϕ for CC(left) and EC(right).

2.6.3 EM_HI: L3

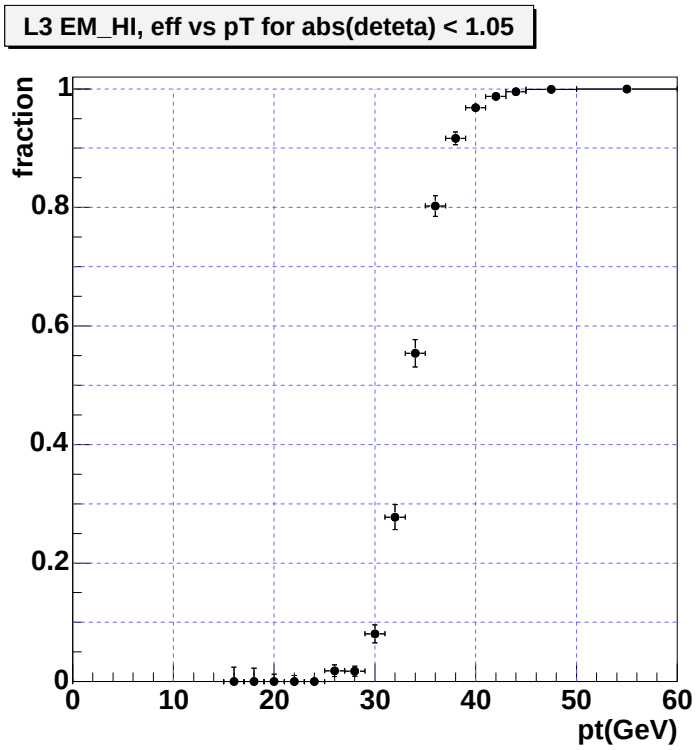

Figure 137: Electron trigger efficiency at L3 for EM_HI as a function of E_T for CC.

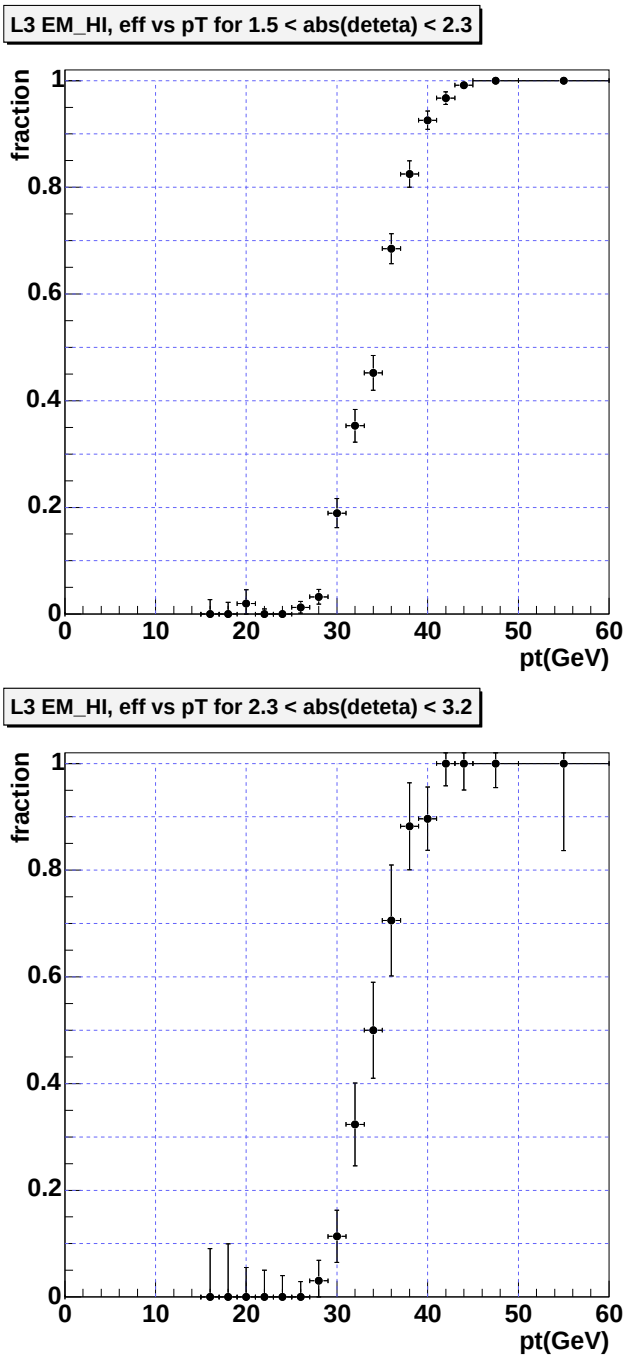

Figure 138: Electron trigger efficiency at L3 for EM_HI as a function of E_T for EC(top) and extended EC($2.3 < |\eta_{detector}| < 3.2$) (bottom).

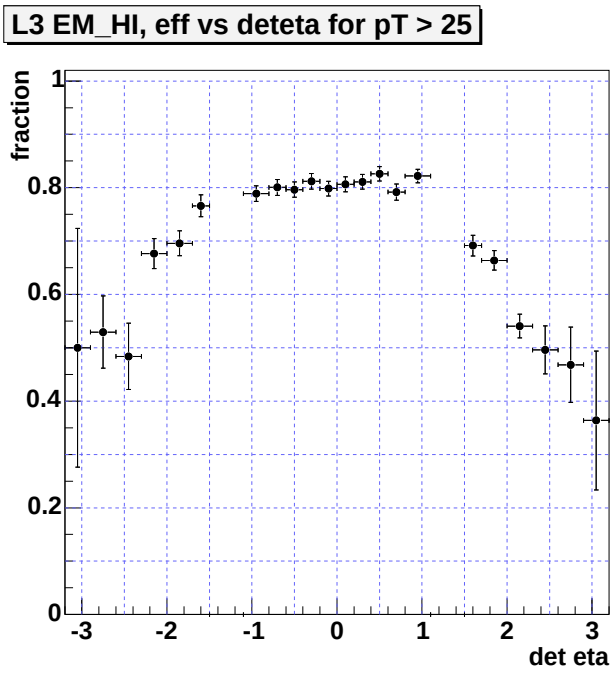

Figure 139: Electron trigger efficiency at L3 for EM_HI as a function of detector η.

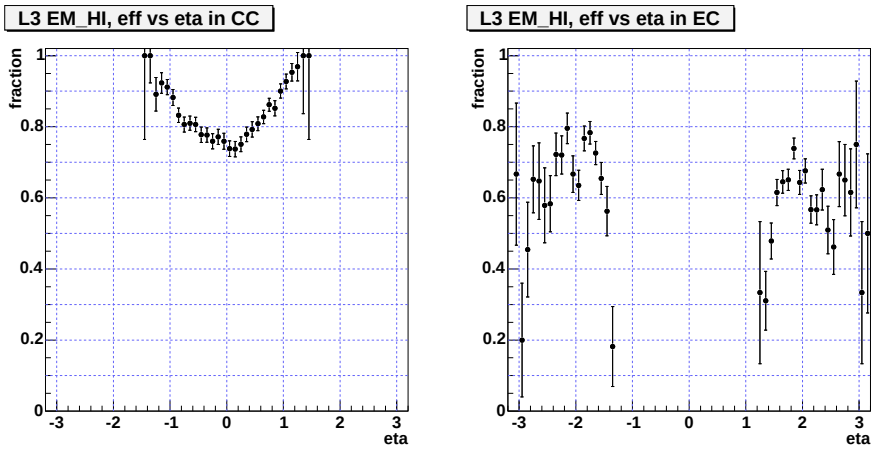

Figure 140: Electron trigger efficiency at L3 for EM_HI as a function of physics η for CC(left) and EC(right).

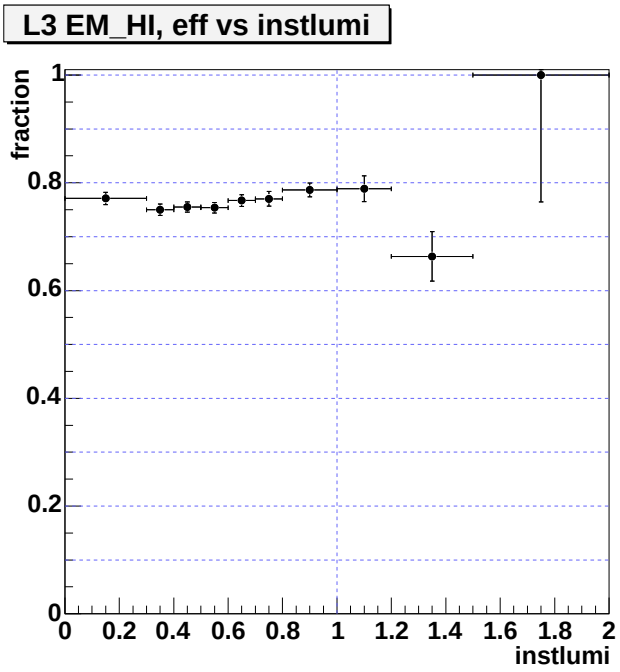

Figure 141: Electron trigger efficiency at L3 for EM_HI as a function of instantaneous luminosity($10^{30} cm^{-2} s^{-1}$) for all probes.

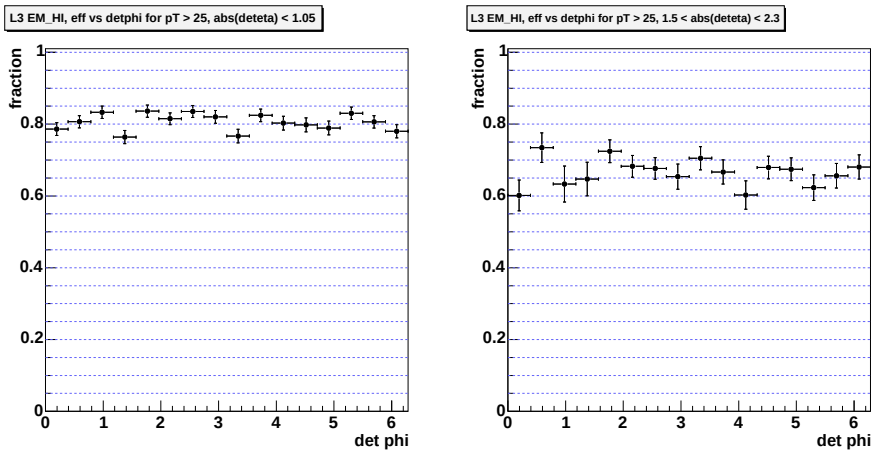

Figure 142: Electron trigger efficiency at L3 for EM_HI as a function of detector ϕ for CC(left) and EC(right).

2.7 EM_MX_SH

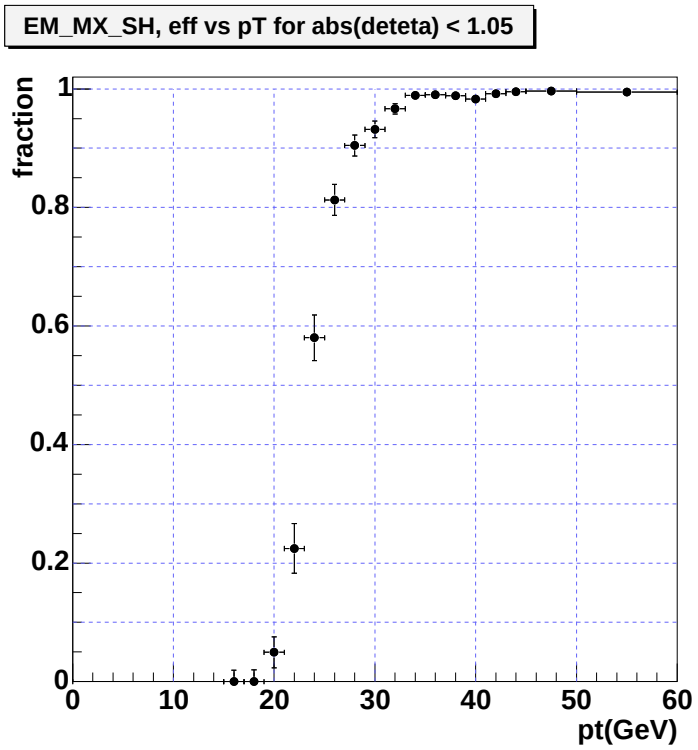

Figure 143: Electron trigger efficiency for EM_MX_SH as a function of E_T for CC.

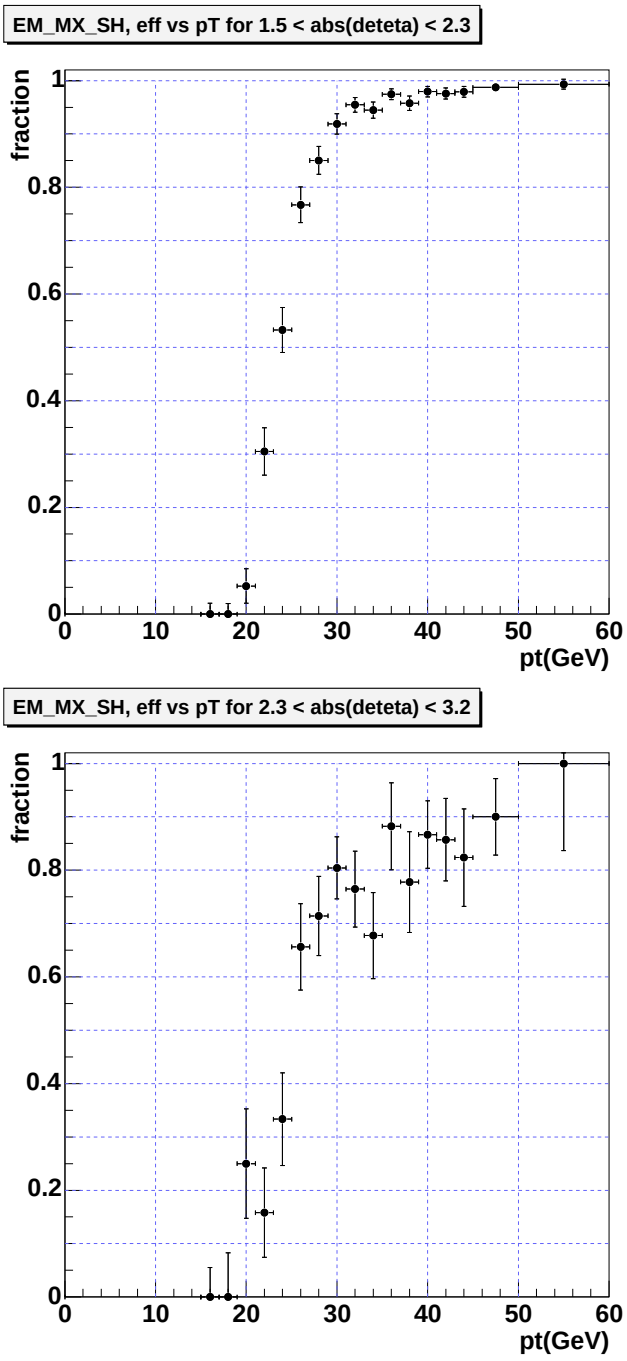

Figure 144: Electron trigger efficiency for EM_MX_SH as a function of E_T for EC(top) and extended EC($2.3 < |\eta_{detector}| < 3.2$) (bottom).

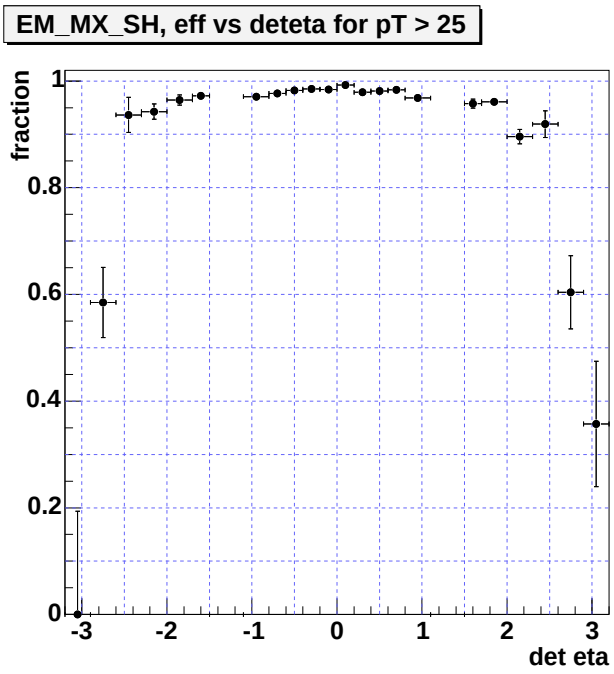

Figure 145: Electron trigger efficiency for EM_MX_SH as a function of detector η.

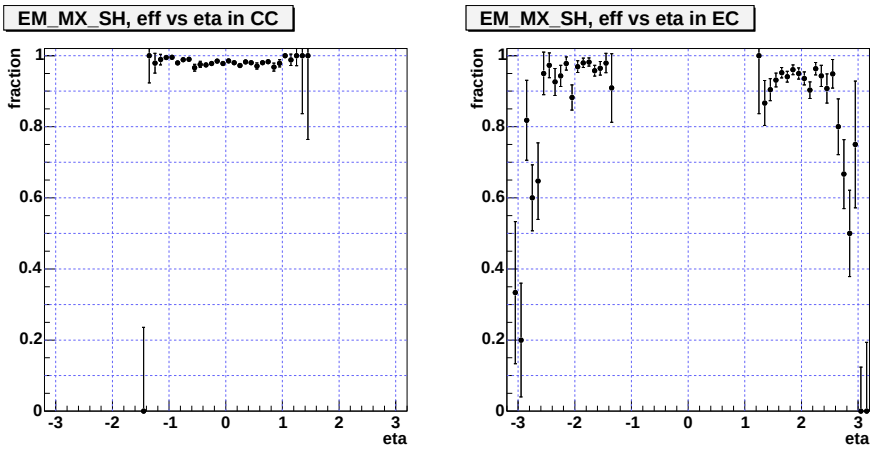

Figure 146: Electron trigger efficiency for EM_MX_SH as a function of physics η for CC(left) and EC(right).

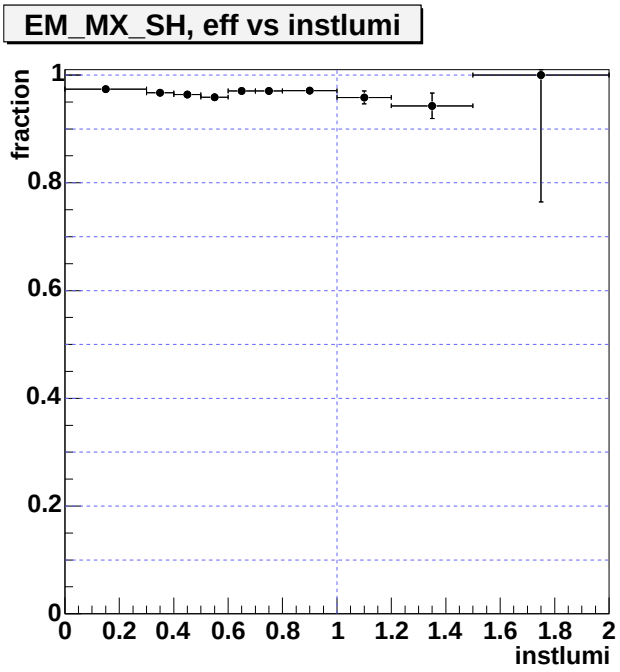

Figure 147: Electron trigger efficiency for EM_MX_SH as a function of instantaneous luminosity($10^{30} cm^{-2} s^{-1}$) for all probes.

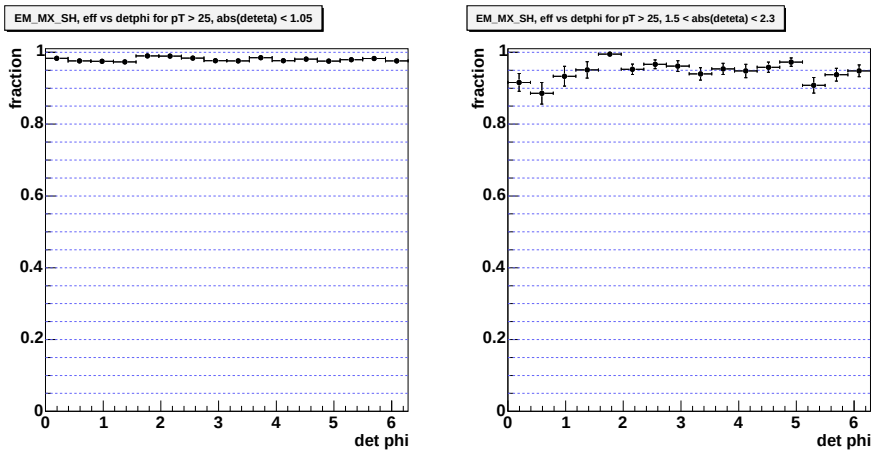

Figure 148: Electron trigger efficiency for EM_MX_SH as a function of detector ϕ for CC(left) and EC(right).

2.7.1 EM_MX_SH: L1

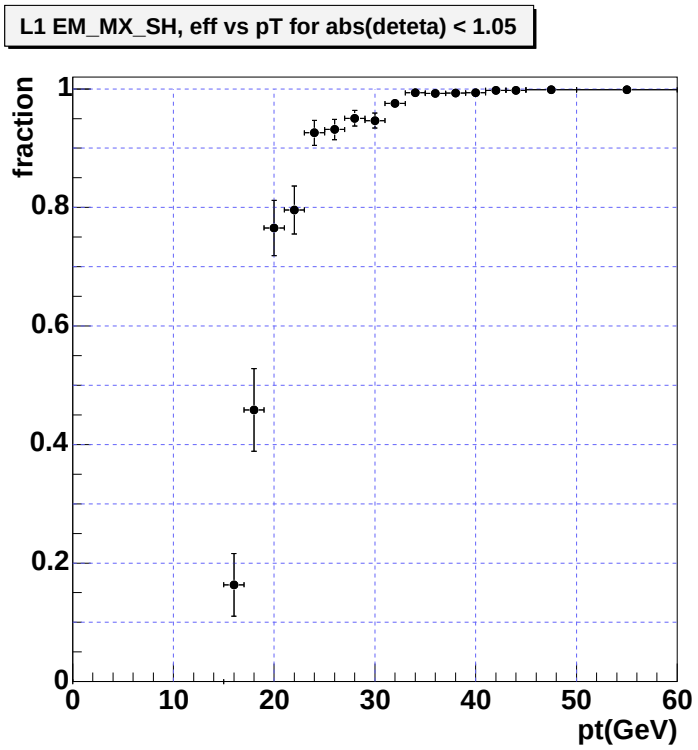

Figure 149: Electron trigger efficiency at L1 for EM_MX_SH as a function of E_T for CC.

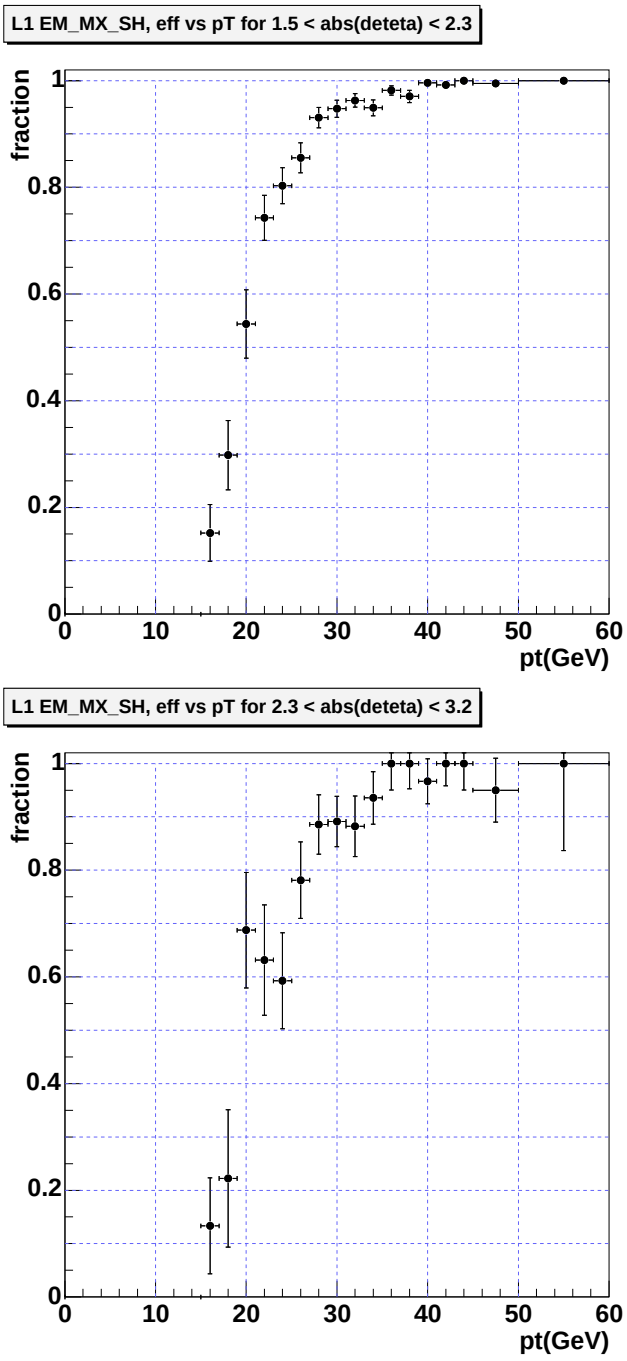

Figure 150: Electron trigger efficiency at L1 for EM_MX_SH as a function of E_T for EC(top) and extended EC($2.3 < |\eta_{detector}| < 3.2$) (bottom).

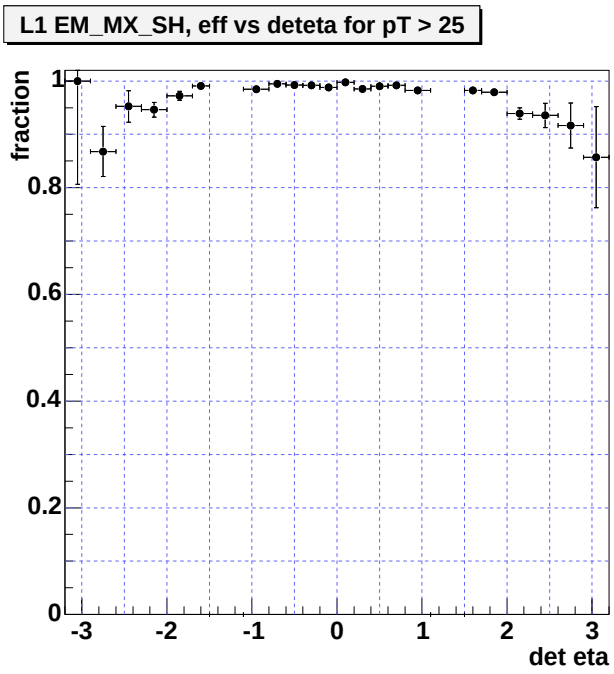

Figure 151: Electron trigger efficiency at L1 for EM_MX_SH as a function of detector η.

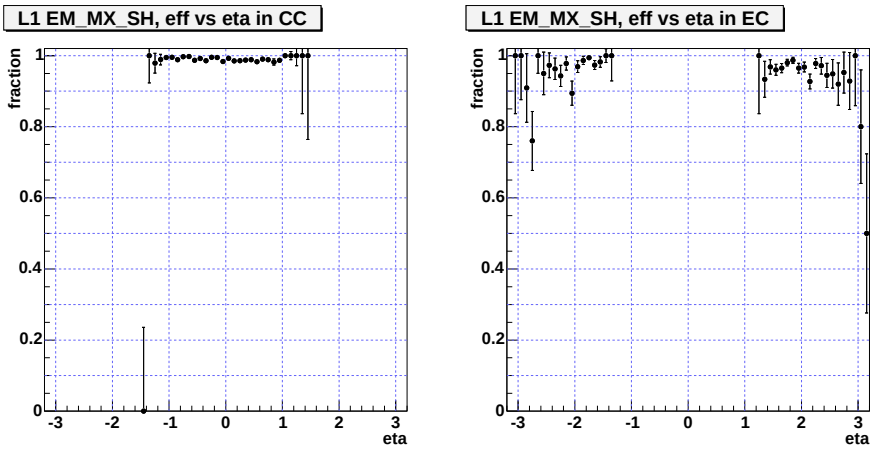

Figure 152: Electron trigger efficiency at L1 for EM_MX_SH as a function of physics η for CC(left) and EC(right).

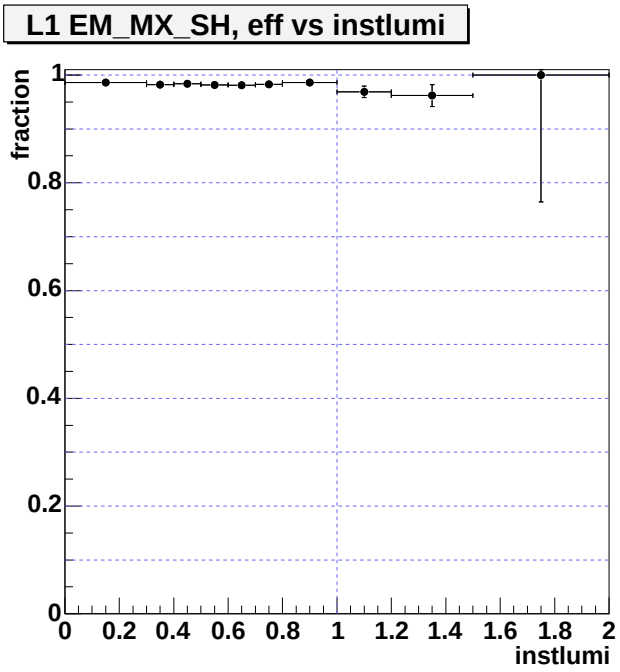

Figure 153: Electron trigger efficiency at L1 for EM_MX_SH as a function of instantaneous luminosity($10^{30} cm^{-2} s^{-1}$) for all probes.

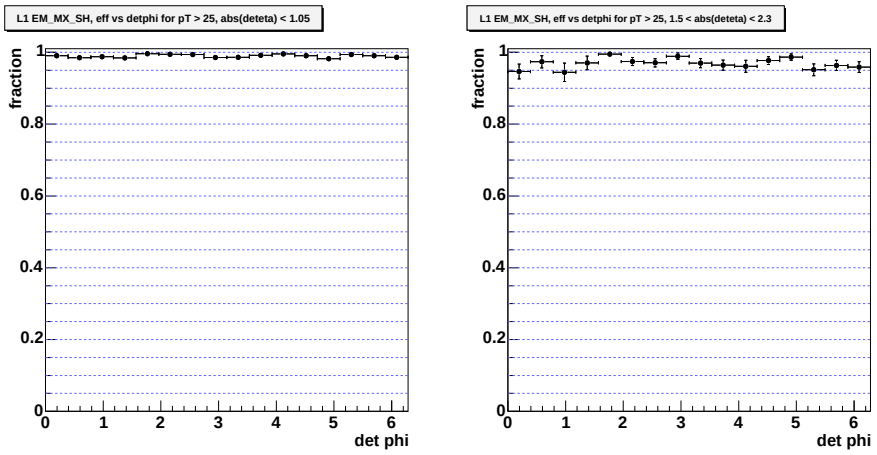

Figure 154: Electron trigger efficiency at L1 for EM_MX_SH as a function of detector ϕ for CC(left) and EC(right).

2.7.2 EM_MX_SH: L3

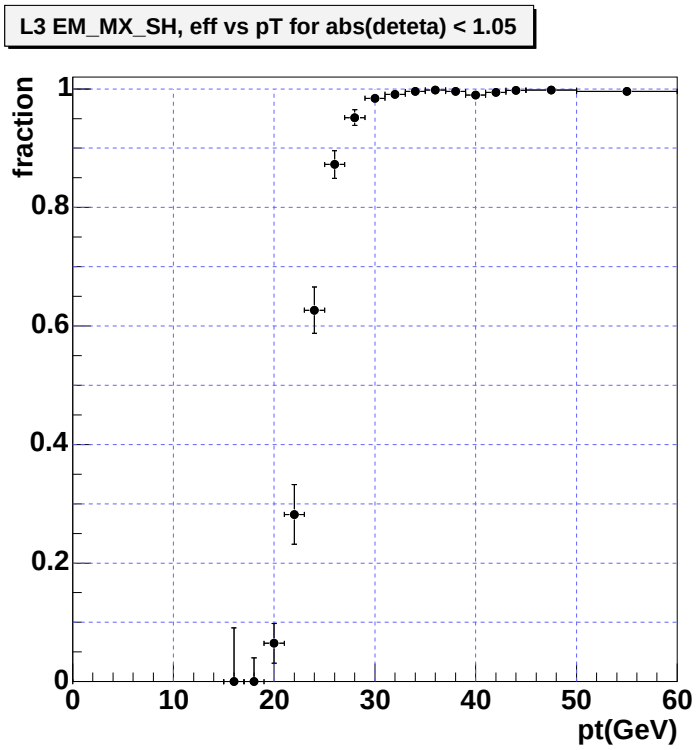

Figure 155: Electron trigger efficiency at L3 for EM_MX_SH as a function of E_T for CC.

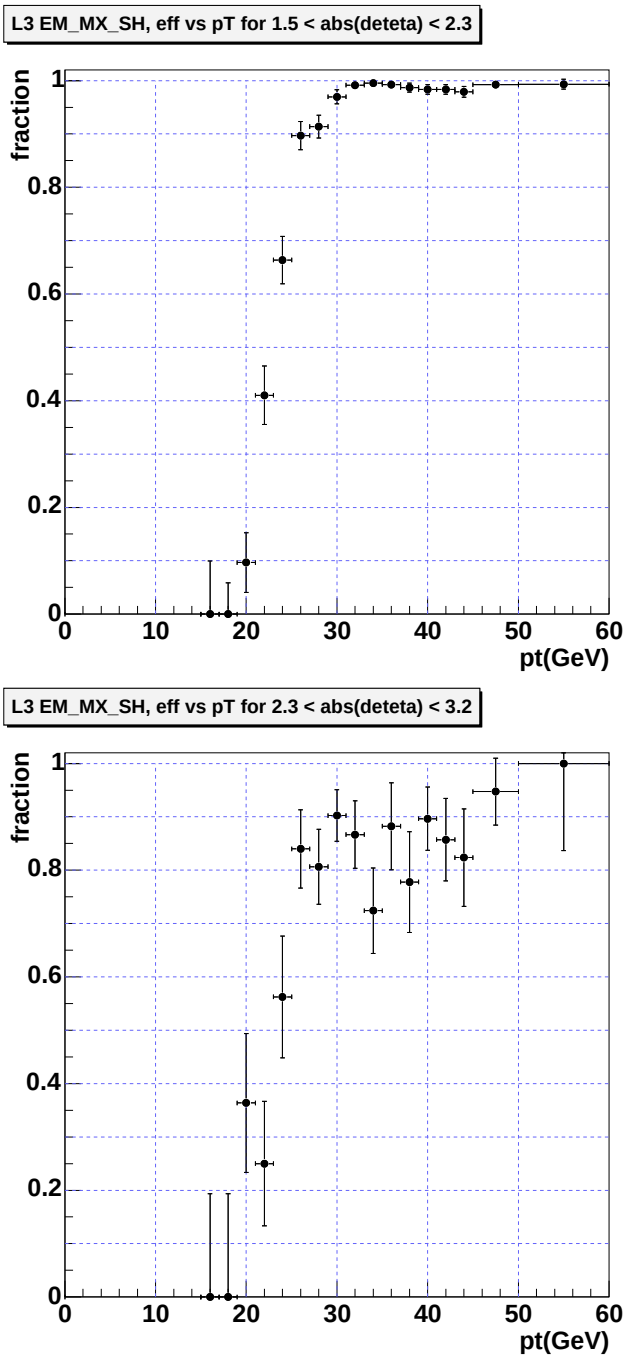

Figure 156: Electron trigger efficiency at L3 for EM_MX_SH as a function of E_T for EC(top) and extended EC($2.3 < |\eta_{detector}| < 3.2$) (bottom).

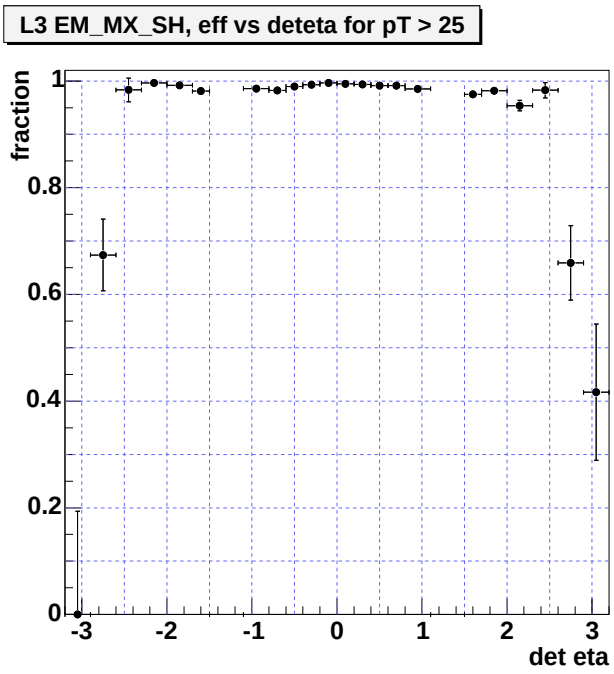

Figure 157: Electron trigger efficiency at L3 for EM_MX_SH as a function of detector η.

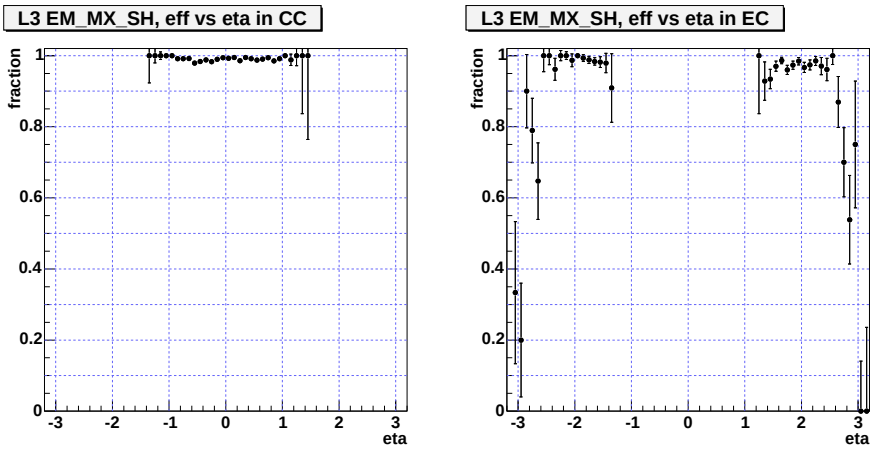

Figure 158: Electron trigger efficiency at L3 for EM_MX_SH as a function of physics η for CC(left) and EC(right).

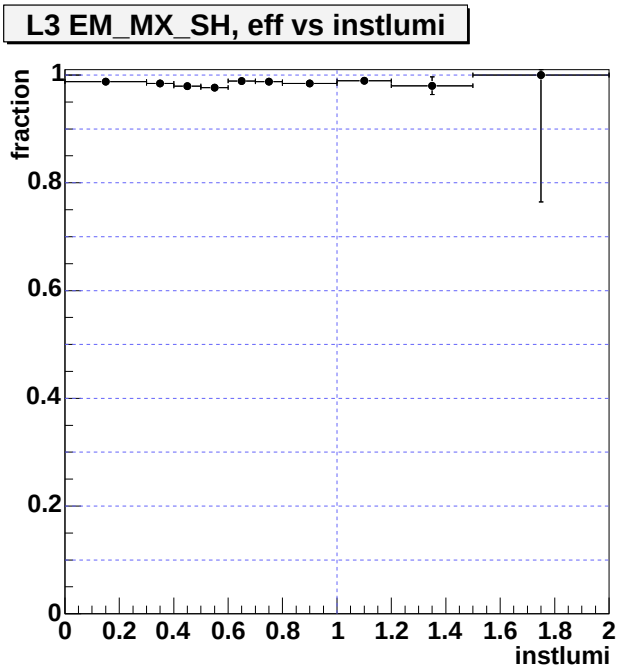

Figure 159: Electron trigger efficiency at L3 for EM_MX_SH as a function of instantaneous luminosity($10^{30} cm^{-2} s^{-1}$) for all probes.

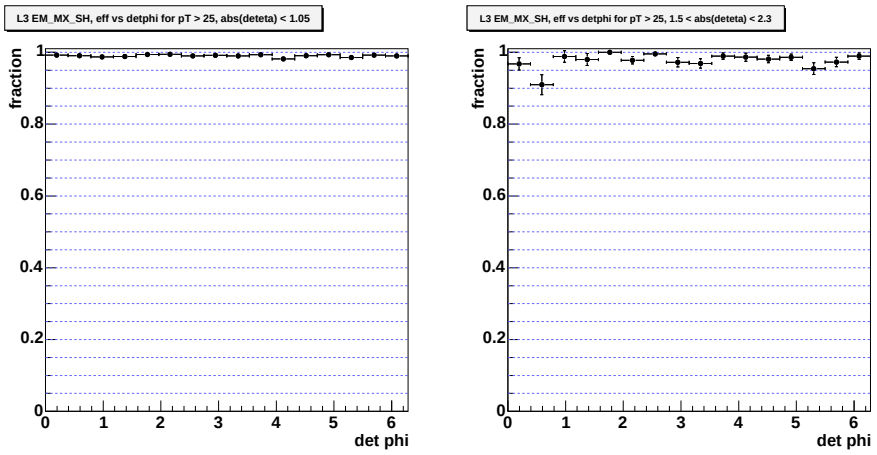

Figure 160: Electron trigger efficiency at L3 for EM_MX_SH as a function of detector ϕ for CC(left) and EC(right).

2.8 EM_MX

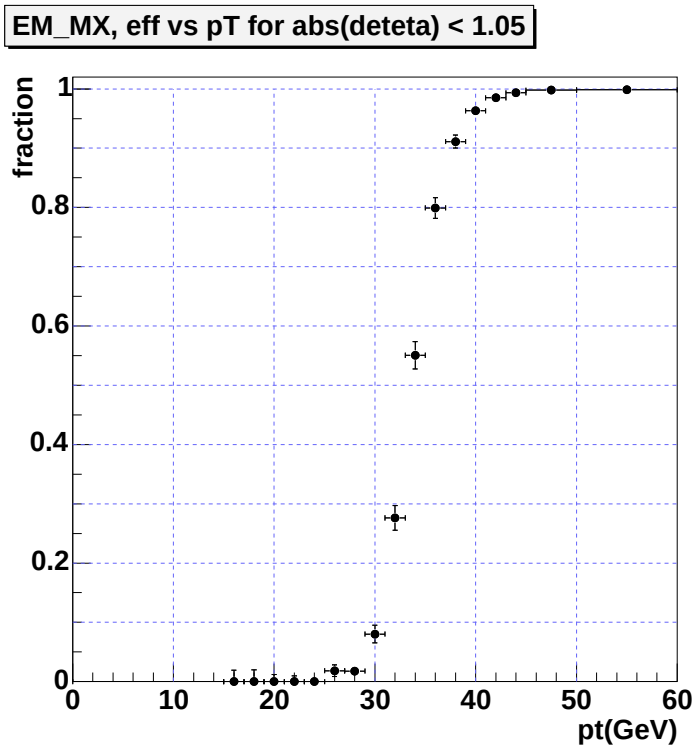

Figure 161: Electron trigger efficiency for EM_MX as a function of E_T for CC.

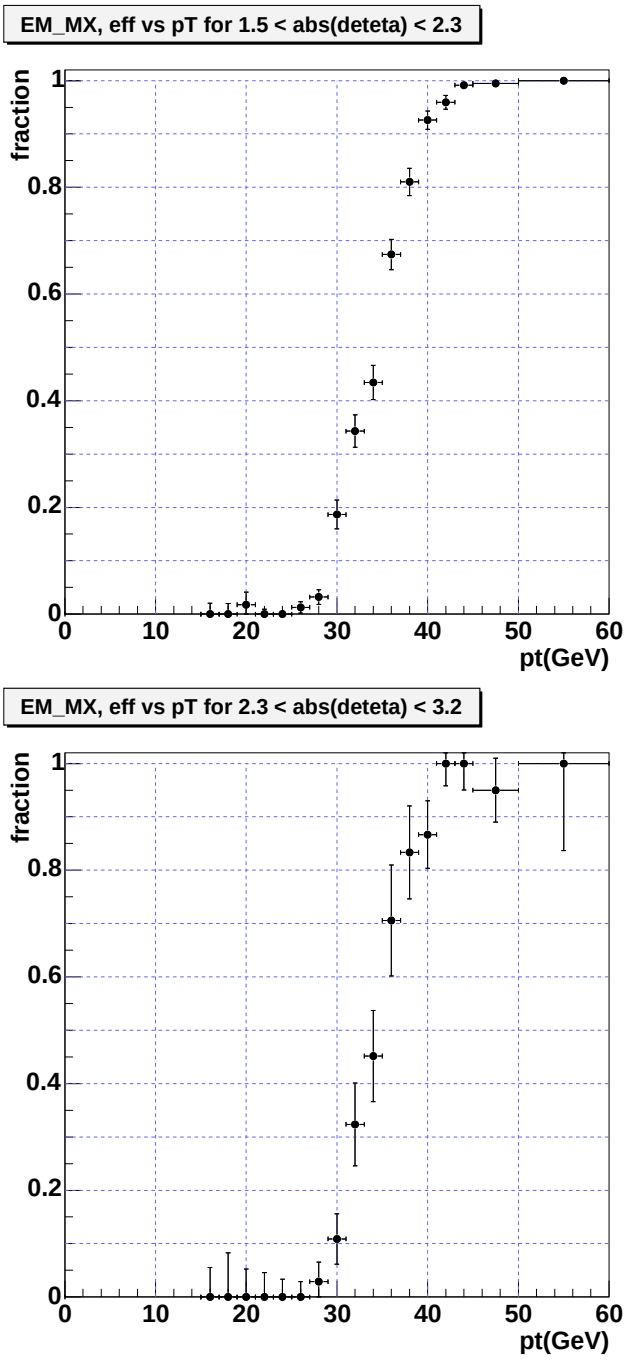

Figure 162: Electron trigger efficiency for EM_MX as a function of E_T for EC(top) and extended EC($2.3 < |\eta_{detector}| < 3.2$) (bottom).

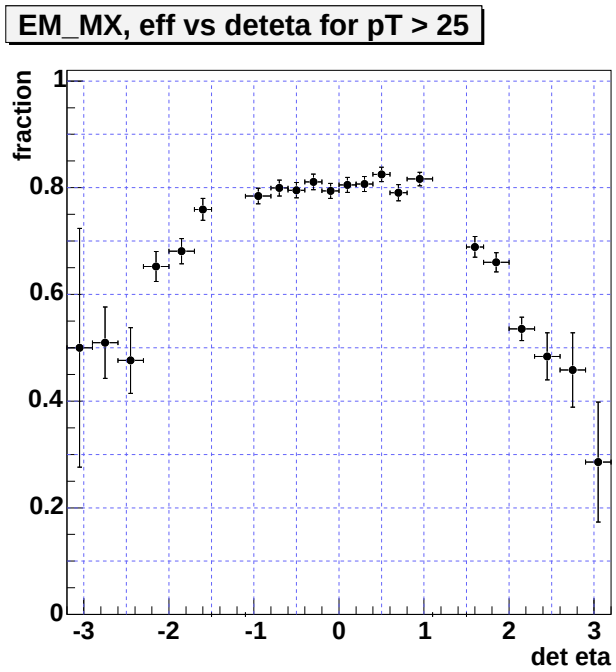

Figure 163: Electron trigger efficiency for EM_MX as a function of detector η.

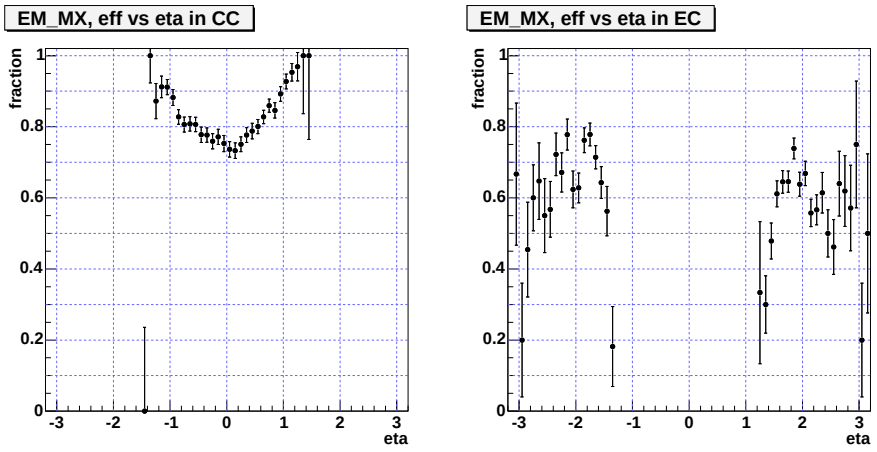

Figure 164: Electron trigger efficiency for EM_MX as a function of physics η for CC(left) and EC(right).

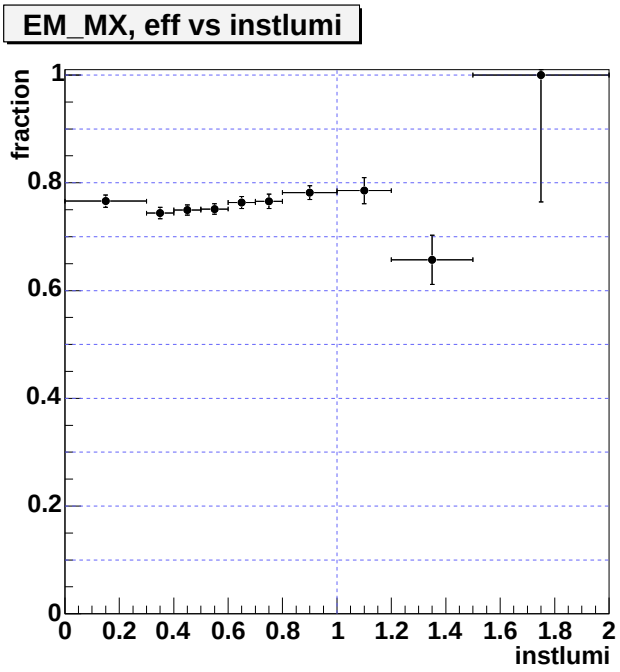

Figure 165: Electron trigger efficiency for EM_MX as a function of instantaneous luminosity($10^{30} cm^{-2} s^{-1}$) for all probes.

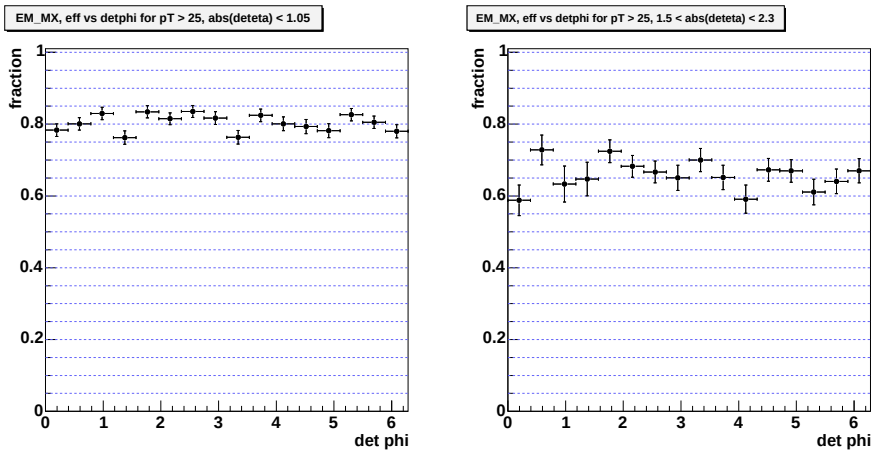

Figure 166: Electron trigger efficiency for EM_MX as a function of detector ϕ for CC(left) and EC(right).

2.8.1 EM_MX: L1

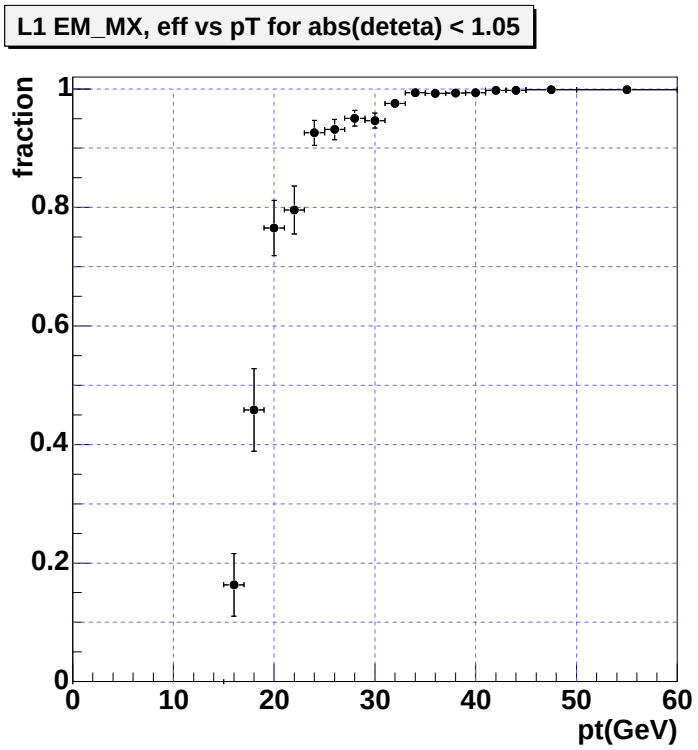

Figure 167: Electron trigger efficiency at L1 for EM_MX as a function of E_T for CC.

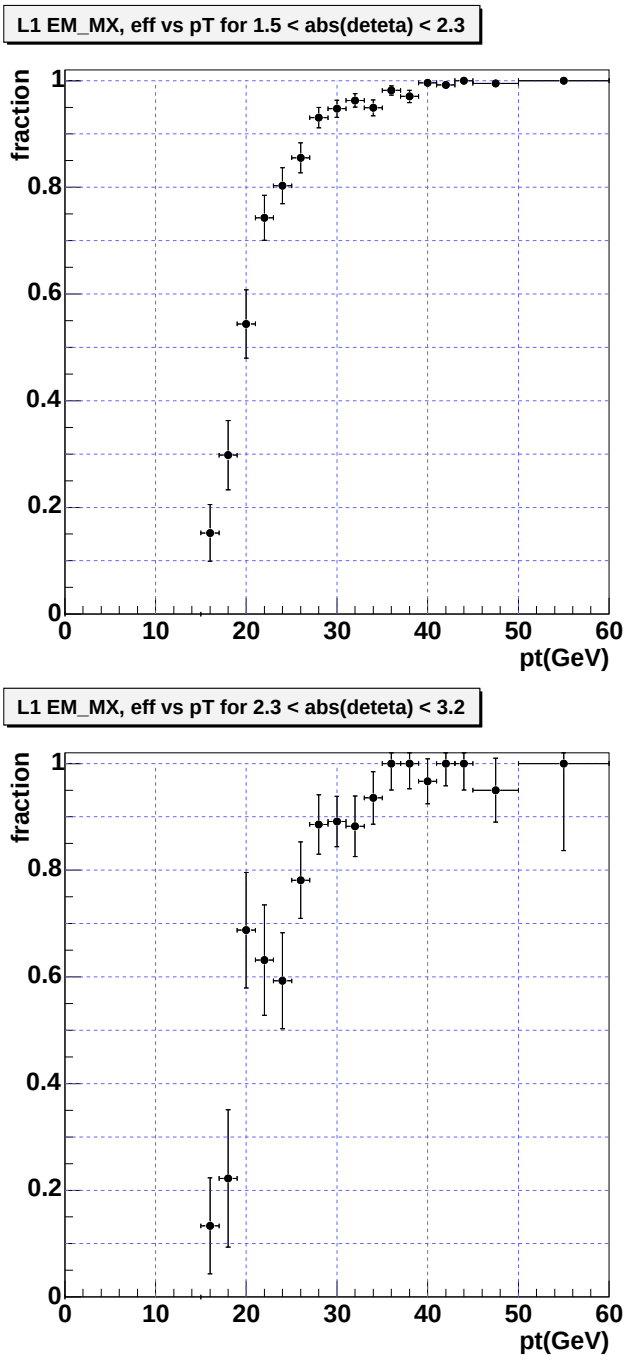

Figure 168: Electron trigger efficiency at L1 for EM_MX as a function of E_T for EC(top) and extended EC($2.3 < |\eta_{detector}| < 3.2$) (bottom).

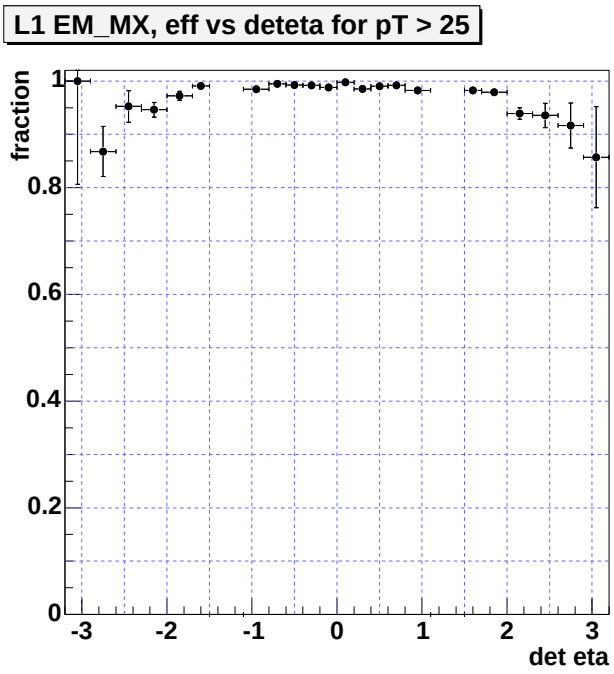

Figure 169: Electron trigger efficiency at L1 for EM_MX as a function of detector η.

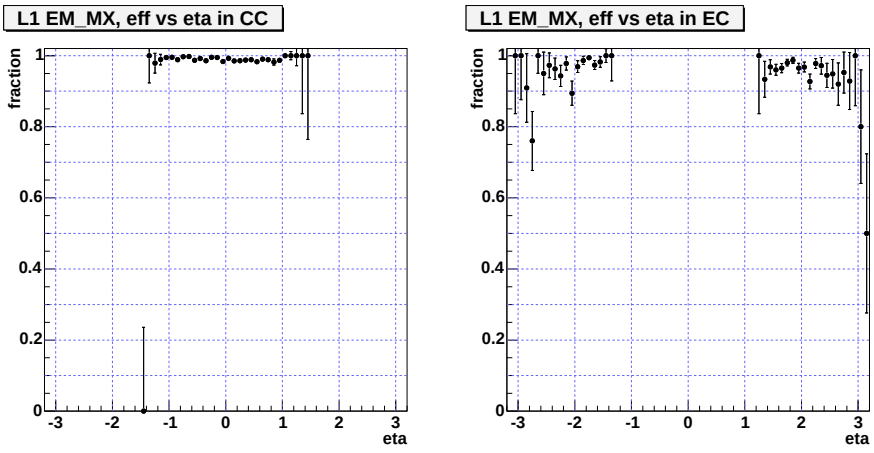

Figure 170: Electron trigger efficiency at L1 for EM_MX as a function of physics η for CC(left) and EC(right).

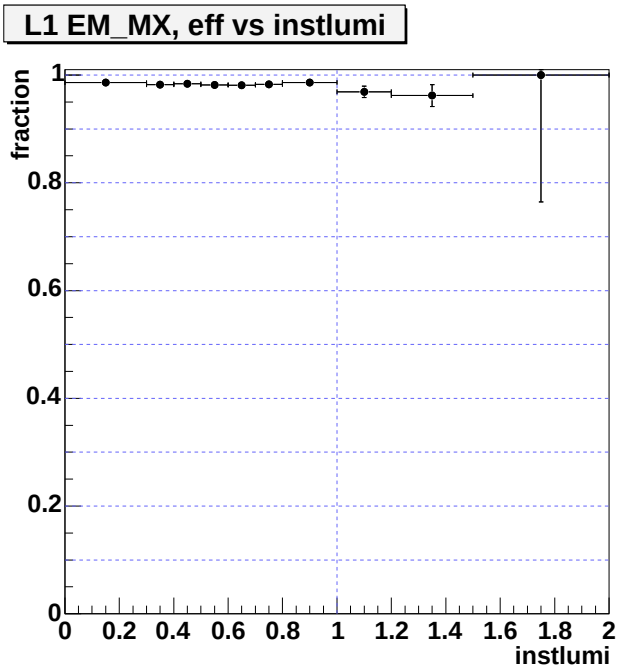

Figure 171: Electron trigger efficiency at L1 for EM_MX as a function of instantaneous luminosity($10^{30} cm^{-2} s^{-1}$) for all probes.

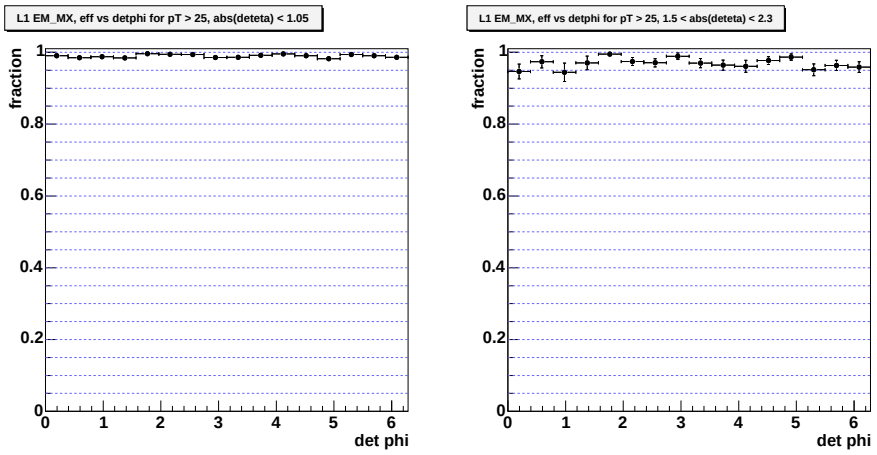

Figure 172: Electron trigger efficiency at L1 for EM_MX as a function of detector ϕ for CC(left) and EC(right).

2.8.2 EM_MX: L3

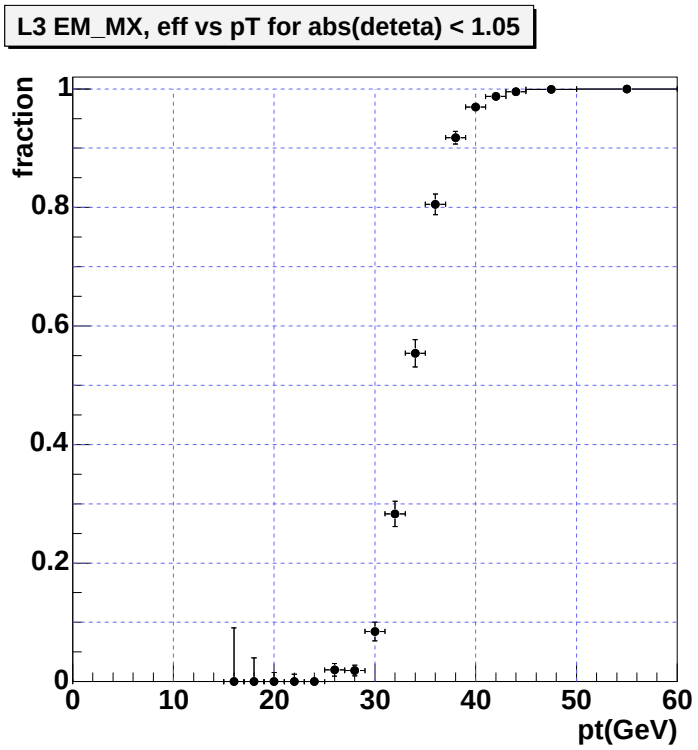

Figure 173: Electron trigger efficiency at L3 for EM_MX as a function of E_T for CC.

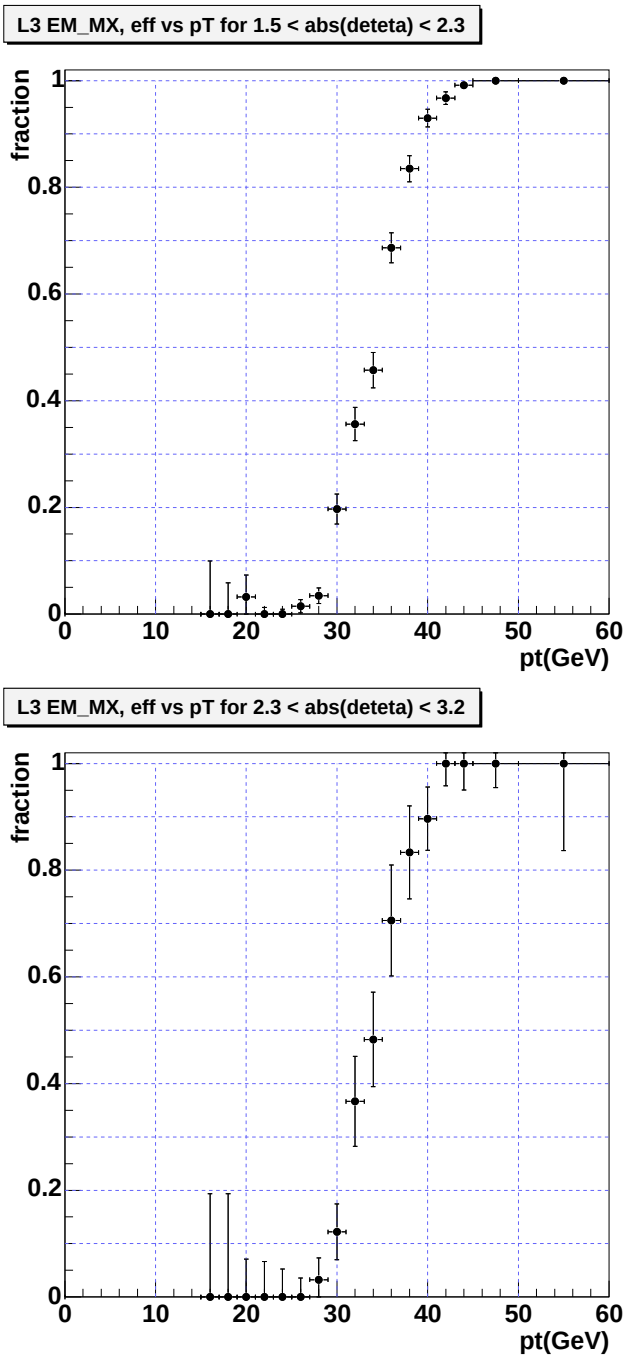

Figure 174: Electron trigger efficiency at L3 for EM_MX as a function of E_T for EC(top) and extended EC($2.3 < |\eta_{detector}| < 3.2$) (bottom).

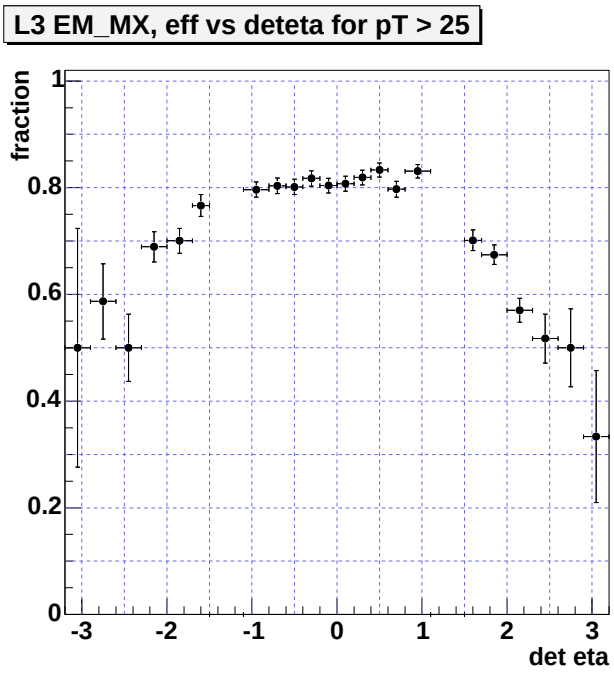

Figure 175: Electron trigger efficiency at L3 for EM_MX as a function of detector η.

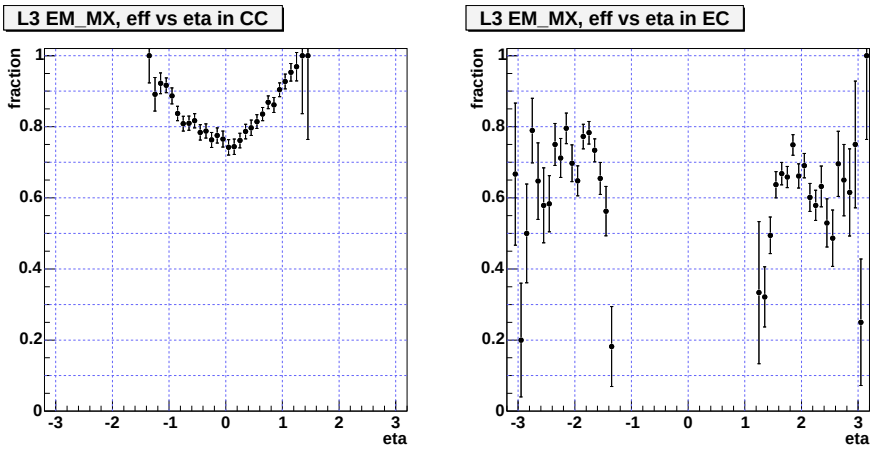

Figure 176: Electron trigger efficiency at L3 for EM_MX as a function of physics η for CC(left) and EC(right).

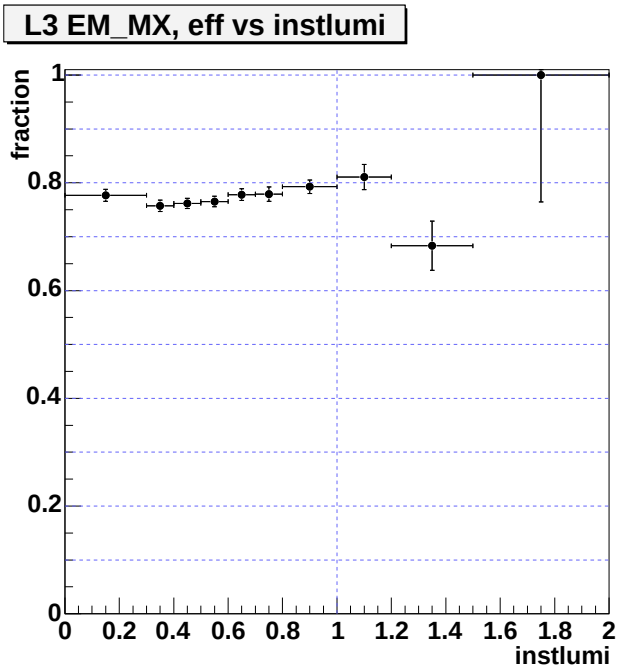

Figure 177: Electron trigger efficiency at L3 for EM_MX as a function of instantaneous luminosity($10^{30} cm^{-2} s^{-1}$) for all probes.

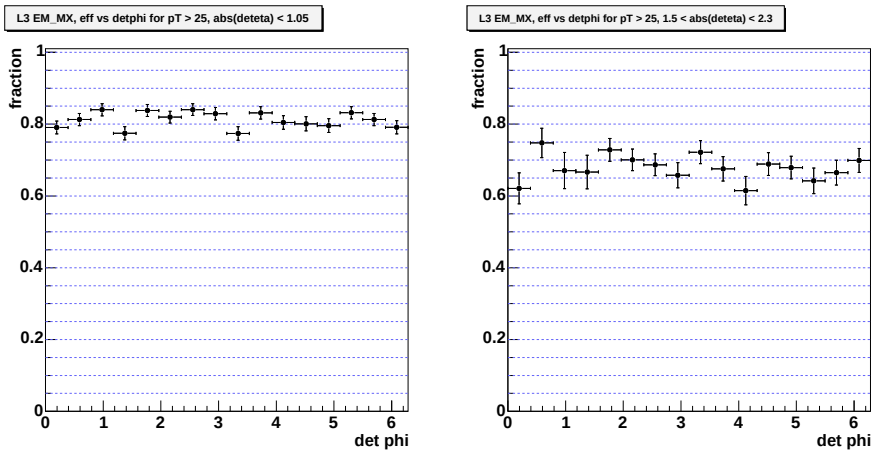

Figure 178: Electron trigger efficiency at L3 for EM_MX as a function of detector ϕ for CC(left) and EC(right).

2.9 E1_SHT20

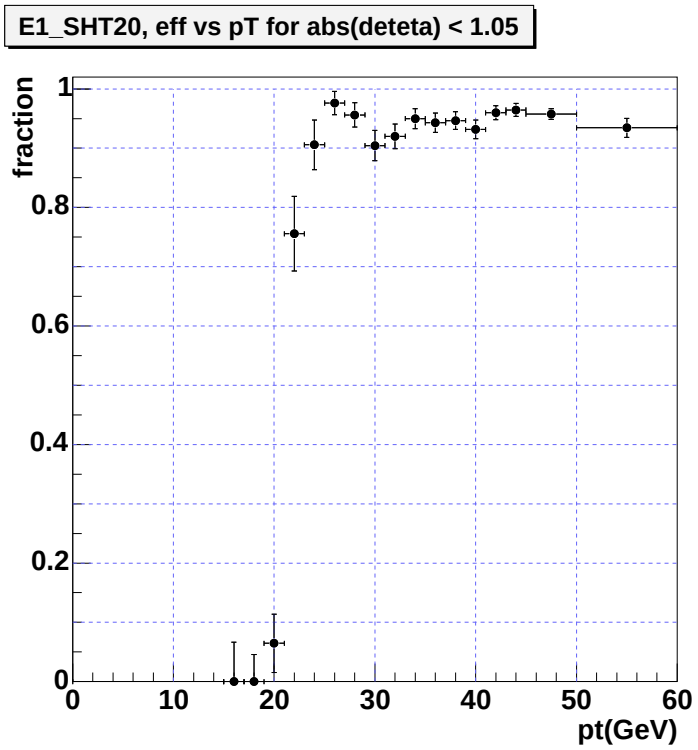

Figure 179: Electron trigger efficiency for E1_SHT20 as a function of E_T for CC.

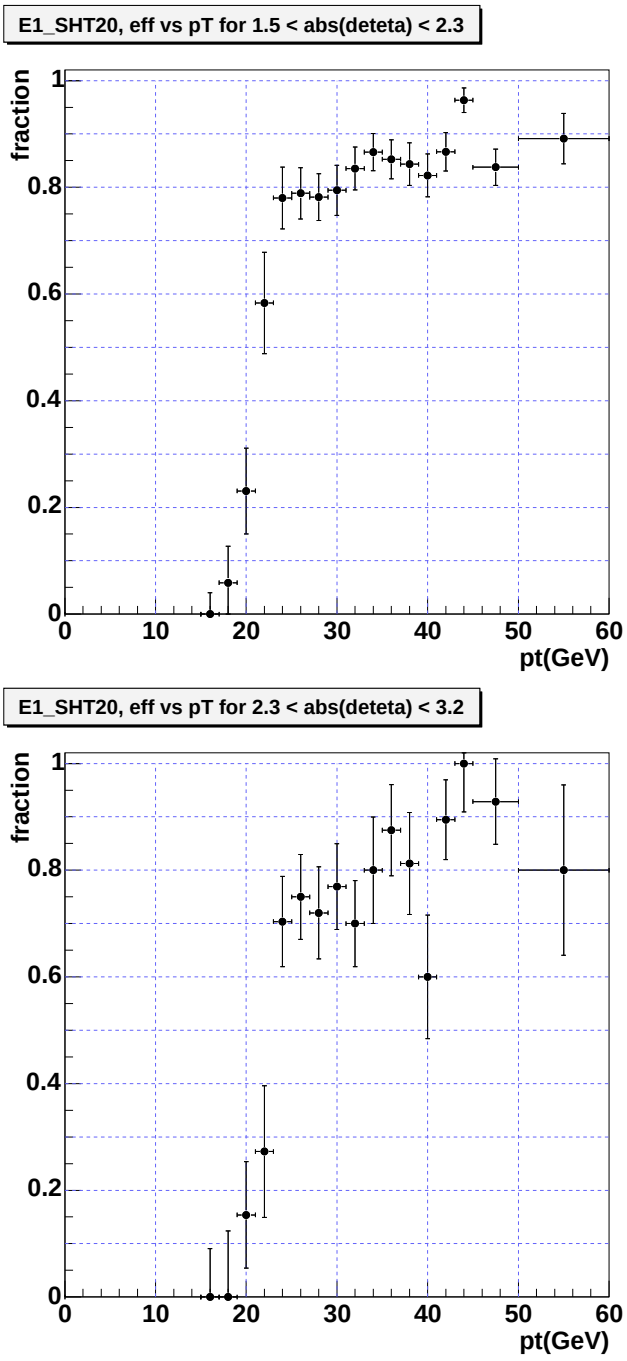

Figure 180: Electron trigger efficiency for E1_SHT20 as a function of E_T for EC(top) and extended EC($2.3 < |\eta_{detector}| < 3.2$) (bottom).

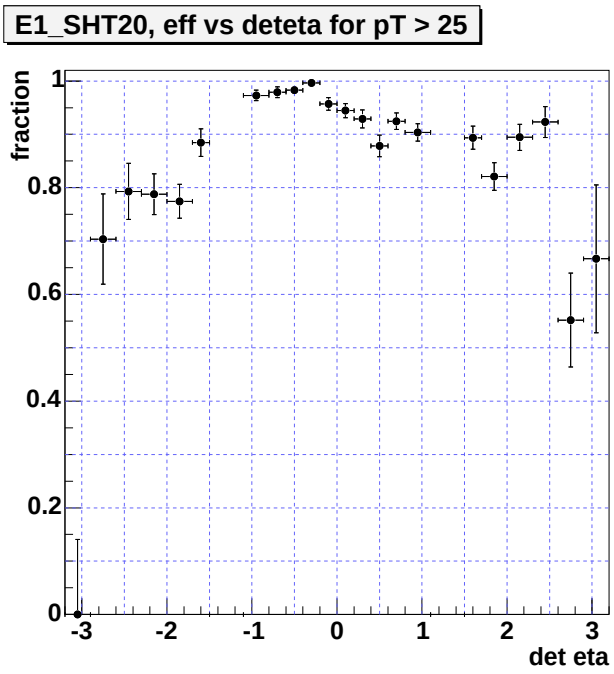

Figure 181: Electron trigger efficiency for E1_SHT20 as a function of detector η.

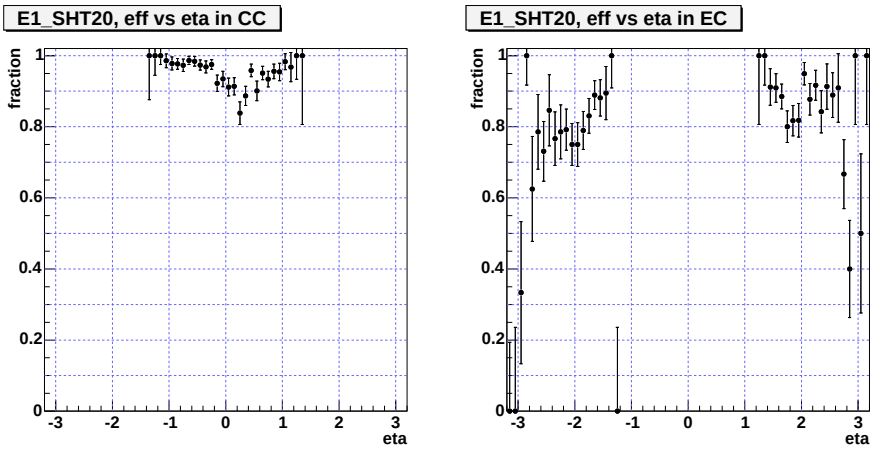

Figure 182: Electron trigger efficiency for E1_SHT20 as a function of physics η for CC(left) and EC(right).

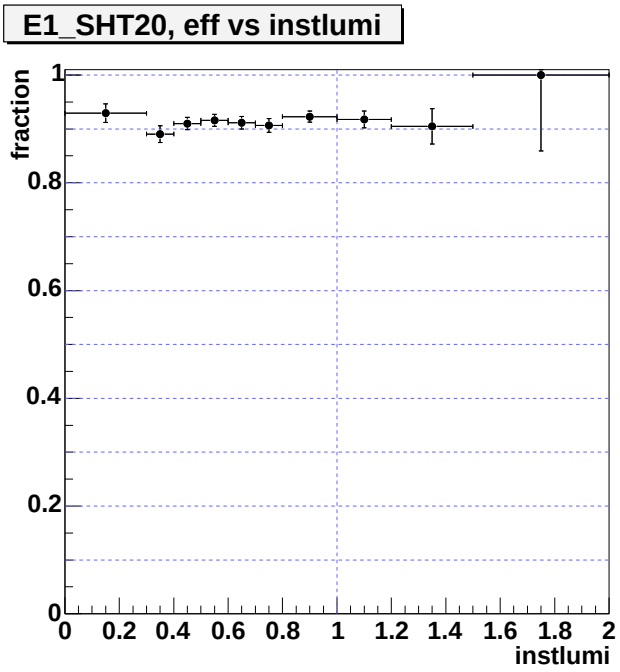

Figure 183: Electron trigger efficiency for E1_SHT20 as a function of instantaneous luminosity($10^{30} cm^{-2} s^{-1}$) for all probes.

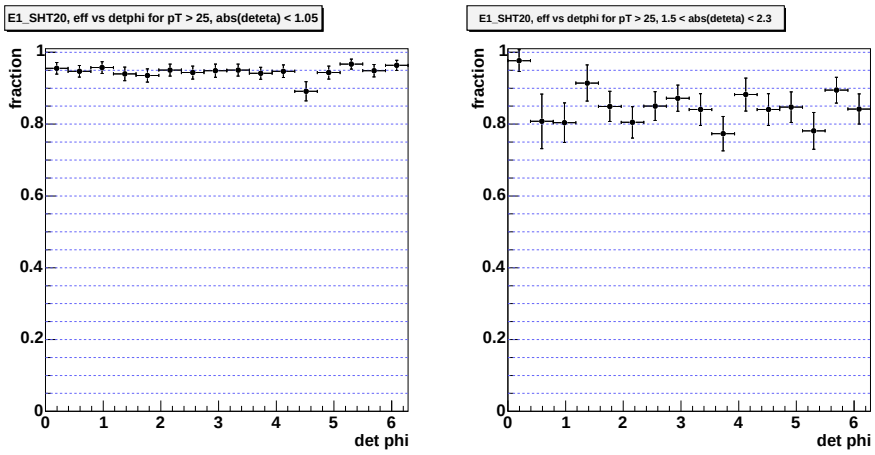

Figure 184: Electron trigger efficiency for E1_SHT20 as a function of detector ϕ for CC(left) and EC(right).

2.9.1 E1_SHT20: L1

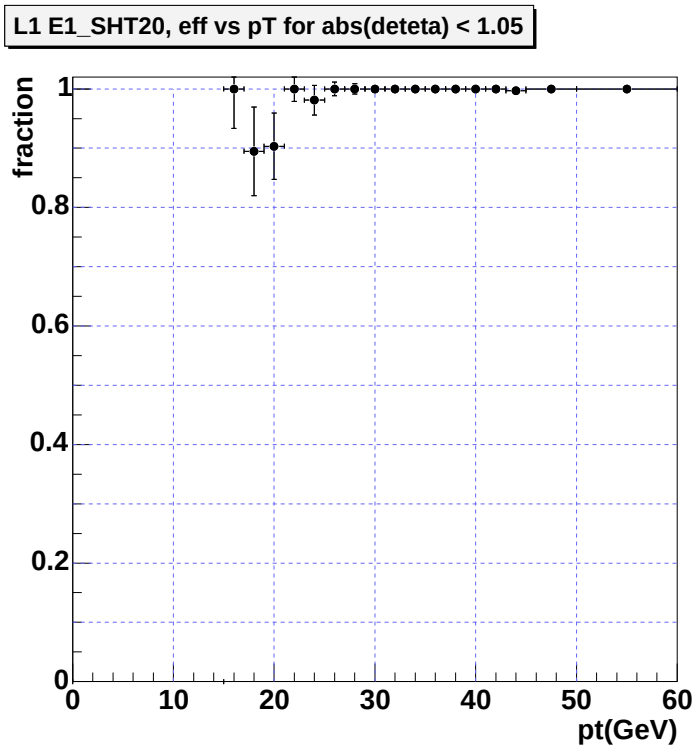

Figure 185: Electron trigger efficiency at L1 for E1_SHT20 as a function of E_T for CC.

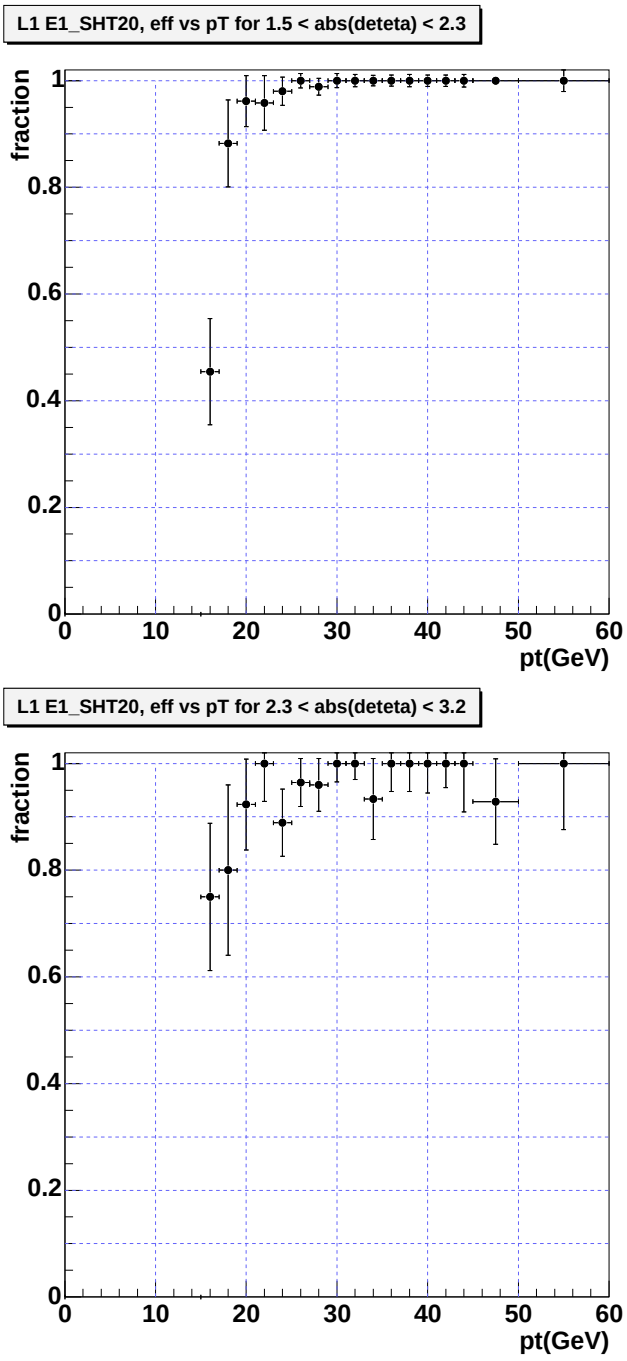

Figure 186: Electron trigger efficiency at L1 for E1_SHT20 as a function of E_T for EC(top) and extended EC($2.3 < |\eta_{detector}| < 3.2$) (bottom).

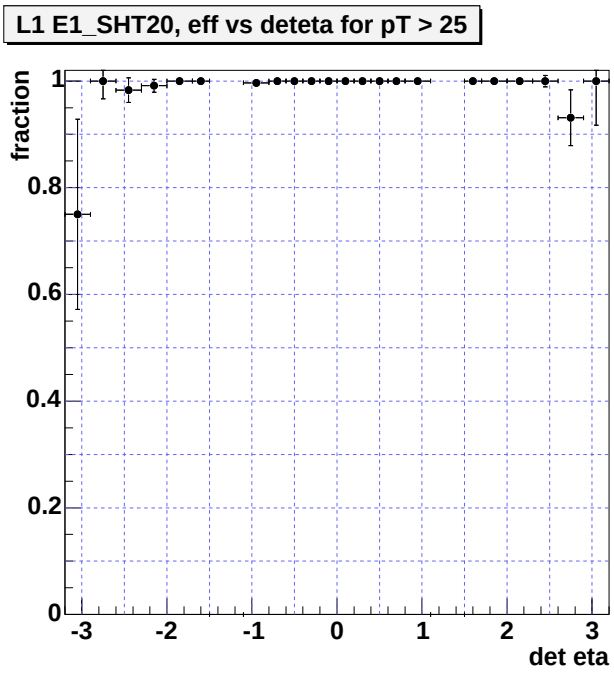

Figure 187: Electron trigger efficiency at L1 for E1_SHT20 as a function of detector η.

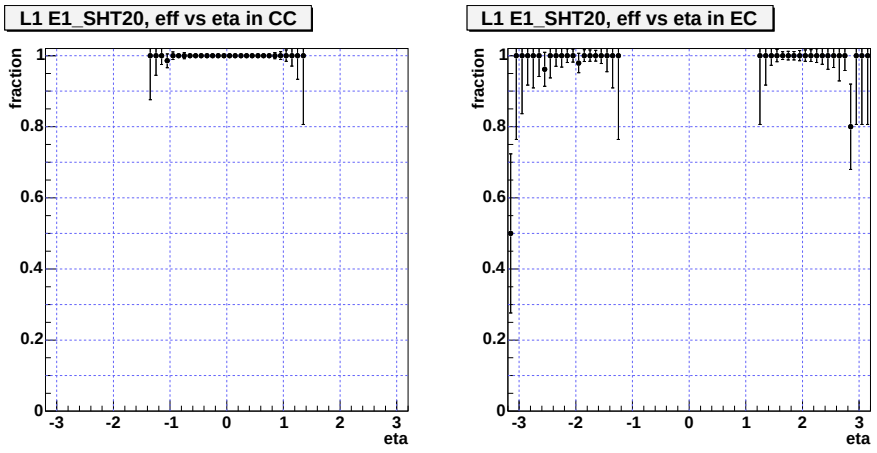

Figure 188: Electron trigger efficiency at L1 for E1_SHT20 as a function of physics η for CC(left) and EC(right).

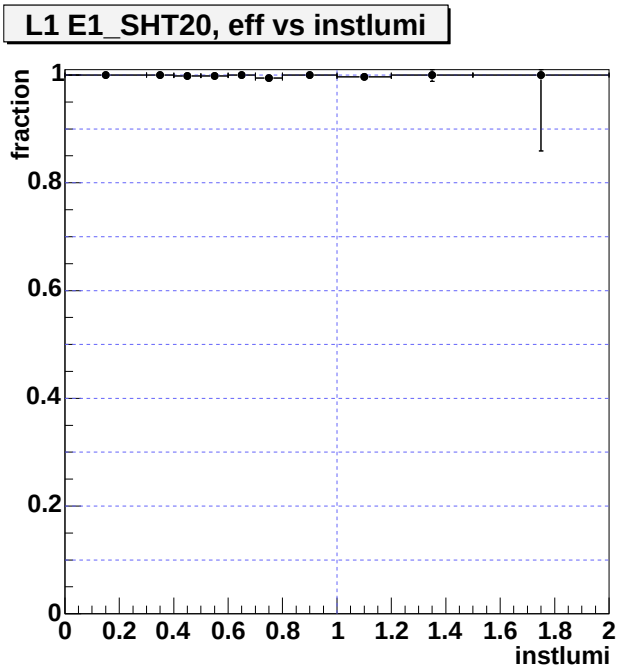

Figure 189: Electron trigger efficiency at L1 for E1_SHT20 as a function of instantaneous luminosity($10^{30} cm^{-2} s^{-1}$) for all probes.

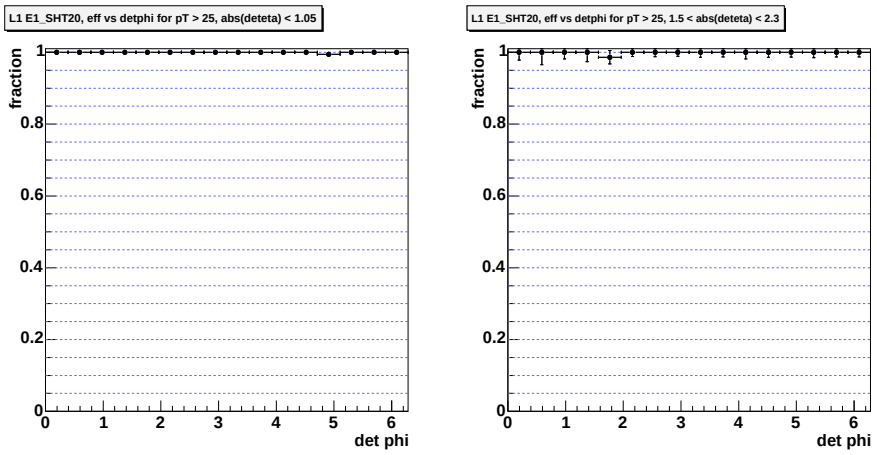

Figure 190: Electron trigger efficiency at L1 for E1_SHT20 as a function of detector ϕ for CC(left) and EC(right).

2.9.2 E1_SHT20: L3

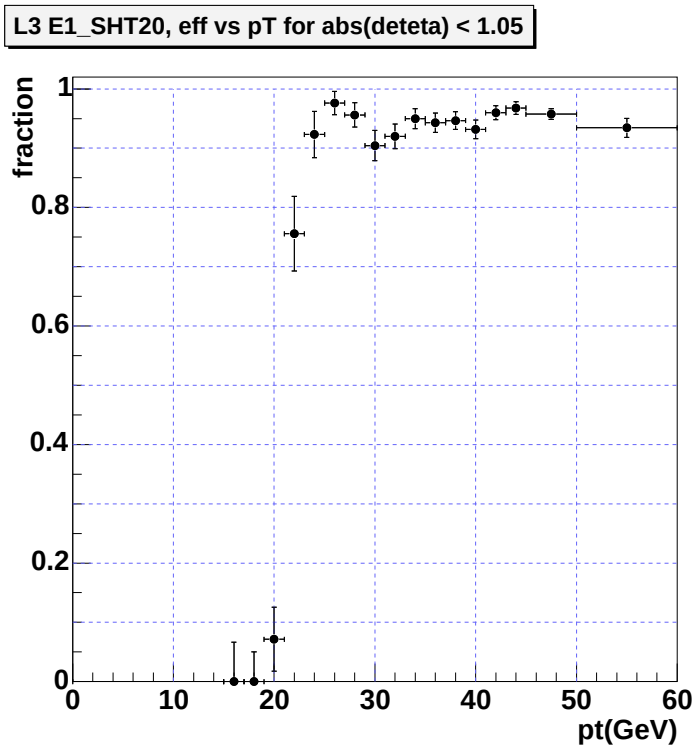

Figure 191: Electron trigger efficiency at L3 for E1_SHT20 as a function of E_T for CC.

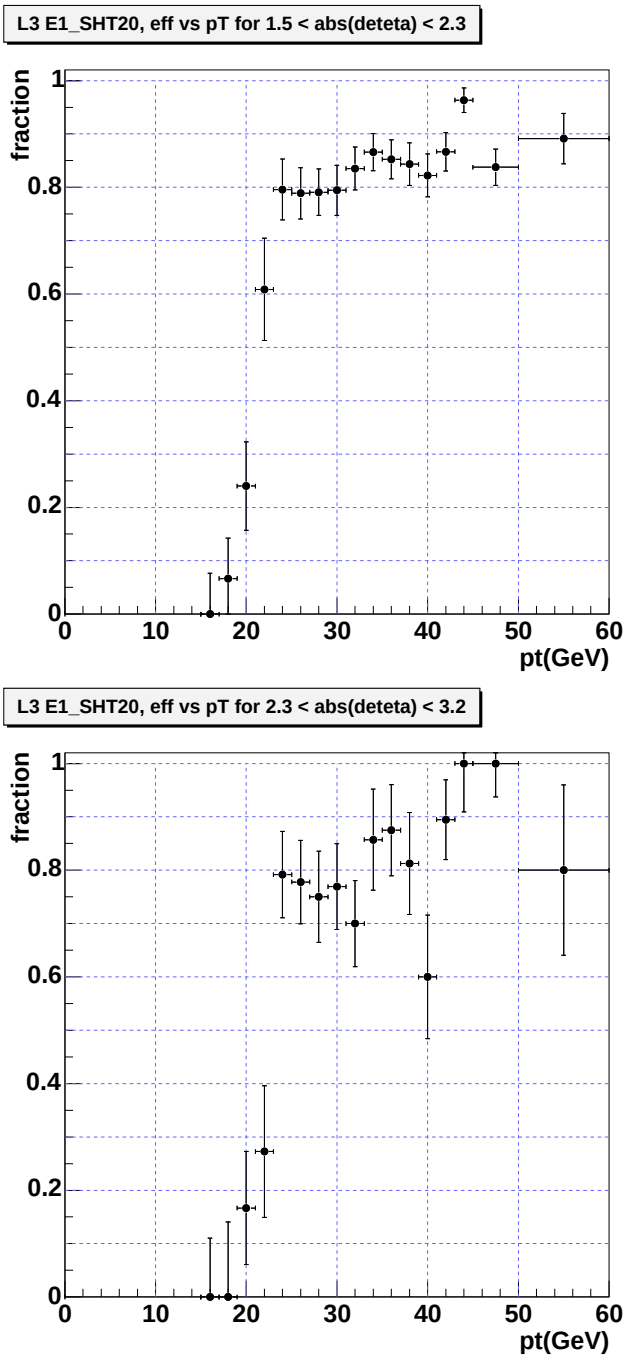

Figure 192: Electron trigger efficiency at L3 for E1_SHT20 as a function of E_T for EC(top) and extended EC($2.3 < |\eta_{detector}| < 3.2$) (bottom).

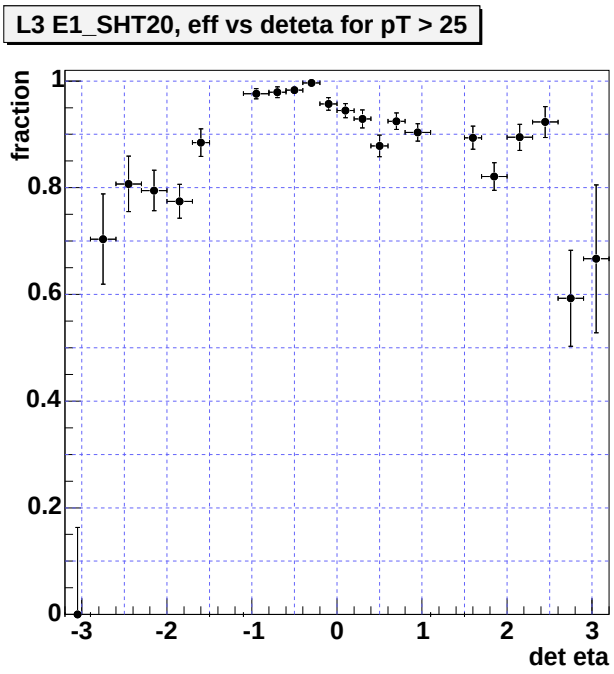

Figure 193: Electron trigger efficiency at L3 for E1_SHT20 as a function of detector η.

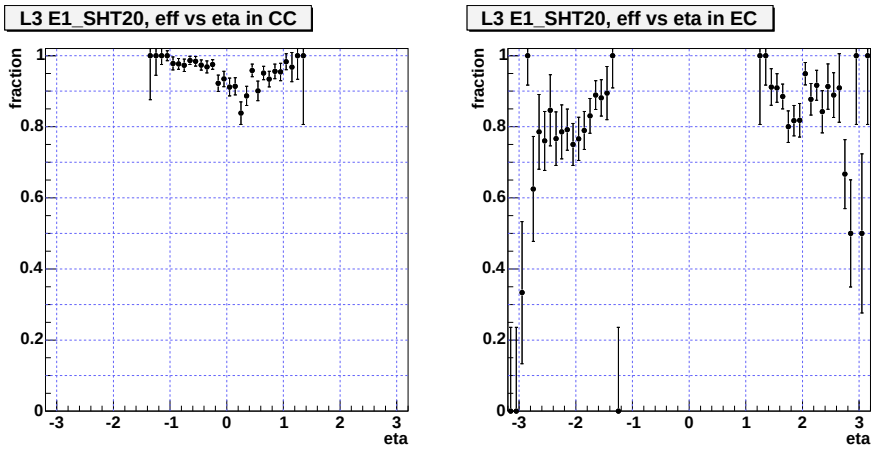

Figure 194: Electron trigger efficiency at L3 for E1_SHT20 as a function of physics η for CC(left) and EC(right).

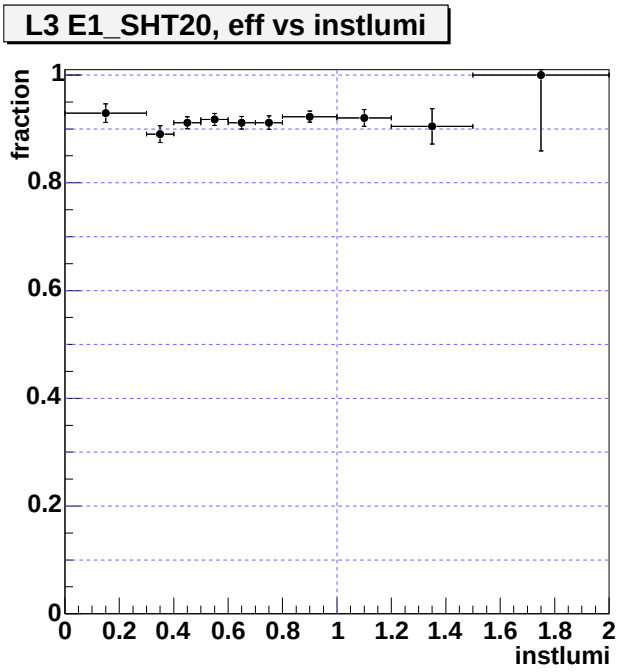

Figure 195: Electron trigger efficiency at L3 for E1_SHT20 as a function of instantaneous luminosity($10^{30} cm^{-2} s^{-1}$) for all probes.

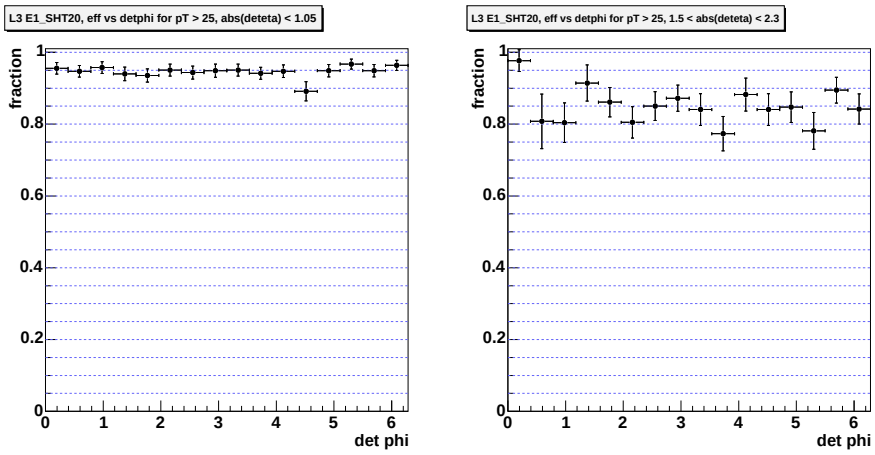

Figure 196: Electron trigger efficiency at L3 for E1_SHT20 as a function of detector ϕ for CC(left) and EC(right).

2.10 E2_SHT20

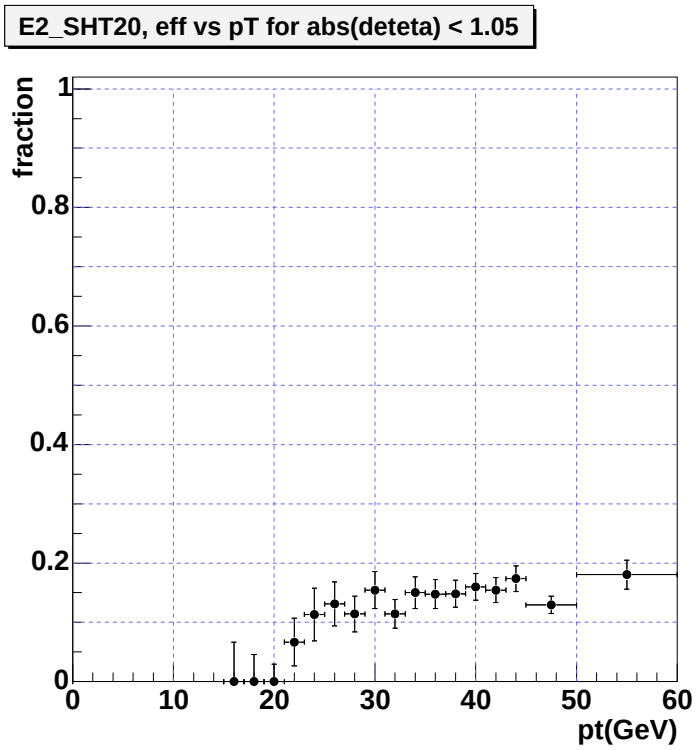

Figure 197: Electron trigger efficiency for E2_SHT20 as a function of E_T for CC.

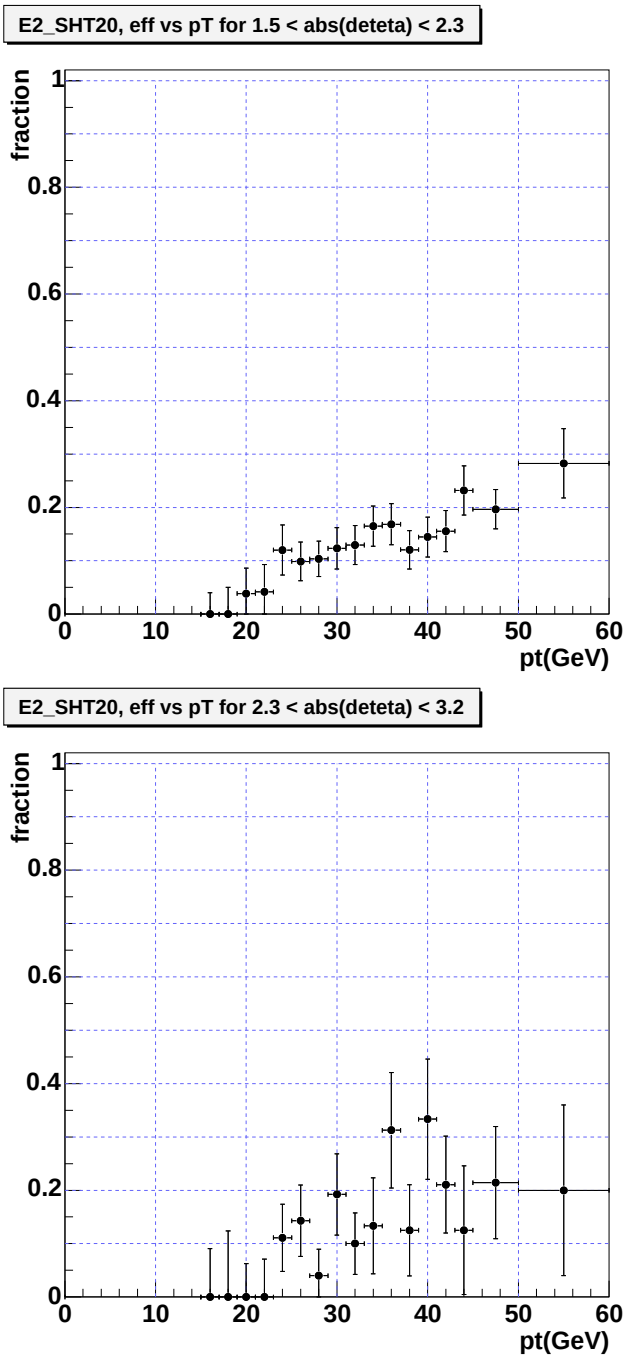

Figure 198: Electron trigger efficiency for E2_SHT20 as a function of E_T for EC(top) and extended EC($2.3 < |\eta_{detector}| < 3.2$) (bottom).

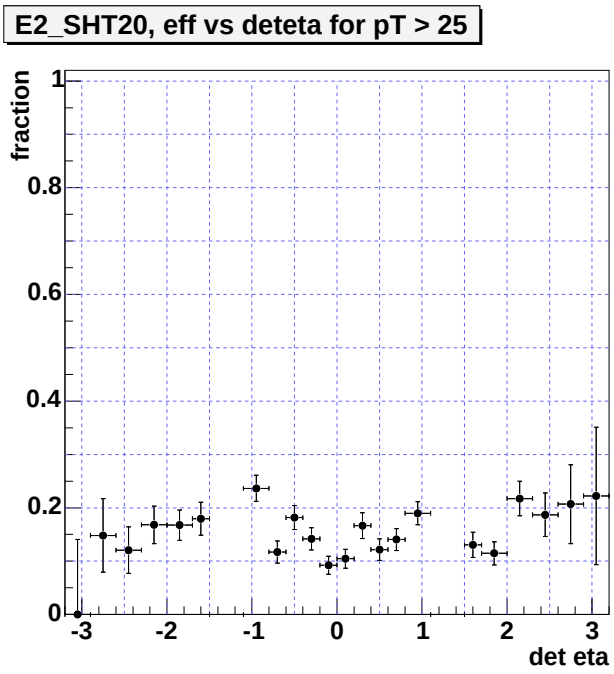

Figure 199: Electron trigger efficiency for E2_SHT20 as a function of detector η.

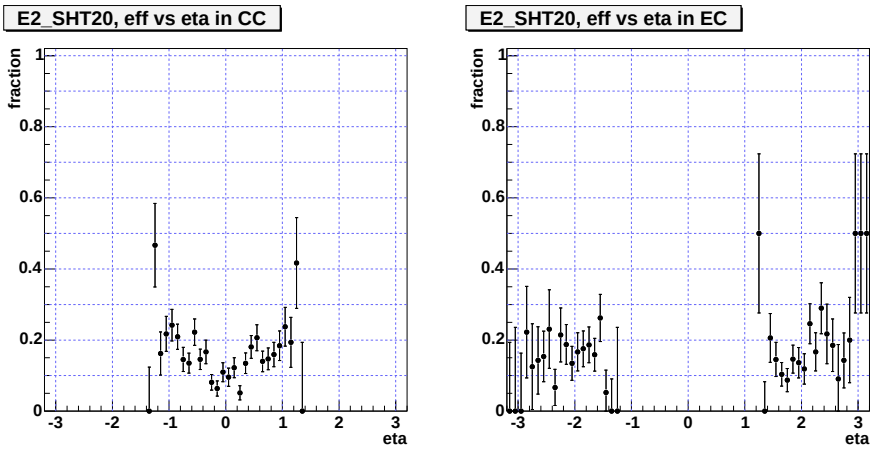

Figure 200: Electron trigger efficiency for E2_SHT20 as a function of physics η for CC(left) and EC(right).

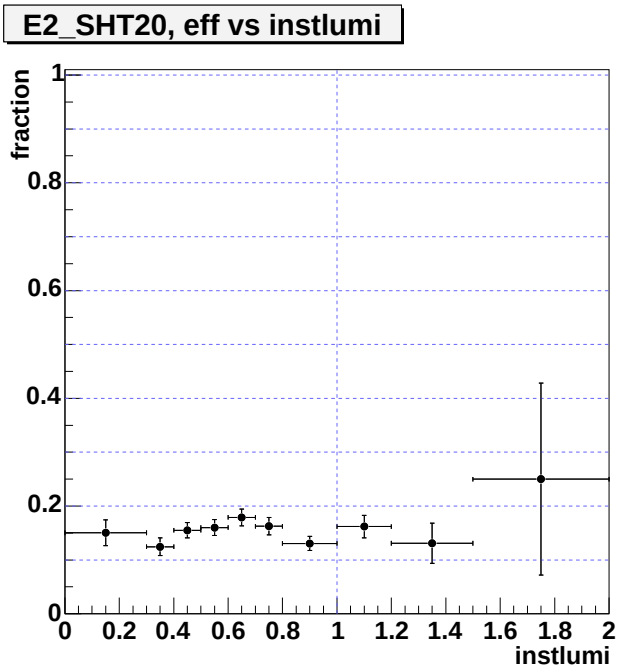

Figure 201: Electron trigger efficiency for E2_SHT20 as a function of instantaneous luminosity($10^{30} cm^{-2} s^{-1}$) for all probes.

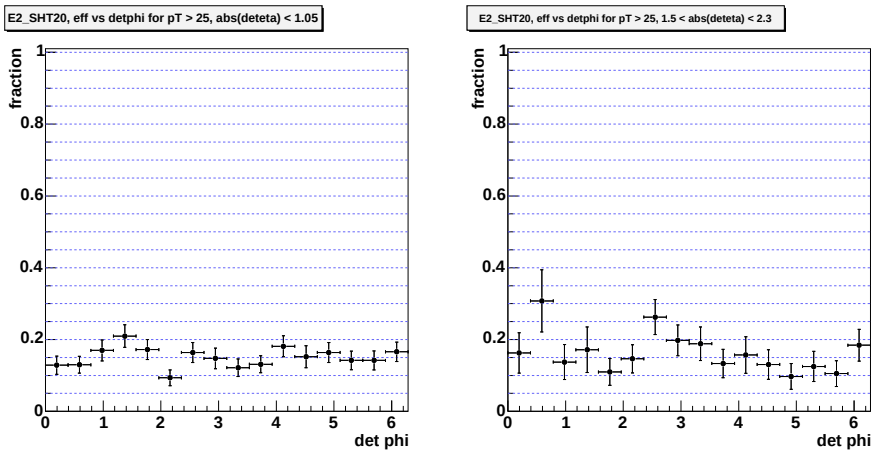

Figure 202: Electron trigger efficiency for E2_SHT20 as a function of detector ϕ for CC(left) and EC(right).

2.10.1 E2_SHT20: L1

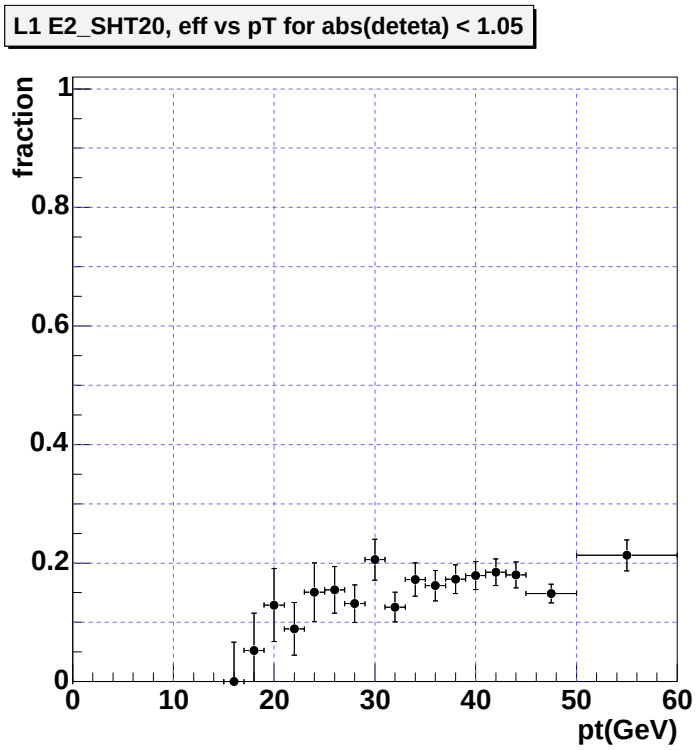

Figure 203: Electron trigger efficiency at L1 for E2_SHT20 as a function of E_T for CC.

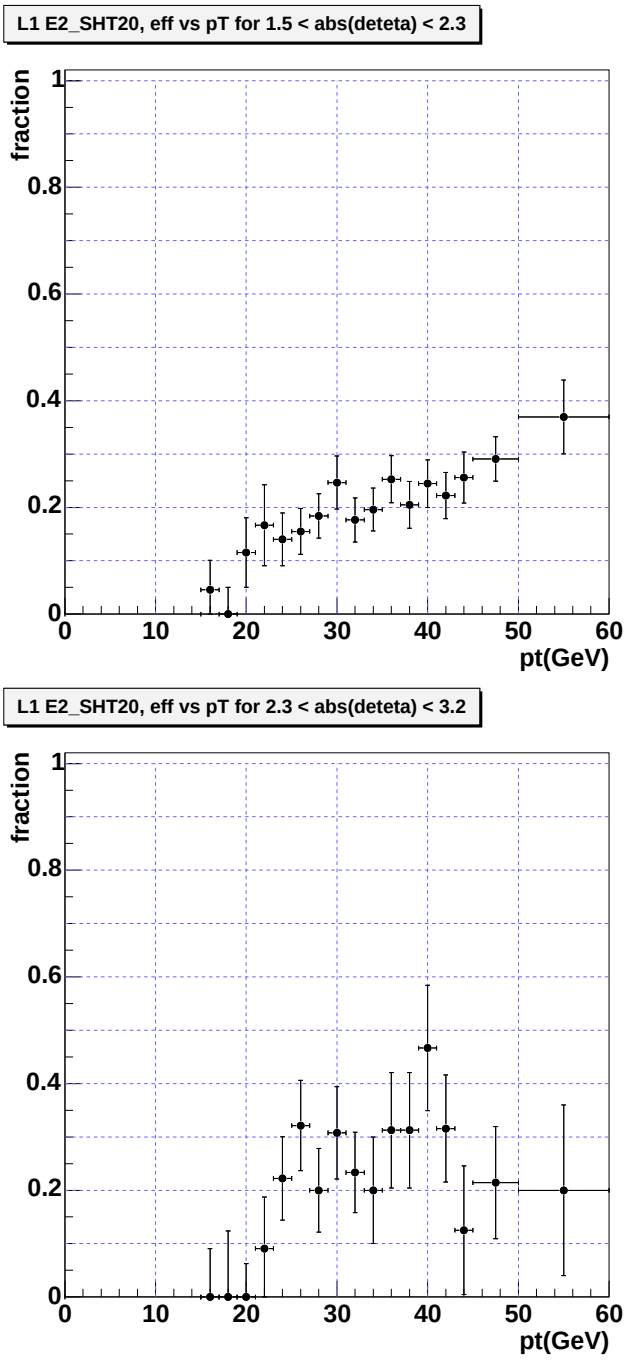

Figure 204: Electron trigger efficiency at L1 for E2_SHT20 as a function of E_T for EC(top) and extended EC($2.3 < |\eta_{detector}| < 3.2$) (bottom).

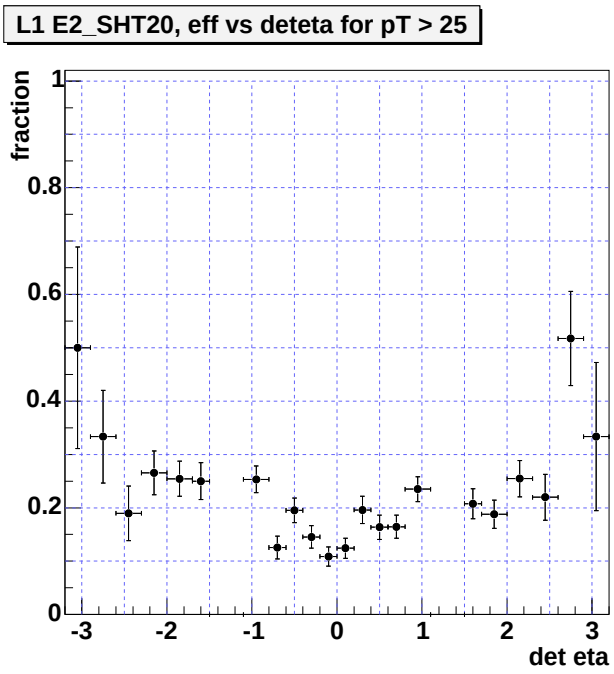

Figure 205: Electron trigger efficiency at L1 for E2_SHT20 as a function of detector η.

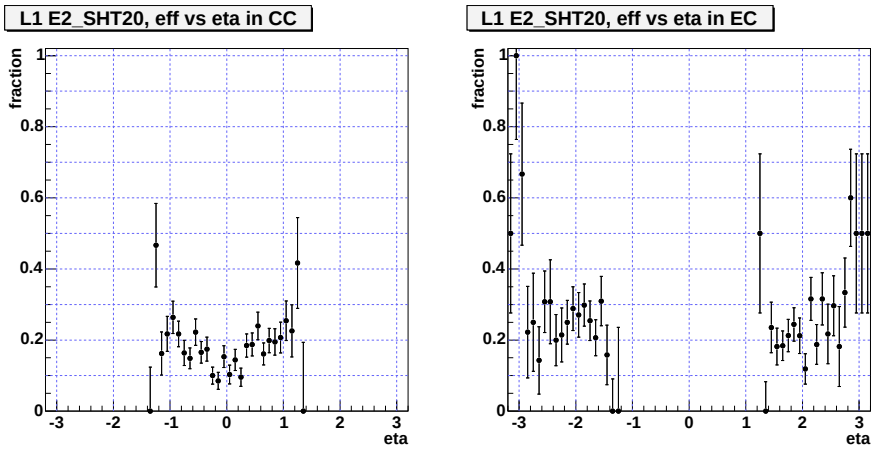

Figure 206: Electron trigger efficiency at L1 for E2_SHT20 as a function of physics η for CC(left) and EC(right).

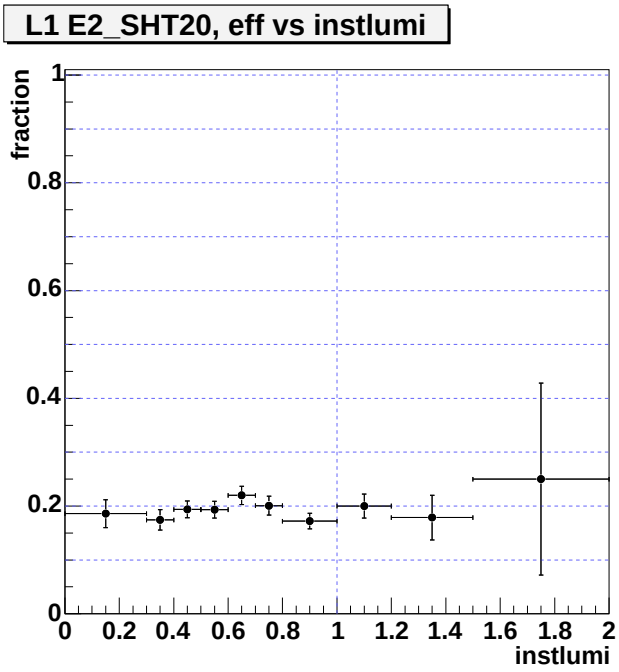

Figure 207: Electron trigger efficiency at L1 for E2_SHT20 as a function of instantaneous luminosity($10^{30} cm^{-2} s^{-1}$) for all probes.

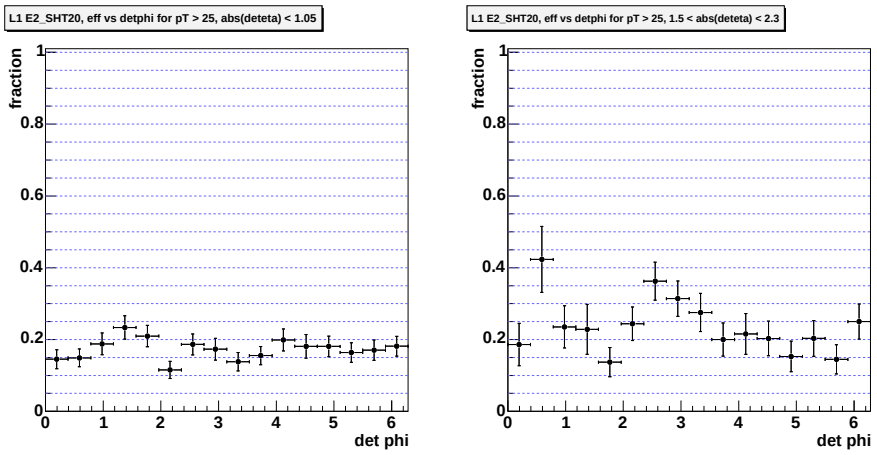

Figure 208: Electron trigger efficiency at L1 for E2_SHT20 as a function of detector ϕ for CC(left) and EC(right).

2.10.2 E2_SHT20: L3

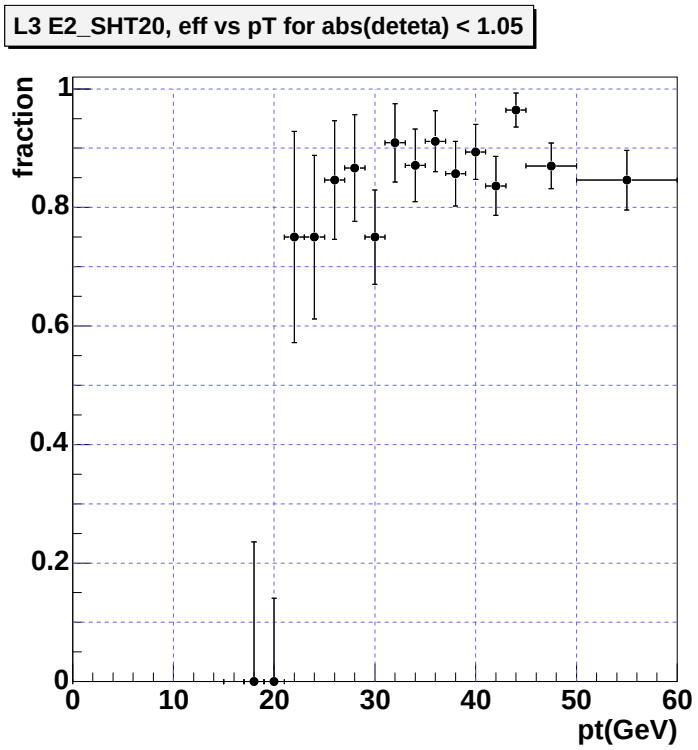

Figure 209: Electron trigger efficiency at L3 for E2_SHT20 as a function of E_T for CC.

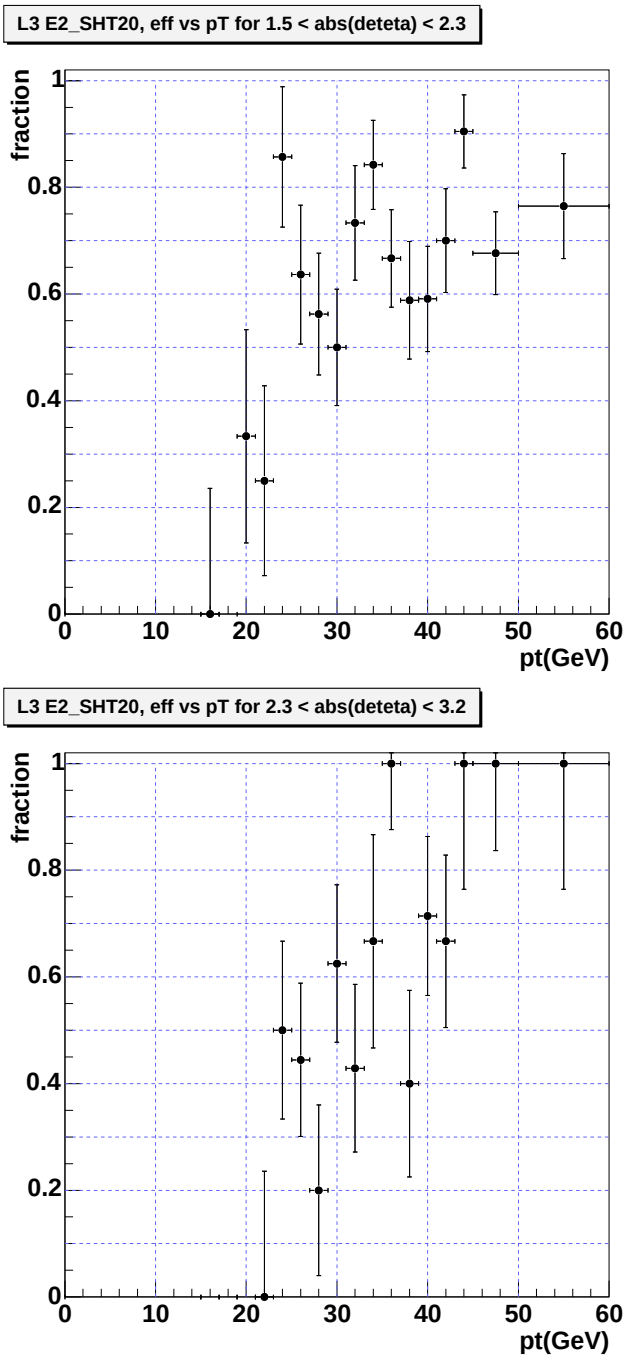

Figure 210: Electron trigger efficiency at L3 for E2_SHT20 as a function of E_T for EC(top) and extended EC($2.3 < |\eta_{detector}| < 3.2$) (bottom).

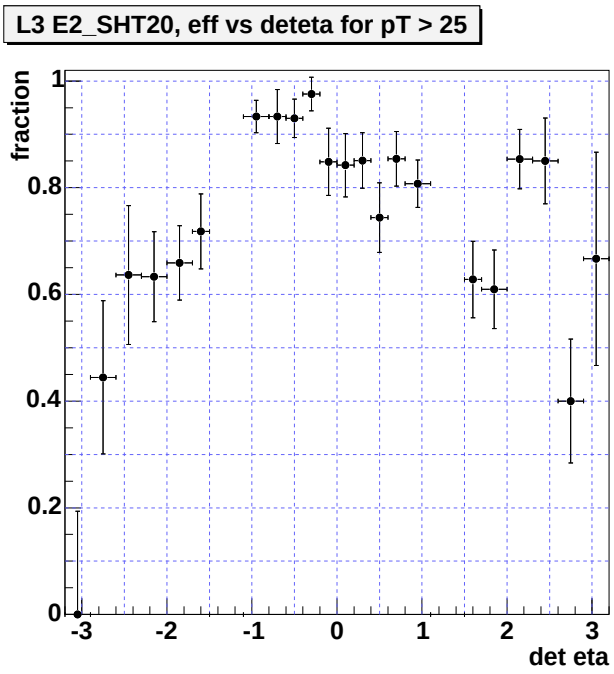

Figure 211: Electron trigger efficiency at L3 for E2_SHT20 as a function of detector η.

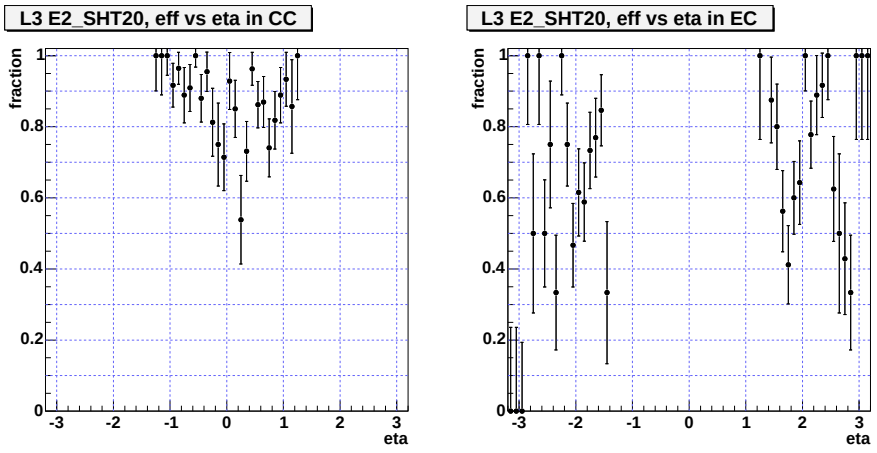

Figure 212: Electron trigger efficiency at L3 for E2_SHT20 as a function of physics η for CC(left) and EC(right).

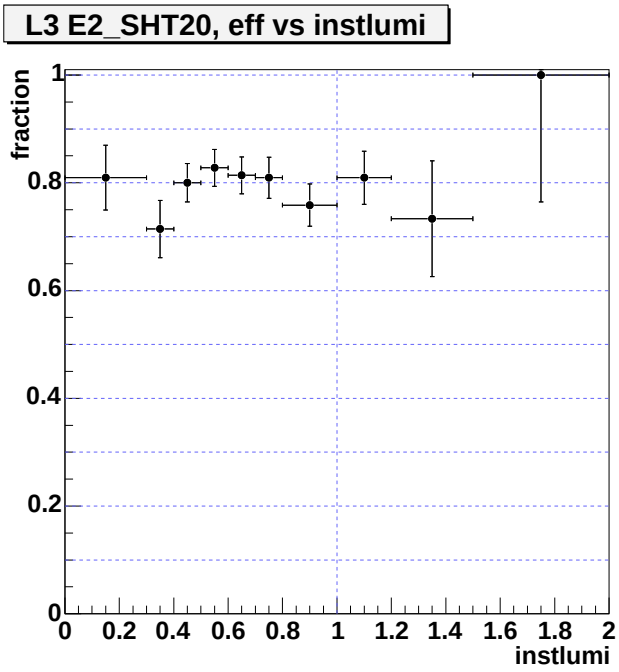

Figure 213: Electron trigger efficiency at L3 for E2_SHT20 as a function of instantaneous luminosity($10^{30} cm^{-2} s^{-1}$) for all probes.

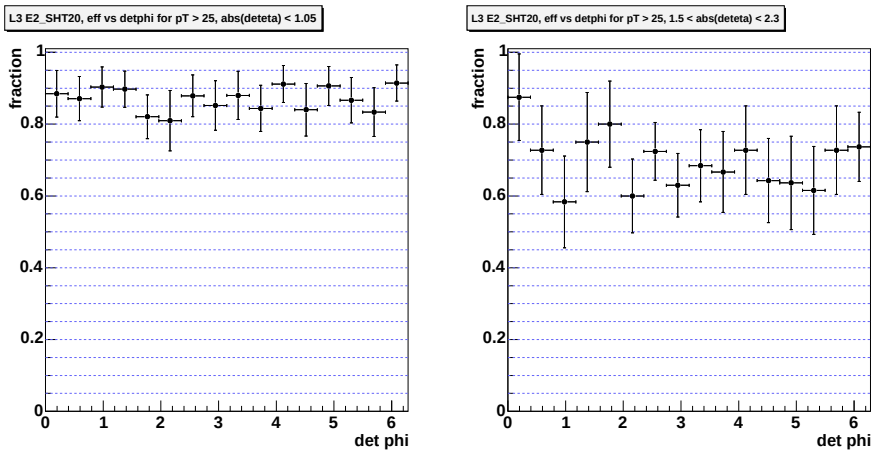

Figure 214: Electron trigger efficiency at L3 for E2_SHT20 as a function of detector ϕ for CC(left) and EC(right).

2.11 E3_SHT20

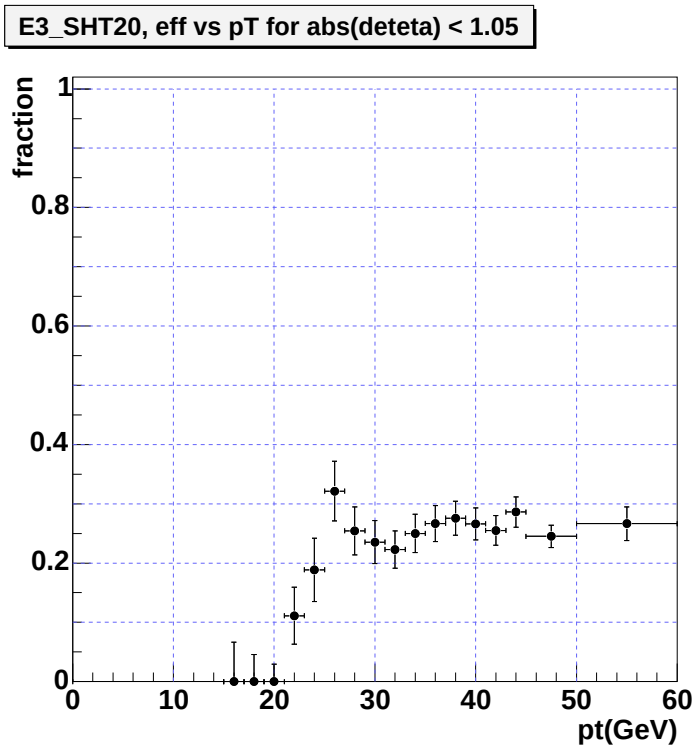

Figure 215: Electron trigger efficiency for E3_SHT20 as a function of E_T for CC.

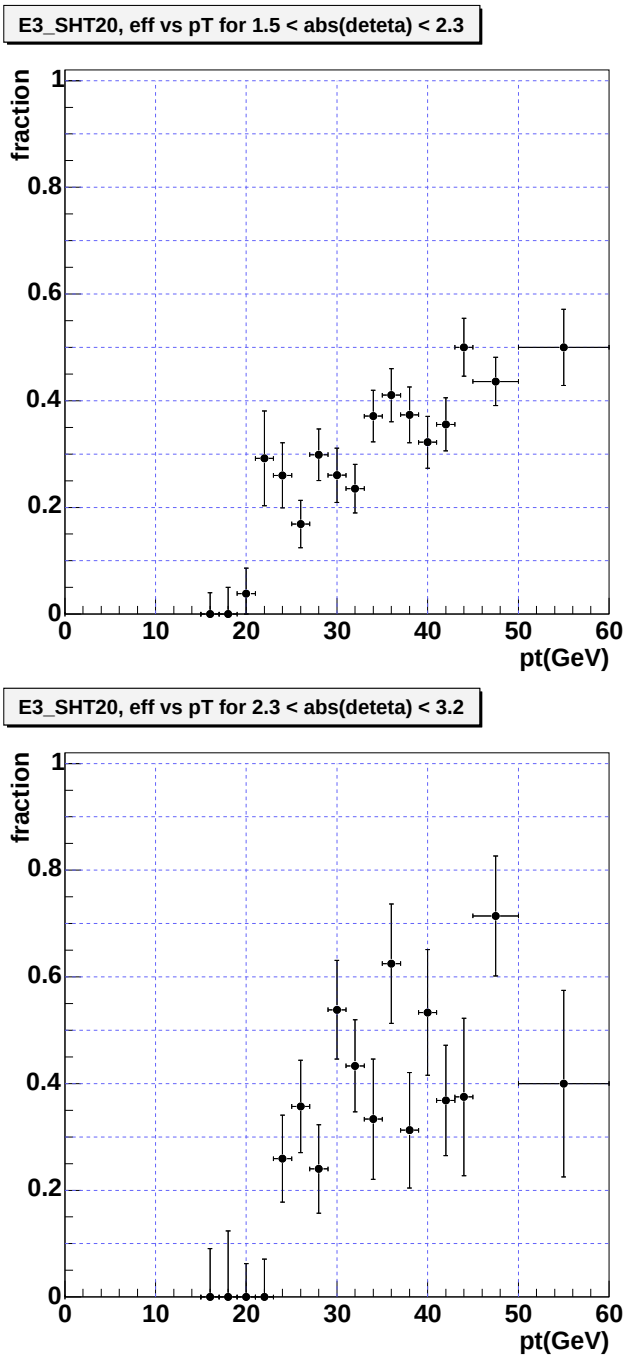

Figure 216: Electron trigger efficiency for E3_SHT20 as a function of E_T for EC(top) and extended EC($2.3 < |\eta_{detector}| < 3.2$) (bottom).

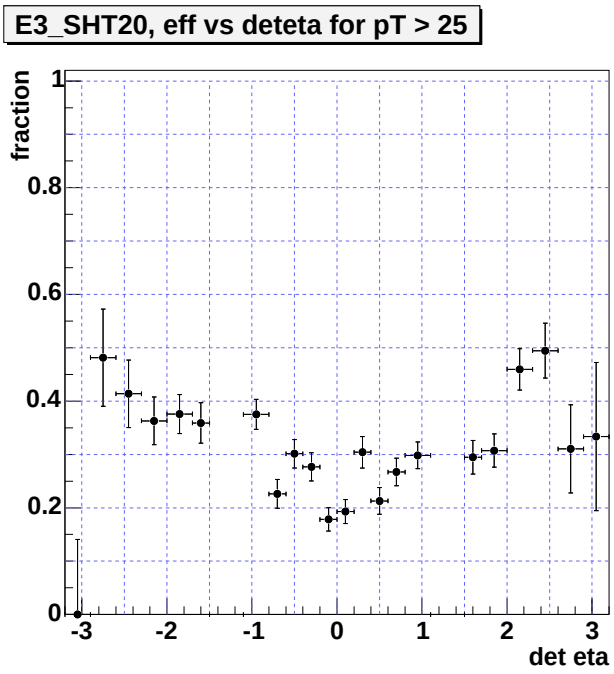

Figure 217: Electron trigger efficiency for E3_SHT20 as a function of detector η.

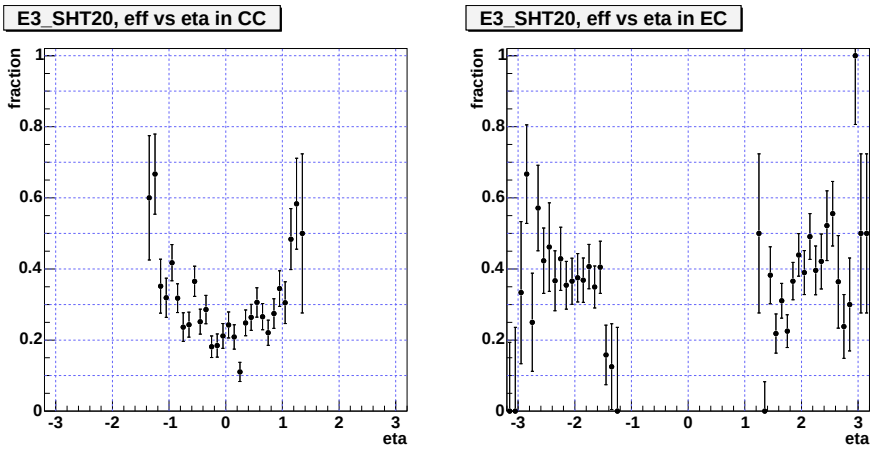

Figure 218: Electron trigger efficiency for E3_SHT20 as a function of physics η for CC(left) and EC(right).

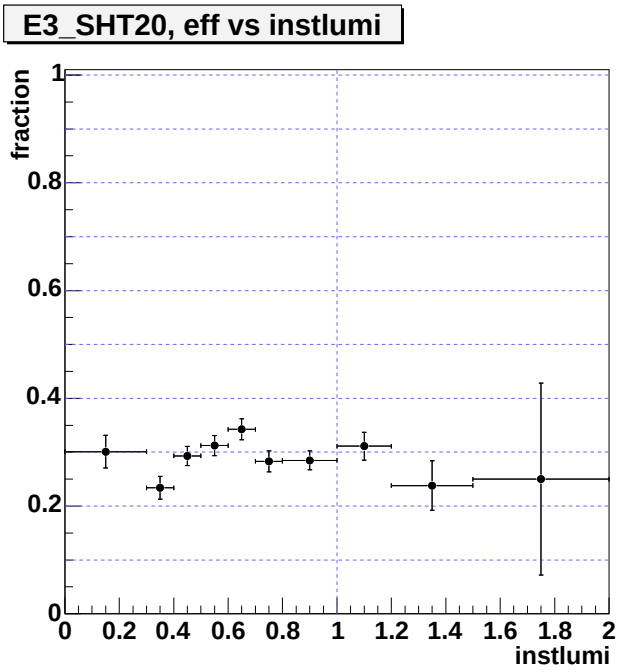

Figure 219: Electron trigger efficiency for E3_SHT20 as a function of instantaneous luminosity($10^{30} cm^{-2} s^{-1}$) for all probes.

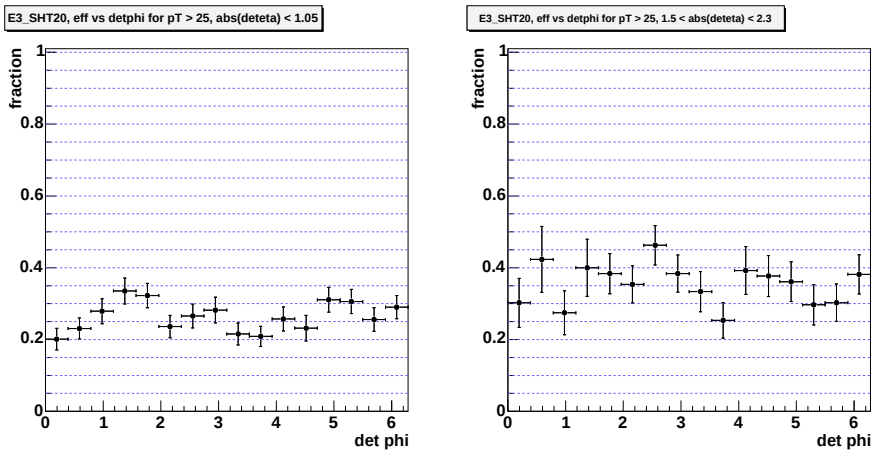

Figure 220: Electron trigger efficiency for E3_SHT20 as a function of detector ϕ for CC(left) and EC(right).

2.11.1 E3_SHT20: L1

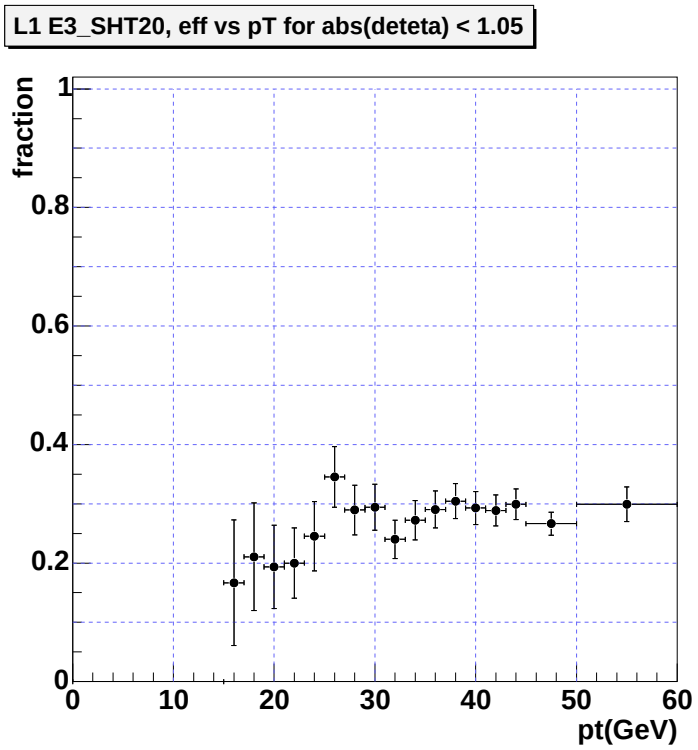

Figure 221: Electron trigger efficiency at L1 for E3_SHT20 as a function of E_T for CC.

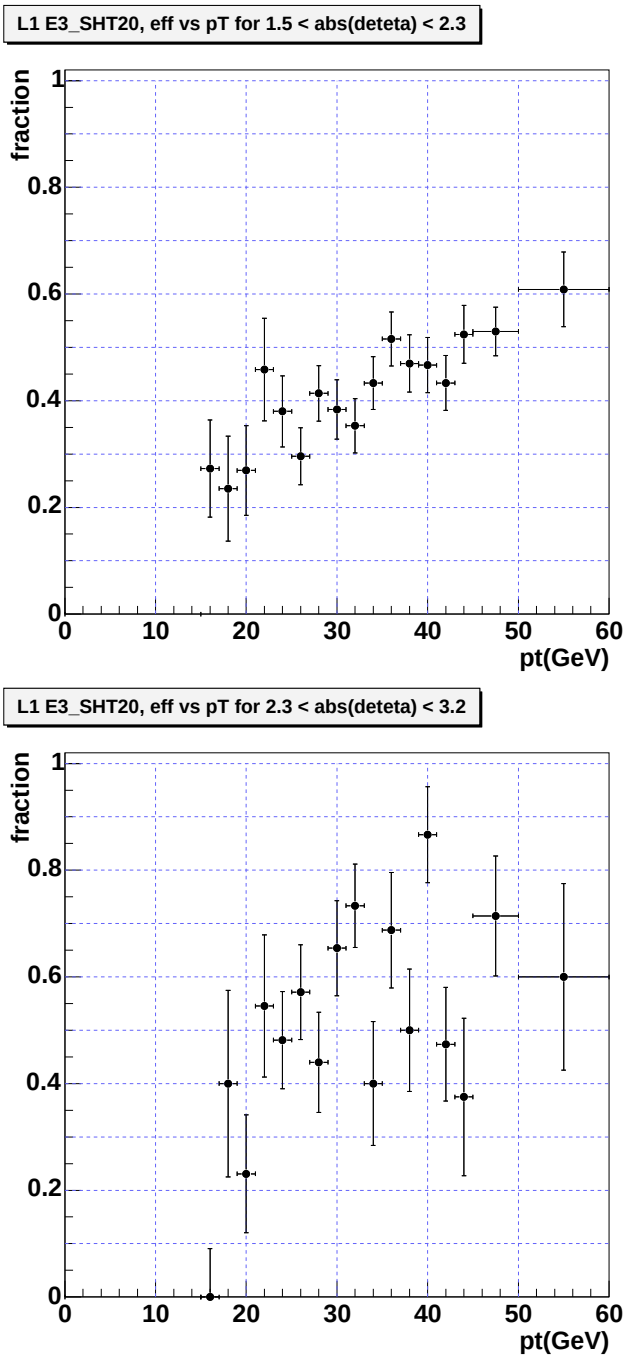

Figure 222: Electron trigger efficiency at L1 for E3_SHT20 as a function of E_T for EC(top) and extended EC($2.3 < |\eta_{detector}| < 3.2$) (bottom).

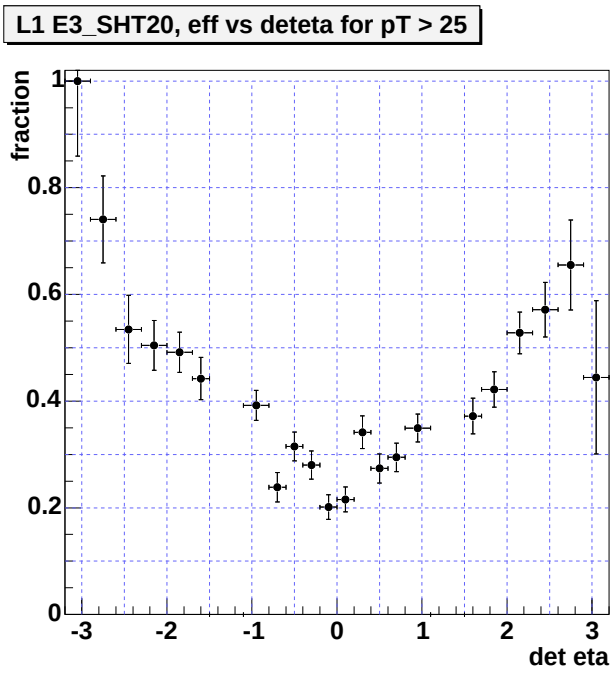

Figure 223: Electron trigger efficiency at L1 for E3_SHT20 as a function of detector η.

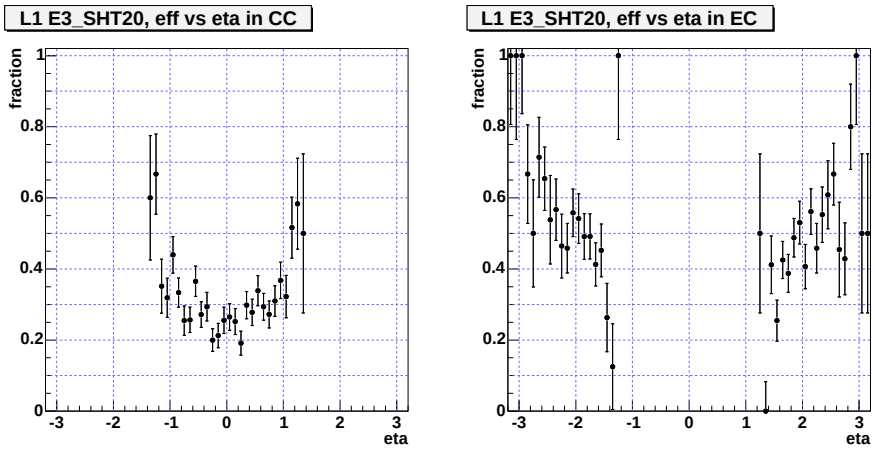

Figure 224: Electron trigger efficiency at L1 for E3_SHT20 as a function of physics η for CC(left) and EC(right).

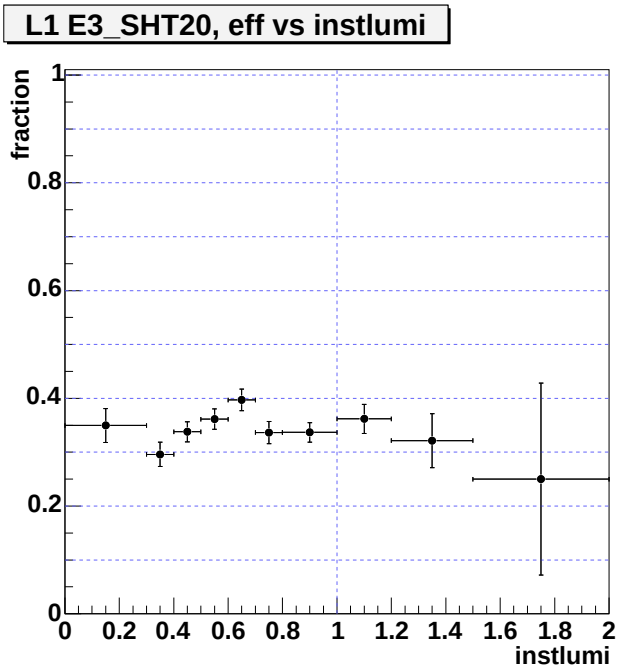

Figure 225: Electron trigger efficiency at L1 for E3_SHT20 as a function of instantaneous luminosity($10^{30} cm^{-2} s^{-1}$) for all probes.

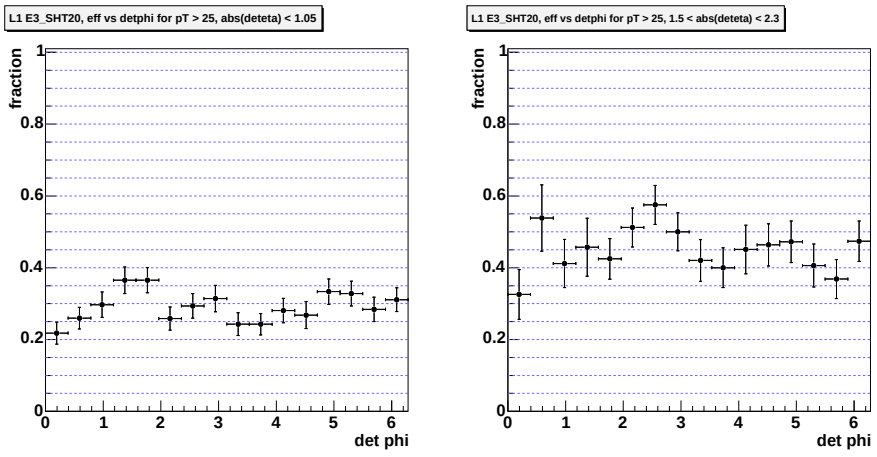

Figure 226: Electron trigger efficiency at L1 for E3_SHT20 as a function of detector ϕ for CC(left) and EC(right).

2.11.2 E3_SHT20: L3

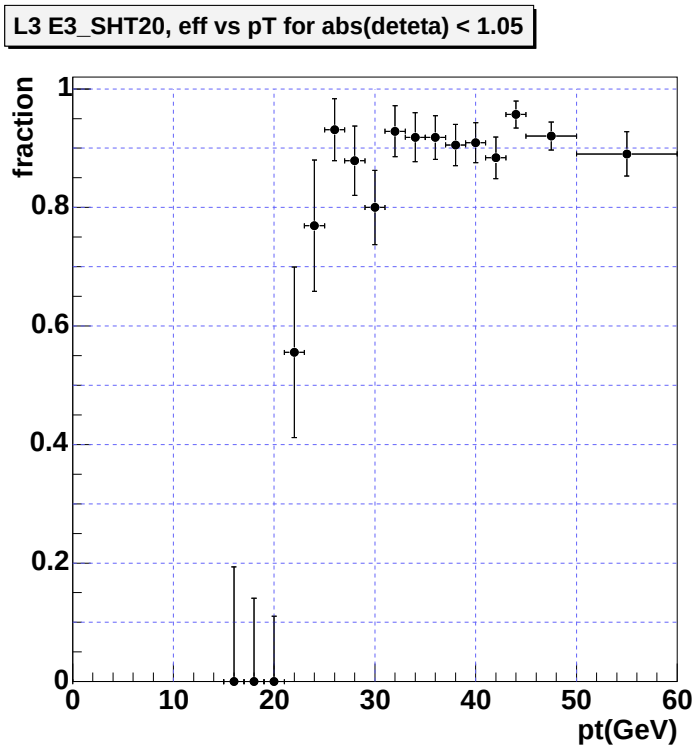

Figure 227: Electron trigger efficiency at L3 for E3_SHT20 as a function of E_T for CC.

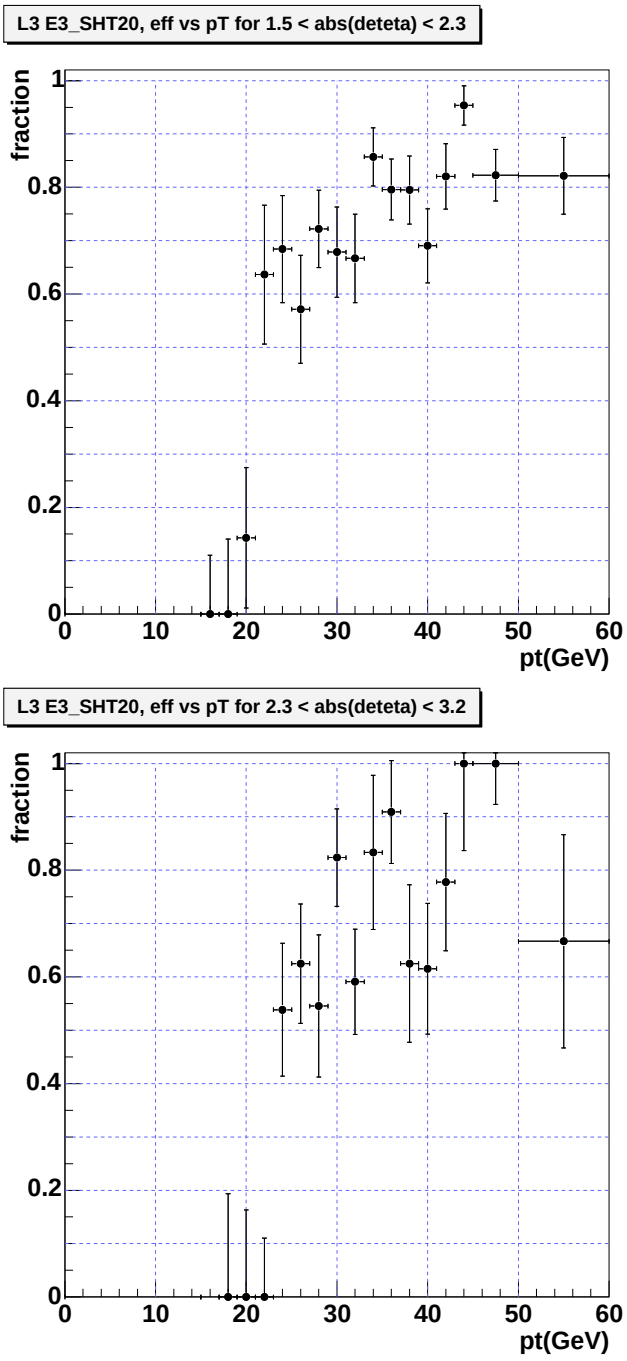

Figure 228: Electron trigger efficiency at L3 for E3_SHT20 as a function of E_T for EC(top) and extended EC($2.3 < |\eta_{detector}| < 3.2$) (bottom).

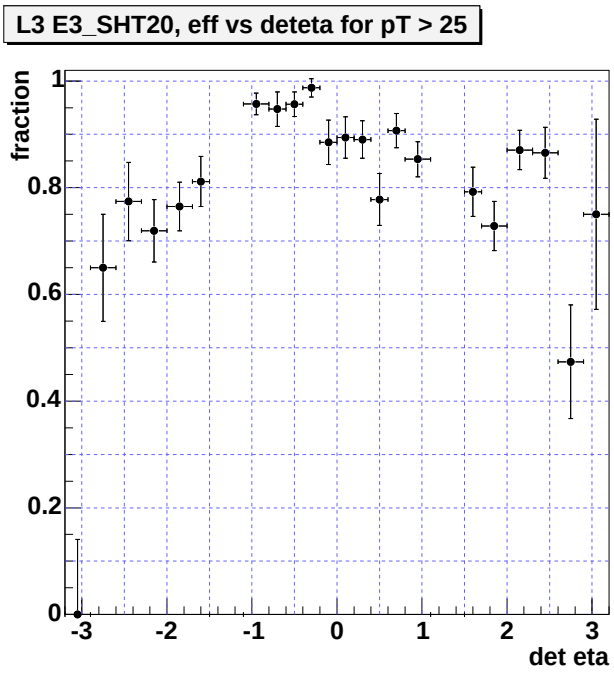

Figure 229: Electron trigger efficiency at L3 for E3_SHT20 as a function of detector η.

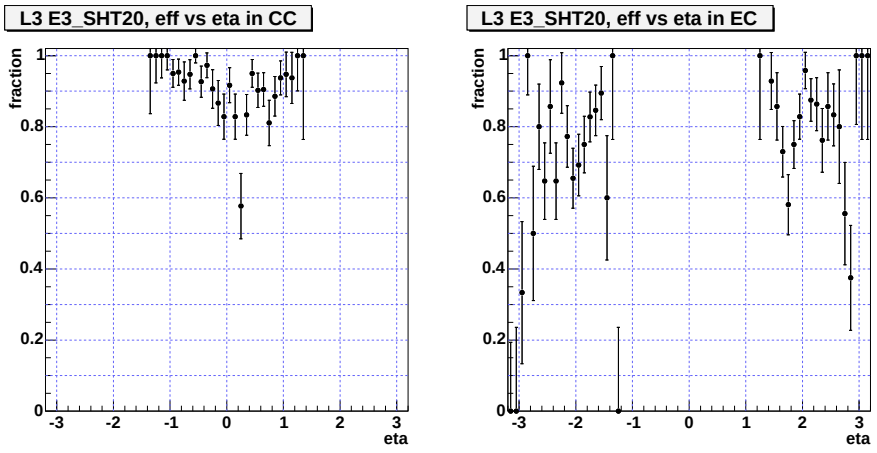

Figure 230: Electron trigger efficiency at L3 for E3_SHT20 as a function of physics η for CC(left) and EC(right).

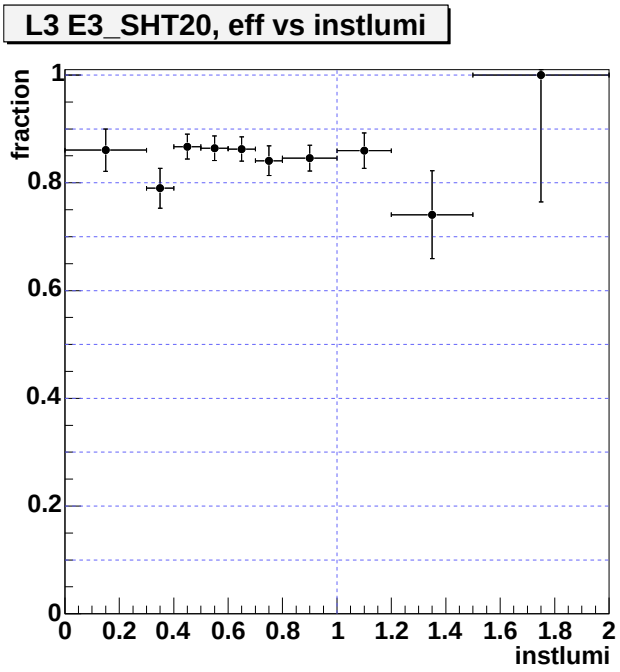

Figure 231: Electron trigger efficiency at L3 for E3_SHT20 as a function of instantaneous luminosity($10^{30} cm^{-2} s^{-1}$) for all probes.

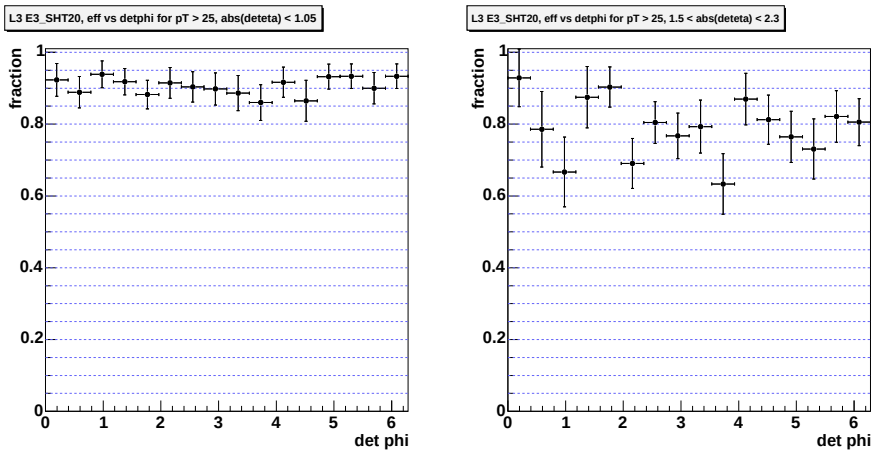

Figure 232: Electron trigger efficiency at L3 for E3_SHT20 as a function of detector ϕ for CC(left) and EC(right).

2.12 E1_SH30

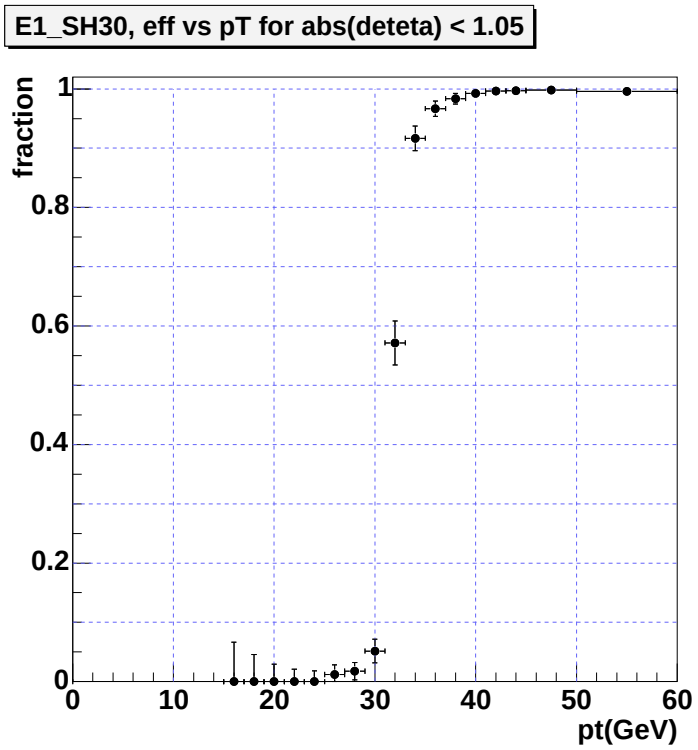

Figure 233: Electron trigger efficiency for E1_SH30 as a function of E_T for CC.

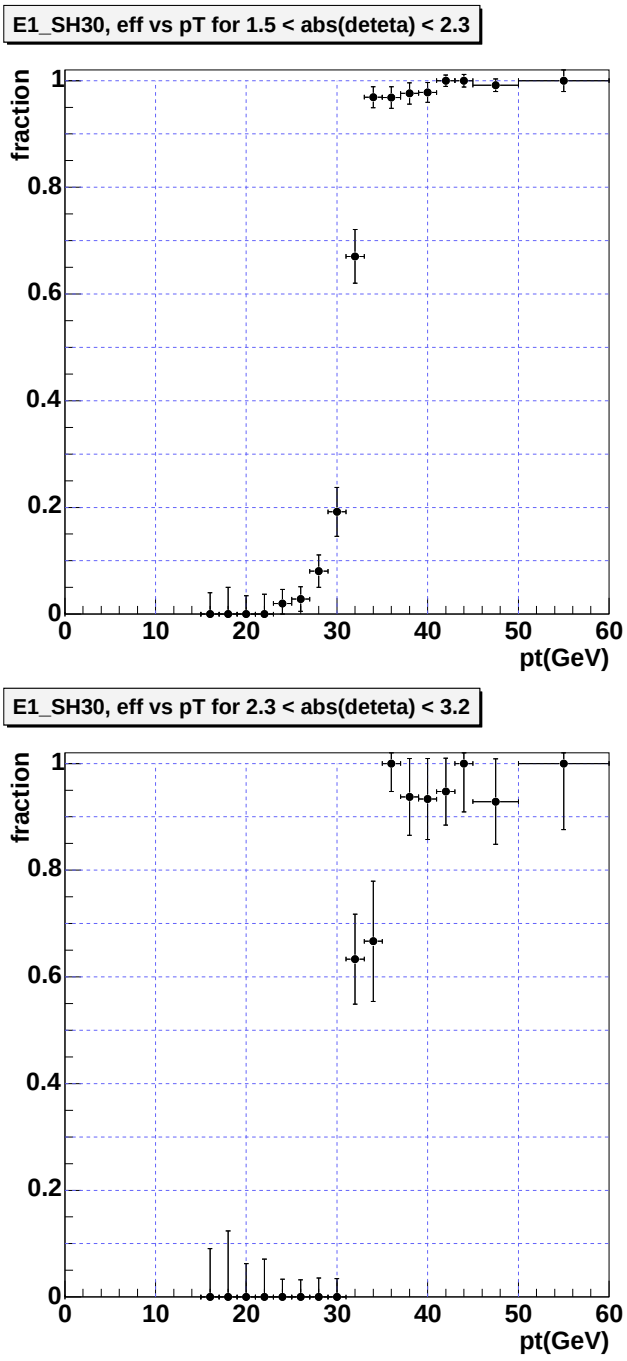

Figure 234: Electron trigger efficiency for E1_SH30 as a function of E_T for EC(top) and extended EC($2.3 < |\eta_{detector}| < 3.2$) (bottom).

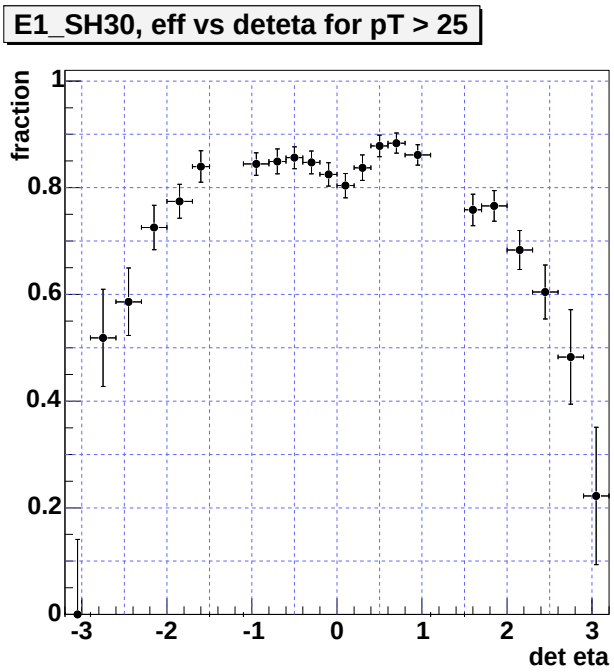

Figure 235: Electron trigger efficiency for E1_SH30 as a function of detector η.

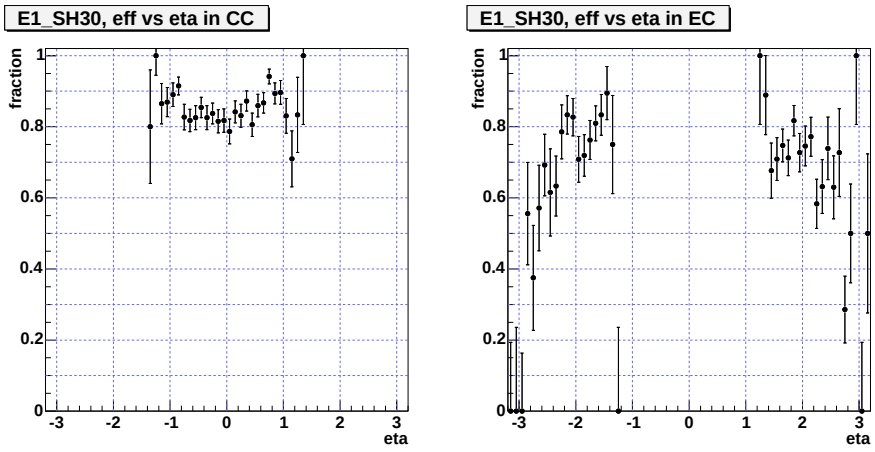

Figure 236: Electron trigger efficiency for E1_SH30 as a function of physics η for CC(left) and EC(right).

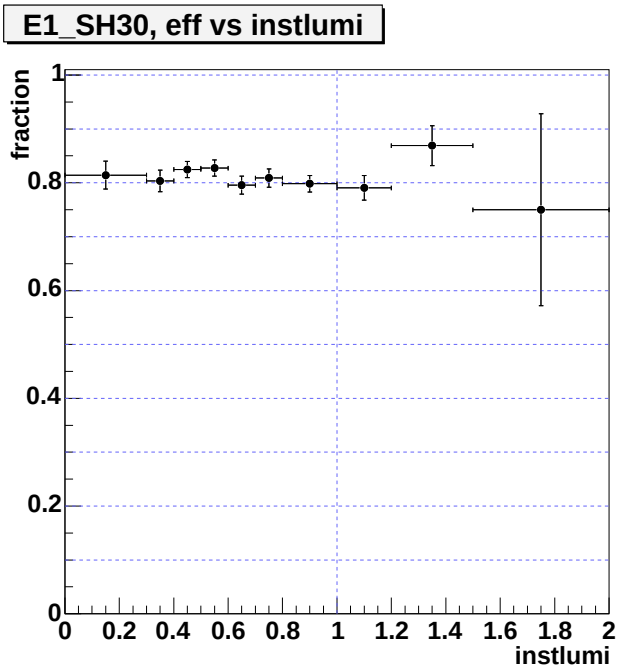

Figure 237: Electron trigger efficiency for E1_SH30 as a function of instantaneous luminosity($10^{30} cm^{-2} s^{-1}$) for all probes.

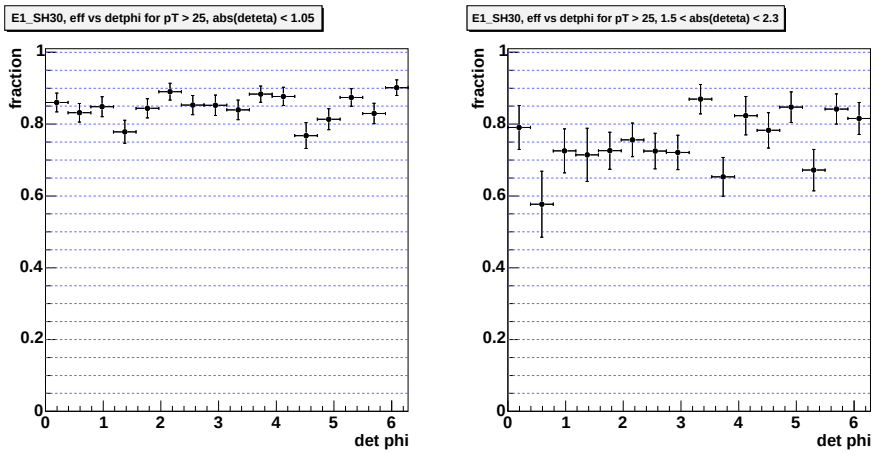

Figure 238: Electron trigger efficiency for E1_SH30 as a function of detector ϕ for CC(left) and EC(right).

2.12.1 E1_SH30: L1

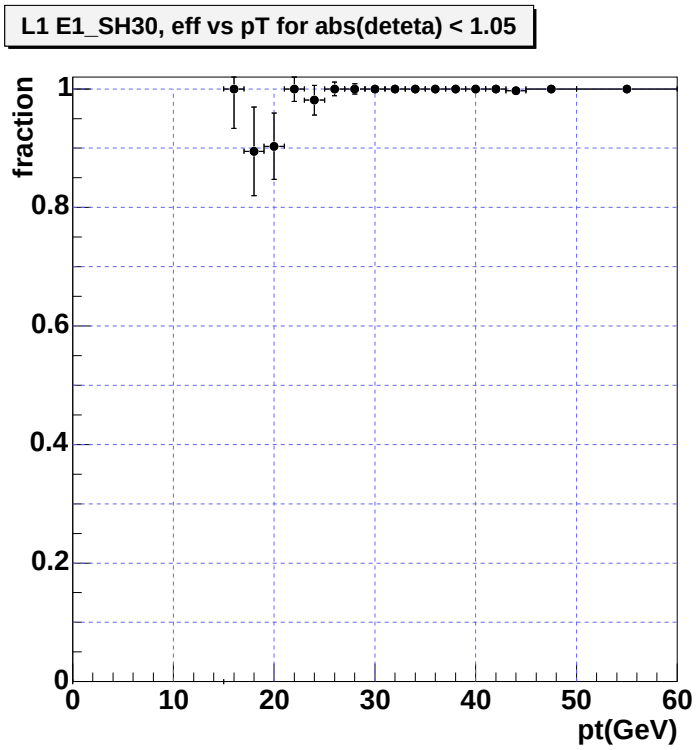

Figure 239: Electron trigger efficiency at L1 for E1_SH30 as a function of E_T for CC.

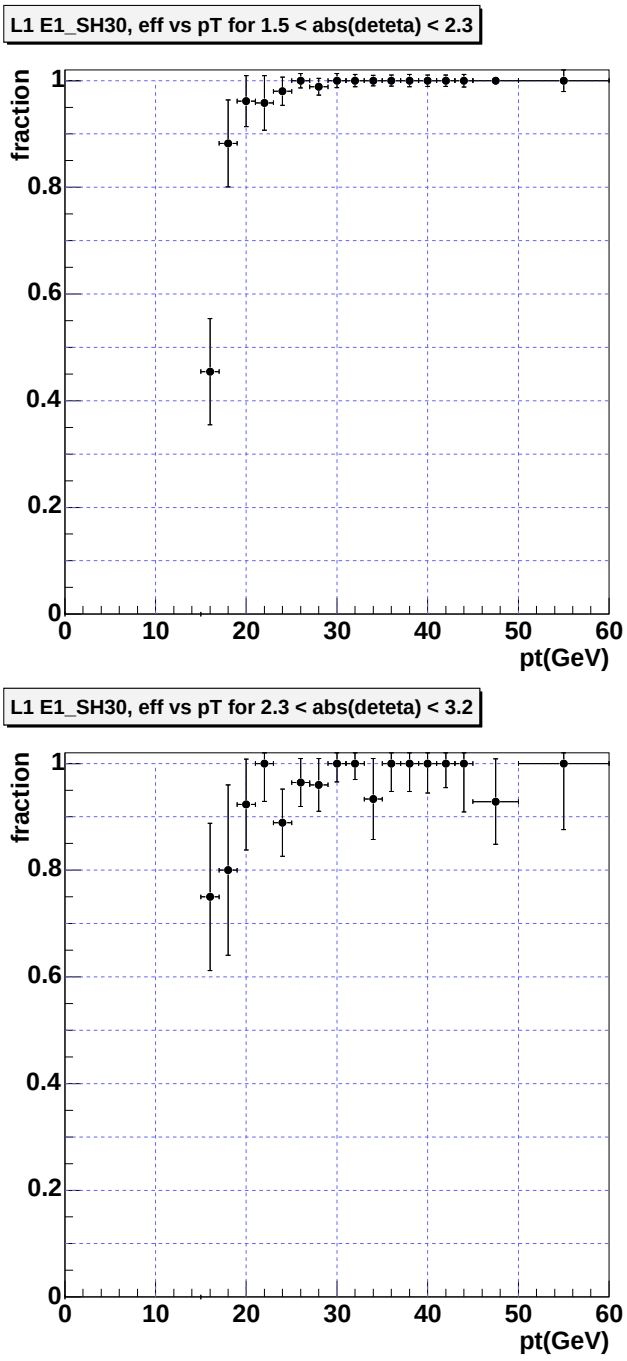

Figure 240: Electron trigger efficiency at L1 for E1_SH30 as a function of E_T for EC(top) and extended EC($2.3 < |\eta_{detector}| < 3.2$) (bottom).

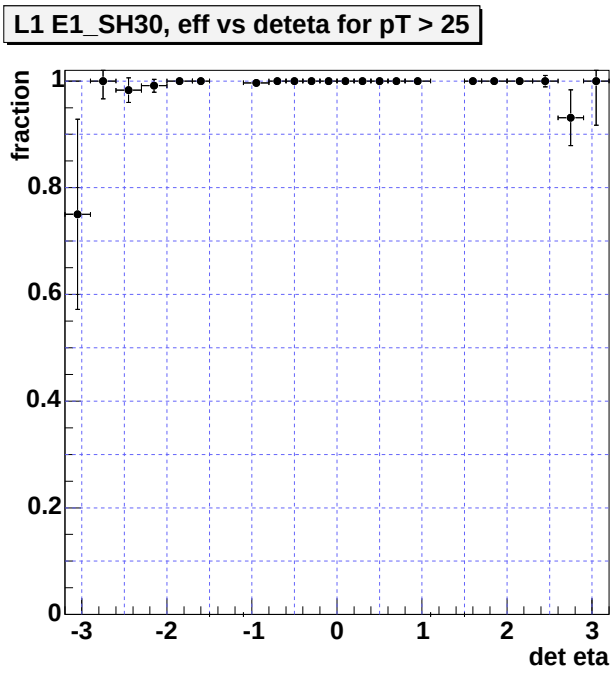

Figure 241: Electron trigger efficiency at L1 for E1_SH30 as a function of detector η.

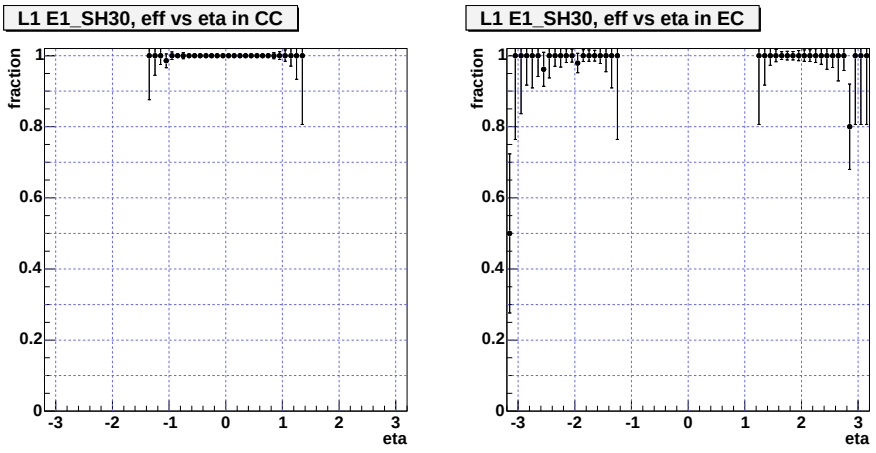

Figure 242: Electron trigger efficiency at L1 for E1_SH30 as a function of physics η for CC(left) and EC(right).

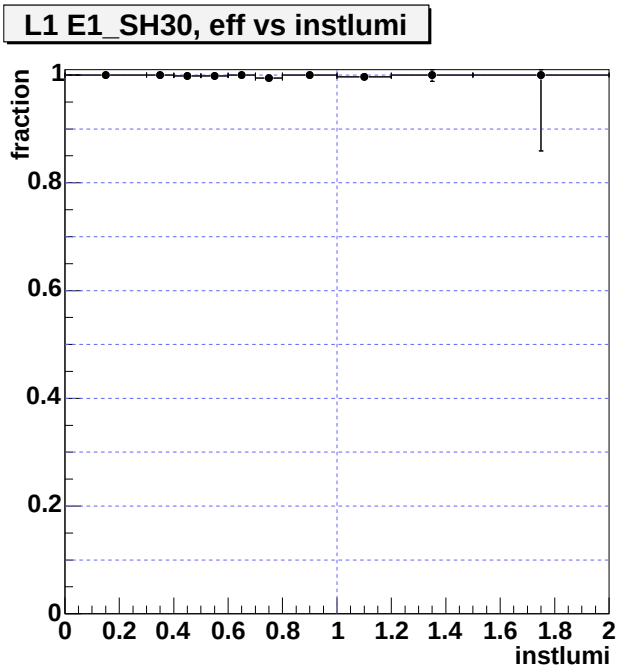

Figure 243: Electron trigger efficiency at L1 for E1_SH30 as a function of instantaneous luminosity($10^{30} cm^{-2} s^{-1}$) for all probes.

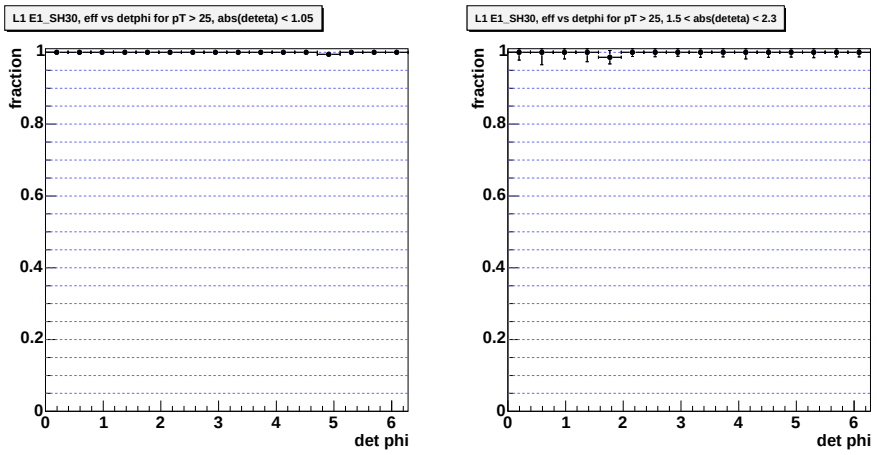

Figure 244: Electron trigger efficiency at L1 for E1_SH30 as a function of detector ϕ for CC(left) and EC(right).

2.12.2 E1_SH30: L3

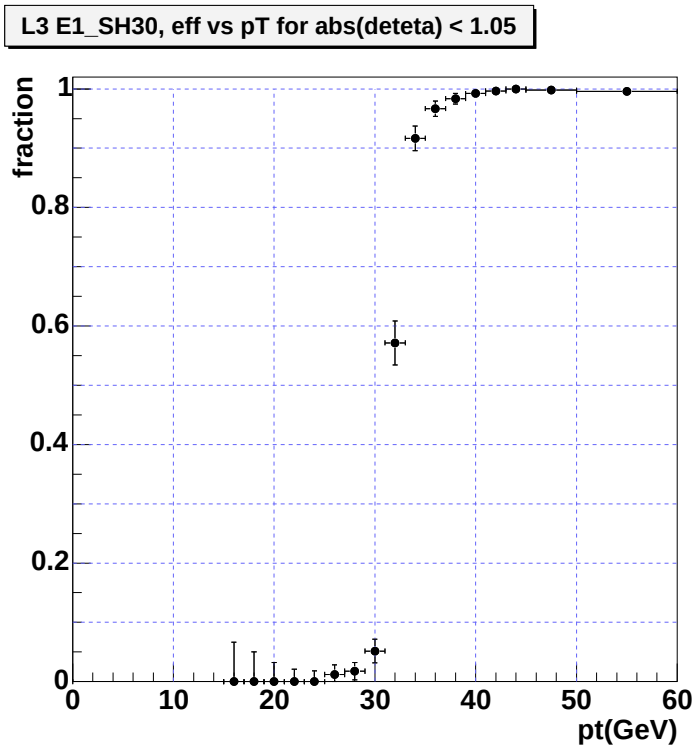

Figure 245: Electron trigger efficiency at L3 for E1_SH30 as a function of E_T for CC.

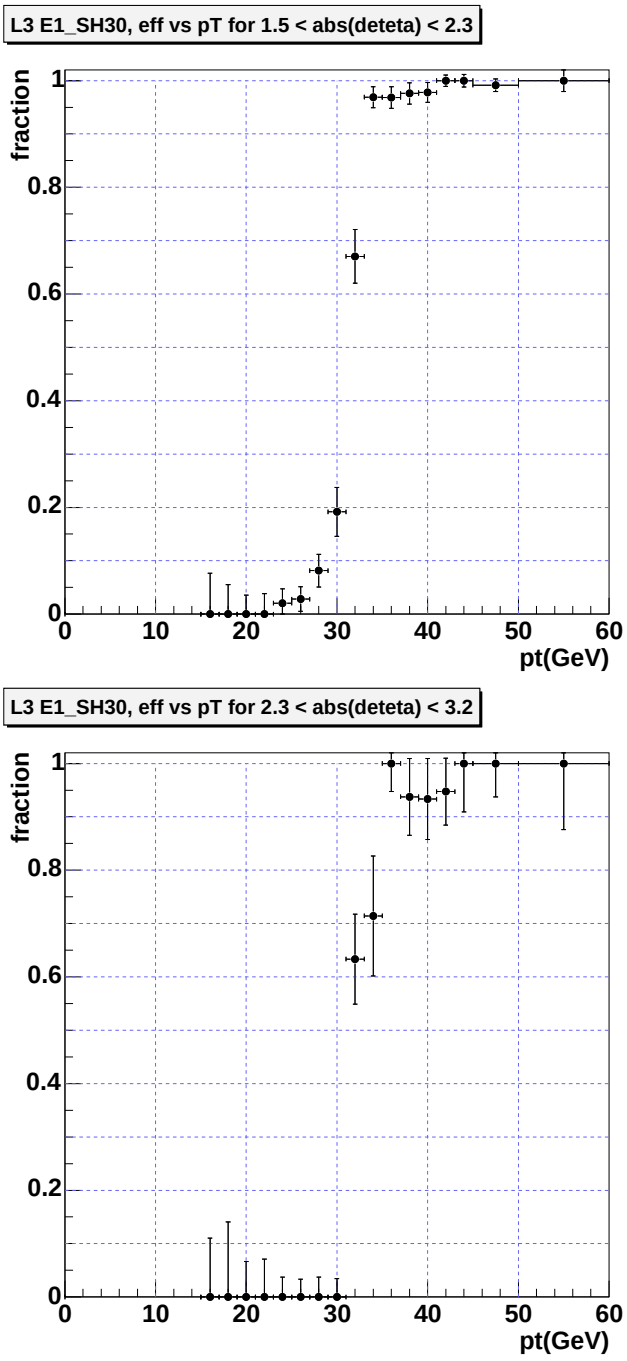

Figure 246: Electron trigger efficiency at L3 for E1_SH30 as a function of E_T for EC(top) and extended EC($2.3 < |\eta_{detector}| < 3.2$) (bottom).

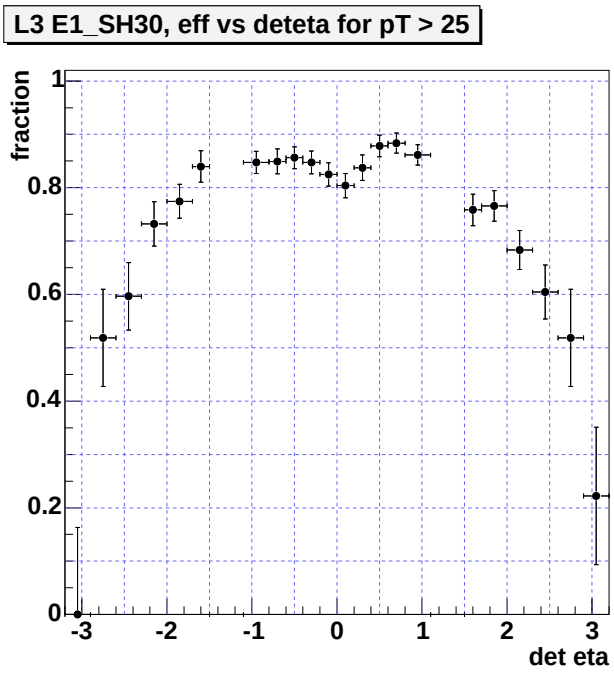

Figure 247: Electron trigger efficiency at L3 for E1_SH30 as a function of detector η.

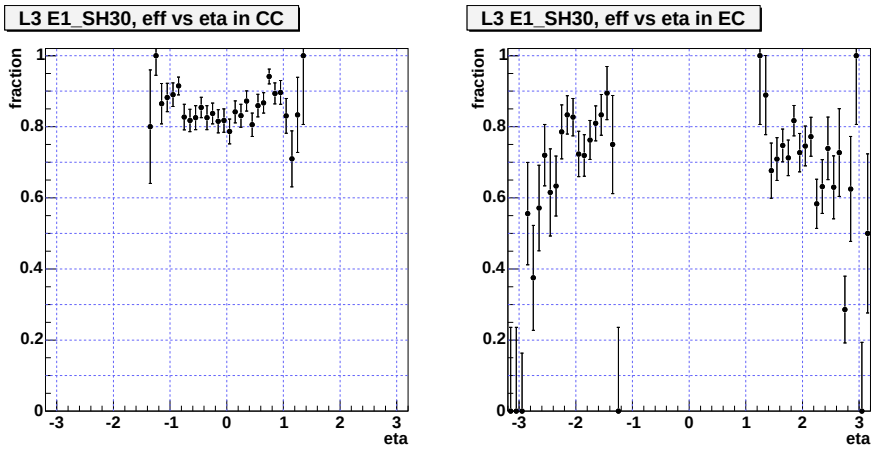

Figure 248: Electron trigger efficiency at L3 for E1_SH30 as a function of physics η for CC(left) and EC(right).

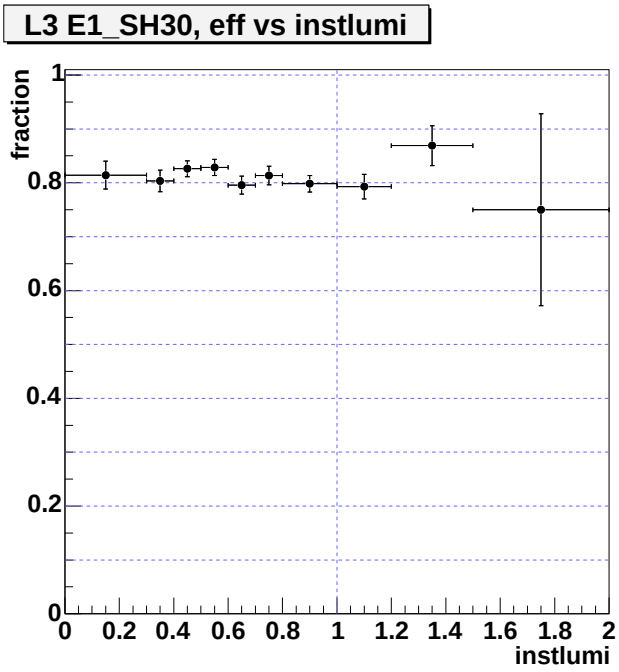

Figure 249: Electron trigger efficiency at L3 for E1_SH30 as a function of instantaneous luminosity($10^{30} cm^{-2} s^{-1}$) for all probes.

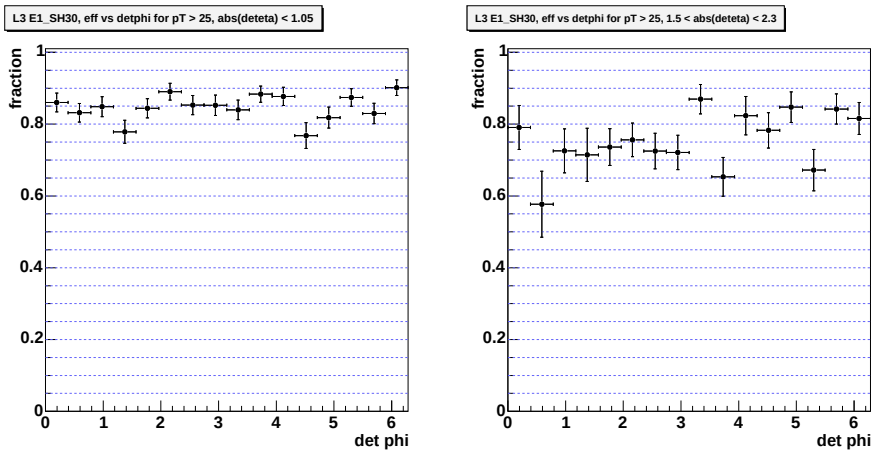

Figure 250: Electron trigger efficiency at L3 for E1_SH30 as a function of detector ϕ for CC(left) and EC(right).